UNIVERSIDADE ESTADUAL DE CAMPINAS

Instituto de Biologia

ANA CAROLINE BRAMBILLA FALVELLA

EFEITO DE ANTIPSICÓTICOS E CANABIDIOL EM CULTURA DE OLIGODENDRÓCITOS TRATADOS COM CUPRIZONA: IMPLICAÇÕES PARA MIELINIZAÇÃO

ANTIPSYCHOTICS AND CANNABIDIOL EFFECTS IN CUPRIZONE-TREATED OLIGODENDROCYTES: IMPLICATIONS FOR MYELINATION

CAMPINAS

2020

ANA CAROLINE BRAMBILLA FALVELLA

EFEITO DE ANTIPSICÓTICOS E CANABIDIOL EM CULTURA DE OLIGODENDRÓCITOS TRATADOS COM CUPRIZONA: IMPLICAÇÕES PARA MIELINIZAÇÃO

ANTIPSYCHOTICS AND CANNABIDIOL EFFECTS IN CUPRIZONE-TREATED OLIGODENDROCYTES: IMPLICATIONS FOR MYELINATION

Dissertação apresentada ao Instituto de Biologia da Universidade Estadual de Campinas como parte dos requisitos exigidos para a obtenção do título Mestra em Biologia Funcional e Molecular, na área de bioquímica.

Dissertation presented to the Institute of Biology of the University of Campinas in partial fulfillment of the requirements for the degree of Master, in Functional and Molecular Biology in the area of Biochemistry.

Orientador: Prof. Dr. Daniel Martins de Souza

ESTE TRABALHO CORRESPONDE À VERSÃO FINAL DA DISSERTAÇÃO DEFENDIDA PELA ALUNA ANA CAROLINE BRAMBILLA FALVELLA, E ORIENTADA PELO PROF. DR. DANIEL MARTINS DE SOUZA

Campinas

2020

Agências de fomento e números de processo: CNPq, 157265/2018-8; FAPESP, 2018/10362-0

Ficha catalográfica
Universidade Estadual de Campinas
Biblioteca do Instituto de Biologia
Mara Janaina de Oliveira - CRB 8/6972

F199e

Falvella, Ana Caroline Brambilla, 1995-
Efeito de antipsicóticos e canabidiol em cultura de oligodendrócitos tratados com cuprizona : implicações para mielinização / Ana Caroline Brambilla Falvella. – Campinas, SP : [s.n.], 2020.

Orientador: Daniel Martins de Souza.
Dissertação (mestrado) – Universidade Estadual de Campinas, Instituto de Biologia.

1. Esquizofrenia. 2. Canabidiol. 3. Haloperidol. 4. Clozapina. 5. Proteoma. 6. Oligodendroglia. 7. Cuprizona. I. Martins-de-Souza, Daniel, 1979-. II. Universidade Estadual de Campinas. Instituto de Biologia. III. Título.

Informações para Biblioteca Digital

Título em outro idioma: Antipsychotics and cannabidiol effects in cuprizone-treated oligodendrocytes : implications for myelination
Palavras-chave em inglês:
Schizophrenia
Cannabidiol
Haloperidol
Clozapine
Proteome
Oligodendroglia
Cuprizone
Área de concentração: Bioquímica
Titulação: Mestra em Biologia Funcional e Molecular
Banca examinadora:
Daniel Martins de Souza [Orientador]
Marcelo Bispo de Jesus
Adriano Silva Sebollela
Data de defesa: 19-10-2020
Programa de Pós-Graduação: Biologia Funcional e Molecular

Identificação e informações acadêmicas do(a) aluno(a)
- ORCID do autor: https://orcid.org/0000-0003-3330-699X
- Currículo Lattes do autor: http://lattes.cnpq.br/1983518195399393

Campinas, 19 de outubro de 2020.

COMISSÃO EXAMINADORA

Prof. Dr. Daniel Martins de Souza (Orientador)

Prof. Dr. Marcelo Bispo de Jesus

Prof. Dr. Adriano Silva Sebollela

Os membros da Comissão Examinadora acima assinaram a Ata de Defesa, que se encontra no processo de vida acadêmica do aluno.

A Ata da defesa com as respectivas assinaturas dos membros encontra-se no SIGA/Sistema de Fluxo de Dissertação/Tese e na Secretaria do Programa de Pós Graduação em Biologia Funcional e Molecular da Unidade (Instituto de Biologia).

Dedicatória

Dedico essa dissertação aos meus pais, que sempre me apoiaram, incentivaram e me deram forças em todos os momentos.

AGRADECIMENTOS

O presente trabalho foi realizado com apoio da Coordenação de Aperfeiçoamento de Pessoal de Nível Superior - Brasil (CAPES) - Código de Financiamento 001.

Agradeço o apoio financeiro da Fundação de Amparo à Pesquisa do Estado de São Paulo (FAPESP), processo nº 2018/10362-0.

À Fapesp e ao Conselho Nacional de Desenvolvimento Científico e Tecnológico (CNPq), processo nº 157265/2018-8.

Ao meu orientador, prof. Dr. Daniel Martins de Souza, por toda orientação e oportunidades que me proporcionou ao longo do mestrado. Obrigada também por toda compreensão e aprendizado que obtive durante esses anos.

À minha coorientadora, Dra. Valéria de Almeida, pelas orientações no desenvolvimento do projeto e em toda a parte experimental. Obrigada por esse exemplo de cientista dedicada e que ama ensinar. Obrigada também por toda compreensão, companhia e aprendizado que obtive durante esses dois anos, sou extremamente grata.

Aos meus colegas do Laboratório de Neuroproteômica, pela companhia e ajuda profissional. Agradeço em especial à Dra. Fernanda Crunfli pelas orientações em relação ao desenvolvimento dos experimentos; à Aline Valença, Brad Smith, Licia Costa, Pamela Carlson e Lívia Ramos pela amizade, ajuda e apoio nesses dois anos; à Danielle Junqueira pela amizade, companhia nos experimentos e na vida; ao Paulinho pelo auxílio nos experimentos de digestão em gel; e a todos do laboratório pela companhia, conversas e trocas de aprendizado.

Aos meus pais, Roseli e Luiz, que sempre me deram forças e apoio para seguir todos os meus sonhos, vocês sempre serão minha inspiração. À minha irmã, Giovanna, que sempre me apoiou e incentivou em todas as minhas escolhas. E a todos os meus familiares que estiveram presentes em todos os momentos.

A todos, minha eterna gratidão.

RESUMO

A esquizofrenia é uma desordem mental que afeta 20 milhões de pessoas em todo o mundo. A desconectividade neural, assim como alterações na substância branca, nos oligodendrócitos e na integridade de mielina, podem estar relacionadas aos sintomas dessa desordem. Neste contexto, os modelos tóxicos de desmielinização são ferramentas utilizadas para a compreensão dos mecanismos envolvidos nestas alterações. Por sua vez, abordagens proteômicas são de suma importância para a compreensão dos processos envolvidos em diferentes distúrbios neurológicos, através da compreensão das bases bioquímicas, por meio da identificação de vias e proteínas diferencialmente expressas. Desta forma, no presente trabalho foi utilizado o modelo farmacológico induzido por cuprizona em culturas de células de oligodendrócitos humanos (linhagem MO3.13), com intuito de testar os efeitos da benzatropina, molécula capaz de induzir mielinização e diferenciação dos oligodendrócitos, e compará-los com os potenciais efeitos protetores ou tóxicos dos antipsicóticos (clozapina e haloperidol) e do canabidiol, os quais afetam os oligodendrócitos de maneira distinta. Após o tratamento dos oligodendrócitos com as drogas citadas acima, foi realizada a extração e digestão do proteoma para análise por meio de nano-cromatografia acoplada à espectrometria de massas, com a finalidade de investigar as proteínas e vias envolvidas nos tratamentos com estes compostos. Nossos resultados indicam que a cuprizona é capaz de induzir efeito citotóxico em oligodendrócitos MO3.13 através de distúrbios em processos biológicos relacionados ao metabolismo energético e de lipídios, à processos genéticos, e à sinalização de fatores de crescimento. Já a administração de antipsicóticos, canabidiol e benzatropina podem modular vias relacionadas ao metabolismo, ao ciclo celular e à fatores genéticos, as quais estão relacionadas com os efeitos tóxicos induzidos pela cuprizona, indicando os seus potenciais efeitos em atenuar a toxicidade desta droga. Apesar da complexidade da fisiopatologia deste transtorno não ser totalmente representada no modelo tóxico por cuprizona, esses resultados fornecem informações sobre os mecanismos dos antipsicóticos e do canabidiol contra os efeitos tóxicos da cuprizona e suas implicações no desenvolvimento de novos alvos terapêuticos e tratamento para a esquizofrenia.

ABSTRACT

Schizophrenia is a psychiatric disorder that affects 20 million people worldwide. Neuronal dysconnectivity can be correlated to symptoms of this disorder, which is related to oligodendrocytes and myelin abnormalities in white matter. In this context, toxic models of demyelination are used to understand the mechanisms involved in these alterations. To achieve this, proteomic approaches are important to understand processes involved in neurological disorders through the elucidation of biochemical bases and identification of differentially expressed pathways and proteins. In this context, we developed an *in vitro* assay of cuprizone-mediated death in a human oligodendrocyte cell line (MO3.13) to test the effect of benztropine, a molecule that enhances myelination and oligodendrocyte differentiation, and compared its effect with the potential protective effects of antipsychotics (clozapine and haloperidol) and cannabidiol. After the treatments mentioned above, the proteomes were extracted and digested for analysis by nano-chromatography coupled to mass spectrometry to investigate the proteins and pathways affected in oligodendrocytes treated by these drugs. We confirmed that the *in vitro* model for cuprizone cell death impairs MO3.13 oligodendrocyte viability through disturbances of several biological processes, including energy and lipid metabolism, genetic processes and growth signaling. Furthermore, the administration of antipsychotics, cannabidiol, and benztropine seems to modulate metabolism, genetic factors, cell cycle and cell signaling, which are related to cuprizone-induced cell death, indicating their potential to act against the cuprizone toxic effect. In conclusion, although modeling oligodendrocyte death with cuprizone does not represent the entirety of the pathophysiology of the disorder, these results provide insight into the mechanisms related to antipsychotics' and cannabidiol's effects against cuprizone toxicity and their implications for developing new pharmaceutical targets and treatment options for schizophrenia.

ÍNDICE DE FIGURAS

INTRODUÇÃO

CAPÍTULO I

CAPÍTULO II

Figure 3. Proteins differentially expressed in OLs treated with 10μM of cuprizone (CUP) for 48 hours, compared to the vehicle (VEH), created with ClustVis.

Figure 4. Prospective network interaction of proteins differentially expressed on oligodendrocytes treated with cuprizone. The network was generated in Cytoscape from differentially expressed proteins resulting from cuprizone treatment (10μM, 48h). Colored lines represent a strong interaction; red spheres are upregulated proteins; blue spheres are downregulated proteins. All colored spheres represent $p<0.05$; to better show potential interconnectivity, gray spheres were added with a higher cutoff ($p<0.10$).

Figure 5. Bar graph of the enriched pathways in OLs resulting from cuprizone treatment (10μM, 48h), generated with Metascape.

Figure 6. Chord diagram where purple curves link identical genes between cuprizone treatment (Cup) and co-treatment with cuprizone and clozapine (CupClz), cannabidiol (CupCBD), haloperidol (CupHal) or benztropine (CupBenz) (A); and a heatmap of enriched pathways of oligodendrocytes co-treated with cuprizone and haloperidol, cannabidiol, clozapine, or benztropine (B), created in Metascape.

MATERIAL SUPLEMENTAR

Figure S1. A MTT assay was used to measure the percentage of live M03.13 cells at 48h with growth medium (DMEM), Vehicle (DMSO, 0.3%), and increasing cuprizone concentrations. (****, $P < 0.0001$; n = 6 wells/condition).

Figure S2. A MTT assay was used to measure the percentage of live M03.13 cells after 8h in growth medium (DMEM), Vehicle (haloperidol and cannabidiol, DMSO, 0.3%; clozapine, DMSO, 0.4%; benztropine was diluted in water), and increasing concentrations of haloperidol (A), clozapine (B), cannabidiol (C), or benztropine (D) (*, $P \leq 0.05$; ***, $P < 0.001$; ****, $P < 0.0001$; n = 6 wells/condition).

Figure S3. Bar graph of enriched biochemical pathways in MO3.13 cells treated with haloperidol, colored by p-value, created in Metascape. Colored lines represent $-\log_{10}(P)$, which significance are representing between 10^{-20} to 10^{-2}.

Figure S4. Bar graph of enriched biochemical pathways in MO3.13 cells treated with clozapine, colored by p-value, created in Metascape. Colored lines represent $-\log_{10}(P)$, which significance are representing between 10^{-20} to 10^{-2}.

Figure S5. Bar graph of enriched biochemical pathways in MO3.13 cells treated with cannabidiol, colored by p-value, created in Metascape. Colored lines represent -$\log_{10}$(P), which significance are representing between 10^{-20} to 10^{-2}.

Figure S6. The network of enriched terms colored by cluster ID (A) and by network-enriched terms, represented as a pie chart (B) in treatment with cuprizone and co-treatments with cuprizone and haloperidol, clozapine, cannabidiol or benztropine, created with Metascape.

LISTAS DE TABELAS

CAPÍTULO II

MATERIAL SUPLEMENTAR

Table S8. Biochemical pathways highlighted in treatment with 1μM of clozapine for 24 hours (Clz) compared to vehicle samples, generated by Reactome.

Table S9. Biochemical pathways highlighted in treatment with 1μM of cannabidiol for 24 hours (CBD) compared to vehicle samples, generated by Reactome.

Table S10. Biochemical pathways highlighted in treatment with 1μM of benztropine for 24 hours (Benz) compared to vehicle samples, generated by Reactome.

Table S11. List of proteins differentially expressed (by ANOVA, $p \leq 0.05$) in MO3.13 oligodendrocytes exposed to cuprizone (CUP; 10μM, 48h) compared to vehicle (VEI).

Table S12. List of proteins differentially expressed (by ANOVA, $p \leq 0.05$) in MO3.13 oligodendrocytes treated with haloperidol (Hal; 1μM, 24h) compared to vehicle (VEI).

Table S13. List of proteins differentially expressed (by ANOVA, $p \leq 0.05$) in MO3.13 oligodendrocytes treated with clozapine (Clz; 1μM, 24h) compared to vehicle (VEI).

Table S14. List of proteins differentially expressed (by ANOVA, $p \leq 0.05$) in MO3.13 oligodendrocytes treated with cannabidiol (CBD; 1μM, 24h) compared to vehicle (VEI).

Table S15. List of proteins differentially expressed (by ANOVA, $p \leq 0.05$) in MO3.13 oligodendrocytes treated with benztropine (Benz; 1μM, 24h) compared to vehicle (VEI).

Table S16. List of proteins differentially expressed (by ANOVA, $p \leq 0.05$) in co-treatment 10μM of cuprizone for 24 hours and 1μM of haloperidol for an additional 24 hours (CupHal), compared to cuprizone treatment alone (Cup).

Table S17. List of proteins differentially expressed (by ANOVA, $p \leq 0.05$) in co-treatment 10μM of cuprizone for 24 hours and 1μM of clozapine for an additional 24 hours (CupClz), compared to cuprizone treatment alone (Cup).

Table S18. List of proteins differentially expressed (by ANOVA, $p \leq 0.05$) in co-treatment 10μM of cuprizone for 24 hours and 1μM of cannabidiol for an additional 24 hours (CupCBD), compared to cuprizone treatment alone (Cup).

LISTAS DE ABREVIATURAS

2-AG - 2-araquidonilglicerol

2D-GE - Eletroforese bidimensional

2D-PAGE - Gel de eletroforese bidimensional de poliacrilamida

ABHD6 ou ABHD12 - Serinas hidrolases, α, β-hidrolase domínios proteínas 6 e 12

ACN - Acetonitrila

AEA – Anandamida, N-arachidonoyl ethanolamine

AF - Ácido fórmico

Ambic - Ammonium bicarbonate

ATP – Adenosine triphosphate

BDNF - Brain-derived neurotrophic factor

BENZ - Benztropine

CB1 - Receptores de canabinoides do tipo 1

CB2 - Receptores de canabinoides do tipo 2

CBD - Canabidiol, cannabidiol

CID - Dissociação induzida por colisão

CLZ - Clozapine

CNP - 2, ′3′-cyclic-nucleotide-3′-phosphodiesterase

CNS - Central nervous system

CUP ou CPZ - cuprizona, cuprizone

CupBenz - Co-treatment with cuprizone (10μM; 48h) and benztropine (1μM; 24h)

CupCBD - Co-treatment with cuprizone (10μM; 48h) and cannabidiol (1μM; 24h)

CupClz - Co-treatment with cuprizone (10μM; 48h) and clozapine (1μM; 24h)

CupHal - Co-treatment with cuprizone (10μM; 48h) and haloperidol (1μM; 24h)

DAG - Diacilglicerol

DAGL - DAG lipase

DIA - Análise independente de dados, data-independent analysis

DISC1 - Disrupted-in-schizophrenia 1

DMEM – Dulbecco's Modified Eagle Medium

DSM-5 - Manual diagnóstico e estatístico de transtornos mentais

DTT - Dithiothreitol stock

EAE - Encefalomielite autoimune experimental

ERK1/2 - Signal-regulated kinases-1 and -2

ESI - Ionização por electrospray

FAAH - Enzima hidrolase de amida de ácidos graxos

FDR – False discovery rate

GalC - Galactocerebroside C

GPR55 - G protein-coupled receptor 55

GSH - Glutathione

GSK3b - Glycogen synthase kinase 3b

HAL - Haloperidol

ICD - Classificação estatística internacional de doenças e problemas relacionados à saúde

IGF-1 - Insulin-like growth factor 1

IT - Ion traps

LC-MS – Cromatografia líquida acoplada à espectrometria de massas

MAG - Glicoproteína associada à mielina, myelin associated glycoprotein

MALDI - Ionização dessorção a laser auxiliada por matriz

MAGL - Lipases monoacilglicerol

MAPKs - Mitogen-activated protein kinases

MBP - Proteína básica de mielina, myelin basic protein

MCT-1 - Monocarboxylate transporter 1

MCT-2 - Monocarboxylate transporter 2

MOG - Glicoproteína da mielina de oligodendrócitos, myelin oligodendrocyte glycoprotein

MS - Espectrometria de massas

mTOR - Mammalian target of rapamycin

NAAA - Enzima N-acetil-etanolamina-hidrólise ácida amidase

NAD+ - Dinucleotídeo de nicotinamida e adenina, nicotinenamide adenine dinucleotide

NAPE - N-acil-fosfatidiletanolamina

NAPE-PLD - Fosfolipase-D-específica de NAPE

NG2 - Neuron-glial antigen 2

NGR - Nogo Receptor

NGF - Nerve growth factor

NMDA - N-metil-D-Aspartato

NPC - Neural progenitor cells

NRG1 - Neuregulin 1

NSC - Neural stem cells

Olig2 - Oligodendrocyte lineage transcription factor 2

OLs - Oligodendrócitos, oligodendrocytes

OPCs - Células precursoras de oligodendrócitos, oligodendrocytes progenitor cells

PBS - Phosphate-buffered saline

PPARs - Peroxisome proliferator activated nuclear receptors

PFC - Prefrontal cortex

PI3K - Phosphoinositide 3-kinase

PLP - Proteína proteolipídica de mielina, proteolipid protein

PPI - Prepulse inhibition

Q - Quadrupolo

QKI - Quaking I

QUE - Quetiapine

ROS - Espécies reativas de oxigênio

Rtn4 - Reticulon 4

SNC – Sistema Nervoso Central

SVZ - Subventricular zone.

THC - Δ-9-tetrahydrocannabinol

TOF - Time of flight mass analyzers

TRPV1 - Transient receptor potential vanilloid-1 channel

SUMÁRIO

1. INTRODUÇÃO

1.1 A esquizofrenia

A esquizofrenia é uma desordem mental grave, crônica e incurável que atinge 1% da população mundial. O início deste transtorno ocorre entre o final da adolescência e o início da vida idade adulta (Owen et al., 2016). Estudos demonstram que pacientes com esquizofrenia têm expectativa de vida de 12 a 15 anos menor do que a da população geral, já que tal distúrbio apresenta alta frequência de suicídio e problemas cardiovasculares (Bruijnzeel et al., 2014; van Os & Kapur, 2009). Os sintomas característicos da esquizofrenia são os sintomas positivos que incluem alucinações, delírios e desorganização do pensamento, os sintomas negativos como a perda motivacional e vivacidade emocional, e os sintomas cognitivos, incluindo comprometimento da memória e de funções executivas (Lewis & Lieberman, 2000; Tarpada & Morris, 2017).

O diagnóstico da esquizofrenia é baseado na anamnese realizada pelo o médico, com base na história e estado mental do paciente. A categorização da mesma é realizada com base no Manual Diagnóstico e Estatístico de Transtornos Mentais (DSM-5) ou através da Classificação Estatística Internacional de Doenças e Problemas Relacionados à Saúde (ICD) (Kahn et al., 2015; Owen et al., 2016). O tratamento medicamentoso de indivíduos com esquizofrenia é baseado na administração de antipsicóticos, os quais atuam efetivamente no tratamento dos sintomas positivos, entretanto possui baixa eficácia no tratamento dos sintomas negativos e cognitivos (Bruijnzeel et al., 2014; van Os & Kapur, 2009). Os antipsicóticos de primeira geração (convencionais ou típicos) descobertos nos anos 1950, como o haloperidol, são antagonista dos receptores D_2, sendo efetivos na redução dos sintomas positivos, porém conduzem a certos efeitos colaterais extrapiramidais (Howes et al., 2015; Howes & Kapur, 2009). Os antipsicóticos de segunda geração (atípicos) como clozapina, risperidona, olanzapina e quetiapina, apresentam afinidade aos receptores D_2 e aos receptores 5-HT_2, sendo mais eficientes na redução dos sintomas negativos, mas podem causar aumento de peso e sedação, quando comparados com os de primeira geração (Leucht et al., 2009; van Os & Kapur, 2009). Neste contexto, os aspectos heterogêneos e multifatorial da esquizofrenia, em conjunto com o conhecimento limitado quanto a causa e a fisiopatologia deste transtorno, dificultam o diagnóstico e a escolha adequada ao tratamento (Nascimento & Martins-de-Souza, 2015).

1.1.1 Fisiopatologia da esquizofrenia

A esquizofrenia é considerada multifatorial, sendo determinada pela interação de fatores genéticos e ambientais, como estresses ocorridos durante a vida fetal (hipóxia, estresse materno e deficiência nutricional) e na infância (Owen et al., 2016). A fisiopatologia desta desordem engloba distúrbios moleculares no sistema nervoso, metabólico, imune e endócrino (Collip et al., 2011; Martins-de-Souza et al., 2011; Pouget et al., 2019; Saia-Cereda et al., 2015). Diversas hipóteses são postuladas para compreender a etiologia da esquizofrenia, porém as hipóteses glutamatérgica e dopaminérgica estão entre as teorias mais estudadas e aceitas, embora evidências sugerem alterações em outros sistemas como o GABAérgico, serotoninérgico, colinérgico e endocanabinoide (Friedman, 2004; Muguruza et al., 2019; Steiner et al., 2016; Yang & Tsai, 2017).

A hipótese dopaminérgica foi postulada na década de 1960, quando foi descoberto o potencial efeito do antipsicótico clorpromazina em atenuar os sintomas positivos em pacientes com esquizofrenia (Yang & Tsai, 2017). Diversos estudos suportam a hipótese que o sistema dopaminérgico estão relacionados com os sintomas psicóticos em pacientes com esquizofrenia (Mackay et al., 1982; Howes & Kapur, 2009). Estudos em cérebros *post-mortem* de pacientes sugerem alterações neuropatológicas na esquizofrenia, incluindo aumento nos níveis de dopamina e na densidade dos receptores D_2 (Mackay et al., 1982). Além disso, o aumento da atividade de dopamina foi observada predominantemente nas regiões do estriado e mesencéfalo em pacientes com alto risco de psicose ou em pacientes que desenvolveram este sintoma mais tardiamente (Edwards et al., 2016; Egerton et al., 2013; Laruelle et al., 1996; Howes et al., 2013). Neste contexto, os antipsicóticos utilizados no tratamento dessa desordem apresentam afinidade pelo receptor de dopamina, bloqueando sua atividade e amenizando os sintomas positivos (Howes et al., 2015; Howes & Kapur, 2009).

Por outro lado, o glutamato é um neurotransmissor excitatório e mais abundante no cérebro. A ação desse neurotransmissor é mediada por receptores metabotrópicos e ionotrópicos, dentre eles os receptores do tipo NMDA (N-metil-D-Aspartato). Suas vias se ligam as regiões do córtex pré-frontal, tálamo e lobo temporal, as quais se encontram alteradas na esquizofrenia (Gao et al., 2000; Goff & Coyle, 2001; Ibrahim et al., 2000). Estudos relatam níveis reduzidos de glutamato no líquido cefalorraquidiano e níveis elevados de metabólitos de glutamato no hipocampo e na região cortical frontal em pacientes com esquizofrenia (Egerton et al., 2017; Howes et al., 2015). Ademais, foi demonstrado que

animais tratados com fenciclidina, um antagonista dos receptores NMDA, apresentam alterações nas expressões de genes no córtex pré-frontal, região relacionada à disfunção cognitiva na esquizofrenia, dentre eles alterações nas expressões de transcritos relacionados à mielina e à linhagens de oligodendrócitos (OLs) (Kaiser et al., 2004). Desta forma, a hipofunção dos receptores NMDA podem desempenhar um grande papel na fisiopatologia da esquizofrenia (Cohen et al., 2015; Paz et al., 2008).

Outras linhas de estudos relacionam as anormalidades na substância branca e a desconectividade neural à fisiopatologia desse transtorno, os quais podem estar relacionados às disfunções na mielinização acarretados por distúrbios em OLs (Cassoli et al., 2015; Jørgensen et al., 2016; Vikhreva et al., 2016). Estudos *post-mortem* e de neuroimagem indicam alterações na mielinização, na área cortical e na substância branca, assim como a redução do número de OLs em pacientes com esquizofrenia (Jørgensen et al., 2016; Mighdoll et al., 2015). Além disso, as anormalidades na conectividade neural e na substância branca podem estar correlacionadas com os sintomas positivos, negativos e cognitivos de pacientes com este transtorno (Bernard et al., 2015; Kochunov et al., 2017; Orban et al., 2017; Saito et al., 2018). Sendo assim, estudos demonstram que as alterações na substância branca, assim como as alterações em OLs e na mielina, podem estar relacionadas com os sintomas da esquizofrenia devido à degradação funcional de importantes circuitos neurais.

1.1.2 O papel dos oligodendrócitos e da mielina na esquizofrenia

Os OLs são células gliais responsáveis pela mielinização dos axônios no sistema nervoso central (SNC), expressando genes que codificam as proteínas da mielina de maneira específica e controlada. Estas células têm origem a partir de células neuroectodérmicas presentes nas zonas sub ventriculares, com posterior migração para as zonas corticais e para substância branca, seguido da maturação em células mielinizantes (Baumann & Pham-Dinh, 2001; Buntix et al., 2003; Pfeiffer et al., 1993). Os processos de oligodendrogênese e de mielinização requerem a ativação de diversas vias de sinalização e da interação com outras células da glia, a fim de fornecer precursores de colesterol e nutrientes para a bainha de mielina, além de propiciar quimiocinas e fatores de crescimento que influenciam os processos de sobrevivência, proliferação, migração e maturação dos OLs (Baror et al., 2019; Camargo et al., 2017; Dziembowska et al., 2005). A mielinização realizada pelos OLs é essencial para a propagação do potencial de ação no axônio, pois devido à composição única (rica em lipídeos e baixo teor de água), e à estrutura segmentar da mielina, a transdução de sinal

elétrico é mais rápida e eficiente nas fibras nervosas mielinizadas (Baumann & Pham-Dinh, 2001; Peferoen et al., 2014; Simons & Nave, 2015). Além disso, essas células possuem um papel importante no metabolismo energético axonal, como a liberação de lactato ou piruvato para o espaço peri-axonal via MCT-1 (*monocarboxylate transporter 1*), que logo em seguida entram nos axônios através de MCT-2 (*monocarboxylate transporter 2)* para a geração de ATP mitocondrial axonal (Philips & Rothstein, 2017; Saab et al., 2013).

Outros estudos indicam que o lactato é capaz de promover a homeostase de ATP nos OLs, sendo importante para a formação e geração de mielina (Rinholm et al., 2011). Estudos proteômicos revelam alterações em proteínas e vias bioquímicas relacionadas ao metabolismo energético, como também demonstrado em estudos de imagens, os quais relatam níveis reduzidos nas taxas metabólicas de glicose em diferentes núcleos talâmicos em pacientes com esquizofrenia (Hazlett et al., 2004; Zuccoli et al., 2017). A privação energética pode inibir eventos de mielinização e acarretar em desmielinização, por meio da limitação da disponibilidade de substratos para a síntese de lipídios na mielina (Rinholm et al., 2011). Estudos com amostras *post-mortem* do córtex pré-frontal indicam uma mielinização anormal em pacientes com esquizofrenia (Migdoll et al., 2015). Ademais, foram relatados desregulações em constituintes essenciais da bainha de mielina, como as proteínas MBP (proteína básica de mielina) e MOG (glicoproteína da mielina de oligodendrócitos) (Saia-Cereda et al., 2015), e alterações nos padrões de RNA mensageiros (mRNA), transcritos e proteínas de OLs (Cassoli et al., 2015).

O ciclo de vida dos OLs consiste em processos altamente regulados e controlados, e estão relacionados a conectividade cerebral adequada (Barateiro & Fernandes, 2014). A desconectividade neural, assim como outras alterações da substância branca na esquizofrenia, podem estar relacionadas à OLs anormais. Descobertas referente à neuropatologia da substância branca no distúrbio em questão incluem a diminuição da densidade de OLs, alterações na distribuição espacial dos mesmos e variações na morfologia dessas células (Bernstein et al., 2015). Estudos indicam que disfunções nos OLs no hipocampo causam alterações no neurocircuito entre o hipocampo e hipotálamo, acarretando em distúrbios cognitivos em pacientes com esquizofrenia (Falkai et al., 2016; Falkai et al., 2020). Além disso, a mielinização anormal e disfunções nas sinapses podem ser correlacionadas com distúrbios na funcionalidade neuronal e glial (Mirnics et al., 2000; Takahashi et al., 2011).

Além dos estudos citados, foram relatadas anormalidades nos processos de diferenciação de células precursoras de oligodendrócitos (OPCs) e de oligodendrogênese na esquizofrenia (Hattori et al., 2014; Santos et al., 2019). Neste último processo as OPCs têm a capacidade de migrar e se diferenciar em OLs maduros, a fim de remielinizar o local lesionado (Dimou et al., 2008). Estudos indicam que o bloqueio da oligodendrogênese acarreta na inibição de eventos que provem a mielinização (Mckenzie et al., 2014). Anormalidades na mielinização ou em fatores que influenciam a mesma podem eventualmente levar à degradação funcional de importantes circuitos neurais, resultando em desorganizações, ineficiências cognitivas e comportamentais, os quais fazem parte da manifestação clínica da esquizofrenia (Mighdoll et al., 2015). Estudos *in vivo* e *in vitro* mostram que diversas drogas, como os antipsicóticos, podem modular a migração, proliferação e diferenciação das OPCs (Ren et al., 2013). Sendo assim, a modulação das OPCs e dos OLs maduros são essenciais para a compreensão de mecanismos relacionados à fisiopatologia e tratamento da esquizofrenia (de Almeida & Martins-de-Souza, 2018). Além disso, os mecanismos relacionados aos distúrbios de OLs, desmielinização e remielinização em transtornos neurológicos podem ser compreendidos a partir de modelos tóxicos de desmielinização (Bénardais et al., 2013). Diversas drogas são investigadas neste modelo para compreender seus potenciais efeitos nos processos de remielinização, neuroproteção e de indução da proliferação de OLs, como os canabinoides e antipsicóticos (Bartzokis, 2012; Zajicek & Apostu, 2011).

1.2 Modelo de estudo de desmielinização e remielinização

1.2.1 Modelo tóxico induzido por cuprizona

A mielinização dos axônios dos neurônios do SNC é essencial para a condução de sinais elétricos e manutenção da integridade do axônio (Taraboletti et al., 2017; Sachs et al., 2014). Desta forma, a desmielinização acarreta sérias consequência neurológicas, incluindo a redução da função motora e comprometimento nas habilidades cognitivas (Skaper, 2019). A compreensão dos mecanismos relacionados a mielinização e desmielinização, assim como anormalidades e mortes de OLs podem ser estudados através de modelos tóxicos induzidos por agentes farmacológicos, como a cuprizona, a qual pode ser

empregada tanto *in vivo* quanto *in vitro* (Bénardais et al., 2013; de Rosa et al., 2019; Xu et al., 2014; Xu et al., 2019).

As propriedades neurotóxicas da cuprizona induzem desmielinização em certas regiões do sistema nervoso de ratos, como no corpo caloso, hipocampo e pedúnculo cerebelar superior, sendo observado um declínio de mRNAs de proteínas relacionados a mielina (Acs et al., 2013a; Pasquini et al., 2007; Sachs et al., 2014). A priori, a sua toxicidade tem sido relacionada com distúrbios na homeostase de cobre no cérebro, devido a sua propriedade de quelação com este íon (Messori et al., 2007; Zatta et al., 2005). Por outro lado, estudos demonstram que a toxicidade desta droga ocorre devido à inibição das enzima monoamina oxidase e citocromo c oxidase (Kesterson & Carlton, 1971; Venturini et al., 1973), à alterações nos complexos da cadeia transportadora de elétrons (Acs et al., 2013b) e a distúrbios na enzima superóxido dismutase de cobre e zinco (De & Subramanian, 1982), os quais acarretam em disfunções mitocondriais e na inibição da geração de energia, culminando na morte dos OLs (Moldovan et al., 2015; Taraboletti et al., 2017). Outros estudos indicam que durante a administração de cuprizona, há diminuição nos níveis de glutationa e consequentemente aumento no estresse oxidativo em OLs (Biancotti et al., 2008). Além disso, durante o uso da cuprizona é observado estresse do retículo endoplasmático, o qual é caracterizado pela proliferação do retículo endoplasmático e redução da síntese de proteínas (Praet et al., 2014). Desta forma, a depleção de energia, a indução de estresse oxidativo e de retículo endoplasmático afetam a viabilidade e proliferação de células em cultura, e consequentemente levam a uma falha no suporte metabólico da mielina (Benetti et al., 2010; Matsushima & Morell, 2001; Zendedel et al., 2013).

Ademais, um estudo demonstrou que a cuprizona pode se acumular intracelularmente, levando à morte de OLs da linhagem MO3.13 (Taraboletti et al., 2017). O estudo de Taraboletti et al. confirmou que há desregulação no metabolismo de NAD+ (dinucleotídeo de nicotinamida e adenina), na capacidade antioxidante da célula e no metabolismo da vitamina B6, em culturas celulares tratadas com cuprizona. Além disso, foi demonstrado que a cuprizona tem a capacidade de reduzir os níveis de MBP e CNP (*2,'3'-cyclic-nucleotide-3'-phosphodiesterase*) em OLs (Xu et al., 2014). Considerando que uma das hipóteses para a toxicidade da cuprizona envolve alterações na geração de energia, e que o metabolismo de NAD+ encontra-se desregulado em células tratadas com essa droga, é

possível que a desregulação do metabolismo NAD+ contribua para a inibição da glicólise aeróbia e para depleção de energia, afetando os OLs maduros.

O modelo de desmielinização induzido por cuprizona é utilizado para compreender os mecanismos de desmielinização e remielinização, auxiliando potencialmente na identificação de novos alvos terapêuticos que possam melhorar a regeneração da mielina em certas doenças (Sachs et al., 2014). A remielinização *in vivo* se assemelha a um processo fisiológico de alta complexidade e regulação, seguindo quatro etapas consecutivas: a proliferação de células progenitoras de OLs, migração das células progenitoras para os axônios desmielinizados, diferenciação das OPCs e interação do OLs prematuro com o axônio (Zendedel et al., 2013). Neste contexto, diversas drogas são empregadas nos modelos de desmielinização com a finalidade de investigar seu potencial efeito na mielinização e nos OLs. Por outro lado, no modelo tóxico induzido por cuprizona *in vitro* é possível avaliar os mecanismos de diversas drogas em OLs em diferentes estágios de desenvolvimento, quanto aos seus potenciais efeitos em prevenir ou atenuar eventos relacionados às anormalidades induzidas nos OLs pela cuprizona e suas implicações para a mielinização.

1.2.2 Drogas potencialmente protetoras

1.2.2.1 Antipsicóticos

Estudos demonstram que a administração de antipsicóticos podem afetar de maneira distinta a expressão da mielina em adultos com esquizofrenia (Bartzokis et al. 2007; Bartzokis et al. 2009). Já em modelo de primatas foi demonstrado que a administração crônica de antipsicóticos de primeira ou segunda geração promovem aumento na densidade glial no córtex pré-frontal (Selemon et al., 1999). Desta forma, estes estudos suportam a hipótese de que administração desses fármacos pode aumentar a mielinização intracortical.

A utilização de haloperidol em modelo *in vivo* induz a mudança da expressão de genes relacionados a mielina e aos OLs, como MBP, PLP (proteína proteolipídica de mielina) e MAG (glicoproteína associada à mielina) (Narayan et al., 2007; Sugai et al., 2004). Já em cultura celular, há indícios que administração do haloperidol promove o aumento na proliferação e inibi a diferenciação de OPCs de rato, porém exerce efeito protetor em OLs contra a privação energética (Niu et al., 2010; Steiner et al., 2011). Por outro lado, diversos antipsicóticos de segunda geração são capazes de reduzir os níveis de espécies reativas de

oxigênio (ROS) e aumentar os níveis de glutationa e superóxido dismutase, levando a proteção contra a apoptose e à danos contra a mielina e OLs (Hendouei et al., 2018; Kriisa et al., 2016; Yan et al., 2014). Além disso, a quetiapina e a clozapina inibem efeitos induzidos pela cuprizona, a qual afeta diretamente a maturação e a diferenciação de OPCs *in vitro* (Xu et al., 2014). Já em modelo *in vivo* de cuprizona, a administração de quetiapina e clozapina induz a regeneração de OLs e o reparo da mielina após os eventos de desmielinização (Templeton et al., 2019; Zhang et al., 2012). Desta forma, diversos estudos indicam os potenciais efeitos dos antipsicóticos em induzir proteção contra danos na mielina e nos OLs. No entanto, diversas classes de drogas vêm sendo estudadas devido aos seus possíveis efeitos protetores, como por exemplo os canabinoides e a benzatropina.

1.2.2.2 Canabinoides

O interesse na modulação do sistema endocanabinoide aumentou desde a descoberta de compostos derivados da *Cannabis sativa.* O sistema endocanabinoide é composto por endocanabinoides (anandamida e 2-araquidonilglicerol), receptores de canabinoides do tipo 1 e tipo 2 (CB1 e CB2) e enzimas que são responsáveis pela síntese e degradação dos endocanabinoides (Khoury et al., 2019). Sendo assim, os endocanabinoides são importantes neuromoduladores responsáveis por controlar diversas funções no SNC (Lu & Mackie, 2016). Devido às propriedades lipofílicas dos endocanabinoides sua síntese ocorre nos neurônios pós-sinápticos, uma vez lançados por estes neurônios ligam-se a receptores dos neurônios pré-sinápticos do tipo canabinoides CB1 e CB2 ou não canabinoides, como os receptores GPR55 (*G protein-coupled receptor 55*), PPARs (*peroxisome proliferator activated nuclear receptors*) e TRPV1 (*transient receptor potential vanilloid-1 channel*) (Nevalainen & Irving, 2010; O'sullivan, 2016; Seabra et al., 2018; Zygmunt et al., 1999).

Embora os endocanabinoides anandamida (AEA, *N-arachidonoyl ethanolamine*) e 2-araquidonilglicerol (2-AG) tenham diferença significativa na seletividade dos receptores, ambos são produzidos em resposta ao aumento da concentração de Ca^{2+}no meio intracelular (Castillo et al., 2012). Resumidamente, a AEA é catalisada a partir de N-acil-fosfatidiletanolamina (NAPE) pela fosfolipase-D-específica de NAPE (NAPE-PLD) e a 2-AG é produzido de diacilglicerol (DAG) pela DAG lipase (DAGL) α ou β (Murataeva et al., 2014; Zou & Kumar, 2018). Nos neurônios a AEA é hidrolisada pela enzima amida hidrolase de ácidos graxos (FAAH) ou pela enzima N-acetil-etanolamina-hidrólise ácida amidase (NAAA), produzindo etanolamina e ácido araquidônico (Cravatt et al., 1996; Tsuboi et al.,

2005). Por outro lado, a 2-AG é degradada pelas lipases monoacilglicerol (MAGL) ou pelas serinas hidrolases α, β-hidrolase domínios proteínas 6 e 12 (ABHD6 e ABHD12) em glicerol e ácido araquidônico (figura 1) (Blankman et al., 2007). Estudos indicam que há uma comunicação mediada por endocanabinoides entre os neurônios e as células da glia, as quais também expressam receptores canabinoides e sintetizam endocanabinoides (de Almeida & Martins-de-Souza, 2018; Lyasov et al., 2018; Scheller & Kirchhof, 2016; Stella, 2009).

Diversos dados têm reforçado a participação do sistema endocanabinoide na fisiopatologia da esquizofrenia (Khoury et al., 2019). Neste contexto, diversos estudos têm indicado que pacientes com esse distúrbio apresentam níveis elevados de AEA (Potvin et al., 2020) e modificações nas expressões de receptores de canabinoides em diversas regiões cerebrais, como o diminuição da expressão receptor CB1 no córtex pré-frontal (Eggan et al., 2008; Muguruza et al., 2019) e diminuição da expressão do receptor CB2 periférico (Bioque et al., 2013). Recentemente foi demonstrado que os receptores CB2 podem estar relacionados com a cognição, psicose e comportamentos relacionados ao humor (ansiedade e depressão), os quais se manifestam em pacientes com esquizofrenia (Banaszkiewicz et al., 2020). Além dos citados acima, estudos indicam que a 2-AG e o bloqueio da enzima MALG estão relacionados com mecanismo de neuroproteção, devido aos seus efeitos anti-inflamatórios e pela redução da citotoxicidade em OLs e da desmielinização (Bernal-Chico et al., 2015; Chen et al., 2012; Panikashvili et al., 2001). Sendo assim, a modulação do sistema endocanabinoide pode ser um novo e promissor alvo farmacológico para tal distúrbio (Rohleder et al., 2016).

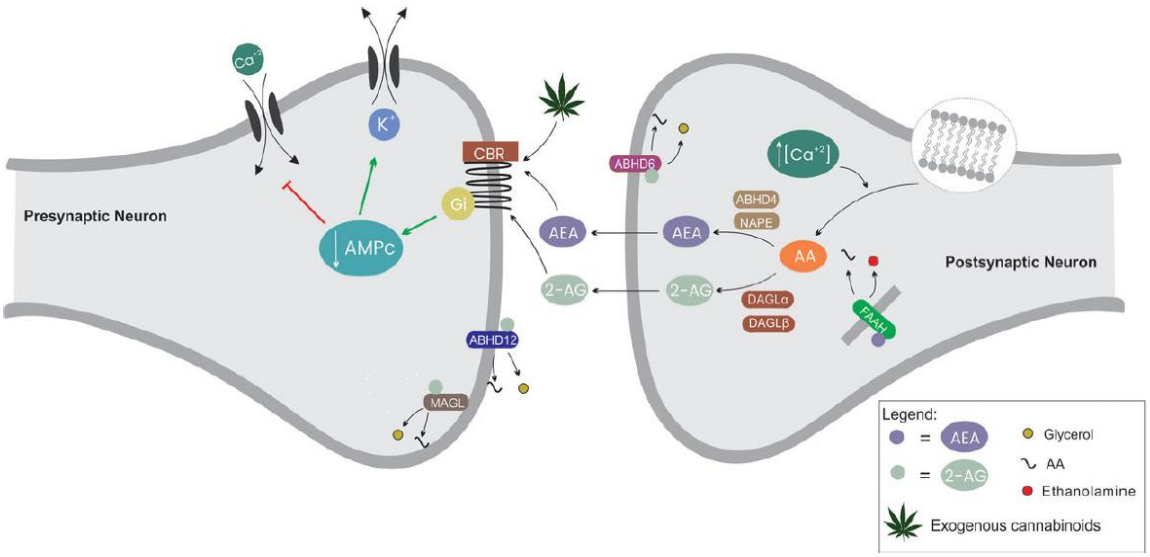

Figura 1. Representação do sistema endocanabinoide, adaptado de Seabra et al., 2018.

Os canabinoides surgiram como uma nova classe de drogas com potenciais efeitos sobre diversos distúrbios neurológicos e psiquiátricos. Já foram identificados mais de 70 canabinoides oriundos da planta *Cannabis sativa*, porém o Δ-9-tetrahidrocanabinol (THC) e o canabidiol (CBD) são os canabinoides mais abundantes (Khoury et al., 2019; Zajicek & Apostu, 2011). Diferente do THC, o CBD não desencadeia efeito psicomimético e ansiogênico (Campos et al., 2017; Khoury et al., 2019), exibindo, em contrapartida, um amplo espectro terapêutico, com propriedades ansiolíticas, antidepressivas e efeito neuroprotetor em uma gama de distúrbios psiquiátricos e neurodegenerativos. Sendo assim, diversos estudos clínicos têm apoiado a utilização do CBD em alguns transtornos, como na ansiedade, esquizofrenia, epilepsia e esclerose múltipla (Campos et al., 2017). Dessa forma, o efeito antipsicótico do CBD vem sendo investigado em diversos modelos de estudo (Rohleder et al., 2016). Estudos relatam que a administração de CBD contribui para a diminuição dos sintomas psicóticos em pacientes com esquizofrenia que não utilizaram antipsicóticos no período de três dias (Leweke et al., 2012). Também foi demonstrado que a administração de CBD em pacientes que respondem de modo parcial a medicação antipsicótica uma diminuição nos sintomas positivos e melhora no desempenho cognitivo (McGuire et al., 2018).

Além dos efeitos sobre o alívio dos sintomas, os canabinoides apresentam efeitos neuroprotetores (de Almeida & Martins-de-Souza, 2018; Zajicek & Apostu, 2011), possivelmente relacionados à efeitos anti-glutamatérgicos, bloqueio dos canais de cálcio, propriedades antioxidantes e ação anti-inflamatória (De Lago et al., 2009). Estudos demonstraram que tais componentes podem alterar a mielinização de células do SNC, e este efeito pode ser via receptores CB1 nos OLs (Tomas-Roig et al., 2016; Rodgers et al., 2013). Em modelo *in vivo* de esclerose múltipla, o CBD pode reduzir a apoptose dos OLs, os danos axonais, as respostas inflamatórias e aumentar a remielinização (Rahimi et al., 2015; Zajicek & Apostu, 2011). Já em modelo *in vitro* foi demonstrado que o CBD apresenta efeito protetor em OPCs contra o estresse oxidativo, pela diminuição de ROS, além de promover proteção contra o estresse de retículo endoplasmático (Mecha et al., 2012). Desta forma, o potencial efeito neuroprotetor do CBD é uma ferramenta farmacológica promissora para o tratamento dos OLs e melina acometidos na esquizofrenia e em outras desordens neurodegenerativas.

1.2.2.3 Benzatropina

Além das citadas acima, outras drogas apresentam efeitos protetores para a mielina. A benzatropina, por exemplo, é um antagonista de receptores muscarínico M1 e M3 e um agente anticolinérgico utilizado no tratamento da doença de Parkinson (Deshmukh et al., 2013; Kremer et al., 2015). Os receptores muscarínicos vem sendo propostos como um novo alvo terapêutico para a esquizofrenia, pois a ativação simultânea dos receptores de glutamato e muscarínicos têm a capacidade de reverter alterações relacionados a esquizofrenia em modelo animal (Cieślik et al., 2018).

Por outro lado, estudos indicam o potencial terapêutico desta droga na esclerose múltipla, devido a sua capacidade de promover a mielinização (Deshmukh et al., 2013; Kremer et al., 2015). Em modelo de desmielinização induzido por cuprizona, a benzatropina contribui para o aumento da remielinização e diminui a porcentagem de desmielinização na substância branca em modelo de encefalomielite autoimune experimental (EAE) (Deshmukh et al., 2013; Thompson et al., 2018). Já em modelo de α-sinucleína foi demonstrado que a benzatropina é capaz de reajustar processos relacionados a mielinização, como a biogênese de membrana e colesterol em OLs acometidos nesse modelo (Ettle et al., 2016). Em modelo *in vitro*, esta droga induz a diferenciação de OPCs de ratos e promove mielinização em co-cultura (Deshmukh et al., 2013), além de exercer efeitos antioxidantes em células neuronais, por meio do aumento de glutationa e pela redução de ROS (Cerles et al., 2019). Sendo assim, nos últimos anos diversos estudos vêm avaliando os efeitos protetores de diversos fármacos e seus potenciais efeitos terapêuticos. Diversas técnicas são utilizadas para a compreensão dos processos envolvidos em diferentes distúrbios neurológicos, como no caso da proteômica, uma tecnologia de suma importância para a avaliação de certas drogas nas células do SNC, assim como na identificação e compreensão de proteínas, vias e bases bioquímicas apresentadas em certos transtornos (Nascimento & Martins-de-Souza, 2015).

1.3 Proteômica

A grande complexidade do SNC vem sendo investigada pelas tecnologias denominadas de "ômicas" (Hosp & Mann, 2017). Neste contexto, a proteômica é uma importante ferramenta para a compreensão da base bioquímica de certos distúrbios cerebrais por meio da identificação de proteínas diferencialmente expressas, tanto no tecido cerebral,

quanto em modelos celulares. Através de metodologias proteômicas, também é possível identificar potenciais biomarcadores, auxiliando no melhoramento do diagnóstico e na escolha de um tratamento adequado (Nascimento & Martins-de-Souza, 2015). Sendo assim, ferramentas proteômicas como a espectrometria de massas (MS, *mass spectrometry*), podem ser utilizadas para elucidar os efeitos de drogas nas células do SNC, desvendando os caminhos de sinalização em distúrbios neurológicos.

Assim, através do uso de metodologias proteômicas, é possível investigar, de maneira quantitativa, a expressão global de proteínas ou grupos de proteínas (e suas modificações pós-traducionais), em um dado momento e local, visto que esses grupos podem mudar para cada tipo de célula e situação fisiológica. Ademais, constitui uma técnica de alto rendimento que fornece um perfil funcional do estado fisiológico atual, reflexo da complexa interação do gene com o ambiente. A importância dessas interações tem aumentado na pesquisa da esquizofrenia e outras doenças neurológicas (Nascimento & Martins-de-Souza, 2015).

1.3.1 Espectrometria de massas

Uma das primeiras ferramentas utilizadas em proteômica foi a eletroforese bidimensional (2D-PAGE), a fim de separar as proteínas de acordo com seu ponto isoelétrico por isoeletrofocalização e por sua massa através da migração em gel SDS-PAGE (Oliveira et al., 2014). A técnica de MS foi inserida combinada com 2D-PAGE para a identificação sistemática de polipeptídeos (Oliveira et al., 2014). A MS é uma técnica analítica utilizada para os estudos de proteínas e de outras biomoléculas na qual a razão massa molecular / carga (m/z) de moléculas ionizadas é mensurada, capaz de determinar a presença de proteínas, seus níveis e suas características estruturais, como sequências de aminoácidos e modificações pós-traducionais (Di Girolamo et al., 2013). Os espectrômetros de massas são compostos em três partes: uma fonte de ionização, um analisador de massas e um detector. A fonte de íons gera íons transferindo moléculas da fase condensada (líquida ou sólida) para a fase gasosa, ionizando as moléculas neste processo (carga positiva ou negativa) (Matthiesen & Bunkenborg, 2013). Os métodos mais comuns de ionização na proteômica são ionização por *electrospray* (ESI, *electrospray ionization*) e ionização dessorção a laser auxiliada por matriz (MALDI, *matrix-assisted laser desorption and ionization*) (Fenn et al., 1989; Karas & Hillenkamp, 1988). Após este processo de ionização, os íons são transferidos para o analisador de massas onde são separados de acordo com a razão m/z e finalmente detectados

por um detector (Domon & Aebersold, 2006; Matthiesen & Bunkenborg, 2013). Os espectrômetros mais novos também são capazes de separar íons através da sua mobilidade iônica, relativa à sua área transversal (Kanu et al., 2008).

A proteômica baseada em espectrometria de massas tem como objetivo identificar e quantificar proteínas e suas modificações pós-traducionais. Para fins de identificação essa técnica pode ser dividida em duas abordagens denominadas como *top-down* e *bottom-up* (ou *shotgun*) (Chait, 2006; Kelleher, 2004; Washburn et al., 2001). Na proteômica por *top-down*, as proteínas e os polipeptídeos intactos são submetidos às análises de MS/MS, a fim de identificar dados relacionados com a degradação de proteínas, isoformas e co-presença de modificações pós-traducionais (Padula et al., 2017). Já a proteômica por *bottom-up* utiliza uma mistura complexa de proteínas que são digeridas em peptídeos, normalmente por tripsina que cliva a sequência onde há resíduos de lisina e arginina, seguida de cromatografia líquida de alto desempenho acoplado ao espectrômetro de massas (Matthiesen & Bunkenborg, 2013). Na cromatografia líquida acoplada à espectrometria de massas (LC-MS), uma série de espectros de MS são adquiridos à medida que as moléculas eluem e por meio de um analisador de massas são gerados espectros MS/MS, onde as identidades de peptídeos podem ser calculadas por meio das razões m/z das transições dos peptídeos, as quais oferecem dados das sequências dos peptídeos. Por fim, a identificação de peptídeos é realizada por *softwares* de processamento de dados que utilizam espectros teóricos, produzidos a partir de bancos de dados de proteínas, a fim de comparar com os dados experimentais determinando as proteínas presentes com base nas sequências de peptídeos. Ao final, é gerada uma lista de proteínas identificadas e quantificadas que serão utilizadas para as análises *in sílico.*

1.3.1.1 Técnicas de ionização

A formação de íons na fase gasosa é de extrema importância antes da mensuração de uma amostra por um analisador de massas. O avanço da espectrometria de massas de proteínas e peptídeos veio com a introdução de fontes de ionização por ESI e MALDI (Fenn et al., 1989; Karas & Hillenkamp, 1988). MALDI é um tipo de ionização por irradiação pulsada a laser, onde as amostras são misturadas a uma matriz que auxilia na sua ionização, por meio da transferência de energia da matriz energizada ao analito (Dass, 2007). Na técnica de ESI os analitos são dissolvidos em um solvente aquoso e bombeados para um capilar, onde existe um campo elétrico que acarreta na dispersão das amostras em aerossol e as ioniza,

por fim as moléculas carregadas repelem uma das outras até que ocorra um colapso na gota e a expulsão das moléculas em forma de íons (Dass, 2007).

1.3.1.2 Analisadores de massa

Atualmente na proteômica baseada em espectrometria de massas são utilizados cinco tipos de analisadores de massas, como quadrupolo (Q, *quadrupole mass filters*), TOF (*time of flight mass analyzers*), IT (*ion traps*), FT-ICR (*Fourier transform ion cyclotron resonance)* e Orbitrap. Nos analisadores de massa TOF, a relação m/z de um íon analítico é deduzida através do seu tempo de "vôo" no vácuo através de um tubo de comprimento conhecido (Andrews et al., 2011). Por outro lado, no analisador de quadrupolo os íons são separados de acordo com a sua m/z por meio de sua trajetória em campos elétricos oscilantes. Sendo assim, analisadores de massa Q-TOF são frequentemente constituídos por analisadores de massa quadrupolo (Q) seguidos de um analisador de massas TOF de alta resolução. Normalmente o Q é usado como guia de íons e para o resfriamento colisional dos íons que entram no instrumento, e em uma câmara de colisão realiza-se a fragmentação dos peptídeos e o TOF separa os íons de acordo com os valores de m/z (Domon & Aebersold, 2006; Matthiesen & Bunkenborg, 2013).

Ao final desses processos, o detector do espectrômetro de massas identifica e amplifica o sinal dos íons obtidos, convertendo os feixes de íons em sinais elétricos, sendo armazenados em espectros de massas, os quais podem ser analisados em programas computacionais como, MASCOT®, PLGS®, Sequest® e Progenesis®.

1.3.2 Synapt G2-Si

O espectrômetro utilizado para esse projeto de mestrado foi o Synapt G2-Si HDMS (Waters Corp, Milford, EUA). Este equipamento é equipado por uma fonte de ionização do tipo ESI e um aparelho do tipo Q-TOF, apresentando um quadrupolo e TOF como analisadores de massas, além de apresentar uma cela para a separação por mobilidade iônica (IMS) de alta eficiência (TriWave) subdividida em três câmaras: trap, câmara de mobilidade e transfer (figura 2). Primeiramente os íons são aprisionados no trap e injetados em períodos regulares na cela de mobilidade iônica, a qual irá separá-los em função *drift-time*, enquanto o transfer conduz os íons para o analisador TOF.

Com esse equipamento é possível fazer análises do tipo aquisição independente de dados (DIA, *data-independent acquisition*), envolvendo a fragmentação de peptídeos seguida da análise de sua composição de aminoácidos. O processo de fragmentação mais utilizado no MSe é a técnica de dissociação induzida por colisão (CID, *Collision Induced Dissociation*), a qual seleciona peptídeos em um quadrupolo e os acelera em uma região do espectrômetro de massas com um gás inerte (hélio, argônio ou nitrogênio) que acarreta na colisão entre os íons e as moléculas desse gás, transferindo a energia dessa colisão para as ligações presentes nos íons (Levin, 2011). Desta forma, o ciclo de aquisições de MS e MS/MS é adquirida ao longo da execução, os dados gerados m/z e o tempo de retenção para os íons precursores e fragmentos são extraídos para a identificação dos peptídeos e proteínas.

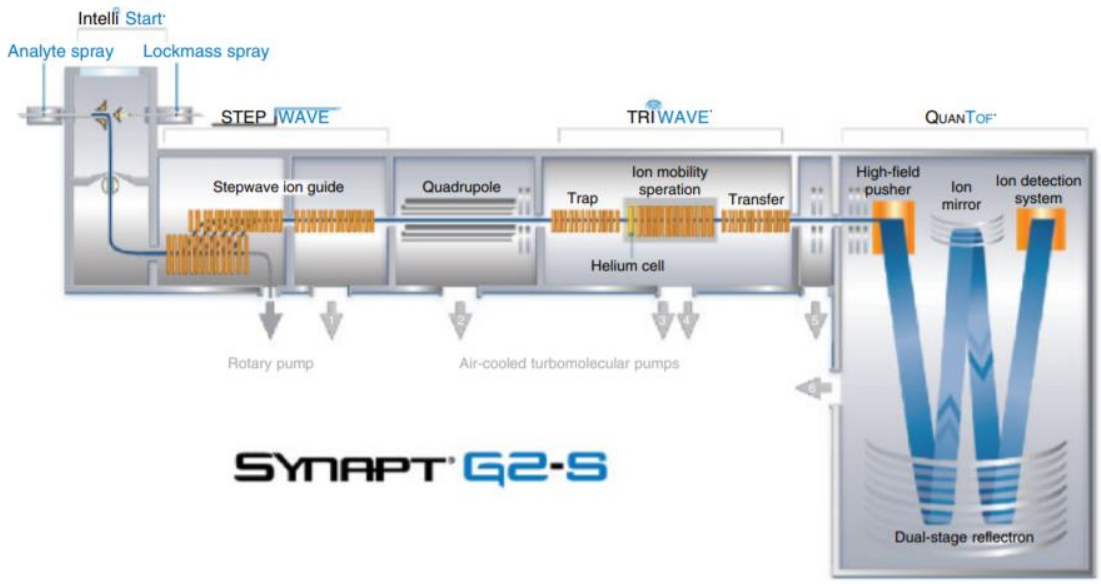

Figura 2. Esquema dos principais componentes do *Synapt* G2-Si HDMS, incluindo analisadores de massas e a cela de mobilidade iônica (trap, câmara de mobilidade e transfer), adaptado de *Waters Corporation*.

2. JUSTIFICATIVA

A esquizofrenia é uma desordem mental que afeta milhões de pessoas globalmente, privando os pacientes de uma vida normal. Diversos estudos, baseados em metodologias, incluindo a proteômica, apontam para anormalidades nos OLs e perda da mielina como fatores importantes na fisiopatologia da esquizofrenia. Neste contexto, modelos toxicológicos de desmielinização, como o induzido por cuprizona, são utilizados para compreender os mecanismos de desmielinização e remielinização, além de levar à identificação de novos alvos terapêuticos que auxiliam na regeneração da mielina em diversos distúrbios (Sachs et al., 2014). O modelo em questão pode ser aplicado tanto *in vitro*, quanto *in vivo* (Zendedel et al., 2013), contribuindo para o *cross-talk* de achados obtidos a partir de diversos estudos. Neste processo é especialmente importante utilizar culturas de OPCs, células neurais indiferenciadas e OLs em um estágio mais avançado de maturação, tanto para avaliar diferenciação, quanto efeitos inflamatórios, testar novos compostos químicos com potencial terapêutico, bem como desenvolver estratégias que ajudem a melhorar a remielinização (Torre-Fuentes et al., 2020). Ferramentas proteômicas, por sua vez, podem auxiliar na compreensão dos processos envolvidos no distúrbio neurológico citado acima, favorecendo a elucidação de bases bioquímicas, e identificação de proteínas e vias diferencialmente expressas, tanto nos distúrbios, quanto em seus tratamentos. Sendo assim, esta dissertação visou estudar os efeitos dos principais representantes de antipsicóticos (haloperidol e clozapina) e do CBD sobre os OLs MO3.13, por meio da utilização do modelo tóxico induzido por cuprizona. Como controle, investigamos também os efeitos da benzatropina, conhecidamente protetora para estas células e indutora de mielinização em modelo *in vivo* e *in vitro*. Com isso, foram identificadas as proteínas e os processos biológicos afetados pelo tratamento com essas drogas. Consequentemente, o presente estudo contribuirá para o entendimento dos mecanismos bioquímicos e moleculares envolvidos na ação dessas drogas sobre os OLs.

3. OBJETIVOS

A presente dissertação teve como objetivo investigar os efeitos da benzatropina, molécula indutora de mielinização e de diferenciação de OLs, e de drogas potencialmente protetoras, como os antipsicóticos (clozapina e haloperidol) e do canabidiol, sobre as alterações proteômicas induzidas pela cuprizona na linhagem celular de OLs humanos MO3.13. Desta forma, por meio da nano-cromatografia líquida acoplada à espectrometria de massas (*shotgun proteomics*) foram identificadas as proteínas e vias bioquímicas afetadas pelo tratamento com as drogas citadas anteriormente. No decorrer do projeto, foram delimitados os seguintes objetivos específicos:

- Cultivar a linhagem celular OLs humanos MO3.13;
- Estabelecer modelo de citoxicidade induzida por cuprizona para esta linhagem;
- Realizar os co-tratamentos de tais células com cuprizona e canabidiol (componente da *C. sativa*), clozapina (antipsicótico de primeira geração), haloperidol (antipsicótico de segunda geração) ou benzatropina;
- Extrair as proteínas das células tratadas e realizar a digestão do proteoma;
- Realizar análise proteômica por meio de nano-cromatografia acoplada à espectrometria de massas;
- Processar os dados e realizar análise de biologia de sistemas *in sílico* dos dados obtidos.

Ao cumprir os objetivos propostos pretendemos colaborar com a hipótese que os antipsicóticos e o CBD podem ser potenciais drogas protetoras, como a benzatropina, e ter a capacidade de prevenir ou atenuar eventos relacionados às anormalidades induzidas nos OLs pela cuprizona. Assim, contribuímos para entendimento de aspectos moleculares envolvidos nas ações destas drogas e seus potenciais efeitos protetores contra à danos gerados em OLs.

4. MATERIAIS E MÉTODOS

4.1 Cultura celular e tratamento

A linhagem de OLs humanos (MO3.13) é um híbrido que expressa características fenotípicas de OLs imaturos (Buntix et al., 2003; Iwata et al., 2013). Esta célula já tem sido utilizada em nosso laboratório e em estudos como modelo *in vitro* para compreender mecanismos relacionados à esquizofrenia (Brandão-Teles et al., 2019; Cassoli et al., 2016; Seabra et al., 2020). Os OLs foram cultivados em meio DMEM (Sigma-Aldrich), suplementado com 10% (v/v) de soro fetal bovino (Gibco), 1% de penicilina (100 U/ml) e estreptomicina (100 μg/mL) (Gibco), e mantidas em incubadora a 37°C em 5% CO_2, com renovação a cada dois dias, como descrito por nosso grupo anteriormente (Brandão-Teles et al., 2017; Iwata et al., 2013). As células foram utilizadas em diferentes passagens, e propagadas sem perder suas características iniciais, conforme as recomendações do fabricante. Para os ensaios de viabilidade celular, as células foram cultivadas na densidade 7.000 células/poço em placas de 96 poços (item 4.2) e nos ensaios de proteômica as células foram cultivadas na densidade de 115.000 células/poço em placas de 6 poços (item 4.3).

As soluções estoques de cuprizona (28,05mM; Sigma), haloperidol (53mM; Cristália), clozapina (25mM; Cristália) e canabidiol (25mM; USP Ribeirão Preto) foram preparadas por meio da solubilização em DMSO, com a concentração máxima de 0,042% de DMSO no meio de cultura. Já a benzatropina (6mM; Merck) foi dissolvida em ddH2O. Salina em DMSO (concentração final de 0,042% de DMSO) foram utilizadas como controle. Baseados nos resultados de MTT e em estudos anteriores, os OLs MO3.13 foram tratados com 10μM de cuprizona por 48 horas ou com 1μM de haloperidol, clozapina, canabidiol ou benzatropina por 24 horas. Para os co-tratamentos, primeiramente foi realizado o insulto com cuprizona por 48 horas, e nas 24 horas finais foram adicionados haloperidol, clozapina, canabidiol ou benzatropina no meio de cultura.

4.2 Ensaio de viabilidade celular (MTT)

Foi utilizado o método de viabilidade celular do MTT (tetrazólio) como parâmetro quantitativo de viabilidade celular. Resumidamente, o ensaio de viabilidade celular pelo método colorimétrico de redução de sais de tetrazólio (MTT- brometo de 3-[4,5-dimetil-tiazol-2-il]-2,5-difeniltetrazólio, Millipore) baseia-se na habilidade de células viáveis que converterem o sal tetrazólio em cristais de formazan (coloração púrpura). Assim, a

quantidade de cristais de formazan formada se compara diretamente com o número de células metabolicamente ativas (Liu et al., 1997). Faltando 1 hora para o fim do tratamento, as células foram incubadas com MTT (0,5 mg/mL) em DMEM não suplementado à 37 ºC durante 2 horas. Após esse período de incubação, foram adicionados 100µL de etanol (100%) para diluição dos cristais de formazan e os valores de absorbância determinados no comprimento de onda de 570nm em um espectrofotômetro para placas. Para avaliação estatística os resultados foram expressos como média ± erro padrão da média (E.P.M.). Para comparação de três ou mais médias foi utilizada análise de variância (ANOVA de uma via), seguido do pós-teste de Dunnet. O nível de significância para rejeição da hipótese de nulidade foi fixado em 5% ($\alpha<0,05$).

4.3 Análise proteômica

4.3.1 Preparo de amostras

Para análise por espectrometria de massas, foram preparadas amostras proteicas de OLs MO3.13 tratados com 10µM de cuprizona por 48 horas, ou com 1µM de haloperidol, clozapina, canabidiol ou benzatropina; e co-tratados com 10µM de cuprizona por 48 horas e com 1µM de haloperidol, clozapina, canabidiol ou benzatropina nas últimas 24 horas do tratamento. Primeiramente as células foram coletadas com auxílio de *scraper* e PBS, (*phosphate-buffered saline*; concentração final 1x) e centrifugadas à 4°C e 14.000 g por 5 min. Logo em seguida, as amostras foram homogeneizadas em tampão de lise (Tris pH 6,8, 1 M; SDS 20%) junto com inibidor de protease (concentração final de 1x, Roche; Mannheim, Germany), sonicadas três vezes, aquecidas a 95°C por 5 minutos e aplicadas no gel de poliacrilamida. Após a corrida, os géis foram cortados e lavados com 50% acetonitrila (ACN) em 50mM de bicarbonato de amônio (Ambic) por 5 min até a remoção total do corante presente nos géis. Depois destes procedimentos foram adicionados 100µL de 10mM de dithiothreitol stock (15.4mg DTT em 10mL de 50mM de Ambic) e incubado por 30 minutos à 80°C. Ademais, as amostras foram incubadas com 100µL de 55mM de iodocetamida stock (102mg IAA em 10mL de 50mM de Ambic) por 20 minutos, lavadas duas vezes com 200µL de ACN 100% por 10 minutos e colocadas no *Speed Vac* por 50 minutos.

Para a digestão das proteínas foi adicionado tripsina (1:50 enzima/substrato–2%) (Sigma-Aldrich / Promega) nas amostras durante o período de 16-18 horas a 37ºC. Após este período, foram adicionados 50µL da solução Ambic 50mM, por 20 minutos, e o volume foi

transferido para um novo *eppendorf* já contendo 50µL da solução 50% ACN/5%AF (ácido fórmico). Nos tubos contendo os géis, foi adicionado 50µL da solução 50% ACN/5% AF por 20 minutos e então o conteúdo foi transferido para o tubo sem os géis. Depois dessas etapas, as amostras foram colocadas no *Speed Vac* até a secagem, e então armazenadas a -80°C.

4.3.2 Análise dos peptídeos por nanoLC-ESI MS/MS

As amostras foram centrifugadas à 4°C e 14.000 g por 5 minutos, a fim de transferir o sobrenadante para tubos *low-binding* e ressuspender em formiato de amônio pH 10. Em seguida as amostras foram injetadas em um sistema nanoAcquity UPLC M-Class (Waters Corporation, Milford, MA) acoplado ao espectrômetro Synapt G2-Si (Waters Corporation, Milford, MA). Primeiramente, as amostras foram fracionadas em cinco frações por meio de etapas descontínuas de ACN (11.4, 14.7, 17.4, 20.7 e 50%) antes da separação com gradientes de ACN contínuo de 7% a 40% (v/v) em colunas de C18 de fase reversa. Os dados MS e MS/MS foram obtidos de maneira dado-independente (DIA) utilizando UDMS^{E} após estabelecer o perfil do método de separação iônica para cada fração, usando DriftScape (version 2.9).

Os espectros MS/MS foram analisados pelo Progenesis® QI para proteômica (version 3.1) com Apex3D, peptideo 3D, e ion accounting informatics (Waters). As proteínas foram identificadas usando o banco de dado humano revisado (obtido em 11/2019) e quantificados usando o método Top3. Os seguintes parâmetros foram utilizados para identificar os peptídeos/proteínas: Digestão por tripsina com no máximo uma clivagem perdida; Massa máxima de 600 kDa; FDR menor que 1%; Pelo menos 2 fragmentos por peptídeo; Dois ou mais peptídeos por proteínas; Pelo menos 5 fragmentos por proteína; Pelo menos um peptídeo único por proteína; Mass error $\leq$ 20ppm. Na lista final de proteínas, foram consideradas para análise *in sílico* aquelas que apresentarem pelo menos um peptídeo único e ANOVA<0,05.

4.3.3 Análise *in sílico*

As proteínas diferencialmente expressas por *shotgun* foram identificadas quanto aos seus processos biológicos e localizações celulares. Para compreender a rede de proteínas alteradas e sua importância para esquizofrenia, foram utilizados as seguintes ferramentas: Reactome (Fabregat et al., 2018), David bioinformatics database (Huang et al., 2009a; Huang et al., 2009b), Proteomaps (Liebermeister et al., 2014), Metascape (Zhou et al., 2019),

Cytoscape (Franz et al., 2016; Szklarczyk et al., 2017) e ClustVis (Metsalu & Vilo, 2015). Nesta etapa, foram considerados os *accessions* das proteínas diferencialmente reguladas, p-valor do teste anova ($p<0,05$) e log_2FC (fold change), considerando a razão entre tratamento e controle, ou co-tratamento e cuprizona. As etapas experimentais descritas até aqui estão representadas na figura 3.

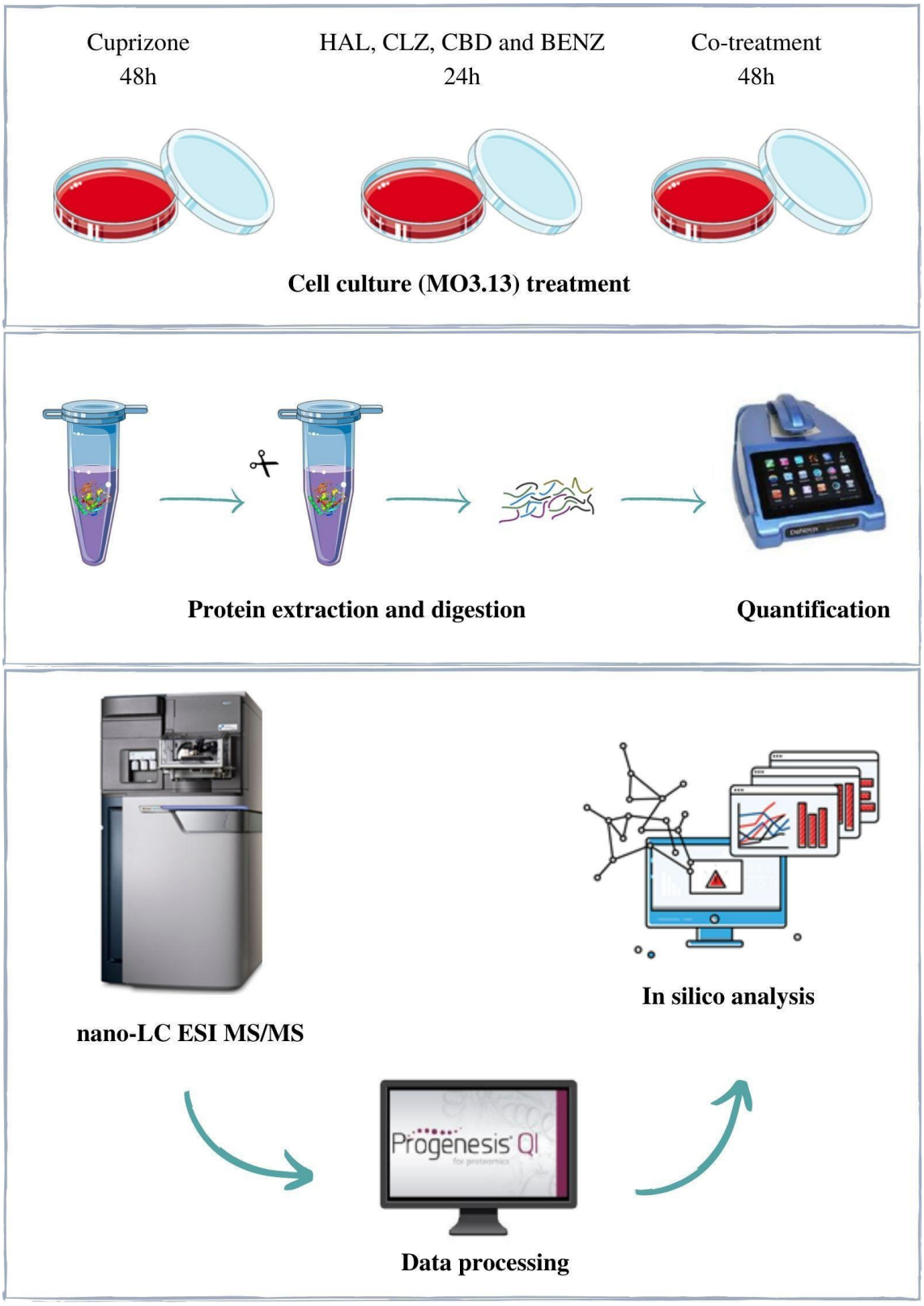

Figura 3. Representação das etapas experimentais, incluindo o tratamento e co-tratamento de OLs MO3.13 com cuprizona e/ou haloperidol (HAL), clozapina (CLZ), cannabidiol (CBD) e benzatropina (BENZ), seguido das etapas de extração e digestão das proteínas,

quantificação dos peptídeos, análise de espectrometria de massas, processamento de dados e análise *in sílico*.

5. CAPÍTULO I

Artigo de revisão publicado no periódico *Frontiers in Psychiatry* em 2020, doi: 10.3389/fpsyt.2020.00379.

NOVEL TREATMENT STRATEGIES TARGETING MYELIN AND OLIGODENDROCYTE DYSFUNCTION IN SCHIZOPHRENIA

Danielle Gouvêa-Junqueira[1], Ana Caroline Brambilla Falvella[1], André Saraiva Leão Marcelo Antunes[1], Gabriela Seabra[1], Caroline Brandão-Teles[1], Daniel Martins-de-Souza[1,2,3,4], Fernanda Crunfli[1,*]

1. Laboratory of Neuroproteomics, Department of Biochemistry and Tissue Biology, Institute of Biology, University of Campinas (UNICAMP), Campinas, Brazil

2. Experimental Medicine Research Cluster (EMRC), University of Campinas, Campinas, SP, Brazil

3. Instituto Nacional de Biomarcadores em Neuropsiquiatria (INBION) Conselho Nacional de Desenvolvimento Científico e Tecnológico, São Paulo, Brazil

4. D'Or Institute for Research and Education (IDOR), São Paulo, Brazil

*Correspondence:

Fernanda Crunfli

fernandacrunfli@gmail.com

REVIEW

published: 30 April 2020 doi: 10.3389/fpsyt.2020.00379

ABSTRACT

Oligodendrocytes are the glial cells responsible for the formation of the myelin sheath around axons. During neurodevelopment, oligodendrocytes undergo maturation and differentiation, and later remyelination in adulthood. Abnormalities in these processes have been associated with behavioral and cognitive dysfunctions and the development of various mental illnesses like schizophrenia. Several studies have implicated oligodendrocyte dysfunction and myelin abnormalities in the disorder, together with altered expression of myelin-related genes such as Olig2, CNP, and NRG1. However, the molecular mechanisms subjacent of these alterations remain elusive. Schizophrenia is a severe, chronic psychiatric disorder affecting more than 23 million individuals worldwide and its symptoms usually appear at the beginning of adulthood. Currently, the major therapeutic strategy for schizophrenia relies on the use of antipsychotics. Despite their widespread use, the effects of antipsychotics on glial cells, especially oligodendrocytes, remain unclear. Thus, in this review we highlight the current knowledge regarding oligodendrocyte dysfunction in schizophrenia, compiling data from (epi)genetic studies and up-to-date models to investigate the role of oligodendrocytes in the disorder. In addition, we examined potential targets currently investigated for the improvement of schizophrenia symptoms. Research in this area has been investigating potential beneficial compounds, including the D-amino acids D-aspartate and D-serine, that act as NMDA receptor agonists, modulating the glutamatergic signaling; the antioxidant N-acetylcysteine, a precursor in the synthesis of glutathione, protecting against the redox imbalance; as well as lithium, an inhibitor of glycogen synthase kinase 3b (GSK3b) signaling, contributing to oligodendrocyte survival and functioning. In conclusion, there is strong evidence linking oligodendrocyte dysfunction to the development of schizophrenia. Hence, a better understanding of oligodendrocyte differentiation, as well as the effects of antipsychotic medication in these cells, could have potential implications for understanding the development of schizophrenia and finding new targets for drug development.

Keywords: schizophrenia, oligodendrocyte, myelin, antipsychotic, glutamate

INTRODUCTION

Oligodendrocytes (OLs) are the neuroglial cells responsible for myelin sheath formation in the central nervous system (CNS). The life cycle of these cells consists of a series of coordinated and highly regulated processes, including migration, proliferation, maturation, and myelination of oligodendroglial cells, leading to adequate brain connectivity (1). In fact, the importance of OL development and myelination in neuronal signaling is well established, as evidenced by several behavioral and cognitive functions (2). Moreover, decreased myelination and OL alterations have been seen in patients with schizophrenia (3), associated with cognitive dysfunction (4). Recently, some studies have also proposed that OLs are more vulnerable to energy metabolism dysfunctions, oxidative damage, and other brain injuries (5, 6), leading to the impaired white matter integrity and brain dysconnectivity observed in schizophrenia (7). Nevertheless, the molecular mechanisms underlying these alterations remain elusive.

Schizophrenia is considered a multifactorial psychiatric disorder that affects more than 23 million individuals worldwide. This disorder is characterized by positive symptoms (delusions and hallucinations), negative symptoms (impaired motivation and social withdrawal), and cognitive impairment. Moreover, environmental and genetic factors, as well as neurodevelopmental dysfunction, play a role in the pathogenesis of schizophrenia (8, 9). The pathophysiology of the disorder includes molecular abnormalities in the nervous, immune, metabolic, and endocrine systems. Several hypotheses have been proposed to describe the etiology of schizophrenia, among which are the well-known dopaminergic and glutamatergic ones.

The dopaminergic hypothesis was developed during the 1970s in association with the discovery of antipsychotics' action on the blockade of D2 dopaminergic receptors (10). Over time, compelling evidence of altered dopaminergic transmission, involving D1 and D2 receptors, was shown in different brain areas linked to the development of positive symptoms and cognitive impairment in schizophrenia (11).

As for the glutamatergic hypothesis, antagonists of N-methyl-D-aspartate (NMDA) receptors mimic alterations and worsen symptoms observed in patients with

schizophrenia such as impaired memory, hallucinations, delusions, and agitation (12,13). This led to the postulation of a glutamatergic hypofunction in the disorder (14). Moreover, altered expressions of NMDA receptors and enzymes involved in glutamate metabolism have been found in patients with schizophrenia (15, 16).

Although there is evidence pointing toward these two aforementioned hypotheses, several lines of evidence also suggest the involvement of white matter abnormalities and neural dysconnectivity in the pathogenesis of schizophrenia (7). For instance, brain imaging and postmortem studies have demonstrated alterations in the myelination of cortical areas and white matter tracts, as well as a reduced number of OLs in patients with schizophrenia (3, 17). During neurodevelopment, dynamic and timely regulated changes in gray/white matter ratios appear to be crucial for adequate brain function (18, 19). During these processes, myelination occurs alongside neuronal development and ensures the brain's functional synchrony. Schizophrenia has been proposed to arise in part from faulty brain connectivity (20) and mounting evidence supports the notion of OL/myelination dysfunction as its underlying cause [reviewed in (21, 22)]. Despite the significant progress achieved in the comprehension of this multifactorial disorder in the past decades, the etiology of schizophrenia still remains unclear (23).

Currently, the main therapeutic strategy for the disorder relies on the use of antipsychotics. These medications mainly attenuate the positive symptoms, though atypical antipsychotics can induce slight improvements in cognitive and negative traits (24). Unfortunately, these same medications are also well known for their severe side effects, including metabolic syndrome and extrapyramidal effects, often leading to treatment discontinuation. In an attempt to change this situation, it is important to investigate the molecular mechanisms involved in antipsychotics' effects beyond neurons and the classical components of neurotransmission. OLs are one of the structures to be investigated to increase the understanding of the development of schizophrenia and find new targets for novel therapies.

In this review, we first describe the differentiation of OLs and myelination, followed by the pathways and signals involved in these processes. Secondly, we discuss how dysregulations in OL function may be linked with schizophrenia, as well as the main pathways and genes involved with OLs and this disorder. We also review current approaches being used to investigate the role of OL dysfunction in schizophrenia. Finally, we provide an

overview of the effects of antipsychotics on the proliferation and differentiation of OLs, and its potential for the discovery of novel therapeutic targets, suggesting new avenues for future research in the field.

OL DEVELOPMENT AND MYELINATION

The oligodendroglial cells are characterized as being cells that progressively mature from OL progenitor cells (OPCs) to myelinating cells through a series of coordinated and highly regulated programs of migration, proliferation, and differentiation, up to the point at which OLs become myelinating cells (1, 25). OPCs originate from neural stem cells (NSCs) that initially differentiate into neural progenitor cells (NPCs) in the subventricular zone (SVZ) (26). NPCs then give rise to OPCs, which migrate radially out of the SVZ to cortical and white matter areas (27, 28).

The maturation of OLs is controlled by transcription factors, and cell-extrinsic molecules, including small metabolic molecules, chemokines, growth factors, neurotransmitters, and hormones that act at defined time points during embryonic and postnatal development (29). Moreover, chromatin remodeling and epigenetic regulation, including methylation and histone modifications, are associated with OL development (30). During the initial stages of differentiation, histone deacetylation promotes chromatin compaction, ensuring that the transcription of non-OL genes is inhibited, followed by the induction of activators of OL cell fate (31, 32). In addition, DNA methylation plays a significant role in OPC expansion and regulates processes required for *de novo* myelination and remyelination, such as RNA splicing and protein synthesis (33, 34).

During maturation, cells committed to an OL lineage go through a series of specific phenotypic stages, including OPCs, pre-OLs, immature (or pre-myelinating) OLs and mature (or myelinating) OLs (1). These differentiation steps can be distinguished by migratory cell capacity, morphological complexity, and sequential expression of stage-specific markers in response to differentiation signals (1).

Initially, OPCs are proliferative cells that migrate and give rise to pre-OLs. These cells project multipolar processes and start to express OPC markers, such as O4, neuron-glial antigen 2 (NG2), A2B5, and OL lineage transcription factor 2 (Olig2) (35, 36). In turn, pre-

OLs differentiate into immature OLs, post-mitotic cells that present long ramified branches (36). Immature OLs begin to express 2′, 3′-cyclic-nucleotide-3-phosphodiesterase (CNP) (37) and galactocerebroside C (GalC) while maintaining O4 expression and losing expression of NG2 and A2B5 markers (38). Throughout differentiation, OLs lose their ability to migrate and proliferate, acquiring a more complex morphology (39). Mature OLs extend axon-wrapping membranes and express myelin-associated proteins, among which are proteolipid protein (PLP), myelin basic protein (MBP), myelin OL glycoprotein (MOG), and myelin-associated glycoprotein (MAG) (40, 41).

Structurally, the myelin sheath is a multilayered, tightly packed membrane wrapped around selected nerve axons. It consists mainly of lipids (70%–80% dry weight—cholesterol and ethanolamine plasmalogen are the most predominant) and proteins (∼20%–30% content) (42). The myelin sheath provides essential conditions for the conduction of saltatory nerve impulses, such as electrical resistance and reduced capacitance. Axonal myelination by OLs is a remarkable example of dynamic cell membrane specialization and remodeling, involving cytoskeletal rearrangements, along with cell–cell and cell–extracellular matrix interactions (43). Cytoplasmic compaction of the myelin lamellae provides the physical stability necessary for membrane wrapping, leading to cytoplasmic extrusion and adhesion of multiple layers of myelin (43). Therefore, during differentiation, the expression of negatively charged sialic acids by OLs is reduced, thereby decreasing electrostatic repulsion forces, which contributes to the adhesiveness and compaction of the myelin bilayer (44).

MBP and PLP are the two principal proteins present in compact myelin, increasing the adhesiveness of the myelin membrane, and contributing to myelin stability (44, 45). In contrast, CNP prevents myelin compaction through the rearrangement of the cytoskeleton (46). Thus, the interaction between MBP, PLP, and CNP is essential to avoid altered myelin compaction and to the maintenance of myelin stabilization (for review see (43)]. Besides those molecules, there are various biochemical pathways and signaling compounds released by other glial and neuronal cells that also contribute to the regulation of various stages of OPC differentiation and OL myelination, resulting in a complex and integrated network.

OL Development and Myelination: Signals and Pathways

In the brain, oligodendrogenesis and myelination require the activation of several signaling pathways, as well as transcription factors, noncoding RNAs, that act on the regulation of the different stages of OLs differentiation (47). Moreover, these processes are influenced by the interaction of astrocytes (48), microglia (49), and neurons with OLs and their precursors (50).

Regarding the role of glial cells in these interactions, astrocytes provide cholesterol precursors and nutrients for myelin sheath synthesis, in addition to chemokines and growth factors that influence OL survival, proliferation, migration, and maturation (48, 51). Similarly, microglia regulate oligodendrogenesis by releasing growth and attraction factors, including platelet-derived growth factor (PDGF), insulin-like growth factor-1 (IGF-1) (52), and hepatocyte growth factor (HGF) (53). Moreover, neurotrophic factors such as brain-derived neurotrophic factor (BDNF) and nerve growth factor (NGF) are known to guide axonal myelination (54, 55). Certain neurotransmitters and hormones can also stimulate oligodendroglial cells by mechanisms not yet completely understood (56).

Several pathways regulate OL differentiation and myelination in the CNS. The phosphatidylinositol-3-phosphate kinase (PI3K)/Akt/mTOR pathway, for example, regulates the initiation of myelination in the CNS through mTORC1 signaling (57). In conjunction, glycogen synthase kinase 3b (GSK3b) signaling regulates OL differentiation (58). Its inhibition induces OL proliferation and differentiation, as well as remyelination in mouse models of demyelination (58). Moreover, *in vivo* studies with mice overexpressing Akt also revealed an essential role of this pathway in inducing myelination rather than the proliferation of OLs (59).

Moreover, extracellular signal-regulated kinases-1 and -2 (ERK1/2), the downstream mediators of the mitogen-activated protein kinases (MAPKs) pathway, regulate myelin growth and maintain the integrity of myelinated axons (60). These MEK/ERK1/2-MAPK-mediated functions are largely independent of mTORC1 (61). Nonetheless, both pathways induce myelin sheath growth mediated by signaling responses involving mTORC1 (61). Therefore, PI3K/Akt/mTOR and MEK/ERK1/2-MAPK signaling pathways act both independently and in conjunction to temporally regulate OL differentiation and myelination (61). Disruptions in the finely tuned regulatory processes of OL development and myelination could result in white matter disturbances linked to the etiology of several mental

illnesses, including schizophrenia. These pathways are also associated with the treatment of this disorder, holding promising findings as potential targets for novel therapeutic strategies.

OLS AND MYELIN IMPAIRMENT IN SCHIZOPHRENIA

Disruptions during brain development caused by (epi)genetic and environmental factors can result in brain damage which could interfere in its ability to maintain normal communication across functional neural networks [for review see (62)]. Myelination is essential for adequate brain function and must occur alongside neuronal development and is only completed within the third decade of life. Disruptions in this process have been linked to the development of schizophrenia [for review see (63)].

The hypothesis that OLs play a major role in schizophrenia is corroborated by genome-wide expression analysis revealing altered expression of myelination-related genes in patients with schizophrenia and white matter pathologies that impair brain functional synchrony thereby resulting in schizophrenic symptoms (64–66).

In addition, structural changes have been reported in white matter tracts in the brains of patients with the disorder (67, 68). The anterior hippocampus plays an important role in the regulation of emotions and deficits in this area have been linked to schizophrenia. Studies have shown a decreased number of OLs in the hippocampus causing a disturbance in the neurocircuitry between the hippocampus and hypothalamus leading to cognitive deficits in patients with schizophrenia (69, 70). Furthermore, myelination deficits and dysfunctional synapses observed in the disorder can be correlated to the dysfunction of neuronal and glial function (71–73), along with cognitive impairment, including deficits in episodic and working memory (74) and in visual processing (75). Moreover, disruptions in OL integrity such as altered morphology and distribution (3), decreased density (76), and altered expression of myelination-related genes and proteins have been reported in patients with schizophrenia (71, 77, 78).

Epigenetics has also been suggested as an etiopathogenic factor for complex mental disorders, including schizophrenia (79). Aberrant epigenetic signatures, like hypermethylation, may be caused by well-known risk factors for schizophrenia during neurodevelopment such as drug abuse during pregnancy, in utero viral infections and hypoxia

(80, 81). Recent advances in sequencing technologies have allowed researchers to identify associations between schizophrenia and epigenetic modulations via DNA methylation and histone modifications (82–86). These have been shown to affect genes well-known for their role in OL lineage development (87), however, the majority of differential epigenetic signatures between OLs of control and schizophrenia brain samples have been found in non-coding regions (88).

Further insight into the pathology of schizophrenia and its connection with OL abnormalities has come from comparative proteomic analyses that reveal differentially expressed proteins and disturbances in biochemical pathways, including energy metabolism, oxidative stress and OL-related functions (78, 89). This is in line with an earlier brain imaging study that demonstrated decreased glucose metabolic rates in different thalamic nuclei in patients with schizophrenia (90). Nevertheless, schizophrenia pathophysiology also includes genetic factors. For this reason, several OL and myelin-related genes are being investigated in *postmortem*, *in vivo* and *in vitro* approaches to understand the contribution of genetic factors to OL development (73).

OL- and Myelin-Related Genes in Schizophrenia

Several (epi)genetic alterations, including risk variants and polymorphisms, have been demonstrated to play an important role in the etiology of schizophrenia (91, 92). Moreover, there are several promising candidate susceptibility genes associated with OL dysfunctions, such as Neuregulin 1 (NRG1)–ERBB4 signaling, Nogo-A/Nogo Receptor, Disrupted-in-schizophrenia 1 (DISC1), and other myelin-related genes (71, 93, 94). In an attempt to unravel the mechanisms involved with OL dysfunction in schizophrenia, OL- and myelin-related genes, as well as its regulatory signaling pathways are being investigated to understand how (epi)genetic and molecular changes lead to schizophrenia. Here we review the data available concerning those candidate myelin-related genes in the disorder.

NRG1–ERBB4 Signaling

NRG1 and its receptor ERBB4 are essential for neuronal, astroglial, and OL development, playing an important role in the survival and differentiation of these glial cells (95, 96). NRG1 is expressed at CNS synapses and activates neurotransmitter receptors, such

as the glutamatergic ones (94). This signaling pathway has been linked to schizophrenia as a potential genetic risk factor in genetic and *in vivo* studies (94, 97). NRG1 mutant mice have been shown to present altered behavior, including hyperactivity and a deficit in prepulse inhibition (PPI), which can be attenuated by treatment with the antipsychotic clozapine (CLZ) (98). The mice that were hypomorphic for NRG1 also had fewer functional NMDA receptors in the brain, a feature observed in schizophrenia patients (94). Moreover, NRG1 risk variants linked to schizophrenia have also been associated with reduced white matter density and integrity (99, 100). Regarding its functions in the CNS, the NRG1/ERBB4 signaling pathway operates in several aspects of neurodevelopment, including neural migration, gliogenesis, and modulation of neurotransmission [for review see (101)]. In addition, NRG1 is also involved with OL survival, migration, and myelination (96, 102, 103). Thus, the oligodendroglial association between this pathway and schizophrenia may be another potential alteration linking NRG1 to the development of the disorder (73).

Nogo-A and Nogo Receptor

The Nogo-A protein and its receptor (NGR) play an important role in the CNS through repairing processes, restricting axonal growth and plasticity (104, 105). This protein is extensively expressed in OLs, acting in the differentiation of these cells (106, 107). *In vivo*, mutant mice lacking Nogo-A exhibited impaired myelin synthesis and delayed differentiation (107). Moreover, Nogo-A knockout mice showed deficiencies in PPI and latent inhibition, as well as hyperactivity and other behavioral traits that resemble alterations observed in patients with schizophrenia (108). The induction of Nogo-A dysfunction in adult mice failed to reproduce the alterations observed in the mutant mice (108). Hence, Nogo-A dysfunction during neurodevelopment may affect neuronal and glial differentiation (107, 109). Altered expression and polymorphisms of the RTN4 (Reticulon 4) gene, which codes for Nogo-A, have been associated with psychiatric disorders like schizophrenia (110). Thus, alterations involving Nogo-A, NGR and other associated pathways, could contribute to some abnormalities observed in the disorder, such as abnormal neuronal organization and connectivity. Further research is needed to help underline the molecular mechanisms linking Nogo-A and NGR to the pathophysiology of schizophrenia [for review see (111)].

Disrupted-in-Schizophrenia 1

DISC1 is a gene disrupted by a chromosomal translocation that has been linked to psychiatric conditions, including schizophrenia, but its association with the disorder remains controversial (93, 112). Studies using *in vivo* models with mutant, truncated DISC1 observed altered OL differentiation and proliferation and alterations in OPC marker levels (113, 114). Investigation of altered gene expression profiles linked to DISC1 has found an association with altered levels of OL markers, such as CNP, MAG, and PLP (114), which contribute to altered white matter functioning and integrity (115). Moreover, postmortem studies have revealed an increased expression of DISC1 protein in OLs in frontal-parietal white matter region in paranoid schizophrenia (116). Thus, DISC1-related polymorphisms may contribute to neurodevelopmental alterations, as well as changes in white matter integrity, participating in the etiology of schizophrenia (115).

Olig2

Olig2 encodes for a transcription factor essential for several aspects of neurodevelopment, including oligodendrogenesis, the formation of motor neurons, and OL differentiation, especially in the early stages of OPC differentiation (117, 118). In postmortem studies, mRNA levels of Olig2 have been found reduced in patients with schizophrenia compared to healthy individuals (71, 119). Studies have described the expression of Olig genes in white matter and during remyelination in a demyelination model (120, 121). Other genes involved with myelination have been correlated with Olig2 expression, including ERBB4 and CNP, which may indicate potential shared pathways and interactions among these genes (122).

Other Myelin-Related Genes

Aside from the genes discussed above, there are other genes that have been found to be differentially expressed in patients with schizophrenia which are related to OLs. MAG, CNP, PLP1, and MBP were found reduced in mRNA samples from patients with schizophrenia in postmortem studies (71, 123). Genetic and neuroimaging data have shown that the MAG, Olig2, and CNP genes can influence white matter integrity and cognitive performance in schizophrenia patients (124). As previously mentioned, CNP is a marker for OLs during neurodevelopment and is also maintained in mature OLs (38, 125). It has been proposed that the inhibition of CNP in OLs can affect an essential glial trophic support mechanism of axons (126).

Another genetic study evaluated the mRNA expression of Quaking I (QKI), finding two splice variants to be downregulated in patients with schizophrenia (127, 128). QKI is an RNAbinding protein important for the development of glial cells and myelin synthesis (129). In an *in vivo* model, mutant mice (qkv) with a deletion in the 5′ regulatory region of the QKI gene presented severe demyelination, altered myelin structure, and reduced lipid content (130, 131). This gene is involved in the regulation of other genes essential for OL differentiation, such as PLP1, MAG, and MBP (132, 133).

Moreover, the Fasciculation and Elongation Protein Zeta-1 (FEZ1) is another myelin-related gene associated with risk for schizophrenia. FEZ1 is a gene involved with OL differentiation and it is known to interact with other schizophrenia-related genes, including DISC1 and QKI, mentioned above (134). FEZ1 has also been found reduced in the hippocampus of patients with schizophrenia and its expression has been associated with disrupted regulation of transcription factors and altered (epi) genetic regulation, including histone acetylation and chromatin remodeling (134, 135).

Changes in (epi)genetic regulation in myelin-related genes have been associated with impaired OL function and development (30). Inhibition of methylation reduces the number of OLs, evidencing the vulnerability of these glial cells to (epi) genetic alterations (136). Moreover, methylome analysis of different cell types isolated from brain tissue of patients with schizophrenia and controls revealed altered methylation associated with OLs (88). For instance, SOX10, a well-known marker of OL development has been shown to be hypermethylated in schizophrenia patients (87); this methylation status may be correlated to its downregulation and OL dysfunction in the disorder.

Therefore, the (epi)genetic components partially explain the etiology of schizophrenia and also support the notion that oligodendroglial abnormalities are among the primary deficits in the disorder (73). However, the individual and collective roles of all these genes remain unknown, making it still somewhat controversial in relation to schizophrenia. Environmental factors have also been associated with the etiology of the disorder, including complications during pregnancy and prenatal maternal infections (137, 138). These scenarios may lead to hypoxic damage and an inflammatory state, which have been linked to gray and white matter dysfunctions (139, 140).

Together, genetic susceptibility and certain environmental conditions may contribute to the development of (epi)genetic dysregulations. Hence, the investigation of the molecular mechanisms behind these different risk factors is essential for the comprehension of the etiology of schizophrenia. Data provided by brain imaging studies, genetic (71, 141) and postmortem studies (142, 143), in addition to animal models (94, 98) have been crucial to unravel these mechanisms as well as to understand the role of OL dysfunction in schizophrenia.

MODELS OF OL AND MYELIN-RELATED DISORDERS

To better understand the molecular changes in OLs and myelination dysfunctions, studies have used different *in vitro* and *in vivo* models to investigate abnormalities observed in OPCdifferentiation and myelination processes. Aiming to bring together the interactions between genetic and environmental factors, experiments using induced pluripotent stem cells (iPSCs) derived from patients with schizophrenia are being developed to generate OPCs and mature OLs. These tools can help us comprehend the association between OL abnormalities and the development of the disorder as well as aid in screenings for novel therapeutics (144, 145). In addition to iPSCs, mouse primary OPC cultures and oligodendroglial cell lines (MO3.13 and HOG) have also been used to understand the biological processes underlying OL differentiation into myelinating OLs (146–148).

Human-Induced Pluripotent Stem Cells-Derived OPCs

For neurobiological studies related to the CNS, patient-derived human iPSCs (hiPSCs) are able to be reprogrammed into neuronal and glial cell types, including OPCs and OLs, offering potential tools to elucidate the molecular and cellular mechanisms behind the etiology of schizophrenia (149). One of the main advantages of iPSCs is the conservation of the original genotype and endophenotype from schizophrenia patients (150, 151). Thus far, studies of psychiatric disorders using patient-derived iPSCs have focused on neuronal differentiation (152–154) and have demonstrated decreased neuronal connectivity, increased oxidative stress and mitochondrial dysfunction and, consequently, an impairment in NPC differentiation and neuronal maturation (151, 155).

Recently, studies have started looking toward OPCs derived from iPSCs in neurodegenerative and psychiatric diseases to understand specific aspects of the myelination process and to investigate how dysfunctional neuron–OL interactions manifest in schizophrenia (146, 156). However, currently available protocols for the differentiation of iPSCs into OPC are still very limited and are not able to induce differentiation into a mature myelinating OL. Wang et al. (2013) developed a protocol to produce myelinogenic OLs fromskin-derived hiPSCs and showed the potential therapeutic of hiPSC-derived OPCs as a treatment for disorders of myelin loss (157). In the context of schizophrenia, a protocol used to generate hiPSC-derived OPCs from patients confirmed that OL dysfunction and anomalies were similar to the alterations in white matter integrity observed in magnetic resonance imaging studies from patients with schizophrenia. Thus, both models confirm OL abnormalities in schizophrenia, linking OL dysfunction with a decreased number of OPCs (145).

Primary OPC Culture and Oligodendroglial Cells Lines

Primary glial cell cultures from mice and rats are the most common and well-established *in vitro* model used for the study of diseases that affect the CNS and allow the study of OPC differentiation and OL function at the cellular and molecular levels (158, 159). One advantage of primary OPC culture is the availability of protocols for the isolation of OLs, microglia and astrocytes from mixed glial cultures. Such protocols are an economical, simple and reproducible way to obtain oligodendroglial cells with high purity and high efficiency, besides requiring a reduced number of animals (160, 161).

Following the pathway of practical, fast and economical *in vitro* models, the oligodendroglial cells lines MO3.13 and HOG have also been used to analyze OL differentiation and abnormalities (162). MO3.13 is an immortal human-human hybrid cell line, created by fusing rhabdomyosarcoma cells with adult OLs (163). The HOG cell line is directly derived from a human glioma that expresses OL markers MBP and CNPase but does not express glial markers, such as GFAP and glutamine synthase (164). MO3.13, however, expresses GFAP and also exhibits GalC and CNPase immunoreactivity (163). Upon differentiation, MO3.13 cells express MBP and PLP, which are markers for mature OLs (163, 165). Both cell lines have been employed as models to study the cellular neurobiology in OL-linked diseases, such as multiple sclerosis (166) and schizophrenia (5, 167). Unfortunately, protocols to differentiate HOG and MO3.13 into mature OLs vary greatly and these cell lines

do not reach a myelinating state, which jeopardizes a more comprehensive study of myelination process using these models (148).

To study the neurobiological alterations in schizophrenia, including the glutamatergic dysfunction in OL, the MO3.13 cell line was treated with MK-801, a glutamatergic NMDA receptor antagonist that mimics the hypofunction in glutamatergic signaling seen in schizophrenia patients (165). The results exhibit differentially expressed proteins related to energy metabolism and glycolysis (5), including proteins previously associated with schizophrenia (165). Moreover, MK-801-treated OLs present more severe alterations compared to neuronal and astrocyte cell lineages, causing OLs to exhibit increased vulnerability to NMDA and glutamatergic dysfunction (5). Given the OLs' high energy demand to promote axon myelination, these metabolic disturbances could lead to white matter dysfunction and, consequently, altered neuronal connectivity, thereby playing a major role in the etiology of schizophrenia (168, 169).

Despite partially representing disturbances observed in schizophrenia and comprising critical tools in understanding OLs and white matter dysfunctions in schizophrenia, the use of isolated OL cell line cultures cannot reproduce complex physiological processes such as the communication between OLs and neurons, which is an essential factor for *in vivo* myelination and remyelination. In this context, the development of neuronal and glial co-culture systems, brain organoids, and organotypic slice cultures come much closer to the biological conditions present in a physiological environment (73, 151) Furthermore, a more robust way to study cell–cell interactions in the pathogenesis of schizophrenia and to better understand how OL-neuron interactions contribute to abnormal myelination, is by using the *in vivo* models of demyelinating diseases and remyelination processes.

In Vivo and *In Vitro* Strategies Using Cuprizone-Induced Demyelination

The cuprizone (CPZ; bis-cyclohexanone oxaldihydrazone) model is a common animal model used to investigate demyelination-associated diseases such as multiple sclerosis and schizophrenia (170). CPZ is a copper chelator that impairs the activity of copper enzymes (cytochrome oxidase and monoamine oxidases), developing reversible, region-specific OL loss and demyelination, as well as stimulating microgliosis and astrogliosis (171–173). The CPZ hypothesis proposes that perturbation in energy metabolism contributes

to OL apoptosis and induces demyelination [for review see (170)]. Furthermore, CPZ reduces the expression of myelin-related genes and proteins, such as MBP, MOG, PLP, and CNP in animals' corpus callosum (174), consequently inducing brain demyelination, myelin disruption, and OL loss (170, 174, 175). This animal model manifests symptoms similar to those observed in schizophrenia patients, such as deficits in working memory (176, 177) and in PPI of the acoustic startle response, less social interaction, and higher dopamine in the prefrontal cortex (PFC) (175), showing that OL dysfunction and abnormal myelination triggers schizophrenia-like symptoms.

The main CPZ-toxic target are mature OLs. CPZ also has a toxic effect in OLs cultured cells, causing a direct disruption of OL function. For instance, Taraboletti (2017) showed that CPZ induces cell death in the MO3.13 cell line through changes in oligodendroglial energy metabolism (178). CPZ is not able to exert toxic effects on microglia, astrocytes, and SH-SY5Y cells, showing a selective effect in OLs.Moreover, CPZ inhibits the differentiation and maturation of cultured OPCs and decreases the levels of CNP and MBP in mature OLs (179). These results highlight the selective demyelination induced by CPZ *in vivo*, showing that the CPZ model may be a potential experimental tool for assessing molecules related to demyelination and remyelination (170, 180).

Currently, it is unknown whether OL dysfunction consists of a primary or a secondary cause of neuronal and synaptic abnormalities in schizophrenia. Thus, it is important to study cell–cell interactions in the schizophrenia pathologic process. All the models described above partially represent OL and myelination disturbances observed in schizophrenia, comprising critical tools in understanding OLs and white matter dysfunction in this disorder. However, schizophrenia is a multifactorial psychiatric disorder, involving environmental and genetic factors, as well as neurodevelopmental dysfunction (8, 9). For this reason, developing a model that links genetic and environmental elements with cellular and molecular alterations associated with positive and negative symptoms, and cognitive impairment is still a challenge.

Molecular pathogenesis research using iPSC-related technologies, such as three-dimensional (3D) culture models and organoids, offers new insight to recapitulate the complexity of the human CNS. Novel findings derived from these models, associated with clinical phenotype in postmortem, *in vivo*, *in vitro* approaches and findings from brain

magnetic resonance imaging and genomic studies, will be increasingly important for a better understanding of the processes involving OL dysfunction in schizophrenia (151).

ANTIPSYCHOTICS AND OLS

Currently, the major therapeutic strategy for schizophrenia relies on the use of antipsychotic drugs. Antipsychotics are high affinity antagonists of dopamine D2 receptors and are categorized into two classes: typical, or first-generation and atypical, or second generation. The typical antipsychotics, such as haloperidol (HAL), act mainly through dopamine D2 antagonism, thereby improving positive symptoms (10, 181). These antipsychotics induce severe extrapyramidal side effects and have a high incidence of nonresponders (182). In contrast, atypical antipsychotics, such as CLZ, inhibit dopamine D2 as well as serotonergic receptors (especially 5-HT2A and 5-HT2C) (183). They attenuate principally positive symptoms and induce fewer neurological side effects; however, they can lead to metabolic disturbances (184).

Antipsychotics were found to target OL development, reinforcing the role of OLs in the pathophysiology and treatment of schizophrenia (185). In *vitro* and *in vivo* studies have been investigating the effects of atypical and typical antipsychotics on the proliferation and differentiation of glial cells (185–187). The results obtained so far remain controversial; while one study reports that the typical antipsychotic HAL promotes proliferation but not the differentiation of OLs (188) another one confirmed HAL inhibition of OL differentiation but found no effects on OL proliferation (186, 188). Regarding the atypical antipsychotics, olanzapine and quetiapine (QUE) induce OL proliferation, however, only QUE promotes OL differentiation, through ERK1/2 signaling and increases CNP and MBP levels (176).

Recent studies have found that the atypical antipsychotic QUE, administered both before or after CPZ-mediated demyelination, significantly enhances OL regeneration and myelin repair by accelerating the maturation of OPCs (187, 189). This acceleration promotes the survival of OLs, linked to a downregulation of the transcription factor Olig2 in the process of cell maturation (189). Regarding behavioral changes, QUE treatment during the remyelination period improves spatial working memory (189) and cognitive impairments (176) and reverses the deficit in PPI of the acoustic startle response in CPZ-treated mice (175, 177). Antipsychotic treatment (CLZ, QUE, and HAL) in the CPZ model reversed higher

dopamine levels in the PFC and lowered spontaneous alternations in Y-maze tests induced by CPZ (175). The study also revealed that, in mice treated with CPZ, the white matter damage in the PFC was reduced after treatment with CLZ or HAL. Moreover, in the caudate–putamen and hippocampus white matter loss was only attenuated by CLZ and QUE (190).

Moreover, in a mouse model of social isolation, animals treated with QUE presented reduced myelin deficits and increased histone methylation in OLs, besides an improvement in social interactions (191). QUE has also been associated with increased methylation of risk factor genes implicated with schizophrenia, providing evidence that epigenetic regulation may be involved in the mechanisms of action of this antipsychotic (192).

Other antipsychotics have also been associated with epigenetic modifications. *In vivo*, OLA induced altered methylation of genes involved with dopaminergic signaling in the hippocampus and cerebellum (193); CLZ was able to reverse epigenetic alterations induced by phencyclidine treatment in mice, improving cognitive dysfunction, memory recognition, and social deficit (194).

Regarding biochemical pathways, it has been shown that antipsychotic effects are associated with cortical and gray/white matter intensity and with lipid metabolism alterations (195, 196). CLZ and HAL can alter OL glucose metabolism, which is deregulated and correlated with abnormal behavior and cognition in schizophrenia patients (196). Moreover, these drugs are able to stimulate the synthesis of cholesterol and fatty acids in glial cells through regulation of gene expression mediated by the sterol regulatory element-binding proteins SREBP-1 and SREBP-2 (197). Glia-derived cholesterol is essential for the formation of myelin and synapses in the CNS (198). Cholesterol metabolism has been implicated in the regulation of many processes, including myelin membrane growth, axon wrapping, and synapse formation. Thus, cholesterol and myelin synthesis are essential for brain physiological homeostasis (199).

Moreover, reduced Akt signaling has been found in the frontal cortex of postmortem brain tissue from patients with schizophrenia (200, 201). *In vivo* animal models modulating Akt signaling have also exhibited schizophrenia-like behaviors and abnormalities (202, 203). Another *in vivo* study investigated the effect of HAL on Akt signaling, finding increased phosphorylation of Akt as a potential protective mechanism of the medication

(200). PI3K/AKT/mTOR signaling is a well established pathway related to several biological processes, including protein synthesis and cell growth, also playing an important role in OL survival (59). Proteomic analyses of the human immature oligodendroglial cell line MO3.13 found altered proteins associated with the mTOR signaling pathway after treatment with atypical (risperidone and QUE) and typical antipsychotics (chlorpromazine and HAL) (204). According to this study, these medications resulted in different protein expression levels, revealing potentially distinct effects of those drugs on OLs.

As such, upstream and downstream processes linked with PI3K/Akt/mTOR signaling may not only influence OL functioning but may also be associated with the molecular mechanisms of antipsychotics. One example is Akt and GSK3b signaling, found to be mediated by cyclin-dependent kinase 5 (Cdk5) (205); in this study, the *in vivo* model for Cdk5 knockout resulted in impaired remyelination and reduced phosphorylation levels of Akt and GSK3b, indicating the potential role of Cdk5 in the regulation of both pathways. Reduced phosphorylation of GSK3b inhibits differentiation and myelination of OLs (58). As a result, GSK3b inhibitors are being investigated as potential targets for remyelinating drugs such as lithium, discussed in the following section.

In summary, aberrations in OL development and myelin contribute to the pathogenesis of schizophrenia and drugs that reverse abnormal OL phenotypes may be a promising treatment strategy. OL development is a target of some antipsychotics (185) and understanding the effects of antipsychotics on OLs reinforces the need for future therapeutic intervention studies.

NOVEL POTENTIAL THERAPEUTIC TARGETS

In this review, OL maturation and function in the CNS have already been discussed, detailing how these cells may be involved in the pathophysiology of schizophrenia. From postmortem brain studies to *in vivo* and *in vitro* models, several approaches were reviewed, all of which have been used to investigate OL dysfunctions in this psychiatric disorder.

Data from these different strategies exhibit alterations in myelin-related genes in patients with schizophrenia. Further investigation of these candidate genes may contribute to

the search for possible targets for drug development. Given the association of white matter dysfunction with brain dysconnectivity and the development of positive, negative, and cognitive symptoms observed in schizophrenia (206–208), the investigation of potential promyelination agents and other protective substances during myelination in the CNS could provide strategies to prevent the damage caused by altered myelination and other OL dysfunctions.

As for typical and atypical antipsychotics, since they are the main therapeutic strategy currently used for the treatment of schizophrenia, a better understanding of their effects on the proliferation and differentiation of OLs is crucial. Their molecular mechanisms and effects on the white matter remain elusive and more data are necessary to determine any protective and negative effects of those drugs after short- and long-term treatment, especially related to white matter integrity.

In regard to glutamatergic dysfunction, altered signaling and receptors dysfunction have been described in schizophrenia (14). Glial cells are especially vulnerable to glutamate excitotoxicity (209), resulting in impaired OL functioning and white matter lesions (210). Therefore, the investigation of compounds able to prevent this excitotoxicity could provide protective effects, especially to attenuate white matter injury. One example is memantine, a non-competitive NMDA antagonist with a low binding affinity that acts by partially blocking this receptor, preventing glutamate toxicity (211, 212).

Other NMDA modulatory compounds include NMDA receptor agonists, such as D-amino acids: D-aspartate and D-serine. D-aspartate also acts as an NMDAr precursor and is essential in several processes in the CNS, including cognitive function (213, 214). Regarding its role in OLs, D-aspartate contributes to remyelination and is also associated with OL maturation and differentiation (215). D-serine is an endogenous ligand for the glycine site of NMDA receptors. Together with glutamatergic signaling, D-serine was found to contribute to the induction and maintenance of long-term potentiation in synaptic plasticity (216). Clinical trials showed that the administration of D-serine alleviated positive, cognitive, and negative symptoms in schizophrenia patients (217).

Given the negative regulation of GSK3b signaling in OLs, GSK3b inhibitors also present promising results for OL differentiation and survival (58). Lithium is one such inhibitor and is a well-known mood stabilizer employed in bipolar disorder treatment. It

exhibits neuroprotective properties, promoting increased expression of myelin-related genes and OL remyelination (218, 219). Lithium was also found to improve symptoms involving emotional withdrawal, motor activity, disorganized thoughts, and positive symptoms in patients with schizophrenia (220).

Altered energy metabolism has also been reported in schizophrenia, leading to an impaired redox balance (78). OPCs are more sensitive to oxidative stress and have lower glutathione (GSH) levels compared to other cells like neurons and astrocytes (168). The tripeptide GSH is an essential intracellular antioxidant also found at reduced levels in patients with schizophrenia (221). It has been suggested that antioxidants such as N-acetylcysteine, which acts as a precursor of cysteine in GSH synthesis, could be an adjunctive strategy in the treatment of psychiatric disorders (222).

Another signaling process that can become a target for drug discovery studies in OLs is the endocannabinoid system. This system acts in the survival, proliferation, migration, and differentiation of OLs (223). OPCs are known to produce the endocannabinoid arachidonoylglycerol (2-AG), consequently stimulating the ERK signaling pathway, inducing OL differentiation and MBP production (224). Cannabidiol (CBD) is a phytocannabinoid that has presented beneficial effects on OLs, protecting OPCs against inflammation-induced damage and oxidative and endoplasmic reticulum stress (225). All potential targets discussed above are summarized in **Figure 1**.

CONCLUSION

Due to the high complexity of and interaction between, (epi)genetic and environmental factors linked to the development of schizophrenia symptoms, several pathways, along with white and gray matter dysfunction, have been implicated in the disorder. To date, investigations have focused on neuronal cells and, more recently, some studies have been shifting their focus toward the role of glial cells in schizophrenia. Combined data from different *in vivo* and *in vitro* models, as well as brain imaging and postmortem studies, provide evidence for white matter dysfunction and dysconnectivity, both observed in schizophrenia. However, the molecular mechanisms underlying these alterations remain unclear.

Thus, continued research in the field could provide further knowledge regarding the role of OLs in the pathophysiology of the disorder, as well as the effects of antipsychotic medication on these cells. This, in turn, would contribute to the discovery of novel targets and the development of new approaches targeting cognitive and negative symptoms, designing adjunctive treatments alongside antipsychotics.

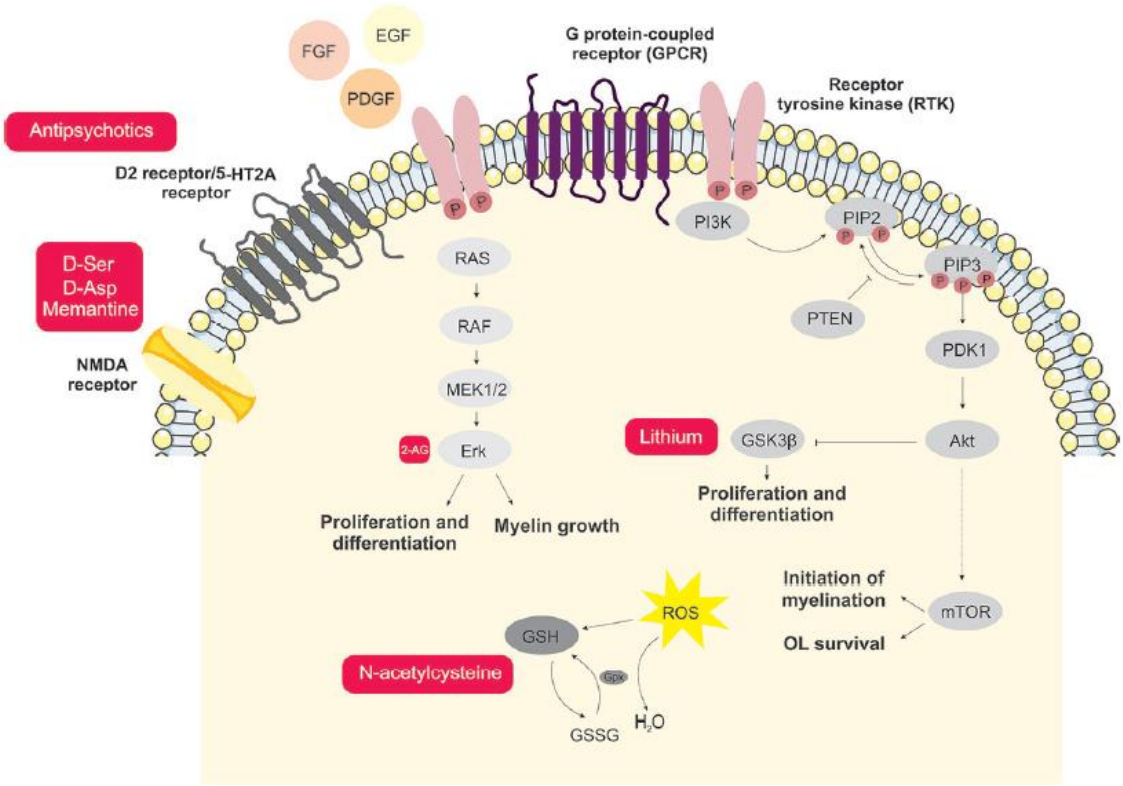

Figure 1. Schematic representation of the main signaling processes and potential novel treatment targets involved with oligodendrocyte dysfunction in schizophrenia. Antipsychotics acting via inhibition of D2 and 5-HT2A receptors are the main therapeutic strategy currently used in schizophrenia treatment. D-amino acids and memantine are shown here as potential targets aiming for improvements in the glutamatergic signaling dysfunction. Endocannabinoids and the GSK3b inhibitor, lithium, contribute to the MEK/ERK1/2-MAPK and PI3K/Akt/mTOR signaling pathways, which are important for oligodendrocyte proliferation and differentiation. Moreover, aiming to attenuate oxidative damage, antioxidants such as N-acetylcysteine may consist of potential therapeutic agents.

NOMENCLATURE

BDNF, brain-derived neurotrophic factor; CBD, cannabidiol; CLZ, clozapine; CNP, 2′ , 3 ′ - cyclic-nucleotide- 3 - phosphodiesterase; CNS, central nervous system; CPZ, cuprizone;

DISC1, disrupted-in-schizophrenia 1; ERK1/2, signal-regulated kinases-1 and -2; GalC, galactocerebroside C; GSH, glutathione; GSK3b, glycogen synthase kinase 3b; HAL, haloperidol; IGF-1, insulin-like growth factor 1; MAG, myelin associated glycoprotein; MAPKs, mitogen-activated protein kinases; MBP, myelin basic protein; MOG, myelin oligodendrocyte glycoprotein; mTOR, mammalian target of rapamycin; NG2, neuron-glial antigen 2; NGR, Nogo Receptor; NGF, nerve growth factor; NMDA, N-methyl-D-aspartate; NPC, neural progenitor cells; NRG1, Neuregulin 1; NSC, neural stem cells; Olig2, oligodendrocyte lineage transcription factor 2; OL, oligodendrocyte; OPCs, oligodendrocyte progenitor cells; PFC, prefrontal cortex; PI3K, phosphoinositide 3-kinase; PLP, proteolipid protein; PPI, prepulse inhibition; QKI, Quaking I; QUE, quetiapine; Rtn4, Reticulon 4; SVZ, subventricular zone.

AUTHOR CONTRIBUTIONS

DG-J conceived the study, designed, and wrote the manuscript. AA helped with data interpretation and manuscript revision. GS and AF conceived the study and assisted with the manuscript draft. CB-T conceived the study and designed the figure. FC and DM-d-S conceived the study, supervised the process, and finalized the manuscript. All authors approved the final version of the manuscript.

FUNDING

DG-J, AF, GS, CB-T, FC, and DM-d-S are supported by the São Paulo Research Foundation (FAPESP, grant numbers 2018/ 25439-9; 2017/25588-1; 2018/03673-0; 2018/10362-0, 2017/ 25055-3; 2019/22398-2). AA and FC are supported by the Coordination for the Improvement of Higher Level Personnel (CAPES/BRAZIL, grant number 465412/2014-9—INBioN).

ACKNOWLEDGMENTS

The authors wish to thank Bradley Smith, MSc for critical comments and English review support during the process.

REFERENCES

1. Barateiro A, Fernandes A. Temporal oligodendrocyte lineage progression: *In vitro* models of proliferation, differentiation and myelination. Biochim Biophys Acta (BBA) - Mol Cell Res (2014) 1843:1917–29. doi: 10.1016/j.bbamcr.2014.04.018

2. Liston C, Watts R, Tottenham N, Davidson MC, Niogi S, Ulug AM, et al. Frontostriatal microstructure modulates efficient recruitment of cognitive control. Cereb Cortex (2006) 16:553–60. doi: 10.1093/cercor/bhj003

3. Hof PR, Haroutunian V, Friedrich VL, Byne W, Buitron C, Perl DP, et al. Loss and altered spatial distribution of oligodendrocytes in the superior frontal gyrus in schizophrenia. Biol Psychiatry (2003) 53:1075–85. doi: 10.1016/s0006-3223(03)00237-3

4. Buchsbaum MS, Tang CY, Peled S, Gudbjartsson H, Lu D, Hazlett EA, et al. Atlas. MRI white matter diffusion anisotropy and PET metabolic rate in schizophrenia. NeuroReport (1998) 9:425–30. doi: 10.1097/00001756-199802160-00013

5. Guest PC, Iwata K, Kato TA, Steiner J, Schmitt A, Turck CW, et al. MK-801 treatment affects glycolysis in oligodendrocytes more than in astrocytes and neuronal cells: insights for schizophrenia. Front Cell Neurosci (2015) 9:180. doi: 10.3389/fncel.2015.00180

6. Giacci M, Fitzgerald M. Oligodendroglia Are Particularly Vulnerable to Oxidative Damage After Neurotrauma In Vivo. J Exp Neurosci (2018) 12:1179069518810004. doi: 10.1177/1179069518810004

7. Friston KJ, Frith CD. Schizophrenia: a disconnection syndrome? Clin Neurosci (1995) 3:89–97.

8. McGrath J, Saha S, Chant D, Welham J. Schizophrenia: A Concise Overview of Incidence, Prevalence, and Mortality. Epidemiol Rev (2008) 30:67–76. doi: 10.1093/epirev/mxn001

9. Gottesman II, Shields J. A polygenic theory of schizophrenia. Proc Natl Acad Sci (1967) 58:199–205. doi: 10.1073/pnas.58.1.199

10. Creese I, Burt D, Snyder S. Dopamine receptor binding predicts clinical and pharmacological potencies of antischizophrenic drugs. Science (1976) 192:481–3. doi: 10.1126/science.3854

11. Howes OD, Montgomery AJ, Asselin M-C, Murray RM, Valli I, Tabraham P, et al. Elevated Striatal Dopamine Function Linked to Prodromal Signs of Schizophrenia. Arch Gen Psychiatry (2009) 66:13. doi: 10.1001/archgenpsychiatry.2008.514

12. Bakker CB, Amini FB. Observations on the psychotomimetic effects of sernyl. Compr Psychiatry (1961) 2:269–80. doi: 10.1016/s0010-440x(61)80033-3

13. Rosenbaum G. Comparison of Sernyl with Other Drugs. AMA Arch Gen Psychiatry (1959) 1:651. doi: 10.1001/archpsyc.1959.03590060113013

14. Olney JW, Farber NB. Glutamate receptor dysfunction and schizophrenia. Arch Gen Psychiatry (1995) 52:998–1007. doi: 10.1001/archpsyc.1995.03950240016004

15. Burbaeva GS, Boksha IS, Turishcheva MS, Vorobyeva EA, Savushkina OK, Tereshkina EB. Glutamine synthetase and glutamate dehydrogenase in the prefrontal cortex of patients with schizophrenia. Prog Neuropsychopharmacol Biol Psychiatry (2003) 27:675–80. doi: 10.1016/s0278-5846(03)00078-2

16. Beneyto M, Kristiansen LV, Oni-Orisan A, McCullumsmith RE, Meador- Woodruff JH. Abnormal glutamate receptor expression in the medial temporal lobe in schizophrenia and mood disorders. Neuropsychopharmacology (2007) 32:1888–902. doi: 10.1038/sj.npp.1301312

17. Jørgensen KN, Nerland S,NorbomLB,Doan NT, Nesvåg R,Mørch-Johnsen L, et al. Increased MRI-based cortical grey/white-matter contrast in sensory and motor regions in schizophrenia and bipolar disorder. psychol Med (2016) 46:1971–85. doi: 10.1017/s0033291716000593

18. Benes FM, Turtle M, Khan Y, Farol P. Myelination of a key relay zone in the hippocampal formation occurs in the human brain during childhood, adolescence, and adulthood. Arch Gen Psychiatry (1994) 51:477–84. doi: 10.1001/archpsyc.1994.03950060041004

19. Fuster JM. Synopsis of function and dysfunction of the frontal lobe. Acta Psychiatr Scand Suppl (1999) 395:51–7. doi: 10.1111/j.1600-0447.1999.tb05983.x

20. Kahn RS, Sommer IE, Murray RM, Meyer-Lindenberg A, Weinberger DR, Cannon TD, et al. Schizophrenia. Nat Rev Dis Primers (2015) 1:15067. doi: 10.1038/nrdp.2015.67

21. Martins-de-Souza D. Proteome and transcriptome analysis suggests oligodendrocyte dysfunction in schizophrenia. J Psychiatr Res (2010) 44:149–56. doi: 10.1016/j.jpsychires.2009.07.007

22. Cassoli JS, Guest PC, Malchow B, Schmitt A, Falkai P, Martins-de-Souza D. Disturbed macro-connectivity in schizophrenia linked to oligodendrocyte dysfunction: from structural findings to molecules. NPJ Schizophr (2015) 1:15034. doi: 10.1038/npjschz.2015.34

23. Hallak JEC, de Paula ALD, Chaves C, Bressan RA, Machado-de-Sousa JP. An Overview on the Search for Schizophrenia Biomarkers. CNS Neurol Disord Drug Targets (2015) 14:996–1000. doi: 10.2174/1871527314666150909114957

24. Woodward ND, Purdon SE, Meltzer HY, Zald DH. A meta-analysis of neuropsychological change to clozapine, olanzapine, quetiapine, and risperidone in schizophrenia. Int J Neuropsychopharmacol (2005) 8:457–72. doi: 10.1017/S146114570500516X

25. Gard AL, Pfeiffer SE. Two proliferative stages of the oligodendrocyte lineage (A2B5 O4- and O4 GaIC-) under different mitogenic control. Neuron (1990) 5:615–25. doi: 10.1016/0896-6273(90)90216-3

26. Miller RH. Oligodendrocyte origins. Trends Neurosci (1996) 19:92–6. doi: 10.1016/s0166-2236(96)80036-1

27. Thomas JL, Spassky N, Perez Villegas EM, Olivier C, Cobos I, Goujet-Zalc C, et al. Spatiotemporal development of oligodendrocytes in the embryonic brain. J Neurosci Res (2000) 59:471–6. doi: 10.1002/(SICI)1097-4547(20000215)59:4<471::AID-JNR1>3.0.CO;2-3

28. Menn B, Garcia-Verdugo JM, Yaschine C, Gonzalez-Perez O, Rowitch D, Alvarez-Buylla A. Origin of Oligodendrocytes in the Subventricular Zone of the Adult Brain. J Neurosci (2006) 26:7907–18. doi: 10.1523/jneurosci.1299-06.2006

29. Emery B. Regulation of oligodendrocyte differentiation and myelination. Science (2010) 330:779–82. doi: 10.1126/science.1190927

30. Emery B, Lu QR. Transcriptional and Epigenetic Regulation of Oligodendrocyte Development and Myelination in the Central Nervous System. Cold Spring Harb Perspect Biol (2015) 7:a020461. doi: 10.1101/cshperspect.a020461

31. Conway GD, O'Bara MA, Vedia BH, Pol SU, Sim FJ. Histone deacetylase activity is required for human oligodendrocyte progenitor differentiation. Glia (2012) 60:1944–53. doi: 10.1002/glia.22410

32. Douvaras P, Rusielewicz T, Kim KH, Haines JD, Casaccia P, Fossati V. Epigenetic Modulation of Human Induced Pluripotent Stem Cell Differentiation to Oligodendrocytes. Int J Mol Sci (2016) 17(4):614. doi: 10.3390/ijms17040614

33. Moyon S, Huynh JL, Dutta D, Zhang F, Ma D, Yoo S, et al. Functional Characterization of DNA Methylation in the Oligodendrocyte Lineage. Cell Rep (2016) 15:748–60. doi: 10.1016/j.celrep.2016.03.060

34. Moyon S, Ma D, Huynh JL, Coutts DJC, Zhao C, Casaccia P, et al. Efficient Remyelination Requires DNA Methylation. eNeuro (2017) 4(2):e0336–16.2017 1–12. doi: 10.1523/ENEURO.0336-16.2017

35. Nishiyama A -H., Lin X, Giese N, Heldin C -H., Stallcup WB. Colocalization of NG2 proteoglycan and PDGF ?-receptor on O2A progenitor cells in the developing rat brain. J Neurosci Res (1996) 43:299–314. doi: 10.1002/(sici)1097-4547(19960201)43:3<299::aid-jnr5>3.0.co;2-e

36. Gard AL, Pfeiffer SE. Oligodendrocyte progenitors isolated directly from developing telencephalon at a specific phenotypic stage: myelinogenic potential in a defined environment. Development (1989) 106:119–32.

37. Sprinkle TJ. 2',3'-cyclic nucleotide 3'-phosphodiesterase, an oligodendrocyte-Schwann cell and myelin-associated enzyme of the nervous system. Crit Rev Neurobiol (1989) 4:235–301.

38. Yu W. Embryonic expression of myelin genes: Evidence for a focal source of oligodendrocyte precursors in the ventricular zone of the neural tube. Neuron (1994) 12:1353–62. doi: 10.1016/0896-6273(94)90450-2

39. Stangel M, Hartung H-P. Remyelinating strategies for the treatment of multiple sclerosis. Prog Neurobiol (2002) 68:361–76. doi: 10.1016/s0301-0082(02)00105-3

40. Dubois-Dalcq M. Emergence of three myelin proteins in oligodendrocytes cultured without neurons. J Cell Biol (1986) 102:384–92. doi: 10.1083/jcb.102.2.384

41. Scolding NJ, Frith S, Linington C, Morgan BP, Campbell AK, Compston DAS. Myelin-oligodendrocyte glycoprotein (MOG) is a surface marker of oligodendrocyte maturation. J Neuroimmunol (1989) 22:169–76. doi: 10.1016/0165-5728(89)90014-3

42. Norton WT, Poduslo SE. Myelination In Rat Brain: Changes In Myelin Composition During Brain Maturation. J Neurochem (1973) 21:759–73. doi: 10.1111/j.1471-4159.1973.tb07520.x

43. Domingues HS, Cruz A, Chan JR, Relvas JB, Rubinstein B, Pinto IM. Mechanical plasticity during oligodendrocyte differentiation and myelination. Glia (2018) 66:5–14. doi: 10.1002/glia.23206

44. Bakhti M, Snaidero N, Schneider D, Aggarwal S, Möbius W, Janshoff A, et al. Loss of electrostatic cell-surface repulsion mediates myelin membrane adhesion and compaction in the central nervous system. Proc Natl Acad Sci U S A (2013) 110:3143–8. doi: 10.1073/pnas.1220104110

45. Lee DW, Banquy X, Kristiansen K, Kaufman Y, Boggs JM, Israelachvili JN. Lipid domains control myelin basic protein adsorption and membrane interactions between model myelin lipid bilayers. Proc Natl Acad Sci U S A (2014) 111:E768–75. doi: 10.1073/pnas.1401165111

46. Snaidero N, Velte C, Myllykoski M, Raasakka A, Ignatev A, Werner HB,et al. Antagonistic Functions of MBP and CNP Establish Cytosolic Channels in CNS Myelin. Cell Rep (2017) 18:314–23. doi: 10.1016/j.celrep.2016.12.053

47. Santos AK, Vieira MS, Vasconcellos R, Goulart VAM, Kihara AH, Resende RR. Decoding cell signalling and regulation of oligodendrocyte differentiation. Semin Cell Dev Biol (2018). 95:54–73. doi: 10.1016/j.semcdb.2018.05.020

48. Camargo N, Goudriaan A, van Deijk A-LF, OtteWM, Brouwers JF, Lodder H, et al. Oligodendroglial myelination requires astrocyte-derived lipids. PloS Biol (2017) 15:e1002605. doi: 10.1371/journal.pbio.1002605

49. Miron VE, Boyd A, Zhao J-W, Yuen TJ, Ruckh JM, Shadrach JL, et al. M2 microglia and macrophages drive oligodendrocyte differentiation during CNS remyelination. Nat Neurosci (2013) 16:1211–8. doi: 10.1038/nn.3469

50. Barres BA, Raff MC. Axonal Control of Oligodendrocyte Development: Figure 1. J Cell Biol (1999) 147:1123–8. doi: 10.1083/jcb.147.6.1123

51. Noble M, Murray K. Purified astrocytes promote the in vitro division of a bipotential glial progenitor cell. EMBO J (1984) 3:2243–7. doi: 10.1002/j.1460-2075.1984.tb02122.x

52. Pang Y, Fan L-W, Tien L-T, Dai X, Zheng B, Cai Z, et al. Differential roles of astrocyte and microglia in supporting oligodendrocyte development and myelination in vitro. Brain Behav (2013) 3:503–14. doi: 10.1002/brb3.152

53. Lalive PH, Paglinawan R, Biollaz G, Kappos EA, Leone DP, Malipiero U, et al. TGF-beta-treated microglia induce oligodendrocyte precursor cell chemotaxis through the HGF-c-Met pathway. Eur J Immunol (2005) 35:727–37. doi: 10.1002/eji.200425430

54. von Büdingen H-C, Mei F, Greenfield A, Jahn S, Shen Y-AA, Reid HH, et al. The myelin oligodendrocyte glycoprotein directly binds nerve growth factor to modulate central axon circuitry. J Cell Biol (2015) 210:891–8. doi: 10.1083/jcb.201504106

55. Xiao J, Wong AW, Willingham MM, van den Buuse M, Kilpatrick TJ, Murray SS. Brain-Derived Neurotrophic Factor Promotes Central Nervous System Myelination via a Direct Effect upon Oligodendrocytes. Neurosignals (2010) 18:186–202. doi: 10.1159/000323170

56. Butt AM, Fern RF, Matute C. Neurotransmitter signaling in white matter. Glia (2014) 62:1762–79. doi: 10.1002/glia.22674

57. Wahl SE, McLane LE, Bercury KK, Macklin WB, Wood TL. Mammalian Target of Rapamycin Promotes Oligodendrocyte Differentiation, Initiation and Extent of CNS Myelination. J Neurosci (2014) 34:4453–65. doi: 10.1523/ jneurosci.4311-13.2014

58. Azim K, Butt AM. GSK3b negatively regulates oligodendrocyte differentiation and myelination in vivo. Glia (2011) 59:540–53. doi: 10.1002/glia.21122

59. Flores AI, Narayanan SP, Morse EN, Shick HE, Yin X, Kidd G, et al. Constitutively Active Akt Induces Enhanced Myelination in the CNS. J Neurosci (2008) 28:7174–83. doi: 10.1523/jneurosci.0150-08.2008

60. Ishii A, Furusho M, Dupree JL, Bansal R. Role of ERK1/2 MAPK signaling in the maintenance of myelin and axonal integrity in the adult CNS. J Neurosci (2014) 34:16031–45. doi: 10.1523/JNEUROSCI.3360-14.2014

61. Ishii A, Furusho M, Macklin W, Bansal R. Independent and cooperative roles of the Mek/ERK1/2-MAPK and PI3K/Akt/mTOR pathways during developmental myelination and in adulthood. Glia (2019) 67:1277–95. doi: 10.1002/glia.23602

62. Bartzokis G. Schizophrenia: breakdown in the well-regulated lifelong process of brain development and maturation. Neuropsychopharmacology (2002) 27:672–83. doi: 10.1016/S0893-133X(02)00364-0

63. Bernstein H-G, Steiner J, Guest PC, Dobrowolny H, Bogerts B. Glial cells as key players in schizophrenia pathology: recent insights and concepts of therapy. Schizophr Res (2015) 161:4–18. doi: 10.1016/j.schres.2014.03.035

64. Hyde TM, Ziegler JC, Weinberger DR. Psychiatric disturbances in metachromatic leukodystrophy. Insights into the neurobiology of psychosis. Arch Neurol (1992) 49:401–6. doi: 10.1001/archneur.1992.00530280095028

65. Weinberger DR, Lipska BK. Cortical maldevelopment, antipsychotic drugs, and schizophrenia: a search for common ground. Schizophr Res (1995) 16:87–110. doi: 10.1016/0920-9964(95)00013-c

66. Bassett AS, Chow EW. 22q11 deletion syndrome: a genetic subtype of schizophrenia. Biol Psychiatry (1999) 46:882–91. doi: 10.1016/s0006-3223

67. Kanaan RA, Picchioni MM, McDonald C, Shergill SS, McGuire PK. White matter deficits in schizophrenia are global and don't progress with age. Aust New Z J Psychiatry (2017) 51:1020–31. doi: 10.1177/0004867417700729

68. Hoptman M, Nierenberg J, Bertisch H, Catalano D, Ardekani B, Branch C, et al. A DTI study of white matter microstructure in individuals at high genetic risk for schizophrenia. Schizophr Res (2008) 106:115–24. doi: 10.1016/j.schres.2008.07.023

69. Falkai P, Raabe F, Bogerts B, Schneider-Axmann T, Malchow B, Tatsch L, et al. Association between altered hippocampal oligodendrocyte number and neuronal circuit structures in schizophrenia: a postmortem analysis. Eur Arch Psychiatry Clin Neurosci (2019). doi: 10.1007/s00406-019-01067-0

70. Falkai P, Steiner J, Malchow B, Shariati J, Knaus A, Bernstein H-G, et al. Oligodendrocyte and Interneuron Density in Hippocampal Subfields in Schizophrenia and Association of Oligodendrocyte Number with Cognitive Deficits. Front Cell Neurosci (2016) 10:78. doi: 10.3389/fncel.2016.00078

71. Tkachev D, Mimmack ML, Ryan MM, Wayland M, Freeman T, Jones PB, et al. Oligodendrocyte dysfunction in schizophrenia and bipolar disorder. Lancet (2003) 362:798–805. doi: 10.1016/s0140-6736(03)14289-4

72. Mirnics K, Middleton FA, Marquez A, Lewis DA, Levitt P. Molecular characterization of schizophrenia viewed by microarray analysis of gene expression in prefrontal cortex. Neuron (2000) 28:53–67. doi: 10.1016/s0896-6273(00)00085-4

73. Takahashi N, Sakurai T, Davis KL, Buxbaum JD. Linking oligodendrocyte and myelin dysfunction to neurocircuitry abnormalities in schizophrenia. Prog Neurobiol (2011) 93:13–24. doi: 10.1016/j.pneurobio.2010.09.004

74. DolatshahiM, Rahmani F, ShadmehrMH, Peoppl T, Shojaie A, Noorizadeh F, et al. Working Memory Function in Recent-Onset Schizophrenia Patients Associated with White Matter Microstructure: Connectometry Approach. Comput Diffusion MRI (2017) 201–9. doi: 10.1007/978-3-319-54130-3_17

75. Palaniyappan L, Al-Radaideh A, Mougin O, Gowland P, Liddle PF. Combined white matter imaging suggests myelination defects in visual processing regions in schizophrenia. Neuropsychopharmacology (2013) 38:1808–15. doi: 10.1038/npp.2013.80

76. Uranova N, Orlovskaya D, Vikhreva O, Zimina I, Kolomeets N, Vostrikov V, et al. Electron microscopy of oligodendroglia in severe mental illness. Brain Res Bull (2001) 55:597–610. doi: 10.1016/s0361-9230(01)00528-7

77. Hakak Y, Walker JR, Li C, Wong WH, Davis KL, Buxbaum JD, et al. Genome-wide expression analysis reveals dysregulation of myelinationrelated genes in chronic schizophrenia. Proc Natl Acad Sci U S A (2001) 98:4746–51. doi: 10.1073/pnas.081071198

78. Martins-de-Souza D, Gattaz WF, Schmitt A, Maccarrone G, Hunyadi- Gulyás E, Eberlin MN, et al. Proteomic analysis of dorsolateral prefrontal cortex indicates the involvement of cytoskeleton, oligodendrocyte, energy metabolism and new potential markers in schizophrenia. J Psychiatr Res (2009) 43:978–86. doi: 10.1016/j.jpsychires.2008.11.006

79. Petronis A. The origin of schizophrenia: genetic thesis, epigenetic antithesis, and resolving synthesis. Biol Psychiatry (2004) 55:965–70. doi: 10.1016/j.biopsych.2004.02.005

80. Abdolmaleky HM, Smith CL, Faraone SV, Shafa R, Stone W, Glatt SJ, et al. Methylomics in psychiatry: Modulation of gene-environment interactions may be through DNA methylation. Am J Med Genet (2004) 127B:51–9. doi: 10.1002/ajmg.b.20142

81. Singh SM, Murphy B, O'Reilly RL. Involvement of gene-diet/drug interaction in DNA methylation and its contribution to complex diseases: from cancer to schizophrenia. Clin Genet (2003) 64:451–60. doi: 10.1046/j.1399-0004.2003.00190.x

82. Akbarian S. Special volume: The genomics and epigenomics of schizophrenia. Schizophr Res (2019). S0920–9964(19):30563–8. doi: 10.1016/j.schres.2019.11.056

83. Alelú-Paz R, Carmona FJ, Sanchez-Mut JV, Cariaga-Martínez A, González- Corpas A, Ashour N, et al. Epigenetics in Schizophrenia: A Pilot Study of Global DNA Methylation in Different Brain Regions Associated with Higher Cognitive Functions. Front Psychol (2016) 7:1496. doi: 10.3389/fpsyg.2016.01496

84. Jiang T, Zong L, Zhou L, Hou Y, Zhang L, Zheng X, et al. Variation in global DNA hydroxymethylation with age associated with schizophrenia. Psychiatry Res (2017) 257:497–500. doi: 10.1016/j.psychres.2017.08.022

85. Chase KA, Gavin DP, Guidotti A, Sharma RP. Histone methylation at H3K9: evidence for a restrictive epigenome in schizophrenia. Schizophr Res (2013) 149:15–20. doi: 10.1016/j.schres.2013.06.021

86. Tang B, Dean B, Thomas EA. Disease- and age-related changes in histone acetylation at gene promoters in psychiatric disorders. Transl Psychiatry (2011) 1:e64. doi: 10.1038/tp.2011.61

87. IwamotoK, BundoM, YamadaK, Takao H, Iwayama-Shigeno Y, Yoshikawa T, et al. DNA methylation status of SOX10 correlates with its downregulation and oligodendrocyte dysfunction in schizophrenia. J Neurosci (2005) 25:5376–81. doi: 10.1523/JNEUROSCI.0766-05.2005

88. Mendizabal I, Berto S, Usui N, Toriumi K, Chatterjee P, Douglas C, et al. Cell type-specific epigenetic links to schizophrenia risk in the brain. Genome Biol (2019) 20:135. doi: 10.1186/s13059-019-1747-7

89. Martins-de-Souza D, Gattaz WF, Schmitt A, Rewerts C, Marangoni S, Novello JC, et al. Alterations in oligodendrocyte proteins, calcium homeostasis and new potential markers in schizophrenia anterior temporal lobe are revealed by shotgun proteome analysis. J Neural Transm (2009) 116:275–89. doi: 10.1007/s00702-008-0156-y

90. Hazlett EA, Buchsbaum MS, Kemether E, Bloom R, Platholi J, Brickman AM, et al. Abnormal glucose metabolism in the mediodorsal nucleus of the thalamus in schizophrenia. Am J Psychiatry (2004) 161:305–14. doi: 10.1176/appi.ajp.161.2.305

91. Schizophrenia Working Group of the Psychiatric Genomics Consortium. Biological insights from 108 schizophrenia-associated genetic loci. Nature (2014) 511:421–7. doi: 10.1038/nature13595

92. Smigielski L, Jagannath V, Rössler W, Walitza S, Grünblatt E. Epigenetic mechanisms in schizophrenia and other psychotic disorders: a systematic review of empirical human findings. Mol Psychiatry (2020). doi: 10.1038/s41380-019-0601-3

93. Millar JK. Disruption of two novel genes by a translocation co-segregating with schizophrenia. Hum Mol Genet (2000) 9:1415–23. doi: 10.1093/hmg/9.9.1415

94. Stefansson H, Sigurdsson E, Steinthorsdottir V, Bjornsdottir S, Sigmundsson T, Ghosh S, et al. Neuregulin 1 and susceptibility to schizophrenia. Am J Hum Genet (2002) 71:877–92. doi: 10.1086/342734

95. Meyer D, Birchmeier C. Multiple essential functions of neuregulin in development. Nature (1995) 378:386–90. doi: 10.1038/378386a0

96. Fernandez PA, Tang DG, Cheng L, Prochiantz A, Mudge AW, Raff MC. Evidence that axon-derived neuregulin promotes oligodendrocyte survival in the developing rat optic nerve. Neuron (2000) 28:81–90. doi: 10.1016/s0896-6273(00)00087-8

97. Norton N, Moskvina V, Morris DW, Bray NJ, Zammit S, Williams NM, et al. Evidence that interaction between neuregulin 1 and its receptor erbB4 increases susceptibility to schizophrenia. Am J Med Genet B Neuropsychiatr Genet (2006) 141B:96–101. doi: 10.1002/ajmg.b.30236

98. Gerlai R, Pisacane P, Erickson S. Heregulin, but not ErbB2 or ErbB3, heterozygous mutant mice exhibit hyperactivity in multiple behavioral tasks. Behav Brain Res (2000) 109:219–27. doi: 10.1016/s0166-4328(99)00175-8

99. McIntosh AM, Moorhead TWJ, Job D, Lymer GKS, Muñoz Maniega S, McKirdy J, et al. The effects of a neuregulin 1 variant on white matter density and integrity. Mol Psychiatry (2008) 13:1054–9. doi: 10.1038/sj.mp.4002103

100. Konrad A, Vucurevic G, Musso F, Stoeter P, Dahmen N, Winterer G. ErbB4 genotype predicts left frontotemporal structural connectivity in human brain. Neuropsychopharmacology (2009) 34:641–50. doi: 10.1038/ npp.2008.112

101. Harrison PJ, Law AJ. Neuregulin 1 and schizophrenia: genetics, gene expression, and neurobiology. Biol Psychiatry (2006) 60:132–40. doi: 10.1016/j.biopsych.2005.11.002

102. Taveggia C, Thaker P, Petrylak A, Caporaso GL, Toews A, Falls DL, et al. Type III neuregulin-1 promotes oligodendrocyte myelination. Glia (2008) 56:284–93. doi: 10.1002/glia.20612

103. Ortega MC, Bribián A, Peregrín S, Gil MT, Marín O, de Castro F. Neuregulin-1/ErbB4 signaling controls the migration of oligodendrocyte precursor cells during development. Exp Neurol (2012) 235:610–20. doi: 10.1016/j.expneurol.2012.03.015

104. GrandPréT, Nakamura F, Vartanian T, Strittmatter SM. Identification of the Nogo inhibitor of axon regeneration as a Reticulon protein. Nature (2000) 403:439–44. doi: 10.1038/35000226

105. Thallmair M, Metz GA, Z'Graggen WJ, Raineteau O, Kartje GL, Schwab ME. Neurite growth inhibitors restrict plasticity and functional recovery following corticospinal tract lesions. Nat Neurosci (1998) 1:124–31. doi: 10.1038/373

106. Wang X, Chun S-J, Treloar H, Vartanian T, Greer CA, Strittmatter SM. Localization of Nogo-A and Nogo-66 Receptor Proteins at Sites of Axon– Myelin and Synaptic Contact. J Neurosci (2002) 22:5505–15. doi: 10.1523/jneurosci.22-13-05505.2002

107. Pernet V, Joly S, Christ F, Dimou L, Schwab ME. Nogo-A and Myelin-Associated Glycoprotein Differently Regulate Oligodendrocyte Maturation and Myelin Formation. J Neurosci (2008) 28:7435–44. doi: 10.1523/jneurosci.0727-08.2008

108. Willi R, Weinmann O, Winter C, Klein J, Sohr R, Schnell L, et al. Constitutive genetic deletion of the growth regulator Nogo-A induces schizophrenia related endophenotypes. J Neurosci (2010) 30:556–67. doi: 10.1523/JNEUROSCI.4393-09.2010

109. Mingorance-Le Meur A, Zheng B, Soriano E, del Río JA. Involvement of the Myelin-Associated Inhibitor Nogo-A in Early Cortical Development and Neuronal Maturation. Cereb Cortex (2007) 17:2375–86. doi: 10.1093/cercor/bhl146

110. Novak G, Kim D, Seeman P, Tallerico T. Schizophrenia and Nogo: elevated mRNA in cortex, and high prevalence of a homozygous CAA insert. Brain Res Mol Brain Res (2002) 107:183–9. doi: 10.1016/s0169-328x(02)00492-8

111. Willi R, Schwab ME. Nogo and Nogo receptor: relevance to schizophrenia? Neurobiol Dis (2013) 54:150–7. doi: 10.1016/j.nbd.2013.01.011

112. Mathieson I, Munafò MR, Flint J. Meta-analysis indicates that common variants at the DISC1 locus are not associated with schizophrenia. Mol Psychiatry (2012) 17:634–41. doi: 10.1038/mp.2011.41

113. Katsel P, Tan W, Abazyan B, Davis KL, Ross C, Pletnikov MV, et al. Expression of mutant human DISC1 in mice supports abnormalities in differentiation of oligodendrocytes. Schizophr Res (2011) 130:238–49. doi: 10.1016/j.schres.2011.04.021

114. Katsel P, Fam P, Tan W, Khan S, Yang C, Jouroukhin Y, et al. Overexpression of Truncated Human DISC1 Induces Appearance of Hindbrain Oligodendroglia in the Forebrain During Development. Schizophr Bull (2018) 44:515–24. doi: 10.1093/schbul/sbx106

115. Sprooten E, Sussmann JE, Moorhead TW, Whalley HC, Ffrench-Constant C, Blumberg HP, et al. Association of white matter integrity with genetic variation in an exonic DISC1 SNP. Mol Psychiatry (2011) 16:688–9. doi: 10.1038/mp.2011.15

116. Bernstein H-G, Jauch E, Dobrowolny H, Mawrin C, Steiner J, Bogerts B. Increased density of DISC1-immunoreactive oligodendroglial cells in frontoparietal white matter of patients with paranoid schizophrenia. Eur Arch Psychiatry Clin Neurosci (2016) 266:495–504. doi: 10.1007/s00406-015-0640-y

117. Zhou Q, Choi G, Anderson DJ. The bHLH Transcription Factor Olig2 Promotes Oligodendrocyte Differentiation in Collaboration with Nkx2.2. Neuron (2001) 31:791–807. doi: 10.1016/s0896-6273(01)00414-7

118. Lu QR, Richard Lu Q, Sun T, Zhu Z, Ma N, Garcia M, et al. Common Developmental Requirement for Olig Function Indicates a Motor Neuron/ Oligodendrocyte Connection. Cell (2002) 109:75–86. doi: 10.1016/s0092-8674(02)00678-5

119. Katsel P, Davis K, Haroutunian V. Variations in myelin and oligodendrocyte-related gene expression across multiple brain regions in schizophrenia: A gene ontology study. Schizophr Res (2005) 79:157–73. doi: 10.1016/j.schres.2005.06.007

120. Ligon KL, Fancy SPJ, Franklin RJM, Rowitch DH. Olig gene function in CNS development and disease. Glia (2006) 54:1–10. doi: 10.1002/glia.20273

121. Woodruff RH, Franklin RJ. Demyelination and remyelination of the caudal cerebellar peduncle of adult rats following stereotaxic injections of lysolecithin, ethidium bromide, and complement/anti-galactocerebroside: a comparative study. Glia (1999) 25:216–28. doi: 10.1002/(sici)1098-1136 (19990201)25:3<216::aid-glia2>3.0.co;2-l

122. Georgieva L, Moskvina V, Peirce T, Norton N, Bray NJ, Jones L, et al. Convergent evidence that oligodendrocyte lineage transcription factor 2 (OLIG2) and interacting genes influence susceptibility to schizophrenia. Proc Natl Acad Sci U S A (2006) 103:12469–74. doi: 10.1073/pnas.0603029103

123. Peirce TR, Bray NJ, Williams NM, Norton N, Moskvina V, Preece A, et al. Convergent evidence for 2',3'-cyclic nucleotide 3'-phosphodiesterase as a possible susceptibility gene for schizophrenia. Arch Gen Psychiatry (2006) 63:18–24. doi: 10.1001/archpsyc.63.1.18

124. Voineskos AN, Felsky D, Kovacevic N, Tiwari AK, Zai C, Mallar Chakravarty M, et al. Oligodendrocyte Genes, White Matter Tract Integrity, and Cognition in Schizophrenia. Cereb Cortex (2013) 23:2044–57. doi: 10.1093/cercor/bhs188

125. Vogel US, Thompson RJ. Molecular Structure, Localization, and Possible Functions of the Myelin-Associated Enzyme 2',3'-Cyclic Nucleotide 3'- Phosphodiesterase. J Neurochem (1988) 50:1667–77. doi: 10.1111/j.1471-4159.1988.tb02461.x

126. Edgar JM, McLaughlin M, Werner HB, McCulloch MC, Barrie JA, Brown A, et al. Early ultrastructural defects of axons and axon-glia junctions in mice lacking expression of Cnp1. Glia (2009) 57:1815–24. doi: 10.1002/glia.20893

127. Åberg K, Saetre P, Lindholm E, Ekholm B, Pettersson U, Adolfsson R, et al. A new candidate gene for schizophrenia involved in myelination. Am J Med Genet Part B: Neuropsychiatr Genet (2006) 141B:84–90. doi: 10.1002/ajmg.b.30243

128. Mccullumsmith R, Gupta D, Beneyto M, Kreger E, Haroutunian V, Davis K, et al. Expression of transcripts for myelination-related genes in the anterior cingulate cortex in schizophrenia☆. Schizophr Res (2007) 90:15–27. doi: 10.1016/j.schres.2006.11.017

129. Chen Y, Tian D, Ku L, Osterhout DJ, Feng Y. The Selective RNA-binding Protein Quaking I (QKI) Is Necessary and Sufficient for Promoting Oligodendroglia Differentiation. J Biol Chem (2007) 282:23553–60. doi: 10.1074/jbc.m702045200

130. Sidman RL, Dickie MM, Appel SH, MUTANT MICE. (Quaking And Jimpy) With Deficient Myelination In The Central Nervous System. Science (1964) 144:309–11. doi: 10.1126/science.144.3616.309

131. Ebersole TA, Chen Q, Justice MJ, Artzt K. The quaking gene product necessary in embryogenesis and myelination combines features of RNA binding and signal transduction proteins. Nat Genet (1996) 12:260–5. doi: 10.1038/ng0396-260

132. Wu JI, Reed RB, Grabowski PJ, Artzt K. Function of quaking in myelination: Regulation of alternative splicing. Proc Natl Acad Sci (2002) 99:4233–8. doi: 10.1073/pnas.072090399

133. Darbelli L, Choquet K, Richard S, Kleinman CL. Transcriptome profiling of mouse brains with qkI-deficient oligodendrocytes reveals major alternative splicing defects including self-splicing. Sci Rep (2017) 7:7554. doi: 10.1038/s41598-017-06211-1

134. Lipska BK, Peters T, Hyde TM, Halim N, Horowitz C, Mitkus S, et al. Expression of DISC1 binding partners is reduced in schizophrenia and associated with DISC1 SNPs. Hum Mol Genet (2006) 15:1245–58. doi: 10.1093/hmg/ddl040

135. Chen X, Ku L, Mei R, Liu G, Xu C, Wen Z, et al. Novel schizophrenia risk factor pathways regulate FEZ1 to advance oligodendroglia development. Transl Psychiatry (2017) 7:1293. doi: 10.1038/s41398-017-0028-z

136. Ransom BR, Yamate CL, Black JA, Waxman SG. Rat optic nerve: Disruption of gliogenesis with 5-azacytidine during early postnatal development. Brain Res (1985) 337:41–9. doi: 10.1016/0006-8993(85)91607-5

137. Khandaker GM, Zimbron J, Lewis G, Jones PB. Prenatal maternal infection, neurodevelopment and adult schizophrenia: a systematic review of population-based studies. psychol Med (2013) 43:239–57. doi: 10.1017/s0033291712000736

138. Kneeland RE, Fatemi SH. Viral infection, inflammation and schizophrenia. Prog Neuropsychopharmacol Biol Psychiatry (2013) 42:35–48. doi: 10.1016/j.pnpbp.2012.02.001

139. Cannon TD, van Erp TGM, Rosso IM, Huttunen M, Lönnqvist J, Pirkola T, et al. Fetal hypoxia and structural brain abnormalities in schizophrenic patients, their siblings, and controls. Arch Gen Psychiatry (2002) 59:35–41. doi: 10.1001/archpsyc.59.1.35

140. Najjar S, Pearlman DM. Neuroinflammation and white matter pathology in schizophrenia: systematic review. Schizophr Res (2015) 161:102–12. doi: 10.1016/j.schres.2014.04.041

141. Aston C, Jiang L, Sokolov BP. Transcriptional profiling reveals evidence for signaling and oligodendroglial abnormalities in the temporal cortex from patients with major depressive disorder. Mol Psychiatry (2005) 10:309–22. doi: 10.1038/sj.mp.4001565

142. Orlovskaya DD, Vostrikov VM, Rachmanova VI, Uranova NA. Decreased numerical density of oligodendroglial cells in postmortem prefrontal cortex in schizophrenia, bipolar affective disorder and major depression. Schizophr Res (2000) 41:105–6. doi: 10.1016/s0920-9964(00)90551-6

143. Uranova NA, Vostrikov VM, Vikhreva OV, Zimina IS, Kolomeets NS, Orlovskaya DD. The role of oligodendrocyte pathology in schizophrenia. Int J Neuropsychopharmacol (2007) 10:537. doi: 10.1017/s1461145707007626

144. de Vrij FMGROUP Study Consortium, , Bouwkamp CG, Gunhanlar N, Shpak G, Lendemeijer B, et al. Candidate CSPG4 mutations and induced pluripotent stem cell modeling implicate oligodendrocyte progenitor cell dysfunction in familial schizophrenia. Mol Psychiatry (2019) 24:757–71. doi: 10.1038/s41380-017-0004-2

145. McPhie DL, Nehme R, Ravichandran C, Babb SM, Ghosh SD, Staskus A, et al. Oligodendrocyte differentiation of induced pluripotent stem cells derived from subjects with schizophrenias implicate abnormalities in development. Transl Psychiatry (2018) 8:230. doi: 10.1038/s41398-018-0284-6

146. Raabe FJ, Galinski S, Papiol S, Falkai PG, Schmitt A, Rossner MJ. Studying and modulating schizophrenia-associated dysfunctions of oligodendrocytes with patient-specific cell systems. NPJ Schizophr (2018) 4:23. doi: 10.1038/ s41537-018-0066-4

147. Buntinx M, Vanderlocht J, Hellings N, Vandenabeele F, Lambrichts I, Raus J, et al. Characterization of three human oligodendroglial cell lines as a model to study oligodendrocyte injury: Morphology and oligodendrocyte-specific gene expression. J Neurocytol (2003) 32:25–38. doi: 10.1023/a:1027324230923

148. De Kleijn KMA, Zuure WA, Peijnenborg J, Heuvelmans JM, Martens GJM. Reappraisal of Human HOG and MO3.13 Cell Lines as a Model to Study Oligodendrocyte Functioning. Cells (2019) 8(9):1096. doi: 10.3390/cells8091096

149. Nakazawa T, Hashimoto R, Takuma K, Hashimoto H.Modeling of psychiatric disorders using induced pluripotent stem cell-related technologies. J Pharmacol Sci (2019) 140:321–4. doi: 10.1016/j.jphs.2019.06.002

150. Gottesman II, Gould TD. The Endophenotype Concept in Psychiatry: Etymology and Strategic Intentions. Am J Psychiatry (2003) 160:636–45. doi: 10.1176/appi.ajp.160.4.636

151. Hoffmann A, Ziller M, Spengler D. Progress in iPSC-Based Modeling of Psychiatric Disorders. Int J Mol Sci (2019) 20:4896. doi: 10.3390/ijms20194896

152. Balan S, ToyoshimaM, Yoshikawa T. Contribution of induced pluripotent stem cell technologies to the understanding of cellular phenotypes in schizophrenia. Neurobiol Dis (2019) 131:104162. doi: 10.1016/j.nbd.2018.04.021

153. Habela CW, Song H, Ming G-L. Modeling synaptogenesis in schizophrenia and autism using human iPSC derived neurons. Mol Cell Neurosci (2016) 73:52–62. doi: 10.1016/j.mcn.2015.12.002

154. Soliman MA, Aboharb F, Zeltner N, Studer L. Pluripotent stem cells in neuropsychiatric disorders. Mol Psychiatry (2017) 22:1241–9. doi: 10.1038/mp.2017.40

155. Brennand KJ, Simone A, Jou J, Gelboin-Burkhart C, Tran N, Sangar S, et al. Modelling schizophrenia using human induced pluripotent stem cells. Nature (2011) 473:221–5. doi: 10.1038/nature09915

156. Douvaras P, Fossati V. Generation and isolation of oligodendrocyte progenitor cells from human pluripotent stem cells. Nat Protoc (2015) 10:1143–54. doi: 10.1038/nprot.2015.075

157. Wang S, Bates J, Li X, Schanz S, Chandler-Militello D, Levine C, et al. Human iPSC-derived oligodendrocyte progenitor cells can myelinate and rescue a mouse model of

congenital hypomyelination. Cell Stem Cell (2013) 12:252–64. doi: 10.1016/j.stem.2012.12.002

158. Abney ER, Bartlett PP, Raff MC. Astrocytes, ependymal cells, and oligodendrocytes develop on schedule in dissociated cell cultures of embryonic rat brain. Dev Biol (1981) 83:301–10. doi: 10.1016/0012-1606 (81)90476-0

159. Mecha M. An easy and fast way to obtain a high number of glial cells from rat cerebral tissue: A beginners approach. Protocol Exchange (2011). doi: 10.1038/protex.2011.218

160. McCarthy KD, de Vellis J. Preparation of separate astroglial and oligodendroglial cell cultures from rat cerebral tissue. J Cell Biol (1980) 85:890–902. doi: 10.1083/jcb.85.3.890

161. Yang Z, Watanabe M, Nishiyama A. Optimization of oligodendrocyte progenitor cell culture method for enhanced survival. J Neurosci Methods (2005) 149:50–6. doi: 10.1016/j.jneumeth.2005.05.003

162. Schoenfeld R, Wong A, Silva J, Li M, Itoh A, Horiuchi M, et al. Oligodendroglial differentiation induces mitochondrial genes and inhibition of mitochondrial function represses oligodendroglial differentiation. Mitochondrion (2010) 10:143–50. doi: 10.1016/j.mito.2009.12.141

163. McLaurin J, Trudel GC, Shaw IT, Antel JP, Cashman NR. A human glial hybrid cell line differentially expressing genes subserving oligodendrocyte and astrocyte phenotype. J Neurobiol (1995) 26:283–93. doi: 10.1002/neu.480260212

164. Post GR, Dawson G. Characterization of a cell line derived from a human oligodendroglioma. Mol Chem Neuropathol (1992) 16:303–17. doi: 10.1007/bf03159976

165. Cassoli JS, Iwata K, Steiner J, Guest PC, Turck CW, Nascimento JM, et al. Effect of MK-801 and Clozapine on the Proteome of Cultured Human Oligodendrocytes. Front Cell Neurosci (2016) 10:52. doi: 10.3389/fncel.2016.00052

166. Dasgupta S, Ray SK. Insights into abnormal sphingolipid metabolism in multiple sclerosis: targeting ceramide biosynthesis as a unique therapeutic strategy. Ther Targets Neurol Dis (2017) 4:e1598. doi: 10.14800/ttnd.1598

167. Brandão-Teles C, Martins-de-Souza D, Guest PC, Cassoli JS. MK-801-Treated Oligodendrocytes as a Cellular Model to Study Schizophrenia. Adv Exp Med Biol (2017) 974:269–77. doi: 10.1007/978-3-319-52479-5_25

168. Thorburne SK, Juurlink BHJ. Low Glutathione and High Iron Govern the Susceptibility of Oligodendroglial Precursors to Oxidative Stress. J Neurochem (1996) 67:1014–22. doi: 10.1046/j.1471-4159.1996.67031014.x 169. Friston KJ. The disconnection hypothesis. Schizophr Res (1998) 30:115–25. doi: 10.1016/s0920-9964(97)00140-0

170. Vega-Riquer JM, Mendez-Victoriano G, Morales-Luckie RA, Gonzalez- Perez O. Five Decades of Cuprizone, an Updated Model to Replicate Demyelinating Diseases. Curr Neuropharmacol (2019) 17:129–41. doi: 10.2174/1570159x15666170717120343

171. Cammer W. The neurotoxicant, cuprizone, retards the differentiation of oligodendrocytes in vitro. J Neurol Sci (1999) 168:116–20. doi: 10.1016/s0022-510x(99)00181-1

172. Kalman B, Laitinen K, Komoly S. The involvement of mitochondria in the pathogenesis of multiple sclerosis. J Neuroimmunol (2007) 188:1–12. doi: 10.1016/j.jneuroim.2007.03.020

173. Pasquini LA, Calatayud CA, Bertone Uña AL, Millet V, Pasquini JM, Soto EF. The neurotoxic effect of cuprizone on oligodendrocytes depends on the presence of pro-inflammatory cytokines secreted by microglia. Neurochem Res (2007) 32:279–92. doi: 10.1007/s11064-006-9165-0

174. Lindner M, Heine S, Haastert K, Garde N, Fokuhl J, Linsmeier F, et al. Sequential myelin protein expression during remyelination reveals fast and efficient repair after central nervous system demyelination. Neuropathol Appl Neurobiol (2008) 34:105–14. doi: 10.1111/j.1365-2990.2007.00879.x

175. Xu H, Yang H-J, Zhang Y, Clough R, Browning R, Li X-M. Behavioral and neurobiological changes in C57BL/6 mice exposed to cuprizone. Behav Neurosci (2009) 123:418–29. doi: 10.1037/a0014477

176. Xiao L, Xu H, Zhang Y, Wei Z, He J, Jiang W, et al. Quetiapine facilitates oligodendrocyte development and prevents mice from myelin breakdown and behavioral changes. Mol Psychiatry (2008) 13:697–708. doi: 10.1038/sj.mp.4002064

177. Wang H-N, Liu G-H, Zhang R-G, Xue F, Wu D, Chen Y-C, et al. Quetiapine Ameliorates Schizophrenia-Like Behaviors and Protects Myelin Integrity in Cuprizone Intoxicated Mice: The Involvement of Notch Signaling Pathway. Int J Neuropsychopharmacol (2015) 19(2):pyv088. doi: 10.1093/ijnp/pyv088

178. Taraboletti A, Walker T, Avila R, Huang H, Caporoso J, Manandhar E, et al. Cuprizone Intoxication Induces Cell Intrinsic Alterations in Oligodendrocyte Metabolism Independent of Copper Chelation. Biochemistry (2017) 56:1518–28. doi: 10.1021/acs.biochem.6b01072

179. Xu H, Yang H-J, Li X-M. Differential effects of antipsychotics on the development of rat oligodendrocyte precursor cells exposed to cuprizone. Eur Arch Psychiatry Clin Neurosci (2014) 264:121–9. doi: 10.1007/s00406-013-0414-3

180. Bénardais K, Kotsiari A, Skuljec J, Koutsoudaki PN, Gudi V, Singh V, et al. Cuprizone [bis(cyclohexylidenehydrazide)] is selectively toxic for mature oligodendrocytes. Neurotox Res (2013) 24:244–50. doi: 10.1007/s12640-013- 9380-9

181. Davis JM, Schaffer CB, Killian GA, Kinard C, Chan C. Important Issues in the Drug Treatment of Schizophrenia. Schizophr Bull (1980) 6:70–87. doi: 10.1093/schbul/6.1.70

182. Ayd FJ Jr. A survey of drug-induced extrapyramidal reactions. JAMA (1961) 175:1054–60. doi: 10.1001/jama.1961.03040120016004

183. Ellenbroek BA. Psychopharmacological treatment of schizophrenia: what do we have, and what could we get? Neuropharmacology (2012) 62:1371–80. doi: 10.1016/j.neuropharm.2011.03.013

184. Allison DB, Mentore JL, Heo M, Chandler LP, Cappelleri JC, Infante MC, et al. Antipsychotic-induced weight gain: a comprehensive research synthesis. Am J Psychiatry (1999) 156:1686–96. doi: 10.1176/ajp.156.11.1686

185. Fang F, Zhang H, Zhang Y, Xu H, Huang Q, Adilijiang A, et al. Antipsychotics promote the differentiation of oligodendrocyte progenitor cells by regulating oligodendrocyte lineage transcription factors 1 and 2. Life Sci (2013) 93:429–34. doi: 10.1016/j.lfs.2013.08.004

186. Kimoto S, Okuda A, Toritsuka M, Yamauchi T, Makinodan M, Okuda H, et al. Olanzapine stimulates proliferation but inhibits differentiation in rat oligodendrocyte precursor cell cultures. Prog Neuropsychopharmacol Biol Psychiatry (2011) 35:1950–6. doi: 10.1016/j.pnpbp.2011.07.011

187. Zhang Y, Xu H, Jiang W, Xiao L, Yan B, He J, et al. Quetiapine alleviates the cuprizone-induced white matter pathology in the brain of C57BL/6 mouse. Schizophr Res (2008) 106:182–91. doi: 10.1016/j.schres.2008.09.013

188. Niu J, Mei F, Li N, Wang H, Li X, Kong J, et al. Haloperidol promotes proliferation but inhibits differentiation in rat oligodendrocyte progenitor cell culturesThis paper is one of a selection of papers published in this special issue entitled “Second International Symposium on Recent Advances in Basic, Clinical, and Social Medicine” and has undergone the Journal's usual peer review process. Biochem Cell Biol (2010) 88:611–20. doi: 10.1139/o09-178

189. Zhang Y, Zhang H, Wang L, Jiang W, Xu H, Xiao L, et al. Quetiapine enhances oligodendrocyte regeneration and myelin repair after cuprizone induced demyelination. Schizophr Res (2012) 138:8–17. doi: 10.1016/j.schres.2012.04.006

190. Xu H, Yang H-J, McConomy B, Browning R, Li X-M. Behavioral and neurobiological changes in C57BL/6 mouse exposed to cuprizone: effects of antipsychotics. Front Behav Neurosci (2010) 4:8. doi: 10.3389/fnbeh.2010.00008

191. Chen X, Liu H, Gan J, Wang X, Yu G, Li T, et al. Quetiapine Modulates Histone Methylation Status in Oligodendroglia and Rescues Adolescent Behavioral Alterations of Socially Isolated Mice. Front Psychiatry (2020) 10:984. doi: 10.3389/fpsyt.2019.00984

192. Melka MG, Rajakumar N, O'Reilly R, Singh SM. Olanzapine-induced DNA methylation in the hippocampus and cerebellum in genes mapped to human 22q11 and implicated in schizophrenia. Psychiatr Genet (2015) 25:88–94. doi: 10.1097/YPG.0000000000000069

193. Melka MG, Laufer BI, McDonald P, Castellani CA, Rajakumar N, O'Reilly R, et al. The effects of olanzapine on genome-wide DNA methylation in the hippocampus and cerebellum. Clin Epigenet (2014) 6:1. doi: 10.1186/1868-7083-6-1

194. Aoyama Y, Mouri A, Toriumi K, Koseki T, Narusawa S, Ikawa N, et al. Clozapine ameliorates epigenetic and behavioral abnormalities induced by phencyclidine through activation of dopamine D1 receptor. Int J Neuropsychopharmacol (2014) 17:723–37. doi: 10.1017/s1461145713001466

195. Gjerde PB, Jørgensen KN, Steen NE, Melle I, Andreassen OA, Steen VM, et al. Association between olanzapine treatment and brain cortical thickness and gray/white matter contrast is moderated by cholesterol in psychotic disorders. Psychiatry Res Neuroimaging (2018) 282:55–63. doi: 10.1016/ j.pscychresns.2018.10.001

196. Steiner J, Martins-de-Souza D, Schiltz K, Sarnyai Z, Westphal S, Isermann B, et al. Clozapine promotes glycolysis and myelin lipid synthesis in cultured oligodendrocytes. Front Cell Neurosci (2014) 8:384. doi: 10.3389/fncel.2014.00384

197. Fernø J, Raeder MB, Vik-Mo AO, Skrede S, Glambek M, Tronstad K-J, et al. Antipsychotic drugs activate SREBP-regulated expression of lipid biosynthetic genes in cultured human glioma cells: a novel mechanism of action? Pharmacogenom J (2005) 5:298–304. doi: 10.1038/sj.tpj.6500323

198. Mauch DH. CNS Synaptogenesis Promoted by Glia-Derived Cholesterol. Science (2001) 294:1354–7. doi: 10.1126/science.294.5545.1354

199. Suzuki R, Lee K, Jing E, Biddinger SB, McDonald JG, Montine TJ, et al. Diabetes and insulin in regulation of brain cholesterol metabolism. Cell Metab (2010) 12:567–79. doi: 10.1016/j.cmet.2010.11.006

200. Emamian ES, Hall D, Birnbaum MJ, Karayiorgou M, Gogos JA. Convergent evidence for impaired AKT1-GSK3beta signaling in schizophrenia. Nat Genet (2004) 36:131–7. doi: 10.1038/ng1296

201. Zhao Z, Ksiezak-Reding H, Riggio S, Haroutunian V, Pasinetti GM. Insulin receptor deficits in schizophrenia and in cellular and animal models of insulin receptor dysfunction. Schizophr Res (2006) 84:1–14. doi: 10.1016/j.schres.2006.02.009

202. Prickaerts J. Transgenic Mice Overexpressing Glycogen Synthase Kinase 3beta: A Putative Model of Hyperactivity and Mania. J Neurosci (2006) 26:9022–9. doi: 10.1523/jneurosci.5216-05.2006

203. Siuta MA, Robertson SD, Kocalis H, Saunders C, Gresch PJ, Khatri V, et al. Dysregulation of the norepinephrine transporter sustains cortical hypodopaminergia and schizophrenia-like behaviors in neuronal rictor null mice. PloS Biol (2010) 8:e1000393. doi: 10.1371/journal.pbio.1000393

204. Brandão-Teles C, de Almeida V, Cassoli JS, Martins-de-Souza D. Biochemical Pathways Triggered by Antipsychotics in Human [corrected] Oligodendrocytes: Potential of Discovering New Treatment Targets. Front Pharmacol (2019) 10:186. doi: 10.3389/fphar.2019.00186

205. Luo F, Burke K, Kantor C, Miller RH, Yang Y. Cyclin-Dependent Kinase 5 Mediates Adult OPC Maturation and Myelin Repair through Modulation of Akt and GsK-3 Signaling. J Neurosci (2014) 34:10415–29. doi: 10.1523/ jneurosci.0710-14.2014

206. Szeszko PR, Robinson DG, Ashtari M, Vogel J, Betensky J, Sevy S, et al. Clinical and Neuropsychological Correlates of White Matter Abnormalities in Recent Onset Schizophrenia. Neuropsychopharmacology (2008) 33:976–84. doi: 10.1038/sj.npp.1301480

207. Nestor PG, Kubicki M, Gurrera RJ, Niznikiewicz M, Frumin M, McCarley RW, et al. Neuropsychological Correlates of Diffusion Tensor Imaging in Schizophrenia. Neuropsychology (2004) 18:629–37. doi: 10.1037/0894-4105.18.4.629

208. Ho B-C, Andreasen NC, Nopoulos P, Arndt S, Magnotta V, Flaum M. Progressive structural brain abnormalities and their relationship to clinical outcome: a longitudinal magnetic resonance imaging study early in schizophrenia. Arch Gen Psychiatry (2003) 60:585–94. doi: 10.1001/

archpsyc.60.6.585

209. Oka A, Belliveau MJ, Rosenberg PA, Volpe JJ. Vulnerability of oligodendroglia to glutamate: pharmacology, mechanisms, and prevention. J Neurosci (1993) 13:1441–53. doi: 10.1523/jneurosci.13-04-01441.1993

210. Agrawal SK, Fehlings MG. Role of NMDA and Non-NMDA Ionotropic Glutamate Receptors in Traumatic Spinal Cord Axonal Injury. J Neurosci (1997) 17:1055–63. doi: 10.1523/jneurosci.17-03-01055.1997

211. Rands GSJ. Memantine as a neuroprotective treatment in schizophrenia. Br J Psychiatry (2005) 186:77–7. doi: 10.1192/bjp.186.1.77-a

212. Manning SM, Talos DM, Zhou C, Selip DB, Park H -K., Park C -J., et al. NMDA Receptor Blockade with Memantine Attenuates White Matter Injury in a Rat Model of Periventricular Leukomalacia. J Neurosci (2008) 28:6670–8. doi: 10.1523/jneurosci.1702-08.2008

213. D'Aniello G. The Role of D-Aspartic Acid and N-Methyl-D-Aspartic Acid in the Regulation of Prolactin Release. Endocrinology (2000) 141:3862–70. doi: 10.1210/en.141.10.3862

214. Errico F, Rossi S, Napolitano F, Catuogno V, Topo E, Fisone G, et al. Daspartate prevents corticostriatal long-term depression and attenuates schizophrenia-like symptoms induced by amphetamine and MK-801. J Neurosci (2008) 28:10404–14. doi: 10.1523/JNEUROSCI.1618-08.2008

215. de Rosa V, Secondo A, Pannaccione A, Ciccone R, Formisano L, Guida N, et al. D-Aspartate treatment attenuates myelin damage and stimulates myelin repair. EMBO Mol Med (2019) 11(1):e9278. doi: 10.15252/emmm.201809278

216. Yang Y, Ge W, Chen Y, Zhang Z, Shen W, Wu C, et al. Contribution of astrocytes to hippocampal long-term potentiation through release of Dserine. Proc Natl Acad Sci (2003) 100:15194–9. doi: 10.1073/pnas.2431073100

217. Tsai G, Yang P, Chung LC, Lange N, Coyle JT. D-serine added to antipsychotics for the treatment of schizophrenia. Biol Psychiatry (1998) 44:1081–9. doi: 10.1016/s0006-3223(98)00279-0

218. Makoukji J, Belle M, Meffre D, Stassart R, Grenier J, Shackleford G, et al. Lithium enhances remyelination of peripheral nerves. Proc Natl Acad Sci (2012) 109:3973–8. doi: 10.1073/pnas.1121367109

219. Fang X-Y, Zhang W-M, Zhang C-F, Wong W-M, Li W, Wu W, et al. Lithium accelerates functional motor recovery by improving remyelination of regenerating axons following ventral root avulsion and reimplantation. Neuroscience (2016) 329:213–25. doi: 10.1016/j.neuroscience.2016.05.010

220. Dube S, Sethi BB. Efficacy of lithium in schizophrenia. Indian J Psychiatry (1981) 23:193–9.

221. Do KQ, Trabesinger AH, Kirsten-Krüger M, Lauer CJ, Dydak U, Hell D, et al. Schizophrenia: glutathione deficit in cerebrospinal fluid and prefrontal cortex in vivo. Eur J Neurosci (2000) 12:3721–8. doi: 10.1046/j.1460-9568.2000.00229.x

222. Berk M, Copolov D, Dean O, Lu K, Jeavons S, Schapkaitz I, et al. N-acetyl cysteine as a glutathione precursor for schizophrenia–a double-blind, randomized, placebo-controlled trial. Biol Psychiatry (2008) 64:361–8. doi: 10.1016/j.biopsych.2008.03.004

223. Molina-Holgado E, Vela JM, Arévalo-Martín A, Almazán G, Molina- Holgado F, Borrell J, et al. Cannabinoids promote oligodendrocyte progenitor survival: involvement of

cannabinoid receptors and phosphatidylinositol-3 kinase/Akt signaling. J Neurosci (2002) 22:9742–53. doi: 10.1523/JNEUROSCI.22-22-09742.2002

224. Gomez O, Sanchez-Rodriguez A, Le M, Sanchez-Caro C, Molina-Holgado F, Molina-Holgado E. Cannabinoid receptor agonists modulate oligodendrocyte differentiation by activating PI3K/Akt and the mammalian target of rapamycin (mTOR) pathways. Br J Pharmacol (2011) 163:1520–32. doi: 10.1111/j.1476-5381.2011.01414.x

225. Mecha M, Torrao AS, Mestre L, Carrillo-Salinas FJ, Mechoulam R, Guaza C. Cannabidiol protects oligodendrocyte progenitor cells from inflammation induced apoptosis by attenuating endoplasmic reticulum stress. Cell Death Dis (2012) 3:e331. doi: 10.1038/cddis.2012.71

Conflict of Interest: The authors declare that the research was conducted in the absence of any commercial or financial relationships that could be construed as a potential conflict of interest.

6. CAPÍTULO II

Artigo em preparação para ser submetido.

THE EFFECTS OF ANTIPSYCHOTICS AND CANNABIDIOL ON THE PROTEOME OF OLIGODENDROCYTES *IN VITRO* IN A DEMYELINATION CONTEXT

Ana Caroline Brambilla Falvella[1], Valéria de Almeida[1], Aline F. Valença[1], Lícia C. Silva-Costa[1], Bradley Joseph Smith[1], Fernanda Crunfli[1], Antônio W. Zuardi[5], Jaime E. Hallak[5], José A. Crippa[5], Daniel Martins-de-Souza[1,2,3,4#]

1. Laboratory of Neuroproteomics, Department of Biochemistry and Tissue Biology, Institute of Biology, University of Campinas (UNICAMP), Campinas, Brazil

2. Instituto Nacional de Biomarcadores em Neuropsiquiatria (INBION) Conselho Nacional de Desenvolvimento Científico e Tecnológico, São Paulo, Brazil

3. Experimental Medicine Research Cluster (EMRC), University of Campinas, Campinas, SP, Brazil

4. D'Or Institute for Research and Education (IDOR), São Paulo, Brazil

5. Department of Neuroscience and Behavior, University of São Paulo, Ribeirão Preto, Brazil

Corresponding author

Daniel Martins-de-Souza

Laboratory of Neuroproteomics

Department of Biochemistry and Tissue Biology

University of Campinas (UNICAMP)

Rua Monteiro Lobato, 255

13083-862 - Campinas, SP, Brazil

Tel: +55 19 3521-6129

E-mail: dmsouza@unicamp.br

ABSTRACT

Schizophrenia is a psychiatric disorder that affects 1% of people worldwide. Antipsychotics are the most commonly chosen option for treatment, and are effective in regards to positive symptoms; however, they are oftentimes not useful for treating negative or cognitive symptoms. All three classes of symptoms have been found to be associated with neuronal dysconnectivity, which has also been implicated in oligodendrocyte abnormalities in white matter. In this context, we developed an *in vitro* assay of cuprizone-mediated death in a human oligodendrocyte precursor cell line (MO3.13) to test the effects of antipsychotics (clozapine and haloperidol), cannabidiol and benztropine in terms of their potential protective effects. After the treatments mentioned above, the proteome was extracted and digested for analysis by nano-chromatography coupled with mass spectrometry to investigate the proteins and pathways affected in oligodendrocytes that were treated by these drugs. We confirm that the *in vitro* model for cuprizone cell death is cytotoxic to MO3.13 oligodendrocyte viability through disturbances of several biological processes, including energy and lipid metabolism, genetic processes and growth signaling. Furthermore, the administration of antipsychotics, cannabidiol, and benztropine seems to modulate metabolism, genetic factors, cell cycle, and cell signaling, pathways related to cuprizone-induced cell death, indicating their potential to act against the cuprizone toxic effect. In conclusion, although modeling OL death with cuprizone does not represent the entirety of the pathophysiology of the disorder, these results provide insight into the mechanisms related to antipsychotics' and cannabidiol's effects against the cuprizone toxicity effect and their implications for developing new pharmaceutical targets and treatment options for schizophrenia.

Keywords: antipsychotics, cannabidiol, cuprizone, MO3.13 oligodendrocyte, schizophrenia.

INTRODUCTION

Schizophrenia is a severe and chronic mental disorder characterized by positive (delusions and hallucinations), negative (lack of motivation, poverty of speech, and social withdrawal) and cognitive symptoms (slower information processing and impaired working memory) (Azorin et al. 2014; Owen et al. 2016). Treatment is based on antipsychotics, which are classified as typical, such as haloperidol, or atypical, including clozapine, the prototype of this drug class (Leucht et al. 2009; van Os and Kapur 2009) and has since become an important treatment option in the clinic. Typical antipsychotics are D_2 receptor antagonists and are effective in reducing the positive symptoms, but often cause extrapyramidal side effects (Howes et al. 2015; Howes and Kapur 2009). In contrast, atypical compounds have an affinity for both D_2 and 5-HT_2 receptors, and can additionally attenuate negative symptoms more than typical antipsychotics (Leucht et al. 2009).

In regards to the physiopathology of schizophrenia, symptoms have been associated with white matter abnormalities and brain dysconnectivity (Bernard et al. 2015; Orban et al. 2017; Saito et al. 2018). Several findings suggest that neuronal dysconnectivity occurs via a dysfunction in axon myelination due to oligodendrocyte (OL) disturbances (Cassoli et al. 2015; Jørgensen et al. 2016; Vikhreva et al. 2016). These glial cells are responsible for forming the myelin sheath in the central nervous system (CNS), ensuring efficient impulse conduction and providing metabolic support for neurons (Buntinx et al. 2003; Lee et al. 2011; Simons and Nave 2015). Studies have demonstrated an abnormality in the expression of genes and proteins related to myelin and OLs in post-mortem brain samples of schizophrenia patients (Georgieva et al. 2006; Saia-Cereda et al. 2015; Voineskos et al. 2008). Additionally, alterations in the density, distribution, and morphology of these cells have been seen in schizophrenia patients (Bernstein et al. 2015; Uranova et al. 2018; Vikhreva et al. 2016). Studies have also shown impairments in oligodendrogenesis and differentiation of the oligodendrocyte progenitor cells (OPCs) in schizophrenia (Hattori et al. 2014; Santos et al. 2019). Thus, the biology of the OPCs and mature OLs is an important hub to understand the role of these cells in the pathophysiology of -- and the development of new treatment for -- schizophrenia (de Almeida and Martins-de-Souza 2018).

Several findings suggest that antipsychotics and cannabidiol affect myelin and OLs, indicating their potential therapeutic in neurodegenerative disorders and schizophrenia (Bartzokis et al. 2007; Bartzokis et al. 2009; Rahimi et al., 2015; Zajicek & Apostu, 2011).

Benztropine is a molecule used for treatment of Parkinson's disease, and enhances OLs differentiation and myelination in an *in vitro* and *in vivo* model (Deshmukh et al., 2013; Ettle et al., 2016; Thompson et al., 2018). That drug probably acts in immature OL and the muscarinic receptors antagonism is the mechanism of action (Deshmukh et al., 2013; Ettle et al., 2016). However, the role of these receptors and the molecular mechanism involved in improvement of myelination and OL differentiation is unclear.

In this context, the molecular mechanisms involved in demyelination, remyelination, and oligodendrocyte abnormalities are investigated by the cuprizone demyelination model. Cuprizone is a copper-chelating agent that inhibits several enzymes that use copper as a cofactor, including cytochrome oxidase, succinyl dehydrogenase and monoamine oxidase (Messori et al. 2007; Petronilli and Zoratti 1990; Venturini 1973). Consequently, this drug induces OL apoptosis, microglial activation and demyelination in the corpus callosum, hippocampus, and superior cerebellar peduncle in the animal models of demyelination (Goldberg et al. 2013; Sachs et al. 2014). Disturbances of energy and protein metabolism have been reported as the molecular mechanisms of cuprizone toxicity, in addition to the resulting increases in oxidative and endoplasmic reticulum stress in OLs (Biancotti et al. 2008; Goldberg et al. 2013; Praet et al. 2014; Taraboletti et al. 2017).

This study aimed to ascertain whether antipsychotics and cannabidiol induce protective molecular mechanisms, such as benztropine, against cuprizone-mediated toxicity in a human oligodendrocyte precursor cell line (MO3.13). Proteomic assays detected changes induced by antipsychotics (haloperidol and clozapine), cannabidiol, and benztropine in MO3.13 cells previously exposed to cuprizone.

METHODS

1. Cell culture and treatment

Human hybrid MO3.13 oligodendrocytes express phenotypic characteristics of immature OLs (Buntinx et al. 2003; Iwata et al. 2013). These cells have been used in our group to understand molecular mechanisms related to schizophrenia and its treatment (Brandão-Teles et al. 2019; Cassoli et al. 2016; Seabra et al. 2020). Here, MO3.13 cells were cultured in DMEM (Sigma) supplemented with 10% FBS and 1% penicillin/streptomycin and grown at 37ºC and 5% CO_2 as described previously (Brandão-Teles et al. 2017; Iwata et al. 2013).

Stocks of cuprizone (28,05mM; Sigma), haloperidol (53mM; Cristália), clozapine (25mM; Cristália), or cannabidiol (25mM; USP Ribeirão) were made in DMSO, and the final concentration of DMSO in the medium was limited to 0.042%. Benztropine (6mM) was dissolved in ddH2O. Saline in DMSO (final concentration of DMSO in medium 0.042%) was used as a control. Based on our pilot experiments and previous studies (Bénardais et al. 2013; Deshmukh et al. 2013; Ettle et al. 2016; Mecha et al. 2012; Xu et al. 2014), MO3.13 cells were seeded in six-well plates at a density of 115.000 cells/well and treated with 10μM of cuprizone for 48 hours or with 1μM of haloperidol, clozapine, cannabidiol, or benztropine for 24 hours. For the co-treatment, the cells were treated with cuprizone for 48 hours, with the other drugs being added for the last 24 hours of the treatment, all at the previously mentioned concentrations.

2. MTT assay

For MTT assays, cells were seeded in 96-well plates at a density of 7.000 cells/well for 24 hours. After incubation, the medium was aspirated and replaced with new media containing increasing concentrations of cuprizone for 48 hours, or haloperidol, clozapine, cannabidiol, or benztropine for 8 hours. Following the treatment, 0.5mg/mL of MTT was added to each well. Each plate was incubated for 2 hours at 37ºC; ethanol, 100% was added and the absorbance was read at 570 nm on a plate spectrophotometer. Data are expressed as mean ± SEM and one-way analysis of variance (ANOVA) was used to analyze the statistical significance, followed by Dunnett post hoc test. ($p<0.05$).

3. Proteome extraction

After treatment, cells were collected and centrifuged at 4°C and 1,200x*g* for 5 min. The pellets were homogenized in a lysis buffer (Tris pH 6,8, 1 M; SDS 20%) with protease

inhibitor (final working concentration, 1x; Roche; Mannheim, Germany). Each sample underwent a short run through a polyacrylamide gel to remove buffer salts and other contaminants before peptide digestion was performed *in gel*. 100µL of 10mM of dithiothreitol stock (15.4mg DTT in 10mL of 50mM ammonium bicarbonate - Ambic), 100µL of 55mM of iodoacetamide stock (102mg IAA in 10mL of 50mM Ambic), and 200µL of acetonitrile 100% were added in each sample. Proteins were digested by trypsin for 16-18 hours at 37ºC and the peptide concentrations were determined by the BSA assay kit (Sigma).

4. NanoLC-ESI MS/MS

Proteomic analyses were performed in a bidimensional nanoAcquity UPLC M-Class (Waters Corporation, Milford, MA) coupled to a Synapt G2-Si mass spectrometer (Waters Corporation, Milford, MA). The samples were fractionated in 5 fractions using discontinuous steps of acetonitrile (11.4, 14.7, 17.4, 20.7, and 50%) before separation with a continuous acetonitrile gradient from 7% to 40% (v/v) on reverse-phase C18 columns. MS/MS analyses were performed in data-independent acquisition (DIA) mode using UDMS^{E} after performing a manual ion selection method profile for each fraction using DriftScape (version 2.9).

5. Data processing and protein identification

MS/MS spectra were analyzed with Progenesis® QI for Proteomics (version 3.1) with Apex3D, peptide 3D, and ion accounting informatics (Waters). Proteins were identified using the Reviewed Uniprot human database (obtained 11/2019) and quantified using the Top3 method. The following parameters were used in the identification of peptides/proteins: Digestion by trypsin with a maximum of one missed cleavage; Maximum protein mass of 600 kDa; False discovery rate (FDR) less than 1%; at least two fragments per peptide; Two or more peptides per protein; Five or more fragments per protein; One or more unique peptide per protein; and a mass error ≤ 20ppm. Proteins were considered to be differentially expressed when one-way analysis of variance (ANOVA) returned a p-value < 0.05.

6. *In silico* analyses

Affected biological processes and biochemical pathways were analyzed using Reactome (Fabregat et al. 2018), David bioinformatics database (Huang et al. 2009; Huang et al. 2009), and Proteomaps (Liebermeister et al. 2014). Biological processes and protein networks were analyzed using Metascape (Zhou et al. 2019), Cytoscape (Franz et al. 2016; Szklarczyk et al. 2017) and ClustVis (Metsalu and Vilo 2015).

RESULTS

1. MTT assay

To determine cuprizone toxicity, we performed an *in vitro* assay of cuprizone-induced death on the oligodendrocyte cell line MO3.13. These cells were treated with increasing concentrations of cuprizone for 48 hours and viability was measured with the MTT assay. All cells treated with cuprizone displayed a loss of viability after 48 hours (figure S1).

We confirmed that the concentrations used in previous studies for these antipsychotics, cannabidiol, and benztropine (Deshmukh et al. 2013; Mecha et al. 2012; Xu et al. 2014) are not cytotoxic to the MO3.13 cell line under this experiment's conditions. To do so, we used the MTT assay to ensure that the cytotoxic cutoff for these compounds is sufficiently above these concentrations after 8 hours of incubation. As the concentrations tested were increased, viability dropped to a significant degree after 75μM of clozapine, 50μM of haloperidol, 4μM of cannabidiol and 100μM of benztropine (figure S2). This confirmed that the previously used concentrations of 10μM for cuprizone induces a cytotoxic effect in these cells and 1μM for antipsychotics, cannabidiol and benztropine (Bénardais et al. 2013; Deshmukh et al. 2013; Taraboletti et al. 2017; Xu et al. 2014) are not cytotoxic and were used during treatment and co-treatment assays for subsequent proteomic analysis.

2. Proteomic analyses

2.1 Proteome of oligodendrocytes treated with benztropine, antipsychotics or cannabidiol

We identified a total of 196 differentially expressed proteins in OLs treated with benztropine (table S1). This drug can affect pathways related to metabolic processes, metabolism of RNA, cell cycle, post-translational modification, immune system and cell redox homeostasis (figure 1 and table S10). When compared to cells treated with vehicle alone, treatment with haloperidol, clozapine or cannabidiol resulted in 91, 292, and 106 differentially expressed proteins, respectively (table S1). Cells treated with clozapine and benztropine had the most overlap of gene names among all groups (figure 2A). Regarding biological processes, all drugs caused changes in RNA metabolism, regulation of chromosome organization, regulation of mRNA metabolic processes, protein localization to the nucleus, the microtubule-based process, regulated exocytosis, RHO GTPase effectors and membrane trafficking (figure 2B).

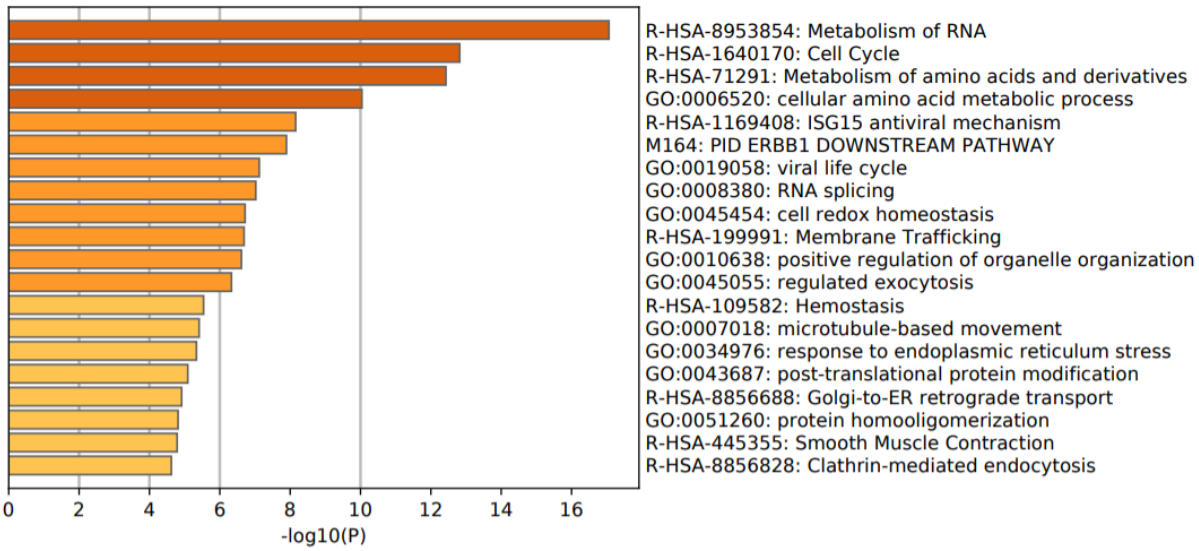

Figure 1. Bar graph of enriched biochemical pathways in MO3.13 cells treated with benztropine, colored by p-value, created in Metascape. Colored lines represent -$\log_{10}$(P), which significance are represent between 10^{-20} to 10^{-2}.

A

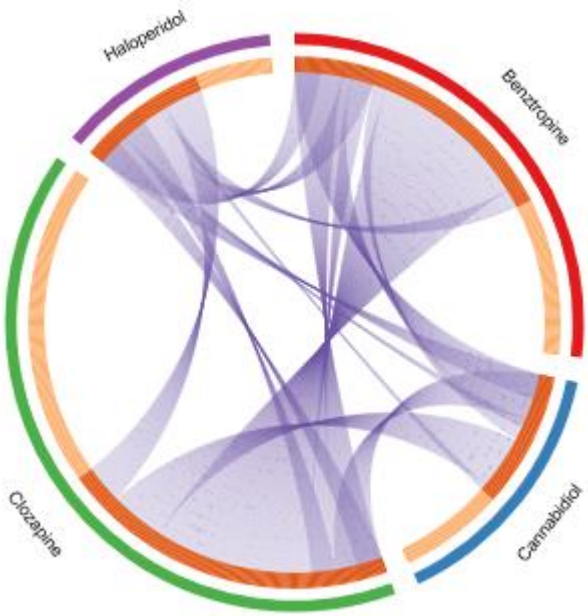

B

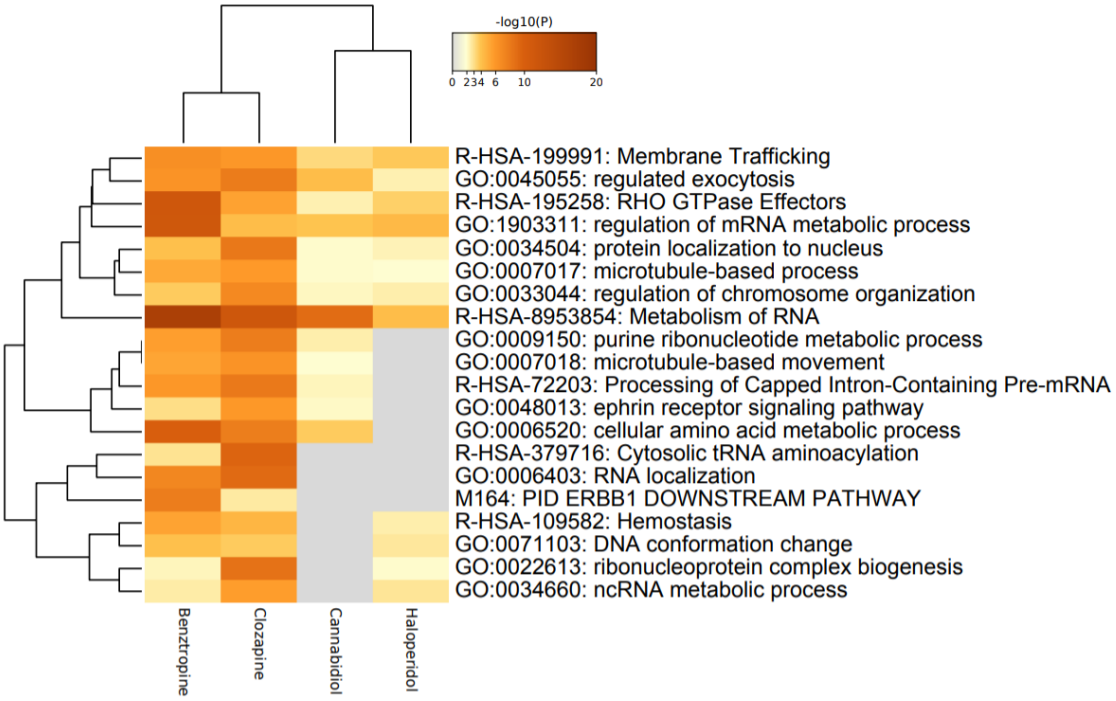

Figure 2. Chord diagram where purple curves link identical genes between clozapine, cannabidiol, haloperidol, and benztropine treatment (A); and a heatmap of enriched pathways in OLs treated with these drugs (B), created in Metascape.

2.3 Proteome of oligodendrocytes treated with cuprizone

A total of 2019 and 1774 proteins were identified and quantified, respectively, 30 of which were differentially expressed in OLs in response to cuprizone treatment (figure 3 and table S1). Citrate synthase (CS) and AMP deaminase 2 (AMPD2), both metabolism-related proteins, were among those differentially expressed. Thioredoxin-dependent peroxide reductase (PRDX3) and E3 ubiquitin/ISG15 ligase (TRIM25), of the immune system, were also present. Serine/arginine-rich splicing factor 9 (SRSF9), related to genetic information processing, and annexin 5 (ANX5) and 26S proteasome non-ATPase regulatory subunit 4 (PSMD4), both associated with apoptosis, were also found (figure 4). Overall, it appears that cuprizone can affect, to a certain degree, pathways related to translation, transcription, signal transduction and DNA maintenance (ribonucleoprotein complex assembly), as well as affecting biosynthesis pathways (carboxylic acid biosynthetic process), the immune system, biological process response to stress, AKT signaling and the cellular process plasma membrane-bounded cell projection assembly (figure 5 and table 1).

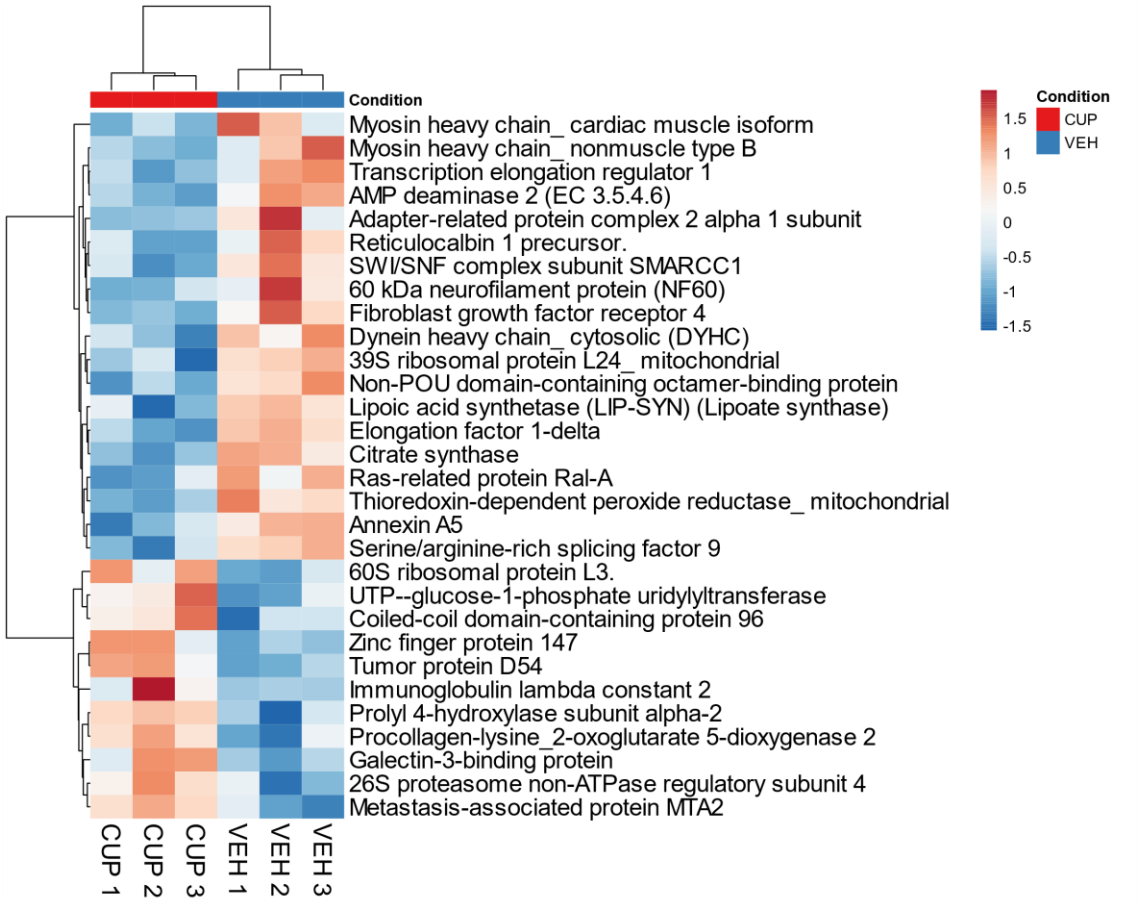

Figure 3. Proteins differentially expressed in OLs treated with 10μM of cuprizone (CUP) for 48 hours, compared to the vehicle (VEH), created with ClustVis.

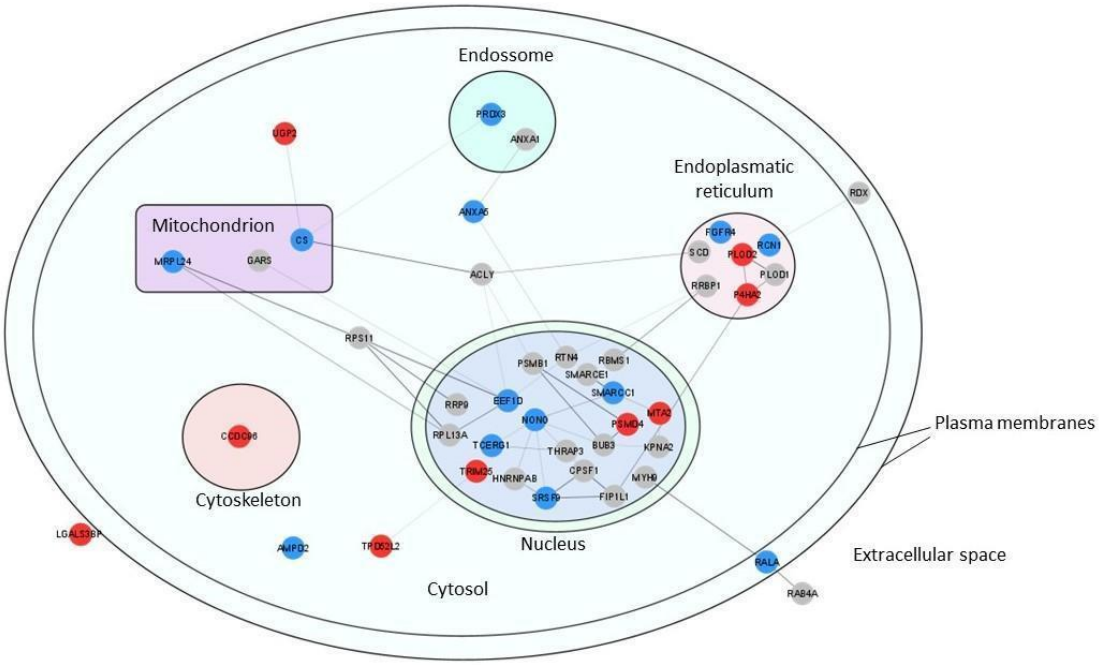

Figure 4. <u>Prospective network interaction of proteins differentially expressed on oligodendrocytes treated with cuprizone.</u> The network was generated in Cytoscape from differentially expressed proteins resulting from cuprizone treatment (10μM, 48h). Colored lines represent a strong interaction; red spheres are upregulated proteins; blue spheres are downregulated proteins. All colored spheres represent $p<0.05$; to better show potential interconnectivity, gray spheres were added with a higher cutoff ($p<0.10$).

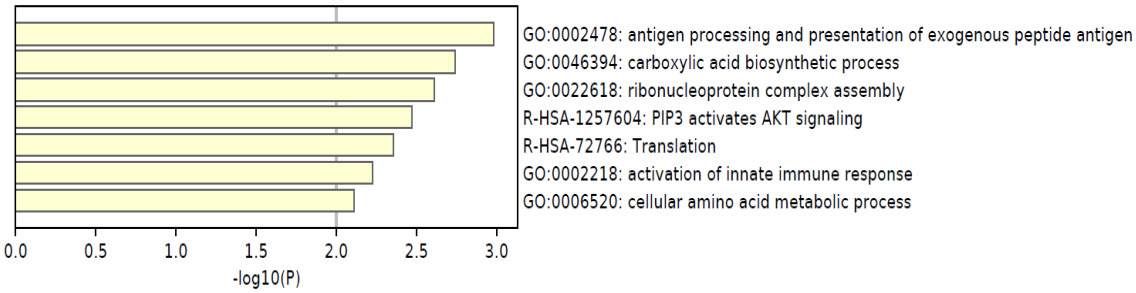

Figure 5. Bar graph of the enriched pathways in OLs resulting from cuprizone treatment (10μM, 48h), generated with Metascape.

Table 1. Biochemical pathways highlighted in treatment with cuprizone (10μM, 48h), generated with Reactome.

Biochemical pathway	p-value
FGFR4 mutant receptor activation	0.003
betaKlotho-mediated ligand binding	0.008
Formation of the active cofactor, UDP-glucuronate	0.008
Collagen biosynthesis and modifying enzymes	0.013
Nef Mediated CD8 Down-regulation	0.021
Collagen formation	0.023
PCP/CE pathway	0.024
EPH-Ephrin signaling	0.024
Nef Mediated CD4 Down-regulation	0.026
Signaling by FGFR4 in disease	0.031
NF-kB activation through FADD/RIP-1 pathway mediated by caspase-8 and -10	0.031
VLDLR internalization and degradation	0.031
WNT5A-dependent internalization of FZD2, FZD5, and ROR2	0.034
Purine salvage	0.034
PIP3 activates AKT signaling	0.035
FGFR4 ligand binding and activation	0.036
Retrograde neurotrophin signaling	0.036
TRAF3-dependent IRF activation pathway	0.036
p38MAPK events	0.036
Signaling by NTRK1 (TRKA)	0.038
Phospholipase C-mediated cascade; FGFR4	0.039
WNT5A-dependent internalization of FZD4	0.039
Glycogen synthesis	0.041
Trafficking of GluR2-containing AMPA receptors	0.044
Platelet degranulation	0.045

2.4 Proteome of oligodendrocytes co-treated with cuprizone and antipsychotics, cannabidiol, or benztropine

When compared to cells treated with cuprizone alone, co-treatment with cuprizone and either haloperidol (CupHal), clozapine (CupClz), cannabidiol (CupCBD), or benztropine

(CupBenz) resulted in 95, 91, 74, and 113 differentially expressed proteins, respectively (table S1). In the antipsychotics groups, proteins were mostly associated with metabolism; the immune system; the cytoskeleton; signal transduction; the genetic information process; cell growth; and cell death. In response to cannabidiol co-treatment, proteins related to energy and lipid metabolism, signal transduction and the genetic information process. Finally, the benztropine co-treatment modulated proteins related to amino acid and lipid metabolism; cellular response to external stimuli (such as amino acid deficiency and DNA damage); signaling transduction; the cytoskeleton; and the genetic information process.

The changes seen in the CupBenz group had some similarities in affected genes when compared with the changes induced by other treatment groups: CupHal, 12 genes (3.8% of total significantly altered genes); CupCLZ, 4 (1.3%); and CupCBD, 10 (3.2%) (figure 6A). All co-treatments caused changes ($-\log_{10}(P)$:10^{-20} to 10^{-2}) in proteins related to RNA metabolism, ribonucleoprotein complex biogenesis, nuclear-transcript mRNA catabolic process, the cell cycle and supramolecular fiber organization (figure 6B). Some biological processes were not found in all co-treatments, such as the ATP metabolic process, altered only in the co-treatment with cannabidiol, and the cellular amino acid metabolic process was changed by benztropine and haloperidol co-treatments (figures 6, S7A, and S7B).

A

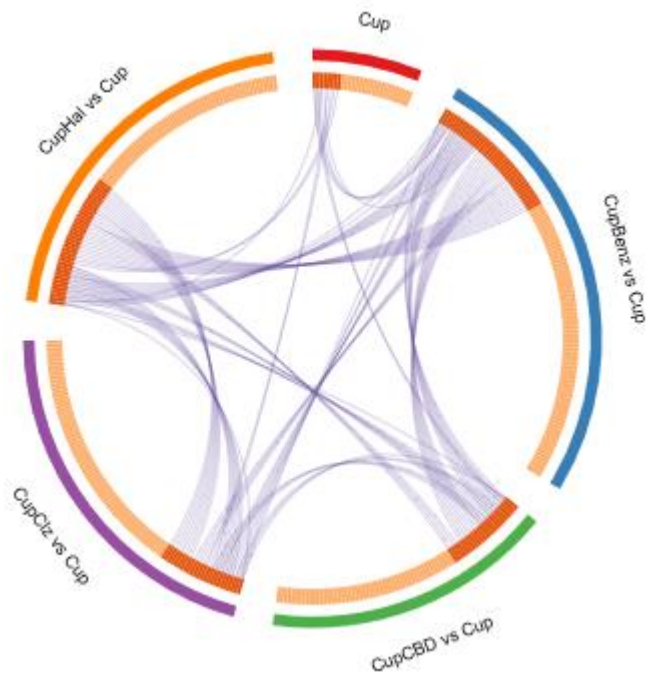

B

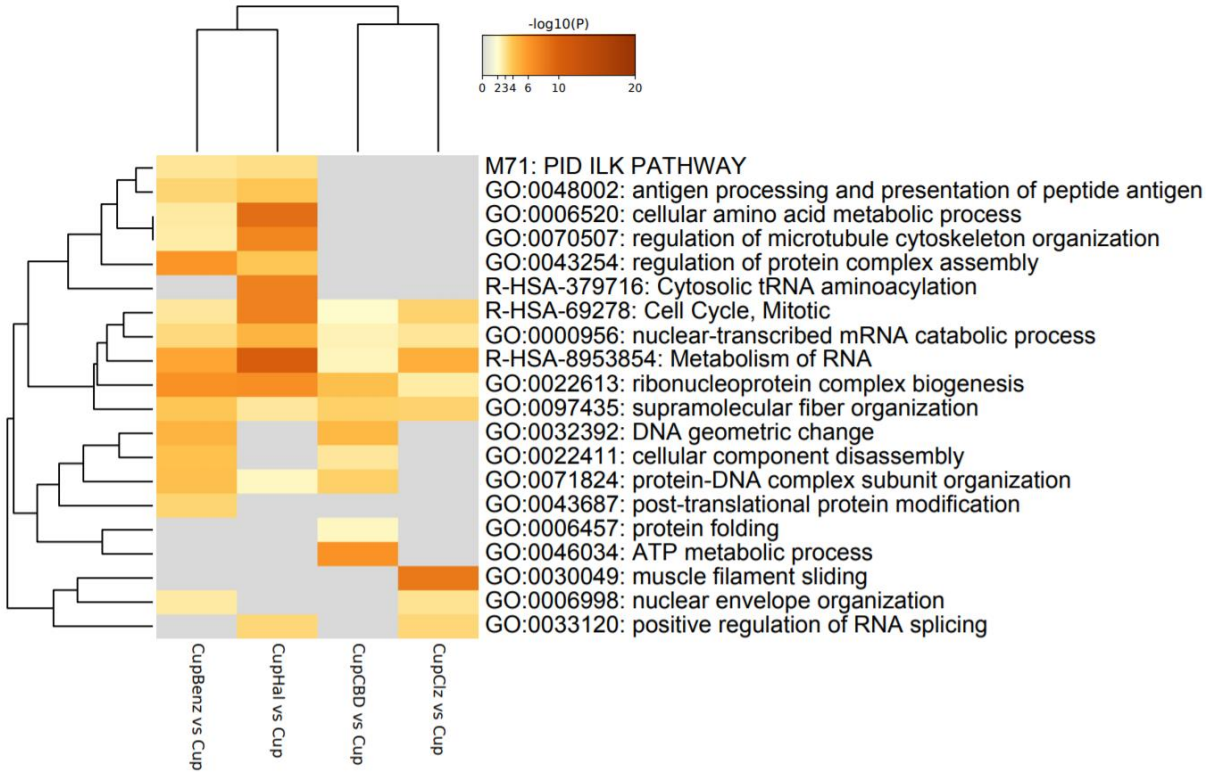

Figure 6. Chord diagram where purple curves link identical genes between cuprizone treatment (Cup) and co-treatment with cuprizone and clozapine (CupClz), cannabidiol (CupCBD), haloperidol (CupHal) or benztropine (CupBenz) (A); and a heatmap of enriched pathways of oligodendrocytes co-treated with cuprizone and haloperidol, cannabidiol, clozapine, or benztropine (B), created in Metascape.

DISCUSSION

Comparing the effects of antipsychotics and cannabidiol with the putative protective effects of benztropine on the proteome of MO3.13 oligodendrocytes

Several studies have demonstrated that many antipsychotics, cannabidiol, and benztropine all have the potential to influence oligodendrocytes (OLs) and induce myelination (Deshmukh et al. 2013; Ren et al. 2013; Xu et al. 2014; Zajicek and Apostu 2011). Here, we found changes in the constituent proteins of several molecular mechanisms and biological processes in OLs resulting from the administration of benztropine, which induces oligodendrocyte progenitor cell (OPC) differentiation and myelination (Deshmukh et al. 2013). We then compared these results with MO3.13 OLs treated with two antipsychotics (haloperidol and clozapine) and cannabidiol, in terms of their hypothesized ability to induce protective molecular mechanisms.

Lipid and Energy Metabolism

Benztropine is a molecule that is known to be able to improve myelination; but a comprehensive understanding of its mechanism of action beyond its primary interacting partners is still lacking (Deshmukh et al. 2013; Ettle et al. 2016). This drug enhances membrane and cholesterol biogenesis in OLs and induces OL formation by decreasing the basal level of sterol (Ettle et al., 2016; Hubler et al. 2018). Benztropine treatment modulates proteins related to the glycolytic, lipid and amino acid pathway (figure 1 and table S10). Our findings reported that benztropine treatment downregulated the levels of 3-hydroxyacyl-CoA dehydrogenase, type-2, which act in mitochondrial fatty acid beta-oxidation (He et al. 1998). Levels of delta (24)-sterol reductase were also found upregulated by benztropine, which reduces an intermediate in cholesterol metabolism and protects cells against oxidative stress (table S15). These results support the hypothesis that benztropine induces myelination and protective effect on OL by molecular mechanisms.

Studies have reported that some drugs such as antipsychotics and cannabidiol can have protective effects against energy deprivation by modulating glucose metabolism (Steiner et al. 2011; Steiner et al. 2014; Sun et al. 2017). In studies involving MK-801, an NMDA receptor antagonist and model for schizophrenia (Li et al. 2013; Paulson et al. 2004), clozapine treatment after MK-801 exposure was found to decrease ALDOC levels, a glycolytic enzyme, and increases cholesterol and triacylglycerol levels in schizophrenia patients (Cassoli et al. 2016; Wu et al. 2006). Haloperidol administration alone similarly modulates proteins related to glycolysis and gluconeogenesis but inhibits cholesterol biosynthesis in cultured cells (Brandão-Teles et al. 2019; Sánchez-Wandelmer et al. 2010). Confirming that haloperidol and clozapine alters cholesterol metabolism in MO3.13 cells has pharmacological relevance to the long-term administration of these drugs. Studies have demonstrated that cannabidiol can attenuate cell damage by promoting mitochondrial function and biogenesis, modulating glucose metabolism via the pentose-phosphate pathway in neurons (Hao et al. 2015; Scarpulla 2011; Sun et al. 2017) and finding that cannabidiol also alters metabolic pathways in MO3.13 cells (figure S5), both supports the previous studies and also helps to validate these findings. As such, the protective effects of these drugs in OLs can be attributed to a modulation of metabolism, similar to benztropine. Moreover, finding that benztropine modulates proteins related to the glycolytic pathway (table S10), just as cannabidiol and antipsychotics do, suggests that this may be a mechanism of action in common, also behind the protective effects of benztropine.

Antioxidant Defense and Stress Pathways

Another set of proteins modulated by benztropine were related to antioxidant defense, selenocysteine synthesis and response to endoplasmic reticulum stress (figure 1 and table S10). When antioxidant defense is insufficient, oxidative stress may occur and it plays a known role in the pathophysiology of schizophrenia (Martins-de-Souza et al. 2011; Sawa and Sedlak 2016). Benztropine exerts effects on neuronal cells, increasing glutathione levels and can reduce the elevated ROS levels induced by oxaliplatin and cell death (Cerles et al., 2019). In contrast, benztropine had an effect on the levels of certain proteins related to antioxidant defense. Antioxidant molecules decrease the ROS level in OPCs; however, some promote OPC to OL differentiation, independent of their antioxidant effect and can therefore promote remyelination (Guo et al., 2018). Here, we suggest that this may be a mechanism of action behind the protective effects of benztropine in OLs. Like benztropine, haloperidol and cannabidiol also modulated proteins related to selenocysteine synthesis (table S7 and S9). While haloperidol has been suggested to induce oxidative stress in rat brains (Andreazza et al. 2015) cannabidiol has been observed to prevent hydrogen peroxide (H2O2)-induced apoptosis in nucleus pulposus cells as well as decrease oxidative species in OPCs (Chen et al. 2016; Mecha et al., 2012), suggesting a possible cause of the differences in the side effect profiles of cannabidiol versus haloperidol.

Similar to our data, studies have reported alterations in proteins responsible for immune system processes and the cell cycle in benztropine treatment (Deshmund et al., 2013; Kudriaeva et al., 2016). Here, we identified ubiquitin and proteasome proteins related to the immune system (figure 1 and table S15). At a molecular level, ubiquitin-proteasome machinery, which is found altered in neurodegenerative disorders, links the immune and neuronal system modulating neurotransmission, oxidative and inflammatory stress, cell cycle and differentiation (Limanaqi et al., 2019; Zheng et al., 2014). The cell progression is inhibited in benztropine-treated OPCs indicating that the drug induces differentiation in immature OL (Deshmund et al., 2013). As such, our results suggest that the efficacy of benztropine is due to an increase in myelination by enhancing oligodendrogenesis and modulating the immune system at molecular level. Moreover, clozapine and cannabidiol also modulated the cell cycle and immune system (table S8-S9 and figure S4-S5). Studies have shown that another atypical antipsychotic, quetiapine which acts in dopamine and serotonin receptors, promotes the cell cycle, OL differentiation, and modulates genes involved in the cell cycle (Mi et al. 2018; Sárvári et al. 2014), and haloperidol has been found to promote

proliferation of rat OPCs (Niu et al. 2010). Here, haloperidol treatment modulated signal transduction by p53 class mediator (figure S3), whose overexpression mediates OL apoptosis (Ma et al., 2017). Along those lines, cell cycle and proliferation changes caused by antipsychotics can be correlated with their long-term administration, differently impacting OLs and expression of myelin in schizophrenia patients (Bartzokis et al., 2007; Bartzokis et al., 2009). Although cannabidiol induces cell cycle arrest in human gastric cancer cells at the G0–G1 phase, reducing cell proliferation (Zhang et al., 2019), it promotes cell proliferation in neural stem cells and neurogenesis (Hill et al., 2018), supporting the hypothesis that cannabidiol promotes OL proliferation by modifying the cell cycle.

Amino Acid Metabolism and Splicing

Proteins related to amino acid metabolism and splicing were also modulated by benztropine, clozapine and cannabidiol treatment (figure S5-6, table S8). Spliceosome machinery has already been documented to be affected by clozapine and haloperidol, especially regarding hnRNPs (Brandão-Teles et al. 2019; Cassoli et al. 2016) and abnormalities in RNA splicing and phosphorylation have already been linked to demyelination and psychiatric disease (Glatt et al. 2011; Szilagyi et al. 2020). More specifically, alterations in alternative splicing and decreases in mRNA-associated genes have been documented in schizophrenia (Cohen et al. 2012; Prabakaran et al. 2004; Saia-Cereda et al. 2017; Santarelli et al. 2019). Therefore, RNA splicing can be another potential therapeutic target of benztropine in the demyelination model.

Lastly, benztropine treatment also modulated proteins related to post-translational modification, being methylation (string, FDR: 1.31e-07) and acetylation (string, FDR: 4.16e-4). Acetylation pathways were also affected by cannabidiol (string, FDR: 4.70e-20) and the two antipsychotics (string, FDR: 1.02e-20; 7.00e-59). Alterations in acetylation and methylation of DNA and proteins have been related to neurodegenerative disorders (Mattson 2003). Furthermore, histone acetylation, which is coordinated by response to metabolic state such as influence of acetyl-CoA, is important for OL differentiation and myelination (Gao et al., 2016; Marin-Husstege et al., 2002) and some drug-mediated acetylation can protect against neurodegenerative events (Ayyadevara et al., 2017). We hypothesize that benztropine can also promote differentiation and myelination by modulating post-translational modification, and that it may be a common protective effect among benztropine, antipsychotics and cannabidiol.

Cuprizone's effects on the proteome of MO3.13 oligodendrocytes

Several models have been created or are under development to comprehend myelination, demyelination, and remyelination mechanisms, including the *in vitro* and *in vivo* cuprizone demyelination model (Bénardais et al. 2013; de Rosa et al. 2019; Taraboletti et al. 2017; Sachs et al. 2014; Xu et al. 2014; Xu et al. 2019; Zahednasab et al. 2019). In this study, we searched for the molecular mechanisms and biological processes that are involved in, and potentially directly behind, cuprizone-mediated toxicity in OLs.

One pathway with altered protein levels in response to OL exposure to cuprizone was NF-kB signaling (table 1). This pathway is known to modulate cell proliferation and myelination by OLs, and can be activated by inflammatory factors, neurotrophic factors, neurotransmitters, and cellular stress molecules (Arnett et al. 2001; Hayden and Ghosh 2008). In some studies on cuprizone models, NF-kB signaling was found to be critical for toxic demyelination and OL death, with its modulation leading to changes in apoptosis, remyelination, and OL differentiation (Elbaz et al. 2018; Raasch et al. 2011). The data obtained in this study further reinforce the role of the NF-kB cascade in cuprizone-induced toxicity.

Cuprizone treatment also had an effect on some growth factor pathways, namely the activation of the FGFR4 receptor and neurotrophic receptor tyrosine kinase 1 (NTRK1, also known as tropomyosin receptor kinase A - TRKA) along with betaKlotho (KLB) signaling (table 1). Certain other soluble factors like fibroblast growth factor (FGF) and nerve growth factor (NGF) are already known to influence CNS myelination by inducing OL proliferation, differentiation, and migration (Bansal and Pfeiffer 1997; Park and Poo 2013). p38 mitogen-activated protein kinase (MAPK) -- a pathway that has a crosstalk with FGF signaling through FGFR and activates MAPK/ERK signaling, regulating myelination and OL maturation (Ahrendsen and Macklin 2013) -- was also found to be altered (table 1). Furthermore, the pathway "PIP3 (phosphatidylinositol (3,4,5) triphosphates) activates AKT (protein kinase B) signaling" was modulated by cuprizone (figure 5), which regulates cell proliferation and apoptosis (Liu et al. 2017). Taken together, these results suggest that cuprizone may lead to OL toxicity by affecting various growth factors and signaling mechanisms that are related to cell proliferation, survival, and myelination.

Proteins related to energy and lipid metabolism were also modulated by cuprizone treatment. Results showed that cuprizone affects, at least indirectly, some mitochondrial proteins,

specifically citrate synthase (figure 5 and table 1). Lipid metabolism may also be affected through changes in FGFR4 activation and VLDLR internalization and degradation (figure 5 and table 1), which are integral to lipogenesis, glucose and lipid homeostasis, and the inflammatory response, potentially also affecting the carboxylic acid biosynthetic process (Adighibe et al. 2006; Sodhi and Singh 2013; Viennois et al. 2011). These results are supported by the dysfunctions in energy and lipid metabolism that have been seen in the corpus callosum and hippocampus of animals administered cuprizone (Maganti et al. 2019; Taraboletti et al. 2017). Disturbances in lipid homeostasis affect OL biology and myelination overall, and an OL primary culture study indicated that these cells take up and use fatty acids for biosynthesis, functioning in brain lipid metabolism machinery (Hofmann et al. 2017).

Cuprizone is also known to disturb energy metabolism and can decrease glucose utilization (Kim et al. 2019; Taraboletti et al. 2017), additionally affecting NAD^+ metabolism, blocking glycolytic pathways and energy production as a result (Fünfschilling et al. 2012; Taraboletti et al. 2017). Moreover, cuprizone administration impairs mitochondria and electron transport chain functionality, leading to a decrease in ATP production (Faizi et al. 2016). Such changes in lipid homeostasis and energy metabolism are especially relevant since OLs are especially vulnerable to metabolic and lipid disturbances, leading in turn to deregulations in proteins related to neuronal structure and transport, cell trafficking, and signal transduction, therefore contributing to a dysfunction in white matter and in neuronal connectivity (Chan et al. 2011; Guest et al. 2015; Hofmann et al. 2017).

Lastly, some proteins related to genetic processes including translation, post-translational modifications, and spliceosome processes (figure 5 and table 1) were found to be dysregulated upon exposure to cuprizone. One post-translational protein modification has already been linked with cuprizone in an *in vivo* study involving mice that found altered levels of phosphorylation on MBP (myelin basic protein) (Szilagyi et al. 2020). Splicing is an important form of RNA processing performed by the spliceosome that affects the translation of all human genes; aberrant splicing events have been confirmed in some neurological disorders, including schizophrenia and multiple sclerosis (Glatt et al. 2011; Hecker et al. 2019). A dysregulation of proteins that comprise the main component of splicing operations has also been reported in both the white and gray matter of patients with schizophrenia, and included the splicing factor serine/arginine-rich 3 (SRSF3) (Saia-Cereda et al. 2017). SRSF9 is involved in alternative pre-RNA splicing and its overexpression affects cell proliferation, cycle arrest, and apoptosis (Bressan et al. 2009; Zhang et al. 2019), and

was found dysregulated in the OLs exposed to cuprizone (figure 4). Thus, these results suggest that the deregulation of proteins related to spliceosome function and post-translational processes can result in cell death in OLs exposed to cuprizone.

The cuprizone model has already been established and used to understand the mechanisms behind OL and myelination dysfunctions. These previous data have been supplemented with the findings of this study, which have determined or confirmed that alterations in proteins involved in metabolic processes, the immune system, genetic factors, signaling pathways, and the regulation of apoptosis can all occur in response to cuprizone. Four therapeutic drugs were then evaluated and compared in this model to understand their effects on MO3.13 OLs at the cellular and molecular levels, as well as their implications for myelination.

Effects of haloperidol, clozapine, cannabidiol, and benztropine on cuprizone-treated cells and their implications on cell survival and myelination

The third part of this study was to administer haloperidol, clozapine, cannabidiol, and benztropine in conjunction with cuprizone to visualize how the protective effects of these compounds may have an effect at the proteomic level. After exposure to cuprizone, one drug was administered, and overall, the resulting proteins that were modulated in response were related to metabolism, the processing of genetic information and the cell cycle.

As detailed in our results, cuprizone appeared to affect mitochondrial proteins and may therefore impair ATP production. Cannabidiol co-treatment also induced changes in ATP metabolic processes (figure 6B), in which modulated proteins were more specifically related to energy metabolism and mitochondrial biogenesis and included cytochrome b-c1 and ATP synthase. Thus, these data indicate a potential of cannabidiol to attenuate the energy metabolism disturbances seen in the cuprizone model. An overall reduction of protein and lipid levels is also observed in animals treated with cuprizone, impacting myelin formation and function (Maganti et al. 2019; Taraboletti et al. 2017). In our results, haloperidol, cannabidiol, and benztropine -- but not clozapine -- co-treatments all modulated proteins involved in lipid and steroid metabolism (tables S12-5). Interestingly, in an *in vivo* cuprizone model, clozapine treatment was unable to prevent demyelination during cuprizone administration, but did enhance functional support after demyelination (Templeton et al. 2019). Benztropine, however, has been found to induce OL formation by decreasing the basal level of sterol (Hubler et al. 2018), and cannabidiol can modulate cholesterol homeostasis and sterol metabolism in microglial cells (Rimmerman et al. 2011). Here, we demonstrated

that haloperidol, cannabidiol, and benztropine modulate proteins and pathways related to lipid metabolism throughout cuprizone insult, suggesting a potential ability to prevent demyelination events.

In cuprizone-treated mice and in schizophrenia, a deregulation of the expression of cell cycle genes has been found to contribute to deficits in OLs, cells which normally respond to injury by accelerating their cell cycle, indicating that CNS remyelination can be mediated by modulating the OPC cell cycle (Fan et al. 2012; Katsel et al. 2008; Palazuelos, et al. 2014). We identified a modulation of the cell cycle in all co-treatments (figure 6B), but this pathway was most significantly affected in co-treatments with haloperidol and clozapine. The antipsychotics modulated the mitotic anaphase, metaphase, prometaphase, and M phase (tables S3 and S4), whereas benztropine co-treatment modulated centrosome maturation, recruitment of mitotic centrosome proteins and complexes, G2/M transition, and mitotic G2-G2/M phases (table S6). Cannabidiol and benztropine co-treatments increased the protein SWI/SNF complex subunit SMARCC1, which is related to the cell cycle (table S2). Clozapine co-treatment decreased 26S proteasome non-ATPase regulatory subunit 6 that participates in many cellular processes, such as cell cycle progression, apoptosis and DNA damage repair (table S2). Though there is overlap between the two antipsychotics tested, each compound seems to affect the OL cell cycle in different ways; nonetheless, these compounds must be tested further regarding their potential to promote cell proliferation.

Lastly, cuprizone treatment was found to induce deregulations in proteins involved with DNA maintenance, spliceosome processes, translation, and post-translational modifications. Alterations in the expression and regulation of post-translational modifications can lead to dysfunctions in multiple cell types, brain regions, and neurotransmitters (Mueller and Meador-Woodruff 2020). All co-treatments modulated proteins related to the spliceosome and RNA metabolism (figure 6B), and was most significant in the co-treatment with haloperidol (figure S6). Moreover, the pathway Positive regulation of RNA splicing was found modulated by clozapine and haloperidol co-treatments (figure 6B), and post-translational modification was modulated by benztropine co-treatment (figure 6B). Though they affect these pathways in different ways, a more developed understanding of how these pathways are affected by antipsychotics, cannabidiol, and benztropine would be important to help determine how OPCs regenerate after toxic effects like those induced by cuprizone, and how schizophrenia and other demyelinating disorders can be better treated.

CONCLUSIONS

In this study, we identified biochemical pathways related to cuprizone toxicity. We confirmed that this *in vitro* model for cuprizone-induced cell death is cytotoxic to MO3.13 oligodendrocytes by disturbing biological processes that are related to the OL deficit hypothesis of schizophrenia. A thorough understanding of the mechanisms regulating myelination would help to develop pharmaceutical targets for the remyelination process, promoting recovery, and preventing the progression of schizophrenia symptoms. In this context, we evaluated the effects of two antipsychotics, cannabidiol, and benztropine on OPCs undergoing treatment with cuprizone; using a proteomic approach, we showed that all of the drugs modulate some biochemical pathways related to cuprizone's toxic effects. Cannabidiol mostly affected ATP production and lipid metabolism, indicating its similarity with benztropine and its potential effect to promote mitochondrial repair. In summary, haloperidol, clozapine, cannabidiol, and benztropine all modulated proteins related to the cell cycle, cell signaling, the spliceosome, and post-translational modifications, which are all pathways related to cuprizone-induced cell death, thus indicating their potential to combat the toxic effects of cuprizone. Even though this model of cuprizone-treated OLs does not represent the entirety of the pathophysiology of schizophrenia, these results allow us to better comprehend some facets of schizophrenia and other demyelinating disorders and to develop novel therapeutic targets and treatment options for OL disturbances.

FUNDING SOURCES

This work was supported by the São Paulo Research Foundation (FAPESP, grant numbers 2018/10362-0, 2017/18242-1, 2018/03422-7, 2018/03450-0, 2019/22398-2), the Coordination for the Improvement of Higher Education Personnel (CAPES, grant numbers 88887.495565/2020-00), and the CNPq (Conselho Nacional de Desenvolvimento Científico e Tecnológico, grant number 157265/2018-8).

REFERENCE

Adighibe, Omanma, Sampath Arepalli, Jaime Duckworth, John Hardy, and Fabienne Wavrant-De Vrièze. 2006. "Genetic Variability at the LXR Gene (NR1H2) May Contribute to the Risk of Alzheimer's Disease." *Neurobiology of Aging* 27 (10): 1431–34.

Ahrendsen, Jared T., and Wendy Macklin. 2013. "Signaling Mechanisms Regulating Myelination in the Central Nervous System." *Neuroscience Bulletin* 29 (2): 199–215.

Almeida, Valéria de, and Daniel Martins-de-Souza. 2018. "Cannabinoids and Glial Cells: Possible Mechanism to Understand Schizophrenia." *European Archives of Psychiatry and Clinical Neuroscience* 268 (7): 727–37.

Andreazza, Ana C., Vilte E. Barakauskas, Salar Fazeli, Abigail Feresten, Li Shao, Vivien Wei, Che Hsuan Wu, Alasdair M. Barr, and Clare L. Beasley. 2015. "Effects of Haloperidol and Clozapine Administration on Oxidative Stress in Rat Brain, Liver and Serum." *Neuroscience Letters* 591 (March): 36–40.

Arnett, H. A., J. Mason, M. Marino, K. Suzuki, G. K. Matsushima, and J. P. Ting. 2001. "TNF Alpha Promotes Proliferation of Oligodendrocyte Progenitors and Remyelination." *Nature Neuroscience* 4 (11): 1116–22.

Ayyadevara, Srinivas, Meenakshisundaram Balasubramaniam, Samuel Kakraba, Ramani Alla, Jawahar L. Mehta, and Robert J. Shmookler Reis. 2017. "Aspirin-Mediated Acetylation Protects Against Multiple Neurodegenerative Pathologies by Impeding Protein Aggregation." *Antioxidants & Redox Signaling* 27 (17): 1383–96.

Azorin, Jean-Michel, Raoul Belzeaux, and Marc Adida. 2014. "Negative Symptoms in Schizophrenia: Where We Have Been and Where We Are Heading." *CNS Neuroscience & Therapeutics* 20 (9): 801–8.

Bansal, R., and S. E. Pfeiffer. 1997. "FGF-2 Converts Mature Oligodendrocytes to a Novel Phenotype." *Journal of Neuroscience Research* 50 (2): 215–28.

Bartzokis, George, Po H. Lu, Keith H. Nuechterlein, Michael Gitlin, Clarissa Doi, Nancy Edwards, Christopher Lieu, Lori L. Altshuler, and Jim Mintz. 2007. "Differential Effects of Typical and Atypical Antipsychotics on Brain Myelination in Schizophrenia." *Schizophrenia Research* 93 (1-3): 13–22.

Bartzokis, George, Po H. Lu, Stephanie B. Stewart, Bolanle Oluwadara, Andrew J. Lucas, Joanna Pantages, Erika Pratt, et al. 2009. “In Vivo Evidence of Differential Impact of Typical and Atypical Antipsychotics on Intracortical Myelin in Adults with Schizophrenia.” *Schizophrenia Research* 113 (2-3): 322–31.

Bénardais, Karelle, Alexandra Kotsiari, Jelena Skuljec, Paraskevi N. Koutsoudaki, Viktoria Gudi, Vikramjeet Singh, Franca Vulinović, Thomas Skripuletz, and Martin Stangel. 2013. “Cuprizone [bis(cyclohexylidenehydrazide)] Is Selectively Toxic for Mature Oligodendrocytes.” *Neurotoxicity Research* 24 (2): 244–50.

Bernard, Jessica A., Joseph M. Orr, and Vijay A. Mittal. 2015. “Abnormal Hippocampal-Thalamic White Matter Tract Development and Positive Symptom Course in Individuals at Ultra-High Risk for Psychosis.” *NPJ Schizophrenia* 1. https://doi.org/10.1038/npjschz.2015.9.

Bernstein, Hans-Gert, Johann Steiner, Paul C. Guest, Henrik Dobrowolny, and Bernhard Bogerts. 2015. “Glial Cells as Key Players in Schizophrenia Pathology: Recent Insights and Concepts of Therapy.” *Schizophrenia Research* 161 (1): 4–18.

Biancotti, Juan Carlos, Shalini Kumar, and Jean de Vellis. 2008. “Activation of Inflammatory Response by a Combination of Growth Factors in Cuprizone-Induced Demyelinated Brain Leads to Myelin Repair.” *Neurochemical Research* 33 (12): 2615–28.

Brandão-Teles, Caroline, Valéria de Almeida, Juliana S. Cassoli, and Daniel Martins-de-Souza. 2019. “Biochemical Pathways Triggered by Antipsychotics in Human [corrected] Oligodendrocytes: Potential of Discovering New Treatment Targets.” *Frontiers in Pharmacology* 10 (March): 186.

Brandão-Teles, Caroline, Daniel Martins-de-Souza, Paul C. Guest, and Juliana S. Cassoli. 2017. “MK-801-Treated Oligodendrocytes as a Cellular Model to Study Schizophrenia.” *Advances in Experimental Medicine and Biology* 974: 269–77.

Bressan, Gustavo C., Eduardo C. Moraes, Adriana O. Manfiolli, Tais M. Kuniyoshi, Dario O. Passos, Marcelo D. Gomes, and Jörg Kobarg. 2009. “Arginine Methylation Analysis of the Splicing-Associated SR Protein SFRS9/SRP30C.” *Cellular & Molecular Biology Letters* 14 (4): 657–69.

Buntinx, M., J. Vanderlocht, N. Hellings, F. Vandenabeele, I. Lambrichts, J. Raus, M. Ameloot, P. Stinissen, and P. Steels. 2003. “Characterization of Three Human Oligodendroglial Cell

Lines as a Model to Study Oligodendrocyte Injury: Morphology and Oligodendrocyte-Specific Gene Expression." *Journal of Neurocytology* 32 (1): 25–38.

Cassoli, Juliana Silva, Paul C. Guest, Berend Malchow, Andrea Schmitt, Peter Falkai, and Daniel Martins-de-Souza. 2015. "Disturbed Macro-Connectivity in Schizophrenia Linked to Oligodendrocyte Dysfunction: From Structural Findings to Molecules." *NPJ Schizophrenia* 1 (September): 15034.

Cassoli, Juliana S., Keiko Iwata, Johann Steiner, Paul C. Guest, Christoph W. Turck, Juliana M. Nascimento, and Daniel Martins-de-Souza. 2016. "Effect of MK-801 and Clozapine on the Proteome of Cultured Human Oligodendrocytes." *Frontiers in Cellular Neuroscience* 10 (March): 52.

Cerles, Olivier, Tânia Cristina Gonçalves, Sandrine Chouzenoux, Evelyne Benoit, Alain Schmitt, Nathaniel Edward Bennett Saidu, Niloufar Kavian, et al. 2019. "Preventive Action of Benztropine on Platinum-Induced Peripheral Neuropathies and Tumor Growth." *Acta Neuropathologica Communications* 7 (1): 9.

Chan, M. K., T. M. Tsang, L. W. Harris, P. C. Guest, E. Holmes, and S. Bahn. 2011. "Evidence for Disease and Antipsychotic Medication Effects in Post-Mortem Brain from Schizophrenia Patients." *Molecular Psychiatry* 16 (12): 1189–1202.

Chen, Jie, Chen Hou, Xin Chen, Dong Wang, Pinglin Yang, Xijing He, Jinsong Zhou, and Haopeng Li. 2016. "Protective Effect of Cannabidiol on Hydrogen Peroxide-induced Apoptosis, Inflammation and Oxidative Stress in Nucleus Pulposus Cells." *Molecular Medicine Reports* 14 (3): 2321–27.

Cohen, Ori S., Sarah Y. Mccoy, Frank A. Middleton, Sean Bialosuknia, Yanli Zhang-James, Lu Liu, Ming T. Tsuang, Stephen V. Faraone, and Stephen J. Glatt. 2012. "Transcriptomic Analysis of Postmortem Brain Identifies Dysregulated Splicing Events in Novel Candidate Genes for Schizophrenia." *Schizophrenia Research* 142 (1-3): 188–99.

Deshmukh, Vishal A., Virginie Tardif, Costas A. Lyssiotis, Chelsea C. Green, Bilal Kerman, Hyung Joon Kim, Krishnan Padmanabhan, et al. 2013. "A Regenerative Approach to the Treatment of Multiple Sclerosis." *Nature* 502 (7471): 327–32.

Elbaz, Eman M., Mahmoud A. Senousy, Dalia M. El-Tanbouly, and Rabab H. Sayed. 2018. "Neuroprotective Effect of Linagliptin against Cuprizone-Induced Demyelination and Behavioural Dysfunction in Mice: A Pivotal Role of AMPK/SIRT1 and JAK2/STAT3/NF-

κB Signalling Pathway Modulation." *Toxicology and Applied Pharmacology* 352 (August): 153–61.

Ettle, Benjamin, Bilal E. Kerman, Elvira Valera, Clarissa Gillmann, Johannes C. M. Schlachetzki, Simone Reiprich, Christian Büttner, et al. 2016. "α-Synuclein-Induced Myelination Deficit Defines a Novel Interventional Target for Multiple System Atrophy." *Acta Neuropathologica* 132 (1): 59–75.

Fabregat, Antonio, Konstantinos Sidiropoulos, Guilherme Viteri, Pablo Marin-Garcia, Peipei Ping, Lincoln Stein, Peter D'Eustachio, and Henning Hermjakob. 2018. "Reactome Diagram Viewer: Data Structures and Strategies to Boost Performance." *Bioinformatics* 34 (7): 1208–14.

Faizi, Mehrdad, Ahmad Salimi, Enayatolla Seydi, Parvaneh Naserzadeh, Mehdi Kouhnavard, Atena Rahimi, and Jalal Pourahmad. 2016. "Toxicity of Cuprizone a Cu(2+) Chelating Agent on Isolated Mouse Brain Mitochondria: A Justification for Demyelination and Subsequent Behavioral Dysfunction." *Toxicology Mechanisms and Methods* 26 (4): 276–83.

Fan, Yongjun, Greger Abrahamsen, John J. McGrath, and Alan Mackay-Sim. 2012. "Altered Cell Cycle Dynamics in Schizophrenia." *Biological Psychiatry* 71 (2): 129–35.

Franz, Max, Christian T. Lopes, Gerardo Huck, Yue Dong, Onur Sumer, and Gary D. Bader. 2016. "Cytoscape.js: A Graph Theory Library for Visualisation and Analysis." *Bioinformatics* 32 (2): 309–11.

Fünfschilling, Ursula, Lotti M. Supplie, Don Mahad, Susann Boretius, Aiman S. Saab, Julia Edgar, Bastian G. Brinkmann, et al. 2012. "Glycolytic Oligodendrocytes Maintain Myelin and Long-Term Axonal Integrity." *Nature* 485 (7399): 517–21.

Gao, Xue, Shu-Hai Lin, Feng Ren, Jin-Tao Li, Jia-Jia Chen, Chuan-Bo Yao, Hong-Bin Yang, et al. 2016. "Acetate Functions as an Epigenetic Metabolite to Promote Lipid Synthesis under Hypoxia." *Nature Communications* 7 (June): 11960.

Georgieva, Lyudmila, Valentina Moskvina, Tim Peirce, Nadine Norton, Nicholas J. Bray, Lesley Jones, Peter Holmans, et al. 2006. "Convergent Evidence That Oligodendrocyte Lineage Transcription Factor 2 (OLIG2) and Interacting Genes Influence Susceptibility to Schizophrenia." *Proceedings of the National Academy of Sciences of the United States of America* 103 (33): 12469–74.

Glatt, Stephen J., Ori S. Cohen, Stephen V. Faraone, and Ming T. Tsuang. 2011. “Dysfunctional Gene Splicing as a Potential Contributor to Neuropsychiatric Disorders.” *American Journal of Medical Genetics. Part B, Neuropsychiatric Genetics: The Official Publication of the International Society of Psychiatric Genetics* 156B (4): 382–92.

Goldberg, Johannes, Moritz Daniel, Yasemin van Heuvel, Marion Victor, Cordian Beyer, Tim Clarner, and Markus Kipp. 2013. “Short-Term Cuprizone Feeding Induces Selective Amino Acid Deprivation with Concomitant Activation of an Integrated Stress Response in Oligodendrocytes.” *Cellular and Molecular Neurobiology* 33 (8): 1087–98.

Guest, Paul C., Keiko Iwata, Takahiro A. Kato, Johann Steiner, Andrea Schmitt, Christoph W. Turck, and Daniel Martins-de-Souza. 2015. “MK-801 Treatment Affects Glycolysis in Oligodendrocytes More than in Astrocytes and Neuronal Cells: Insights for Schizophrenia.” *Frontiers in Cellular Neuroscience* 9 (May): 180.

Guo, Yu-E, Na Suo, Xue Cui, Qianting Yuan, and Xin Xie. 2018. “Vitamin C Promotes Oligodendrocytes Generation and Remyelination.” *Glia* 66 (7): 1302–16.

Hao, Enkui, Partha Mukhopadhyay, Zongxian Cao, Katalin Erdélyi, Eileen Holovac, Lucas Liaudet, Wen-Shin Lee, György Haskó, Raphael Mechoulam, and Pál Pacher. 2015. “Cannabidiol Protects against Doxorubicin-Induced Cardiomyopathy by Modulating Mitochondrial Function and Biogenesis.” *Molecular Medicine* 21 (January): 38–45.

Hattori, Tsuyoshi, Shoko Shimizu, Yoshihisa Koyama, Hisayo Emoto, Yuji Matsumoto, Natsuko Kumamoto, Kohei Yamada, et al. 2014. “DISC1 (disrupted-in-Schizophrenia-1) Regulates Differentiation of Oligodendrocytes.” *PloS One* 9 (2): e88506.

Hayden, Matthew S., and Sankar Ghosh. 2008. “Shared Principles in NF-kappaB Signaling.” *Cell* 132 (3): 344–62.

Hecker, Michael, Annelen Rüge, Elena Putscher, Nina Boxberger, Paulus Stefan Rommer, Brit Fitzner, and Uwe Klaus Zettl. 2019. “Aberrant Expression of Alternative Splicing Variants in Multiple Sclerosis - A Systematic Review.” *Autoimmunity Reviews* 18 (7): 721–32.

He, X. Y., H. Schulz, and S. Y. Yang. 1998. “A Human Brain L-3-Hydroxyacyl-Coenzyme A Dehydrogenase Is Identical to an Amyloid Beta-Peptide-Binding Protein Involved in Alzheimer’s Disease.” *The Journal of Biological Chemistry* 273 (17): 10741–46.

Hill, Jeremy D., Viviana Zuluaga-Ramirez, Sachin Gajghate, Malika Winfield, and Yuri Persidsky. 2018. “Activation of GPR55 Increases Neural Stem Cell Proliferation and Promotes Early Adult Hippocampal Neurogenesis.” *British Journal of Pharmacology* 175 (16): 3407–21.

Hofmann, Kristina, Rosalia Rodriguez-Rodriguez, Anne Gaebler, Núria Casals, Anja Scheller, and Lars Kuerschner. 2017. “Astrocytes and Oligodendrocytes in Grey and White Matter Regions of the Brain Metabolize Fatty Acids.” *Scientific Reports* 7 (1): 10779.

Howes, Oliver D., and Shitij Kapur. 2009. “The Dopamine Hypothesis of Schizophrenia: Version III--the Final Common Pathway.” *Schizophrenia Bulletin* 35 (3): 549–62.

Howes, Oliver, Rob McCutcheon, and James Stone. 2015. “Glutamate and Dopamine in Schizophrenia: An Update for the 21st Century.” *Journal of Psychopharmacology* 29 (2): 97–115.

Huang, Da Wei, Brad T. Sherman, and Richard A. Lempicki. 2009a. “Systematic and Integrative Analysis of Large Gene Lists Using DAVID Bioinformatics Resources.” *Nature Protocols* 4 (1): 44–57.

———. 2009b. “Bioinformatics Enrichment Tools: Paths toward the Comprehensive Functional Analysis of Large Gene Lists.” *Nucleic Acids Research* 37 (1): 1–13.

Hubler, Zita, Dharmaraja Allimuthu, Ilya Bederman, Matthew S. Elitt, Mayur Madhavan, Kevin C. Allan, H. Elizabeth Shick, et al. 2018. “Accumulation of 8,9-Unsaturated Sterols Drives Oligodendrocyte Formation and Remyelination.” *Nature* 560 (7718): 372–76.

Iwata, Keiko, Cecilia C. Café-Mendes, Andrea Schmitt, Johann Steiner, Takayuki Manabe, Hideo Matsuzaki, Peter Falkai, Christoph W. Turck, and Daniel Martins-de-Souza. 2013. “The Human Oligodendrocyte Proteome.” *Proteomics* 13 (23-24): 3548–53.

Jørgensen, K. N., S. Nerland, L. B. Norbom, N. T. Doan, R. Nesvåg, L. Mørch-Johnsen, U. K. Haukvik, et al. 2016. “Increased MRI-Based Cortical Grey/white-Matter Contrast in Sensory and Motor Regions in Schizophrenia and Bipolar Disorder.” *Psychological Medicine* 46 (9): 1971–85.

Katsel, Pavel, Kenneth L. Davis, Celeste Li, Weilun Tan, Elizabeth Greenstein, Lisa B. Kleiner Hoffman, and Vahram Haroutunian. 2008. “Abnormal Indices of Cell Cycle Activity in Schizophrenia and Their Potential Association with Oligodendrocytes.”

Neuropsychopharmacology: Official Publication of the American College of Neuropsychopharmacology 33 (12): 2993–3009.

Kim, Woosuk, Kyu Ri Hahn, Hyo Young Jung, Hyun Jung Kwon, Sung Min Nam, Jong Whi Kim, Joon Ha Park, et al. 2019. "Melatonin Ameliorates Cuprizone-Induced Reduction of Hippocampal Neurogenesis, Brain-Derived Neurotrophic Factor, and Phosphorylation of Cyclic AMP Response Element-Binding Protein in the Mouse Dentate Gyrus." *Brain and Behavior* 9 (9): e01388.

Kudriaeva, A. A., N. A. Khaustova, D. V. Maltseva, E. S. Kuzina, I. S. Glagoleva, E. A. Surina, V. D. Knorre, A. A. Belogurov Jr, A. G. Tonevitsky, and A. G. Gabibov. 2016. "mRNA Expression Profile of Mouse Oligodendrocytes in Inflammatory Conditions." *Doklady. Biochemistry and Biophysics* 469 (1): 264–68.

Lee, Jung-Min, Jasmine J. Han, Gary Altwerger, and Elise C. Kohn. 2011. "Proteomics and Biomarkers in Clinical Trials for Drug Development." *Journal of Proteomics* 74 (12): 2632–41.

Leucht, Stefan, Caroline Corves, Dieter Arbter, Rolf R. Engel, Chunbo Li, and John M. Davis. 2009. "Second-Generation versus First-Generation Antipsychotic Drugs for Schizophrenia: A Meta-Analysis." *The Lancet* 373 (9657): 31–41.

Li, Cui, Lin Xiao, Xiuyun Liu, Wenjing Yang, Weiran Shen, Chun Hu, Guang Yang, and Cheng He. 2013. "A Functional Role of NMDA Receptor in Regulating the Differentiation of Oligodendrocyte Precursor Cells and Remyelination." *Glia* 61 (5): 732–49.

Liebermeister, Wolfram, Elad Noor, Avi Flamholz, Dan Davidi, Jörg Bernhardt, and Ron Milo. 2014. "Visual Account of Protein Investment in Cellular Functions." *Proceedings of the National Academy of Sciences of the United States of America* 111 (23): 8488–93.

Limanaqi, Fiona, Francesca Biagioni, Anderson Gaglione, Carla Letizia Busceti, and Francesco Fornai. 2019. "A Sentinel in the Crosstalk Between the Nervous and Immune System: The (Immuno)-Proteasome." *Frontiers in Immunology* 10 (March): 628.

Liu, Jing, Weiyan Chen, Haiyan Zhang, Ting Liu, and Lin Zhao. 2017. "miR-214 Targets the PTEN-Mediated PI3K/Akt Signaling Pathway and Regulates Cell Proliferation and Apoptosis in Ovarian Cancer." *Oncology Letters* 14 (5): 5711–18.

Maganti, Rajanikanth J., Xiaoping L. Hronowski, Robert W. Dunstan, Brian T. Wipke, Xueli Zhang, Luke Jandreski, Stefan Hamann, and Peter Juhasz. 2019. “Defining Changes in the Spatial Distribution and Composition of Brain Lipids in the Shiverer and Cuprizone Mouse Models of Myelin Disease.” *The Journal of Histochemistry and Cytochemistry: Official Journal of the Histochemistry Society* 67 (3): 203–19.

Ma, Lan, Hai-Jun Yu, Sheng-Wei Gan, Rui Gong, Ke-Jie Mou, Jun Xue, and Shan-Quan Sun. 2017. “p53-Mediated Oligodendrocyte Apoptosis Initiates Demyelination after Compressed Spinal Cord Injury by Enhancing ER-Mitochondria Interaction and E2F1 Expression.” *Neuroscience Letters* 644 (March): 55–61.

Marin-Husstege, Mireya, Michela Muggironi, Aixiao Liu, and Patricia Casaccia-Bonnefil. 2002. “Histone Deacetylase Activity Is Necessary for Oligodendrocyte Lineage Progression.” *The Journal of Neuroscience: The Official Journal of the Society for Neuroscience* 22 (23): 10333–45.

Martins-de-Souza, Daniel, Laura W. Harris, Paul C. Guest, and Sabine Bahn. 2011. “The Role of Energy Metabolism Dysfunction and Oxidative Stress in Schizophrenia Revealed by Proteomics.” *Antioxidants & Redox Signaling* 15 (7): 2067–79.

Mecha, M., A. S. Torrao, L. Mestre, F. J. Carrillo-Salinas, R. Mechoulam, and C. Guaza. 2012. “Cannabidiol Protects Oligodendrocyte Progenitor Cells from Inflammation-Induced Apoptosis by Attenuating Endoplasmic Reticulum Stress.” *Cell Death & Disease* 3 (June): e331.

Messori, Luigi, Angela Casini, Chiara Gabbiani, Lorenzo Sorace, Maurizio Muniz-Miranda, and Paolo Zatta. 2007. “Unravelling the Chemical Nature of Copper Cuprizone.” *Dalton Transactions* , no. 21 (June): 2112–14.

Metsalu, Tauno, and Jaak Vilo. 2015. “ClustVis: A Web Tool for Visualizing Clustering of Multivariate Data Using Principal Component Analysis and Heatmap.” *Nucleic Acids Research* 43 (W1): W566–70.

Mi, Guiyun, Yunyun Gao, Shuai Liu, Enmao Ye, Yanyan Li, Xiao Jin, Hongju Yang, and Zheng Yang. 2016. “Cyclin-Dependent Kinase Inhibitor Flavopiridol Promotes Remyelination in a Cuprizone Induced Demyelination Model.” *Cell Cycle* 15 (20): 2780–91.

Mi, Guiyun, Yituo Wang, Enmao Ye, Yunyun Gao, Qiaowei Liu, Pinhong Chen, Yuyang Zhu, Hongju Yang, and Zheng Yang. 2018. “The Antipsychotic Drug Quetiapine Stimulates

Oligodendrocyte Differentiation by Modulating the Cell Cycle." *Neurochemistry International* 118 (September): 242–51.

Mueller, Toni M., and James H. Meador-Woodruff. 2020. "Post-Translational Protein Modifications in Schizophrenia." *NPJ Schizophrenia* 6 (1): 5.

Niu, Jianqin, Feng Mei, Nan Li, Hanzhi Wang, Xinmin Li, Jiming Kong, and Lan Xiao. 2010. "Haloperidol Promotes Proliferation but Inhibits Differentiation in Rat Oligodendrocyte Progenitor Cell Cultures." *Biochemistry and Cell Biology = Biochimie et Biologie Cellulaire* 88 (4): 611–20.

Orban, Pierre, Martin Desseilles, Adrianna Mendrek, Josiane Bourque, Pierre Bellec, and Emmanuel Stip. 2017. "Altered Brain Connectivity in Patients with Schizophrenia Is Consistent across Cognitive Contexts." *Journal of Psychiatry & Neuroscience: JPN* 42 (1): 17–26.

Os, Jim van, and Shitij Kapur. 2009. "Schizophrenia." *The Lancet* 374 (9690): 635–45.

Owen, Michael J., Akira Sawa, and Preben B. Mortensen. 2016. "Schizophrenia." *The Lancet* 388 (10039): 86–97.

Palazuelos, Javier, Michael Klingener, and Adan Aguirre. 2014. "TGFβ Signaling Regulates the Timing of CNS Myelination by Modulating Oligodendrocyte Progenitor Cell Cycle Exit through SMAD3/4/FoxO1/Sp1." *The Journal of Neuroscience: The Official Journal of the Society for Neuroscience* 34 (23): 7917–30.

Park, Hyungju, and Mu-Ming Poo. 2013. "Neurotrophin Regulation of Neural Circuit Development and Function." *Nature Reviews. Neuroscience* 14 (1): 7–23.

Paulson, Linda, Peter Martin, Carol L. Nilsson, Elisabeth Ljung, Ann Westman-Brinkmalm, Kaj Blennow, and Pia Davidsson. 2004. "Comparative Proteome Analysis of Thalamus in MK-801-Treated Rats." *Proteomics* 4 (3): 819–25.

Petronilli, V., and M. Zoratti. 1990. "A Characterization of Cuprizone-Induced Giant Mouse Liver Mitochondria." *Journal of Bioenergetics and Biomembranes* 22 (5): 663–77.

Prabakaran, S., J. E. Swatton, M. M. Ryan, S. J. Huffaker, J. T-J Huang, J. L. Griffin, M. Wayland, et al. 2004. "Mitochondrial Dysfunction in Schizophrenia: Evidence for Compromised Brain Metabolism and Oxidative Stress." *Molecular Psychiatry* 9 (7): 684–97, 643.

Praet, Jelle, Caroline Guglielmetti, Zwi Berneman, Annemie Van der Linden, and Peter Ponsaerts. 2014. “Cellular and Molecular Neuropathology of the Cuprizone Mouse Model: Clinical Relevance for Multiple Sclerosis.” *Neuroscience and Biobehavioral Reviews* 47 (November): 485–505.

Raasch, Jenni, Nicolas Zeller, Geert van Loo, Doron Merkler, Alexander Mildner, Daniel Erny, Klaus-Peter Knobeloch, et al. 2011. “IkappaB Kinase 2 Determines Oligodendrocyte Loss by Non-Cell-Autonomous Activation of NF-kappaB in the Central Nervous System.” *Brain: A Journal of Neurology* 134 (Pt 4): 1184–98.

Rahimi, A., M. Faizi, F. Talebi, F. Noorbakhsh, F. Kahrizi, and N. Naderi. 2015. “Interaction between the Protective Effects of Cannabidiol and Palmitoylethanolamide in Experimental Model of Multiple Sclerosis in C57BL/6 Mice.” *Neuroscience* 290 (April): 279–87.

Ren, Yuan, Hanzhi Wang, and Lan Xiao. 2013. “Improving Myelin/oligodendrocyte-Related Dysfunction: A New Mechanism of Antipsychotics in the Treatment of Schizophrenia?” *The International Journal of Neuropsychopharmacology / Official Scientific Journal of the Collegium Internationale Neuropsychopharmacologicum* 16 (3): 691–700.

Rimmerman, Neta, Ana Juknat, Ewa Kozela, Rivka Levy, Heather B. Bradshaw, and Zvi Vogel. 2011. “The Non-Psychoactive Plant Cannabinoid, Cannabidiol Affects Cholesterol Metabolism-Related Genes in Microglial Cells.” *Cellular and Molecular Neurobiology* 31 (6): 921–30.

Rosa, Valeria de, Agnese Secondo, Anna Pannaccione, Roselia Ciccone, Luigi Formisano, Natascia Guida, Roberta Crispino, et al. 2019. “D-Aspartate Treatment Attenuates Myelin Damage and Stimulates Myelin Repair.” *EMBO Molecular Medicine* 11 (1). https://doi.org/10.15252/emmm.201809278.

Sachs, Hilary H., Kathryn K. Bercury, Daniela C. Popescu, S. Priya Narayanan, and Wendy B. Macklin. 2014. “A New Model of Cuprizone-Mediated Demyelination/remyelination.” *ASN Neuro* 6 (5). https://doi.org/10.1177/1759091414551955.

Saia-Cereda, Verônica M., Juliana S. Cassoli, Andrea Schmitt, Peter Falkai, Juliana M. Nascimento, and Daniel Martins-de-Souza. 2015. “Proteomics of the Corpus Callosum Unravel Pivotal Players in the Dysfunction of Cell Signaling, Structure, and Myelination in Schizophrenia Brains.” *European Archives of Psychiatry and Clinical Neuroscience* 265 (7): 601–12.

Saia-Cereda, Verônica M., Aline G. Santana, Andrea Schmitt, Peter Falkai, and Daniel Martins-de-Souza. 2017. “The Nuclear Proteome of White and Gray Matter from Schizophrenia Postmortem Brains.” *Molecular Neuropsychiatry* 3 (1): 37–52.

Saito, Yukiko, Marek Kubicki, Inga Koerte, Tatsui Otsuka, Yogesh Rathi, Ofer Pasternak, Sylvain Bouix, et al. 2018. “Impaired White Matter Connectivity between Regions Containing Mirror Neurons, and Relationship to Negative Symptoms and Social Cognition, in Patients with First-Episode Schizophrenia.” *Brain Imaging and Behavior* 12 (1): 229–37.

Sánchez-Wandelmer, J., A. Dávalos, G. de la Peña, S. Cano, M. Giera, A. Canfrán-Duque, F. Bracher, et al. 2010. “Haloperidol Disrupts Lipid Rafts and Impairs Insulin Signaling in SH-SY5Y Cells.” *Neuroscience* 167 (1): 143–53.

Santarelli, Danielle M., Adam P. Carroll, Heath M. Cairns, Paul A. Tooney, and Murray J. Cairns. 2019. “Schizophrenia-Associated MicroRNA-Gene Interactions in the Dorsolateral Prefrontal Cortex.” *Genomics, Proteomics & Bioinformatics* 17 (6): 623–34.

Santos, A. K., M. S. Vieira, R. Vasconcellos, V. A. M. Goulart, A. H. Kihara, and R. R. Resende. 2019. “Decoding Cell Signalling and Regulation of Oligodendrocyte Differentiation.” *Seminars in Cell & Developmental Biology* 95 (November): 54–73.

Sárvári, Anitta K., Zoltán Veréb, Iván P. Uray, László Fésüs, and Zoltán Balajthy. 2014. “Atypical Antipsychotics Induce Both Proinflammatory and Adipogenic Gene Expression in Human Adipocytes in Vitro.” *Biochemical and Biophysical Research Communications* 450 (4): 1383–89.

Sawa, Akira, and Thomas W. Sedlak. 2016. “Oxidative Stress and Inflammation in Schizophrenia.” *Schizophrenia Research* 176 (1): 1–2.

Scarpulla, Richard C. 2011. “Metabolic Control of Mitochondrial Biogenesis through the PGC-1 Family Regulatory Network.” *Biochimica et Biophysica Acta* 1813 (7): 1269–78.

Seabra, Gabriela, Valéria de Almeida, Guilherme Reis-de-Oliveira, Fernanda Crunfli, André Saraiva Leão Marcelo Antunes, and Daniel Martins-de-Souza. 2020. “Ubiquitin-Proteasome System, Lipid Metabolism and DNA Damage Repair Are Triggered by Antipsychotic Medication in Human Oligodendrocytes: Implications in Schizophrenia.” *Scientific Reports* 10 (1): 12655.

Simons, Mikael, and Klaus-Armin Nave. 2015. “Oligodendrocytes: Myelination and Axonal Support.” *Cold Spring Harbor Perspectives in Biology* 8 (1): a020479.

Sodhi, Rupinder K., and Nirmal Singh. 2013. “Liver X Receptors: Emerging Therapeutic Targets for Alzheimer’s Disease.” *Pharmacological Research: The Official Journal of the Italian Pharmacological Society* 72 (June): 45–51.

Steiner, Johann, Daniel Martins-de-Souza, Kolja Schiltz, Zoltan Sarnyai, Sabine Westphal, Berend Isermann, Henrik Dobrowolny, et al. 2014. “Clozapine Promotes Glycolysis and Myelin Lipid Synthesis in Cultured Oligodendrocytes.” *Frontiers in Cellular Neuroscience* 8 (November): 384.

Steiner, Johann, Zoltán Sarnyai, Sabine Westphal, Tomasz Gos, Hans-Gert Bernstein, Bernhard Bogerts, and Gerburg Keilhoff. 2011. “Protective Effects of Haloperidol and Clozapine on Energy-Deprived OLN-93 Oligodendrocytes.” *European Archives of Psychiatry and Clinical Neuroscience* 261 (7): 477–82.

Sun, Shanshan, Fangyuan Hu, Jihong Wu, and Shenghai Zhang. 2017. “Cannabidiol Attenuates OGD/R-Induced Damage by Enhancing Mitochondrial Bioenergetics and Modulating Glucose Metabolism via Pentose-Phosphate Pathway in Hippocampal Neurons.” *Redox Biology* 11 (April): 577–85.

Szilagyi, Gabor T., Arkadiusz M. Nawrocki, Krisztian Eros, Janos Schmidt, Katalin Fekete, Maria L. Elkjaer, Kirsten H. Hyrlov, Martin R. Larsen, Zsolt Illes, and Ferenc Gallyas Jr. 2020. “Proteomic Changes during Experimental de- and Remyelination in the Corpus Callosum.” *PloS One* 15 (4): e0230249.

Szklarczyk, Damian, John H. Morris, Helen Cook, Michael Kuhn, Stefan Wyder, Milan Simonovic, Alberto Santos, et al. 2017. “The STRING Database in 2017: Quality-Controlled Protein-Protein Association Networks, Made Broadly Accessible.” *Nucleic Acids Research* 45 (D1): D362–68.

Taraboletti, Alexandra, Tia Walker, Robin Avila, He Huang, Joel Caporoso, Erendra Manandhar, Thomas C. Leeper, David A. Modarelli, Satish Medicetty, and Leah P. Shriver. 2017. “Cuprizone Intoxication Induces Cell Intrinsic Alterations in Oligodendrocyte Metabolism Independent of Copper Chelation.” *Biochemistry* 56 (10): 1518–28.

Templeton, Nikki, Bronwyn Kivell, Amy McCaughey-Chapman, Bronwen Connor, and Anne Camille La Flamme. 2019. “Clozapine Administration Enhanced Functional Recovery after Cuprizone Demyelination.” *PloS One* 14 (5): e0216113.

Thompson, Kaitlyn K., Jillian C. Nissen, Amanda Pretory, and Stella E. Tsirka. 2018. “Tuftsin Combines With Remyelinating Therapy and Improves Outcomes in Models of CNS Demyelinating Disease.” *Frontiers in Immunology* 9 (November): 2784.

Uranova, Natalya A., Olga V. Vikhreva, Valentina I. Rakhmanova, and Diana D. Orlovskaya. 2018. “Ultrastructural Pathology of Oligodendrocytes Adjacent to Microglia in Prefrontal White Matter in Schizophrenia.” *NPJ Schizophrenia* 4 (1): 26.

Venturini, G. 1973. “Enzymic Activities and Sodium, Potassium and Copper Concentrations in Mouse Brain and Liver after Cuprizone Treatment in Vivo.” *Journal of Neurochemistry* 21 (5): 1147–51.

Viennois, Emilie, Aurélien J. C. Pommier, Kévin Mouzat, Abdelkader Oumeddour, Fatim-Zohra El Hajjaji, Julie Dufour, Françoise Caira, David H. Volle, Silvère Baron, and Jean-Marc A. Lobaccaro. 2011. “Targeting Liver X Receptors in Human Health: Deadlock or Promising Trail?” *Expert Opinion on Therapeutic Targets* 15 (2): 219–32.

Vikhreva, O. V., V. I. Rakhmanova, D. D. Orlovskaya, and N. A. Uranova. 2016. “Ultrastructural Alterations of Oligodendrocytes in Prefrontal White Matter in Schizophrenia: A Post-Mortem Morphometric Study.” *Schizophrenia Research* 177 (1-3): 28–36.

Voineskos, Aristotle N., Vincenzo de Luca, Natalie L. Bulgin, Quinton van Adrichem, Sajid Shaikh, Donna J. Lang, William G. Honer, and James L. Kennedy. 2008. “A Family-Based Association Study of the Myelin-Associated Glycoprotein and 2’,3'-Cyclic Nucleotide 3'-Phosphodiesterase Genes with Schizophrenia.” *Psychiatric Genetics* 18 (3): 143–46.

Wu, Ren-Rong, Jing-Ping Zhao, Zhe-Ning Liu, Jin-Guo Zhai, Xiao-Feng Guo, Wen-Bing Guo, and Jing-Song Tang. 2006. “Effects of Typical and Atypical Antipsychotics on Glucose-Insulin Homeostasis and Lipid Metabolism in First-Episode Schizophrenia.” *Psychopharmacology* 186 (4): 572–78.

Xu, Haiyun, Hong-Ju Yang, and Xin-Min Li. 2014. “Differential Effects of Antipsychotics on the Development of Rat Oligodendrocyte Precursor Cells Exposed to Cuprizone.” *European Archives of Psychiatry and Clinical Neuroscience* 264 (2): 121–29.

Xu, Zhizhong, Abulimiti Adilijiang, Wenqiang Wang, Pan You, Duoduo Lin, Xinmin Li, and Jue He. 2019. “Arecoline Attenuates Memory Impairment and Demyelination in a Cuprizone-Induced Mouse Model of Schizophrenia.” *Neuroreport* 30 (2): 134–38.

Zahednasab, Hamid, Masoumeh Firouzi, Sussan Kaboudanian-Ardestani, Zahra Mojallal-Tabatabaei, Sajad Karampour, and Hossein Keyvani. 2019. “The Protective Effect of Rifampicin on Behavioral Deficits, Biochemical, and Neuropathological Changes in a Cuprizone Model of Demyelination.” *Cytokine* 113 (January): 417–26.

Zajicek, John P., and Vicentiu I. Apostu. 2011. “Role of Cannabinoids in Multiple Sclerosis.” *CNS Drugs* 25 (3): 187–201.

Zhang, Qianwen, Rui Lv, Wenjia Guo, and Xiaoning Li. 2019. “microRNA-802 Inhibits Cell Proliferation and Induces Apoptosis in Human Cervical Cancer by Targeting Serine/arginine-Rich Splicing Factor 9.” *Journal of Cellular Biochemistry* 120 (6): 10370–79.

Zhang, Xin, Yao Qin, Zhaohai Pan, Minjing Li, Xiaona Liu, Xiaoyu Chen, Guiwu Qu, et al. 2019. “Cannabidiol Induces Cell Cycle Arrest and Cell Apoptosis in Human Gastric Cancer SGC-7901 Cells.” *Biomolecules* 9 (8). https://doi.org/10.3390/biom9080302.

Zheng, Chen, Thangiah Geetha, and Jeganathan Ramesh Babu. 2014. “Failure of Ubiquitin Proteasome System: Risk for Neurodegenerative Diseases.” *Neuro-Degenerative Diseases* 14 (4): 161–75.

Zhou, Yingyao, Bin Zhou, Lars Pache, Max Chang, Alireza Hadj Khodabakhshi, Olga Tanaseichuk, Christopher Benner, and Sumit K. Chanda. 2019. “Metascape Provides a Biologist-Oriented Resource for the Analysis of Systems-Level Datasets.” *Nature Communications* 10 (1): 1523.

7. CONCLUSÃO E PERSPECTIVAS

Como mencionado no decorrer desta dissertação, a esquizofrenia é uma desordem mental complexa e de caráter multifatorial. Sendo assim, o estudo desta desordem deve englobar estudos clínicos, biológicos e moleculares para sua compreensão. Estudos com tecido *post-mortem*, genéticos, proteômicos e de imagem relatam que os distúrbios na desconectividade neural e na substância branca, assim como anormalidades nos OLs e na mielina, podem estar relacionadas à fisiopatologia da esquizofrenia. Desta forma, modelos tóxicos de desmielinização, como o induzido por cuprizona, são utilizados para compreender os mecanismos moleculares relacionados aos distúrbios de OLs e de mielina. Neste processo, é de suma importância utilizar culturas de OPCs, para avaliar os efeitos de novos compostos químicos com potencial terapêutico.

Neste estudo, confirmamos que a cuprizona é capaz de induzir citoxicidade em OLs da linhagem MO3.13, através de alterações em processos biológicos, os quais estão relacionados com a hipótese de déficits de OLs na esquizofrenia. Ademais, demonstramos que os antipsicóticos, CBD e a benzatropina podem modular vias bioquímicas e proteínas relacionadas com os efeitos tóxicos induzidos pela cuprizona, como a alteração de proteínas relacionadas com o metabolismo, ao ciclo celular e à processos genéticos, evidenciando seus potenciais efeitos protetores. Desta forma, pretendemos contribuir para o melhor entendimento dos mecanismos relacionados às anormalidades de OLs e como se relacionam à fisiopatologia da esquizofrenia, além da sua relação com o desenvolvimento de futuros alvos terapêuticos para esta desordem. Sendo assim, trabalhos futuros que utilizem diferentes estágios celulares, como células neurais indiferenciadas e OLs em um estágio mais avançado de maturação, são de suma importância para avaliar os processos de diferenciação, efeitos inflamatórios, testar novos compostos químicos com potencial terapêutico, bem como desenvolver estratégias que ajudem atenuar estas anormalidades relacionados aos OLs e a mielina neste distúrbio.

8. REFERÊNCIAS (introdução, justificativa e materiais e métodos)

ACS, P. *et al.* **Distribution of oligodendrocyte loss and mitochondrial toxicity in the cuprizone-induced experimental demyelination model**. Journal of neuroimmunology, v. 262, n. 1-2, p. 128–131, 2013 a.

ACS, P. *et al.* **Distribution of oligodendrocyte loss and mitochondrial toxicity in the cuprizone-induced experimental demyelination model**. Journal of neuroimmunology, v. 262, n. 1-2, p. 128–131, 2013 b.

ADIGHIBE, O. *et al.* **Genetic variability at the LXR gene (NR1H2) may contribute to the risk of Alzheimer's disease**. Neurobiology of aging, v. 27, n. 10, p. 1431–1434, 2006.

AHRENDSEN, J. T.; MACKLIN, W. **Signaling mechanisms regulating myelination in the central nervous system**. Neuroscience bulletin, v. 29, n. 2, p. 199–215, 2013.

ANDREAZZA, A. C. *et al.* **Effects of haloperidol and clozapine administration on oxidative stress in rat brain, liver and serum**. Neuroscience letters, v. 591, p. 36–40, 2015.

ANDREWS, G. L. *et al.* **Performance characteristics of a new hybrid quadrupole time-of-flight tandem mass spectrometer (TripleTOF 5600)**. Analytical chemistry, v. 83, n. 13, p. 5442–5446, 2011.

AQUINO, A. *et al.* **Blood-Based Lipidomics Approach to Evaluate Biomarkers Associated With Response to Olanzapine, Risperidone, and Quetiapine Treatment in Schizophrenia Patients**. Frontiers in psychiatry / Frontiers Research Foundation, v. 9, p. 209, 2018.

ARETI, S. *et al.* **Selenocysteine vs Cysteine: Tuning the Derivatization on Benzenesulfonyl Moiety of a Triazole Linked Dansyl Connected Glycoconjugate for Selective Recognition of Selenocysteine and the Applicability of the Conjugate in Buffer, in Serum, on Silica Gel, and in HepG2 Cells**. Analytical chemistry, v. 88, n. 14, p. 7259–7267, 2016.

ARNETT, H. A. *et al.* **TNF alpha promotes proliferation of oligodendrocyte progenitors and remyelination**. Nature neuroscience, v. 4, n. 11, p. 1116–1122, 2001.

AZORIN, J.-M.; BELZEAUX, R.; ADIDA, M. **Negative Symptoms in Schizophrenia: Where We have been and Where We are Heading**. CNS neuroscience & therapeutics, v. 20, n. 9, p. 801–808, 2014.

BANASZKIEWICZ, I.; BIALA, G.; KRUK-SLOMKA, M. **Contribution of CB2 receptors in schizophrenia-related symptoms in various animal models: Short review**. Neuroscience and biobehavioral reviews, v. 114, p. 158–171, 2020.

BANSAL, R.; PFEIFFER, S. E. **FGF-2 converts mature oligodendrocytes to a novel phenotype**. Journal of neuroscience research, v. 50, n. 2, p. 215–228, 1997.

BARATEIRO, A.; FERNANDES, A. **Temporal oligodendrocyte lineage progression: in vitro models of proliferation, differentiation and myelination**. Biochimica et biophysica acta, v. 1843, n. 9, p. 1917–1929, 2014.

BAROR, R. *et al.* **Transforming growth factor-beta renders ageing microglia inhibitory to oligodendrocyte generation by CNS progenitors**. Glia, v. 67, n. 7, p. 1374–1384, 2019.

BARTZOKIS, G. *et al.* **Differential effects of typical and atypical antipsychotics on brain myelination in schizophrenia**. Schizophrenia research, v. 93, n. 1-3, p. 13–22, 2007.

BARTZOKIS, G. *et al.* **In vivo evidence of differential impact of typical and atypical antipsychotics on intracortical myelin in adults with schizophrenia**. Schizophrenia research, v. 113, n. 2-3, p. 322–331, 2009.

BARTZOKIS, G. **Neuroglialpharmacology: myelination as a shared mechanism of action of psychotropic treatments**. Neuropharmacology, v. 62, n. 7, p. 2137–2153, 2012.

BAUMANN, N.; PHAM-DINH, D. **Biology of oligodendrocyte and myelin in the mammalian central nervous system**. Physiological reviews, v. 81, n. 2, p. 871–927, 2001.

BÉNARDAIS, K. *et al.* **Cuprizone [bis(cyclohexylidenehydrazide)] is selectively toxic for mature oligodendrocytes.** Neurotoxicity research, v. 24, n. 2, p. 244–250, 2013.

BENETTI, F. *et al.* **Cuprizone neurotoxicity, copper deficiency and neurodegeneration**. Neurotoxicology, v. 31, n. 5, p. 509–517, 2010.

BERNAL-CHICO, A. *et al.* **Blockade of monoacylglycerol lipase inhibits oligodendrocyte excitotoxicity and prevents demyelination in vivo**. Glia, v. 63, n. 1, p. 163–176, 2015.

BERNARD, J. A.; ORR, J. M.; MITTAL, V. A. **Abnormal hippocampal-thalamic white matter tract development and positive symptom course in individuals at ultra-high risk for psychosis**. NPJ schizophrenia, v. 1, 2015.

BERNSTEIN, H.-G. *et al.* **Glial cells as key players in schizophrenia pathology: recent insights and concepts of therapy.** Schizophrenia research, v. 161, n. 1, p. 4–18, 2015.

BIANCOTTI, J. C.; KUMAR, S.; DE VELLIS, J. **Activation of inflammatory response by a combination of growth factors in cuprizone-induced demyelinated brain leads to myelin repair.** Neurochemical research, v. 33, n. 12, p. 2615–2628, 2008.

BIOQUE, M. *et al.* **Peripheral endocannabinoid system dysregulation in first-episode psychosis**. Neuropsychopharmacology: official publication of the American College of Neuropsychopharmacology, v. 38, n. 13, p. 2568–2577, 2013.

BLANKMAN, J. L.; SIMON, G. M.; CRAVATT, B. F. **A comprehensive profile of brain enzymes that hydrolyze the endocannabinoid 2-arachidonoylglycerol**. Chemistry & biology, v. 14, n. 12, p. 1347–1356, 2007.

BRANDÃO-TELES, C. *et al.* M**K-801-Treated Oligodendrocytes as a Cellular Model to Study Schizophrenia**. Advances in experimental medicine and biology, v. 974, p. 269–277, 2017.

BRANDÃO-TELES, C. *et al.* **Biochemical Pathways Triggered by Antipsychotics in Human [corrected] Oligodendrocytes: Potential of Discovering New Treatment Targets**. Frontiers in pharmacology, v. 10, p. 186, 2019.

BRESSAN, G. C. *et al.* **Arginine methylation analysis of the splicing-associated SR protein SFRS9/SRP30C**. Cellular & molecular biology letters, v. 14, n. 4, p. 657–669, 2009.

BRUIJNZEEL, D.; SURYADEVARA, U.; TANDON, R. **Antipsychotic treatment of schizophrenia: an update**. Asian journal of psychiatry, v. 11, p. 3–7, 2014.

BUNTINX, M. *et al.* **Characterization of three human oligodendroglial cell lines as a model to study oligodendrocyte injury: morphology and oligodendrocyte-specific gene expression**. Journal of neurocytology, v. 32, n. 1, p. 25–38, 2003.

CAMARGO, N. *et al.* **Oligodendroglial myelination requires astrocyte-derived lipids**. PLoS biology, v. 15, n. 5, p. e1002605, 2017.

CAMPOS, A. C. *et al.* **Plastic and Neuroprotective Mechanisms Involved in the Therapeutic Effects of Cannabidiol in Psychiatric Disorders**. Frontiers in pharmacology, v. 8, p. 269, 2017.

CASSOLI, J. S. *et al.* **Disturbed macro-connectivity in schizophrenia linked to oligodendrocyte dysfunction: from structural findings to molecules**. NPJ schizophrenia, v. 1, p. 15034, 2015.

CASSOLI, J. S. *et al.* **Effect of MK-801 and Clozapine on the Proteome of Cultured Human Oligodendrocytes**. Frontiers in cellular neuroscience, v. 10, p. 52, 2016.

CASTILLO, P. E. *et al.* **Endocannabinoid signaling and synaptic function**. Neuron, v. 76, n. 1, p. 70–81, 2012.

CERLES, O. *et al.* **Preventive action of benztropine on platinum-induced peripheral neuropathies and tumor growth**. Acta neuropathologica communications, v. 7, n. 1, p. 9, 2019.

CHAIT, B. T. Chemistry. **Mass spectrometry: bottom-up or top-down?.** Science, 2006.

CHAN, M. K. *et al.* E**vidence for disease and antipsychotic medication effects in post-mortem brain from schizophrenia patients**. Molecular psychiatry, v. 16, n. 12, p. 1189–1202, 2011.

CHEN, J. *et al.* P**rotective effect of cannabidiol on hydrogen peroxide-induced apoptosis, inflammation and oxidative stress in nucleus pulposus cells**. Molecular medicine reports, v. 14, n. 3, p. 2321–2327, 2016.

CHEN, R. *et al.* **Monoacylglycerol lipase is a therapeutic target for Alzheimer's disease**. Cell reports, v. 2, n. 5, p. 1329–1339, 2012.

CIEŚLIK, P. *et al.* **Mutual activation of glutamatergic mGlu4 and muscarinic M4 receptors reverses schizophrenia-related changes in rodents**. Psychopharmacology, v. 235, n. 10, p. 2897–2913, 2018.

COHEN, O. S. *et al.* **Transcriptomic analysis of postmortem brain identifies dysregulated splicing events in novel candidate genes for schizophrenia**. Schizophrenia research, v. 142, n. 1-3, p. 188–199, 2012.

COHEN, S. M. *et al.* **The impact of NMDA receptor hypofunction on GABAergic neurons in the pathophysiology of schizophrenia**. Schizophrenia research, v. 167, n. 1-3, p. 98–107, 2015.

COLLIP, D. *et al.* **Daily cortisol, stress reactivity and psychotic experiences in individuals at above average genetic risk for psychosis**. Psychological medicine, v. 41, n. 11, p. 2305–2315, 2011.

CRAVATT, B. F. *et al.* **Molecular characterization of an enzyme that degrades neuromodulatory fatty-acid amides**. Nature, v. 384, n. 6604, p. 83–87, 1996.

DASS, C. **Fundamentals of Contemporary Mass Spectrometry**. Hoboken, NJ, USA: John Wiley & Sons, Inc., 2007. *E-book*.

DE, A. K.; SUBRAMANIAN, M. **Effect of cuprizone feeding on hepatic superoxide dismutase and cytochrome oxidase activities in mice**. Experientia, v. 38, n. 7, p. 784–785, 1982.

DE ALMEIDA, V. *et al.* **Changes in the blood plasma lipidome associated with effective or poor response to atypical antipsychotic treatments in schizophrenia patients**. Progress in neuro-psychopharmacology & biological psychiatry, v. 101, p. 109945, 2020.

DE ALMEIDA, V.; MARTINS-DE-SOUZA, D. **Cannabinoids and glial cells: possible mechanism to understand schizophrenia**. European archives of psychiatry and clinical neuroscience, v. 268, n. 7, p. 727–737, 2018.

DE LAGO, E. *et al.* **Cannabinoids, multiple sclerosis and neuroprotection**. Expert review of clinical pharmacology, *[S. l.]*, v. 2, n. 6, p. 645–660, 2009.

DE ROSA, V. et al. **D-Aspartate treatment attenuates myelin damage and stimulates myelin repair**. EMBO molecular medicine, v. 11, n. 1, 2019.

DESHMUKH, V. A. *et al.* **A regenerative approach to the treatment of multiple sclerosis. Nature,** v. 502, n. 7471, p. 327–332, 2013.

DIETZ, K. C. *et al.* **Targeting human oligodendrocyte progenitors for myelin repair**. Experimental neurology, v. 283, n. Pt B, p. 489–500, 2016.

DI GIROLAMO, F. *et al.* **The Role of Mass Spectrometry in the "Omics" Era**. Current organic chemistry, v. 17, n. 23, p. 2891–2905, 2013.

DIMOU, L. *et al.* **Progeny of Olig2-expressing progenitors in the gray and white matter of the adult mouse cerebral cortex**. The Journal of neuroscience: the official journal of the Society for Neuroscience, v. 28, n. 41, p. 10434–10442, 2008.

DOMON, B.; AEBERSOLD, R. **Mass spectrometry and protein analysis.** Science, v. 312, n. 5771, p. 212–217, 2006.

DZIEMBOWSKA, M. *et al.* **A role for CXCR4 signaling in survival and migration of neural and oligodendrocyte precursors**. Glia, v. 50, n. 3, p. 258–269, 2005.

EDWARDS, A. C. *et al.* **Evaluating the dopamine hypothesis of schizophrenia in a large-scale genome-wide association study**. Schizophrenia research, v. 176, n. 2-3, p. 136–140, 2016.

EGAWA, J. *et al.* **Membrane lipid rafts and neurobiology: age-related changes in membrane lipids and loss of neuronal function**. The Journal of physiology, v. 594, n. 16, p. 4565–4579, 2016.

EGERTON, A. *et al.* **Presynaptic striatal dopamine dysfunction in people at ultra-high risk for psychosis: findings in a second cohort**. Biological psychiatry, v. 74, n. 2, p. 106–112, 2013.

EGERTON, A. *et al.* **Effects of Antipsychotic Administration on Brain Glutamate in Schizophrenia: A Systematic Review of Longitudinal 1H-MRS Studies**. Frontiers in psychiatry / Frontiers Research Foundation, v. 8, p. 66, 2017.

EGGAN, S. M.; HASHIMOTO, T.; LEWIS, D. A. **Reduced cortical cannabinoid 1 receptor messenger RNA and protein expression in schizophrenia**. Archives of general psychiatry, v. 65, n. 7, p. 772–784, 2008.

ELBAZ, E. M. *et al.* **Neuroprotective effect of linagliptin against cuprizone-induced demyelination and behavioural dysfunction in mice: A pivotal role of AMPK/SIRT1 and JAK2/STAT3/NF-κB signalling pathway modulation**. Toxicology and applied pharmacology, v. 352, p. 153–161, 2018.

ETTLE, B. *et al.* **α-Synuclein-induced myelination deficit defines a novel interventional target for multiple system atrophy**. Acta neuropathologica, v. 132, n. 1, p. 59–75, 2016.

EYSTER, K. M. **The membrane and lipids as integral participants in signal transduction: lipid signal transduction for the non-lipid biochemist**. Advances in physiology education, v. 31, n. 1, p. 5–16, 2007.

FABREGAT, A. *et al.* **Reactome diagram viewer: data structures and strategies to boost performance.** Bioinformatics , v. 34, n. 7, p. 1208–1214, 2018.

FAIZI, M. *et al.* **Toxicity of cuprizone a Cu(2+) chelating agent on isolated mouse brain mitochondria: a justification for demyelination and subsequent behavioral dysfunction**. Toxicology mechanisms and methods, v. 26, n. 4, p. 276–283, 2016.

FALKAI, P. *et al.* **Oligodendrocyte and Interneuron Density in Hippocampal Subfields in Schizophrenia and Association of Oligodendrocyte Number with Cognitive Deficits**. Frontiers in cellular neuroscience, v. 10, p. 78, 2016.

FALKAI, P. *et al.* **Association between altered hippocampal oligodendrocyte number and neuronal circuit structures in schizophrenia: a postmortem analysis**. European archives of psychiatry and clinical neuroscience, v. 270, n. 4, p. 413–424, 2020.

FAN, Y. *et al.* **Altered cell cycle dynamics in schizophrenia**. Biological psychiatry, v. 71, n. 2, p. 129–135, 2012.

FENN, J. B. *et al.* **Electrospray ionization for mass spectrometry of large biomolecules**. Science, v. 246, n. 4926, p. 64–71, 1989.

FRANZ, M. *et al.* **Cytoscape.js: a graph theory library for visualisation and analysis.** Bioinformatics , v. 32, n. 2, p. 309–311, 2016.

FRIEDMAN, J. I. **Cholinergic targets for cognitive enhancement in schizophrenia: focus on cholinesterase inhibitors and muscarinic agonists**. Psychopharmacology, v. 174, n. 1, p. 45–53, 2004.

FÜNFSCHILLING, U. *et al.* **Glycolytic oligodendrocytes maintain myelin and long-term axonal integrity**. Nature, v. 485, n. 7399, p. 517–521, 2012.

GAO, X. M. *et al.* **Ionotropic glutamate receptors and expression of N-methyl-D-aspartate receptor subunits in subregions of human hippocampus: effects of schizophrenia**. The American journal of psychiatry, v. 157, n. 7, p. 1141–1149, 2000.

GATTAZ, W. F.; BRUNNER, J. **Phospholipase A2 and the hypofrontality hypothesis of schizophrenia**. Prostaglandins, leukotrienes, and essential fatty acids, v. 55, n. 1-2, p. 109–113, 1996.

GEORGIEVA, L. *et al.* **Convergent evidence that oligodendrocyte lineage transcription factor 2 (OLIG2) and interacting genes influence susceptibility to schizophrenia**. Proceedings of the National Academy of Sciences of the United States of America, v. 103, n. 33, p. 12469–12474, 2006.

GLATT, S. J. *et al.* **Dysfunctional gene splicing as a potential contributor to neuropsychiatric disorders. American journal of medical genetics**. Part B, Neuropsychiatric genetics: the official publication of the International Society of Psychiatric Genetics, v. 156B, n. 4, p. 382–392, 2011.

GOFF, D. C.; COYLE, J. T. T**he emerging role of glutamate in the pathophysiology and treatment of schizophrenia**. The American journal of psychiatry, v. 158, n. 9, p. 1367–1377, 2001.

GOLDBERG, J. *et al.* **Short-term cuprizone feeding induces selective amino acid deprivation with concomitant activation of an integrated stress response in oligodendrocytes**. Cellular and molecular neurobiology, v. 33, n. 8, p. 1087–1098, 2013.

GOUVÊA-JUNQUEIRA *et al*. **Novel treatment strategies targeting myelin and oligodendrocyte dysfunction in schizophrenia**. Frontiers in psychiatry, v. 11, p. 379, 2020.

GUEST, P. C. *et al.* **MK-801 treatment affects glycolysis in oligodendrocytes more than in astrocytes and neuronal cells: insights for schizophrenia**. Frontiers in cellular neuroscience, v. 9, p. 180, 2015.

HAO, E. *et al.* **Cannabidiol Protects against Doxorubicin-Induced Cardiomyopathy by Modulating Mitochondrial Function and Biogenesis**. Molecular medicine, v. 21, p. 38–45, 2015.

HATTORI, T. *et al.* **DISC1 (disrupted-in-schizophrenia-1) regulates differentiation of oligodendrocytes**. PloS one, v. 9, n. 2, p. e88506, 2014.

HAYDEN, M. S.; GHOSH, S. **Shared principles in NF-kappaB signaling**. Cell, v. 132, n. 3, p. 344–362, 2008.

HAZLETT, E. A. *et al.* **Abnormal glucose metabolism in the mediodorsal nucleus of the thalamus in schizophrenia**. The American journal of psychiatry, v. 161, n. 2, p. 305–314, 2004.

HECKER, M. *et al.* **Aberrant expression of alternative splicing variants in multiple sclerosis - A systematic review**. Autoimmunity reviews, v. 18, n. 7, p. 721–732, 2019.

HENDOUEI, N. *et al.* **Alterations in oxidative stress markers and its correlation with clinical findings in schizophrenic patients consuming perphenazine, clozapine and risperidone**. Biomedicine & pharmacotherapy = Biomedecine & pharmacotherapie, v. 103, p. 965–972, 2018.

HOFMANN, K. *et al.* **Astrocytes and oligodendrocytes in grey and white matter regions of the brain metabolize fatty acids**. Scientific reports, v. 7, n. 1, p. 10779, 2017.

HOSP, F.; MANN, M. **A Primer on Concepts and Applications of Proteomics in Neuroscience**. Neuron, v. 96, n. 3, p. 558–571, 2017.

HOWES, O. D. *et al.* **Midbrain dopamine function in schizophrenia and depression: a post-mortem and positron emission tomographic imaging study**. Brain: a journal of neurology, v. 136, n. Pt 11, p. 3242–3251, 2013.

HOWES, O. D.; KAPUR, S. **The dopamine hypothesis of schizophrenia: version III--the final common pathway**. Schizophrenia bulletin, v. 35, n. 3, p. 549–562, 2009.

HOWES, O.; MCCUTCHEON, R.; STONE, J. **Glutamate and dopamine in schizophrenia: an update for the 21st century**. Journal of psychopharmacology , v. 29, n. 2, p. 97–115, 2015.

HUANG, D. W.; SHERMAN, B. T.; LEMPICKI, R. A. **Systematic and integrative analysis of large gene lists using DAVID bioinformatics resources**. Nature protocols, v. 4, n. 1, p. 44–57, 2009 a.

HUANG, D. W.; SHERMAN, B. T.; LEMPICKI, R. A. **Bioinformatics enrichment tools: paths toward the comprehensive functional analysis of large gene lists**. Nucleic acids research, v. 37, n. 1, p. 1–13, 2009 b.

HUBLER, Z. *et al.* **Accumulation of 8,9-unsaturated sterols drives oligodendrocyte formation and remyelination.** Nature, v. 560, n. 7718, p. 372–376, 2018.

HUGHES, A. N.; APPEL, B. **Oligodendrocytes express synaptic proteins that modulate myelin sheath formation**. Nature communications, v. 10, n. 1, p. 4125, 2019.

HUSSAIN, G. *et al.* **Role of cholesterol and sphingolipids in brain development and neurological diseases**. Lipids in health and disease, v. 18, n. 1, p. 26, 2019.

IBRAHIM, H. M. *et al.* **Ionotropic glutamate receptor binding and subunit mRNA expression in thalamic nuclei in schizophrenia**. The American journal of psychiatry, v. 157, n. 11, p. 1811–1823, 2000.

ILYASOV, A. A. *et al.* **The Endocannabinoid System and Oligodendrocytes in Health and Disease**. Frontiers in neuroscience, v. 12, p. 733, 2018.

IWATA, K. *et al.* T**he human oligodendrocyte proteome**. Proteomics, v. 13, n. 23-24, p. 3548–3553, 2013.

JØRGENSEN, K. N. *et al.* **Increased MRI-based cortical grey/white-matter contrast in sensory and motor regions in schizophrenia and bipolar disorder**. Psychological medicine, v. 46, n. 9, p. 1971–1985, 2016.

KAHN, R. S. *et al.* **Schizophrenia**. Nature reviews. Disease primers, v. 1, p. 15067, 2015.

KAISER, S. *et al.* P**hencyclidine-induced changes in rat cortical gene expression identified by microarray analysis: implications for schizophrenia**. Neurobiology of disease, v. 16, n. 1, p. 220–235, 2004.

KANU, A. B. *et al.* **Ion mobility-mass spectrometry**. Journal of mass spectrometry: JMS, v. 43, n. 1, p. 1–22, 2008.

KARAS, M.; HILLENKAMP, F. **Laser desorption ionization of proteins with molecular masses exceeding 10,000 daltons**. Analytical chemistry, v. 60, n. 20, p. 2299–2301, 1988.

KATSEL, P. *et al.* **Abnormal indices of cell cycle activity in schizophrenia and their potential association with oligodendrocytes**. Neuropsychopharmacology: official publication of the American College of Neuropsychopharmacology, v. 33, n. 12, p. 2993–3009, 2008.

KEIRSTEAD, H. S.; BLAKEMORE, W. F. The role of oligodendrocytes and oligodendrocyte progenitors in CNS remyelination. Advances in experimental medicine and biology, v. 468, p. 183–197, 1999.

KELLEHER, N. L. **Top-down proteomics**. Analytical chemistry, v. 76, n. 11, p. 197A–203A, 2004.

KESTERSON, J. W.; CARLTON, W. W. **Monoamine oxidase inhibition and the activity of other oxidative enzymes in the brains of mice fed cuprizone**. Toxicology and applied pharmacology, v. 20, n. 3, p. 386–395, 1971.

KHOURY, J. M. *et al.* **Is there a role for cannabidiol in psychiatry?** The world journal of biological psychiatry: the official journal of the World Federation of Societies of Biological Psychiatry, v. 20, n. 2, p. 101–116, 2019.

KIM, W. *et al.* **Melatonin ameliorates cuprizone-induced reduction of hippocampal neurogenesis, brain-derived neurotrophic factor, and phosphorylation of cyclic AMP response element-binding protein in the mouse dentate gyrus**. Brain and behavior, v. 9, n. 9, p. e01388, 2019.

KIRBY, L. *et al.* **Oligodendrocyte precursor cells present antigen and are cytotoxic targets in inflammatory demyelination**. Nature communications, v. 10, n. 1, p. 3887, 2019.

KOCHUNOV, P. *et al.* **Association of White Matter With Core Cognitive Deficits in Patients With Schizophrenia**. JAMA psychiatry, v. 74, n. 9, p. 958–966, 2017.

KOWALCHUK, C. *et al.* **Antipsychotics differentially regulate insulin, energy sensing, and inflammation pathways in hypothalamic rat neurons**. Psychoneuroendocrinology, *[S. l.]*, v. 104, p. 42–48, 2019.

KREMER, D.; KÜRY, P.; DUTTA, R. **Promoting remyelination in multiple sclerosis: current drugs and future prospects.** Multiple sclerosis, v. 21, n. 5, p. 541–549, 2015.

KRIISA, K. *et al.* **Antipsychotic Treatment Reduces Indices of Oxidative Stress in First-Episode Psychosis Patients**. Oxidative medicine and cellular longevity, v. 2016, p. 9616593, 2016.

KRIISA, K. *et al.* **Profiling of Acylcarnitines in First Episode Psychosis before and after Antipsychotic Treatment**. Journal of proteome research, v. 16, n. 10, p. 3558–3566, 2017.

LARUELLE, M. *et al.* **Single photon emission computerized tomography imaging of amphetamine-induced dopamine release in drug-free schizophrenic subjects**. Proceedings of the National Academy of Sciences of the United States of America, v. 93, n. 17, p. 9235–9240, 1996.

LEE, J.-M. *et al.* **Proteomics and biomarkers in clinical trials for drug development**. Journal of proteomics, v. 74, n. 12, p. 2632–2641, 2011.

LEPPIK, L. *et al.* **Profiling of lipidomics before and after antipsychotic treatment in first-episode psychosis.** European archives of psychiatry and clinical neuroscience, v. 270, n. 1, p. 59–70, 2020.

LEUCHT, S. *et al.* **Second-generation versus first-generation antipsychotic drugs for schizophrenia: a meta-analysis**. The Lancet, v. 373, n. 9657, p. 31–41, 2009.

LEVIN, Y.; HRADETZKY, E.; BAHN, S. **Quantification of proteins using data-independent analysis (MSE) in simple andcomplex samples: a systematic evaluation.** Proteomics, v. 11, n. 16, p. 3273–3287, 2011.

LEWEKE, F. M. *et al.* **Cannabidiol enhances anandamide signaling and alleviates psychotic symptoms of schizophrenia**. Translational psychiatry, v. 2, p. e94, 2012.

LEWIS, D. A.; LIEBERMAN, J. A. C**atching up on schizophrenia: natural history and neurobiology**. Neuron, v. 28, n. 2, p. 325–334, 2000.

LI, C. *et al.* **A functional role of NMDA receptor in regulating the differentiation of oligodendrocyte precursor cells and remyelination**. Glia, v. 61, n. 5, p. 732–749, 2013.

LIEBERMEISTER, W. *et al.* **Visual account of protein investment in cellular functions**. Proceedings of the National Academy of Sciences of the United States of America, v. 111, n. 23, p. 8488–8493, 2014.

LI, F. *et al.* R**edox active motifs in selenoproteins**. Proceedings of the National Academy of Sciences of the United States of America, v. 111, n. 19, p. 6976–6981, 2014.

LIU, J. *et al.* **miR-214 targets the PTEN-mediated PI3K/Akt signaling pathway and regulates cell proliferation and apoptosis in ovarian cancer**. Oncology letters, v. 14, n. 5, p. 5711–5718, 2017.

LIU, Y. *et al.* **Mechanism of cellular 3-(4,5-dimethylthiazol-2-yl)-2,5-diphenyltetrazolium bromide (MTT) reduction**. Journal of neurochemistry, v. 69, n. 2, p. 581–593, 1997.

LU, H.-C.; MACKIE, K. **An Introduction to the Endogenous Cannabinoid System**. Biological psychiatry, v. 79, n. 7, p. 516–525, 2016.

MACKAY, A. V. *et al.* **Increased brain dopamine and dopamine receptors in schizophrenia**. Archives of general psychiatry, v. 39, n. 9, p. 991–997, 1982.

MAGANTI, R. J. *et al.* **Defining Changes in the Spatial Distribution and Composition of Brain Lipids in the Shiverer and Cuprizone Mouse Models of Myelin Disease**. The journal of histochemistry and cytochemistry: official journal of the Histochemistry Society, v. 67, n. 3, p. 203–219, 2019.

MAGISTRETTI, P. J.; ALLAMAN, I. **Brain Energy Metabolism**. *In*: PFAFF, D. W. (org.). Neuroscience in the 21st Century: From Basic to Clinical. New York, NY: Springer New York, 2013. p. 1591–1620. *E-book.*

MALHOTRA, A. K. *et al.* **Association between common variants near the melanocortin 4 receptor gene and severe antipsychotic drug-induced weight gain**. Archives of general psychiatry, v. 69, n. 9, p. 904–912, 2012.

MARTINS-DE-SOUZA, D. *et al.* **The role of energy metabolism dysfunction and oxidative stress in schizophrenia revealed by proteomics**. Antioxidants & redox signaling, v. 15, n. 7, p. 2067–2079, 2011.

MARTINS-DE-SOUZA, D. *et al.* **Proteomic analysis identifies dysfunction in cellular transport, energy, and protein metabolism in different brain regions of atypical frontotemporal lobar degeneration**. Journal of proteome research, v. 11, n. 4, p. 2533–2543, 2012.

MATSUSHIMA, G. K.; MORELL, P. **The neurotoxicant, cuprizone, as a model to study demyelination and remyelination in the central nervous system**. Brain pathology , *[S. l.]*, v. 11, n. 1, p. 107–116, 2001.

MATTHIESEN, R.; BUNKENBORG, J. **Introduction to mass spectrometry-based proteomics**. Methods in molecular biology, v. 1007, p. 1–45, 2013.

MCGUIRE, P. *et al.* **Cannabidiol (CBD) as an Adjunctive Therapy in Schizophrenia: A Multicenter Randomized Controlled Trial**. The American journal of psychiatry, v. 175, n. 3, p. 225–231, 2018.

MCKENZIE, I. A. *et al.* **Motor skill learning requires active central myelination**. Science, v. 346, n. 6207, p. 318–322, 2014.

MECHA, M. *et al.* **Cannabidiol protects oligodendrocyte progenitor cells from inflammation-induced apoptosis by attenuating endoplasmic reticulum stress**. Cell death & disease, v. 3, p. e331, 2012.

MENN, B. *et al.* **Origin of oligodendrocytes in the subventricular zone of the adult brain**. The Journal of neuroscience: the official journal of the Society for Neuroscience, v. 26, n. 30, p. 7907–7918, 2006.

MESSORI, L. *et al.* **Unravelling the chemical nature of copper cuprizone**. Dalton transactions, n. 21, p. 2112–2114, 2007.

METSALU, T.; VILO, J. **ClustVis: a web tool for visualizing clustering of multivariate data using Principal Component Analysis and heatmap**. Nucleic acids research, v. 43, n. W1, p. W566–70, 2015.

MI, G. *et al.* **Cyclin-dependent kinase inhibitor flavopiridol promotes remyelination in a cuprizone induced demyelination model**. Cell cycle, v. 15, n. 20, p. 2780–2791, 2016.

MI, G. *et al.* **The antipsychotic drug quetiapine stimulates oligodendrocyte differentiation by modulating the cell cycle**. Neurochemistry international, v. 118, p. 242–251, 2018.

MIGHDOLL, M. I. *et al.* **Myelin, myelin-related disorders, and psychosis**. Schizophrenia research, v. 161, n. 1, p. 85–93, 2015.

MIRNICS, K. *et al.* **Molecular characterization of schizophrenia viewed by microarray analysis of gene expression in prefrontal cortex**. Neuron, v. 28, n. 1, p. 53–67, 2000.

MITEW, S. *et al.* **Mechanisms regulating the development of oligodendrocytes and central nervous system myelin**. Neuroscience, v. 276, p. 29–47, 2014.

MOLDOVAN, N. *et al.* **Altered transition metal homeostasis in the cuprizone model of demyelination**. Neurotoxicology, v. 48, p. 1–8, 2015.

MOLINA-HOLGADO, E. *et al.* C**annabinoids promote oligodendrocyte progenitor survival: involvement of cannabinoid receptors and phosphatidylinositol-3 kinase/Akt signaling**. The Journal of neuroscience: the official journal of the Society for Neuroscience, v. 22, n. 22, p. 9742–9753, 2002.

MUELLER, T. M.; MEADOR-WOODRUFF, J. H. **Post-translational protein modifications in schizophrenia**. NPJ schizophrenia, v. 6, n. 1, p. 5, 2020.

MUGURUZA, C. *et al.* **Endocannabinoid system imbalance in the postmortem prefrontal cortex of subjects with schizophrenia**. Journal of psychopharmacology, v. 33, n. 9, p. 1132–1140, 2019.

MURATAEVA, N.; STRAIKER, A.; MACKIE, K. **Parsing the players: 2-arachidonoylglycerol synthesis and degradation in the CNS**. British journal of pharmacology, v. 171, n. 6, p. 1379–1391, 2014.

NARAYAN, S.; KASS, K. E.; THOMAS, E. A. **Chronic haloperidol treatment results in a decrease in the expression of myelin/oligodendrocyte-related genes in the mouse brain**. Journal of neuroscience research, v. 85, n. 4, p. 757–765, 2007.

NASCIMENTO, J. M.; MARTINS-DE-SOUZA, D. **The proteome of schizophrenia**. NPJ schizophrenia, v. 1, p. 14003, 2015.

NEVALAINEN, T.; IRVING, A. J. **GPR55, a lysophosphatidylinositol receptor with cannabinoid sensitivity?** Current topics in medicinal chemistry, v. 10, n. 8, p. 799–813, 2010.

NIU, J. *et al.* **Haloperidol promotes proliferation but inhibits differentiation in rat oligodendrocyte progenitor cell cultures**. Biochemistry and cell biology = Biochimie et biologie cellulaire, v. 88, n. 4, p. 611–620, 2010.

OLIVEIRA, B. M.; COORSSEN, J. R.; MARTINS-DE-SOUZA, D. **2DE: the phoenix of proteomics**. Journal of proteomics, v. 104, p. 140–150, 2014.

ORBAN, P. *et al.* **Altered brain connectivity in patients with schizophrenia is consistent across cognitive contexts**. Journal of psychiatry & neuroscience: JPN, v. 42, n. 1, p. 17–26, 2017.

O'SULLIVAN, S. E. **An update on PPAR activation by cannabinoids**. British journal of pharmacology, v. 173, n. 12, p. 1899–1910, 2016.

OWEN, M. J.; SAWA, A.; MORTENSEN, P. B. **Schizophrenia**. The Lancet, v. 388, n. 10039, p. 86–97, 2016.

PADULA, M. P. *et al.* **A Comprehensive Guide for Performing Sample Preparation and Top-Down Protein Analysis**. Proteomes, v. 5, n. 2, 2017. Disponível em: https://doi.org/10.3390/proteomes5020011

PALAZUELOS, J.; KLINGENER, M.; AGUIRRE, A. **TGFβ signaling regulates the timing of CNS myelination by modulating oligodendrocyte progenitor cell cycle exit through SMAD3/4/FoxO1/Sp1**. The Journal of neuroscience: the official journal of the Society for Neuroscience, v. 34, n. 23, p. 7917–7930, 2014.

PANIKASHVILI, D. *et al.* **An endogenous cannabinoid (2-AG) is neuroprotective after brain injury**. Nature, v. 413, n. 6855, p. 527–531, 2001.

PARK, H.; POO, M.-M. **Neurotrophin regulation of neural circuit development and function**. Nature reviews. Neuroscience, v. 14, n. 1, p. 7–23, 2013.

PASQUINI, L. A. *et al.* **The neurotoxic effect of cuprizone on oligodendrocytes depends on the presence of pro-inflammatory cytokines secreted by microglia**. Neurochemical research, v. 32, n. 2, p. 279–292, 2007.

PAULSON, L. *et al.* **Comparative proteome analysis of thalamus in MK-801-treated rats**. Proteomics, v. 4, n. 3, p. 819–825, 2004.

PAZ, R. D. *et al.* **Glutamatergic dysfunction in schizophrenia: from basic neuroscience to clinical psychopharmacology**. European neuropsychopharmacology: the journal of the European College of Neuropsychopharmacology, v. 18, n. 11, p. 773–786, 2008.

PEFEROEN, L. *et al.* **Oligodendrocyte-microglia cross-talk in the central nervous system**. Immunology, v. 141, n. 3, p. 302–313, 2014.

PETRONILLI, V.; ZORATTI, M. **A characterization of cuprizone-induced giant mouse liver mitochondria**. Journal of bioenergetics and biomembranes, v. 22, n. 5, p. 663–677, 1990.

PFEIFFER, S. E.; WARRINGTON, A. E.; BANSAL, R. **The oligodendrocyte and its many cellular processes**. Trends in cell biology, v. 3, n. 6, p. 191–197, 1993.

PHILIPS, T.; ROTHSTEIN, J. D. **Oligodendroglia: metabolic supporters of neurons**. The Journal of clinical investigation, v. 127, n. 9, p. 3271–3280, 2017.

POLYMEROPOULOS, M. H. *et al.* **Common effect of antipsychotics on the biosynthesis and regulation of fatty acids and cholesterol supports a key role of lipid homeostasis in schizophrenia**. Schizophrenia research, v. 108, n. 1-3, p. 134–142, 2009.

POTVIN, S. *et al.* **Peripheral Endogenous Cannabinoid Levels Are Increased in Schizophrenia Patients Evaluated in a Psychiatric Emergency Setting**. Frontiers in psychiatry / Frontiers Research Foundation, v. 11, p. 628, 2020.

POUGET, J. G. *et al.* **Cross-disorder analysis of schizophrenia and 19 immune-mediated diseases identifies shared genetic risk**. Human molecular genetics, v. 28, n. 20, p. 3498–3513, 2019.

PRABAKARAN, S. *et al.* **Mitochondrial dysfunction in schizophrenia: evidence for compromised brain metabolism and oxidative stress**. Molecular psychiatry, v. 9, n. 7, p. 684–97, 643, 2004.

PRAET, J. *et al.* **Cellular and molecular neuropathology of the cuprizone mouse model: clinical relevance for multiple sclerosis**. Neuroscience and biobehavioral reviews, v. 47, p. 485–505, 2014.

RAASCH, J. *et al.* **IkappaB kinase 2 determines oligodendrocyte loss by non-cell-autonomous activation of NF-kappaB in the central nervous system**. Brain: a journal of neurology, v. 134, n. Pt 4, p. 1184–1198, 2011.

RAHIMI, A. *et al.* **Interaction between the protective effects of cannabidiol and palmitoylethanolamide in experimental model of multiple sclerosis in C57BL/6 mice**. Neuroscience, v. 290, p. 279–287, 2015.

REN, Y.; WANG, H.; XIAO, L. **Improving myelin/oligodendrocyte-related dysfunction: a new mechanism of antipsychotics in the treatment of schizophrenia?** The international journal of neuropsychopharmacology / official scientific journal of the Collegium Internationale Neuropsychopharmacologicum, v. 16, n. 3, p. 691–700, 2013.

RIMMERMAN, N. *et al.* **The non-psychoactive plant cannabinoid, cannabidiol affects cholesterol metabolism-related genes in microglial cells**. Cellular and molecular neurobiology, v. 31, n. 6, p. 921–930, 2011.

RINHOLM, J. E. *et al.* **Regulation of oligodendrocyte development and myelination by glucose and lactate.** The Journal of neuroscience: the official journal of the Society for Neuroscience, v. 31, n. 2, p. 538–548, 2011.

RODGERS, J. M.; ROBINSON, A. P.; MILLER, S. D. **Strategies for protecting oligodendrocytes and enhancing remyelination in multiple sclerosis**. Discovery medicine, v. 16, n. 86, p. 53–63, 2013.

ROHLEDER, C. *et al.* **Cannabidiol as a Potential New Type of an Antipsychotic.** A Critical Review of the Evidence. Frontiers in pharmacology, v. 7, p. 422, 2016.

SAAB, A. S.; TZVETANOVA, I. D.; NAVE, K.-A. **The role of myelin and oligodendrocytes in axonal energy metabolism.** Current opinion in neurobiology, v. 23, n. 6, p. 1065–1072, 2013.

SACHS, H. H. et al**. A new model of cuprizone-mediated demyelination/remyelination**. ASN neuro, v. 6, n. 5, 2014.

SAIA-CEREDA, V. M. *et al.* **Proteomics of the corpus callosum unravel pivotal players in the dysfunction of cell signaling, structure, and myelination in schizophrenia brains**. European archives of psychiatry and clinical neuroscience, v. 265, n. 7, p. 601–612, 2015.

SAIA-CEREDA, V. M. *et al.* **The Nuclear Proteome of White and Gray Matter from Schizophrenia Postmortem Brains**. Molecular neuropsychiatry, v. 3, n. 1, p. 37–52, 2017.

SAITO, Y. *et al.* **Impaired white matter connectivity between regions containing mirror neurons, and relationship to negative symptoms and social cognition, in patients with first-episode schizophrenia**. Brain imaging and behavior, v. 12, n. 1, p. 229–237, 2018.

SÁNCHEZ-WANDELMER, J. *et al.* **Haloperidol disrupts lipid rafts and impairs insulin signaling in SH-SY5Y cells**. Neuroscience, v. 167, n. 1, p. 143–153, 2010.

SANTARELLI, D. M. *et al.* **Schizophrenia-associated MicroRNA-Gene Interactions in the Dorsolateral Prefrontal Cortex**. Genomics, proteomics & bioinformatics, v. 17, n. 6, p. 623–634, 2019.

SANTOS, A. K. *et al.* **Decoding cell signalling and regulation of oligodendrocyte differentiation**. Seminars in cell & developmental biology, v. 95, p. 54–73, 2019.

SÁRVÁRI, A. K. *et al.* **Atypical antipsychotics induce both proinflammatory and adipogenic gene expression in human adipocytes in vitro**. Biochemical and biophysical research communications, v. 450, n. 4, p. 1383–1389, 2014.

SAWA, A.; SEDLAK, T. W. **Oxidative stress and inflammation in schizophrenia**. Schizophrenia research, v. 176, n. 1, p. 1–2, 2016.

SCARPULLA, R. C. **Metabolic control of mitochondrial biogenesis through the PGC-1 family regulatory network**. Biochimica et biophysica acta, v. 1813, n. 7, p. 1269–1278, 2011.

SCHELLER, A.; KIRCHHOFF, F. **Endocannabinoids and Heterogeneity of Glial Cells in Brain Function**. Frontiers in integrative neuroscience, v. 10, p. 24, 2016.

SEABRA, G. *et al.* P**roteomics and Lipidomics in the Elucidation of Endocannabinoid Signaling in Healthy and Schizophrenia Brains**. Proteomics, v. 18, n. 18, p. e1700270, 2018.

SEABRA, G. *et al.* **Ubiquitin-proteasome system, lipid metabolism and DNA damage repair are triggered by antipsychotic medication in human oligodendrocytes: implications in schizophrenia**. Scientific reports, v. 10, n. 1, p. 12655, 2020.

SELEMON, L. D.; LIDOW, M. S.; GOLDMAN-RAKIC, P. S. **Increased volume and glial density in primate prefrontal cortex associated with chronic antipsychotic drug exposure**. Biological psychiatry, v. 46, n. 2, p. 161–172, 1999.

SIMONS, M.; NAVE, K.-A. **Oligodendrocytes: Myelination and Axonal Support**. Cold Spring Harbor perspectives in biology, v. 8, n. 1, p. a020479, 2015.

SKAPER, S. D. Chapter 4 - **Oligodendrocyte precursor cells as a therapeutic target for demyelinating diseases**. *In*: SHARMA, A.; SHARMA, H. S. (org.). Progress in Brain Research. Elsevier, 2019. v. 245p. 119–144. *E-book*.

SODHI, R. K.; SINGH, N. **Liver X receptors: emerging therapeutic targets for Alzheimer's disease**. Pharmacological research: the official journal of the Italian Pharmacological Society, v. 72, p. 45–51, 2013.

STADELMANN, C. *et al.* **Myelin in the Central Nervous System: Structure, Function, and Pathology**. Physiological reviews, v. 99, n. 3, p. 1381–1431, 2019.

STEINER, J. *et al.* **Protective effects of haloperidol and clozapine on energy-deprived OLN-93 oligodendrocytes**. European archives of psychiatry and clinical neuroscience, v. 261, n. 7, p. 477–482, 2011.

STEINER, J. *et al.* **GABAergic system impairment in the hippocampus and superior temporal gyrus of patients with paranoid schizophrenia: A post-mortem study**. Schizophrenia research, v. 177, n. 1-3, p. 10–17, 2016.

STELLA, N. **Endocannabinoid signaling in microglial cells**. Neuropharmacology, v. 56 Suppl 1, p. 244–253, 2009.

STORCK, E. M.; ÖZBALCI, C.; EGGERT, U. S. **Lipid Cell Biology: A Focus on Lipids in Cell Division**. Annual review of biochemistry, v. 87, p. 839–869, 2018.

SUGAI, T. *et al.* **Prefrontal abnormality of schizophrenia revealed by DNA microarray: impact on glial and neurotrophic gene expression**. Annals of the New York Academy of Sciences, v. 1025, p. 84–91, 2004.

SUN, S. *et al.* **Cannabidiol attenuates OGD/R-induced damage by enhancing mitochondrial bioenergetics and modulating glucose metabolism via pentose-phosphate pathway in hippocampal neurons**. Redox biology, v. 11, p. 577–585, 2017.

SZILAGYI, G. T. *et al.* **Proteomic changes during experimental de- and remyelination in the corpus callosum.** PloS one, v. 15, n. 4, p. e0230249, 2020.

SZKLARCZYK, D. *et al.* **The STRING database in 2017: quality-controlled protein-protein association networks, made broadly accessible**. Nucleic acids research, v. 45, n. D1, p. D362–D368, 2017.

TAHA, A. Y. *et al.* **Altered fatty acid concentrations in prefrontal cortex of schizophrenic patients**. Journal of psychiatric research, v. 47, n. 5, p. 636–643, 2013.

TAKAHASHI, N. *et al.* **Linking oligodendrocyte and myelin dysfunction to neurocircuitry abnormalities in schizophrenia**. Progress in neurobiology, v. 93, n. 1, p. 13–24, 2011.

TARABOLETTI, A. *et al.* **Cuprizone Intoxication Induces Cell Intrinsic Alterations in Oligodendrocyte Metabolism Independent of Copper Chelation**. Biochemistry, v. 56, n. 10, p. 1518–1528, 2017.

TARPADA, S. P.; MORRIS, M. T. **Physical Activity Diminishes Symptomatic Decline in Chronic Schizophrenia: A Systematic Review**. Psychopharmacology bulletin, v. 47, n. 4, p. 29–40, 2017.

TEMPLETON, N. *et al.* **Clozapine administration enhanced functional recovery after cuprizone demyelination**. PloS one, v. 14, n. 5, p. e0216113, 2019.

THOMPSON, K. K. *et al.* **Tuftsin Combines With Remyelinating Therapy and Improves Outcomes in Models of CNS Demyelinating Disease**. Frontiers in immunology, v. 9, p. 2784, 2018.

TOMAS-ROIG, J. *et al.* **The Cannabinoid CB1/CB2 Agonist WIN55212.2 Promotes Oligodendrocyte Differentiation In Vitro and Neuroprotection During the Cuprizone-Induced Central Nervous System Demyelination**. CNS neuroscience & therapeutics, v. 22, n. 5, p. 387–395, 2016.

TORRE-FUENTES, L. *et al.* **Experimental models of demyelination and remyelination**. Neurologia, v. 35, n. 1, p. 32–39, 2020.

TSUBOI, K. *et al.* **Molecular characterization of N-acylethanolamine-hydrolyzing acid amidase, a novel member of the choloylglycine hydrolase family with structural and functional similarity to acid ceramidase**. The Journal of biological chemistry, v. 280, n. 12, p. 11082–11092, 2005.

URANOVA, N. A. *et al.* **Ultrastructural pathology of oligodendrocytes adjacent to microglia in prefrontal white matter in schizophrenia**. NPJ schizophrenia, v. 4, n. 1, p. 26, 2018.

VAN OS, J.; KAPUR, S. **Schizophrenia**. The Lancet, v. 374, n. 9690, p. 635–645, 2009.

VENTURINI, G. **Enzymic activities and sodium, potassium and copper concentrations in mouse brain and liver after cuprizone treatment in vivo**. Journal of neurochemistry, v. 21, n. 5, p. 1147–1151, 1973.

VIENNOIS, E. *et al.* **Targeting liver X receptors in human health: deadlock or promising trail?** Expert opinion on therapeutic targets, v. 15, n. 2, p. 219–232, 2011.

VIKHREVA, O. V. *et al.* **Ultrastructural alterations of oligodendrocytes in prefrontal white matter in schizophrenia: A post-mortem morphometric study**. Schizophrenia research, v. 177, n. 1-3, p. 28–36, 2016.

VOINESKOS, A. N. *et al.* **A family-based association study of the myelin-associated glycoprotein and 2',3'-cyclic nucleotide 3'-phosphodiesterase genes with schizophrenia**. Psychiatric genetics, v. 18, n. 3, p. 143–146, 2008.

WANG, D. *et al.* **Metabolic profiling identifies phospholipids as potential serum biomarkers for schizophrenia**. Psychiatry research, v. 272, p. 18–29, 2019.

WASHBURN, M. P.; WOLTERS, D.; YATES, J. R., **3rd. Large-scale analysis of the yeast proteome by multidimensional protein identification technology**. Nature biotechnology, v. 19, n. 3, p. 242–247, 2001.

WERNER, S. R. *et al.* **Proteomic analysis of demyelinated and remyelinating brain tissue following dietary cuprizone administration.** Journal of molecular neuroscience: MN, v. 42, n. 2, p. 210–225, 2010.

WU, R.-R. *et al.* **Effects of typical and atypical antipsychotics on glucose-insulin homeostasis and lipid metabolism in first-episode schizophrenia**. Psychopharmacology, v. 186, n. 4, p. 572–578, 2006.

XU, H.; YANG, H.-J.; LI, X.-M. **Differential effects of antipsychotics on the development of rat oligodendrocyte precursor cells exposed to cuprizone**. European archives of psychiatry and clinical neuroscience, v. 264, n. 2, p. 121–129, 2014.

XU, Z. *et al.* **Arecoline attenuates memory impairment and demyelination in a cuprizone-induced mouse model of schizophrenia.** Neuroreport, v. 30, n. 2, p. 134–138, 2019.

YAN, B. C. *et al.* **Neuroprotection of posttreatment with risperidone, an atypical antipsychotic drug, in rat and gerbil models of ischemic stroke and the maintenance of antioxidants in a gerbil model of ischemic stroke**. Journal of neuroscience research, v. 92, n. 6, p. 795–807, 2014.

YANG, A. C.; TSAI, S.-J. **New Targets for Schizophrenia Treatment beyond the Dopamine Hypothesis**. International journal of molecular sciences, v. 18, n. 8, 2017.

YANG, J. *et al.* **Potential metabolite markers of schizophrenia**. Molecular psychiatry, v. 18, n. 1, p. 67–78, 2013.

ZAHEDNASAB, H. *et al.* **The protective effect of rifampicin on behavioral deficits, biochemical, and neuropathological changes in a cuprizone model of demyelination**. Cytokine, v. 113, p. 417–426, 2019.

ZAJICEK, J. P.; APOSTU, V. I. **Role of cannabinoids in multiple sclerosis**. CNS drugs, v. 25, n. 3, p. 187–201, 2011.

ZATTA, P. *et al.* **Copper and zinc dismetabolism in the mouse brain upon chronic cuprizone treatment**. Cellular and molecular life sciences: CMLS, v. 62, n. 13, p. 1502–1513, 2005.

ZENDEDEL, A.; BEYER, C.; KIPP, M. **Cuprizone-induced demyelination as a tool to study remyelination and axonal protection**. Journal of molecular neuroscience: MN, v. 51, n. 2, p. 567–572, 2013.

ZHANG, Q. *et al.* **microRNA-802 inhibits cell proliferation and induces apoptosis in human cervical cancer by targeting serine/arginine-rich splicing factor 9**. Journal of cellular biochemistry, v. 120, n. 6, p. 10370–10379, 2019.

ZHANG, Y. *et al.* **Quetiapine enhances oligodendrocyte regeneration and myelin repair after cuprizone-induced demyelination**. Schizophrenia research, v. 138, n. 1, p. 8–17, 2012.

ZHOU, Y. *et al.* **Metascape provides a biologist-oriented resource for the analysis of systems-level datasets**. Nature communications, v. 10, n. 1, p. 1523, 2019.

ZOU, S.; KUMAR, U. **Cannabinoid Receptors and the Endocannabinoid System: Signaling and Function in the Central Nervous System**. International journal of molecular sciences, v. 19, n. 3, 2018.

ZUCCOLI, G. S. *et al.* **The Energy Metabolism Dysfunction in Psychiatric Disorders Postmortem Brains: Focus on Proteomic Evidence**. Frontiers in neuroscience, v. 11, p. 493, 2017.

ZYGMUNT, P. M. *et al.* **Vanilloid receptors on sensory nerves mediate the vasodilator action of anandamide**. Nature, v. 400, n. 6743, p. 452–457, 1999.

9. MATERIAL SUPLEMENTAR

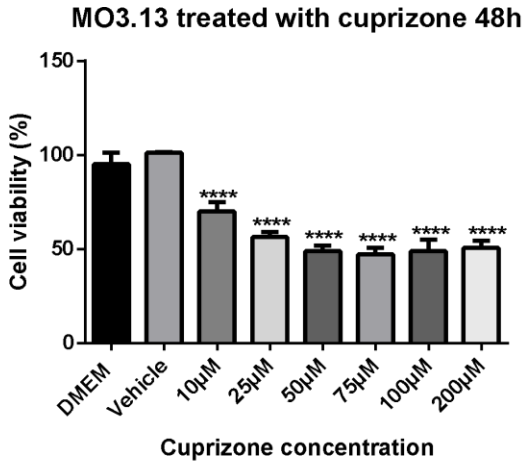

Figure S1. An MTT assay was used to measure the percentage of live M03.13 cells at 48h with growth medium (DMEM), Vehicle (DMSO, 0.3%), and increasing cuprizone concentrations. (****, P < 0.0001; n = 6 wells/condition).

A **B**

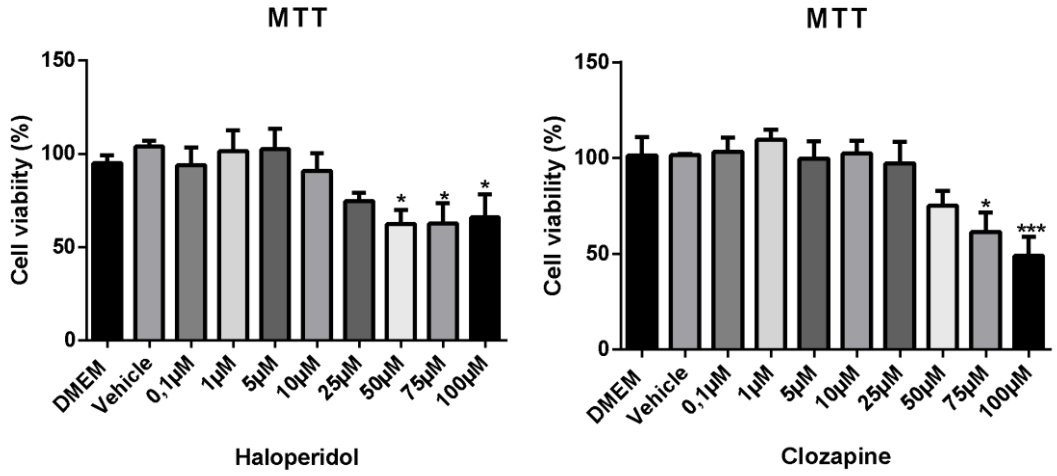

C **D**

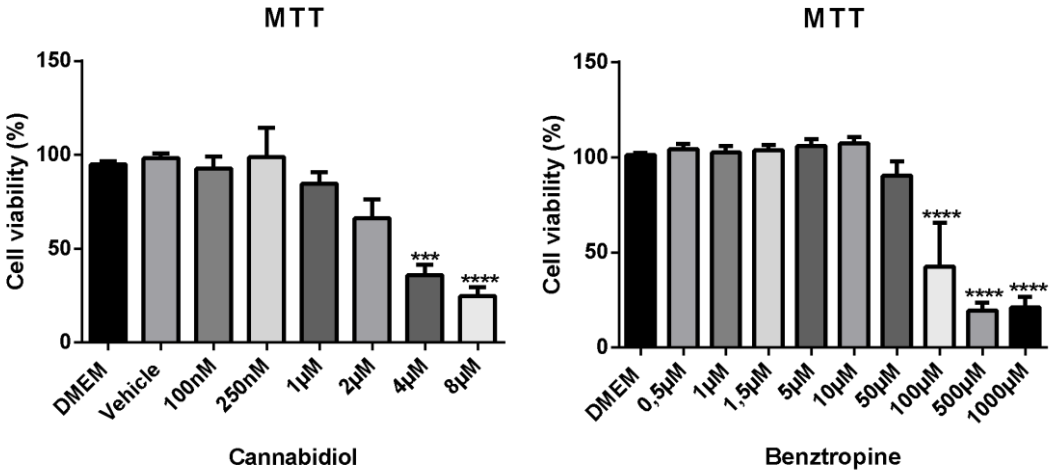

Figure S2. A MTT assay was used to measure the percentage of live M03.13 cells after 8h in growth medium (DMEM), Vehicle (haloperidol and cannabidiol, DMSO, 0.3%; clozapine, DMSO, 0.4%; benztropine was diluted in water), and increasing concentrations of haloperidol (A), clozapine (B), cannabidiol (C), or benztropine (D) (*, $P \leq 0.05$; ***, $P < 0.001$; ****, $P < 0.0001$; n = 6 wells/condition).

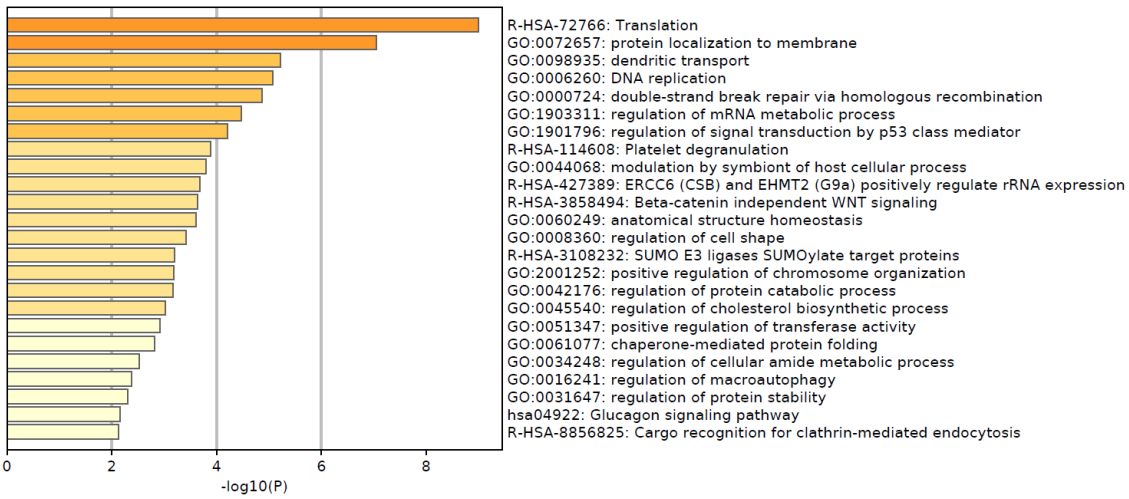

Figure S3. Bar graph of enriched biochemical pathways in MO3.13 cells treated with haloperidol, colored by p-value, created in Metascape. Colored lines represent $-\log_{10}(P)$, which significance are representing between 10^{-20} to 10^{-2}.

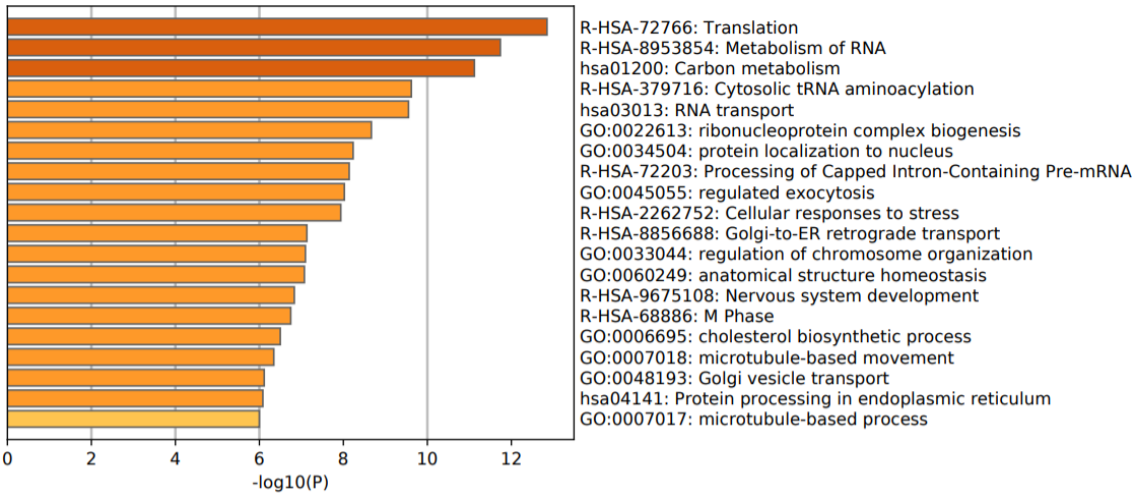

Figure S4. Bar graph of enriched biochemical pathways in MO3.13 cells treated with clozapine, colored by p-value, created in Metascape. Colored lines represent -$\log_{10}$(P), which significance are representing between 10^{-20} to 10^{-2}.

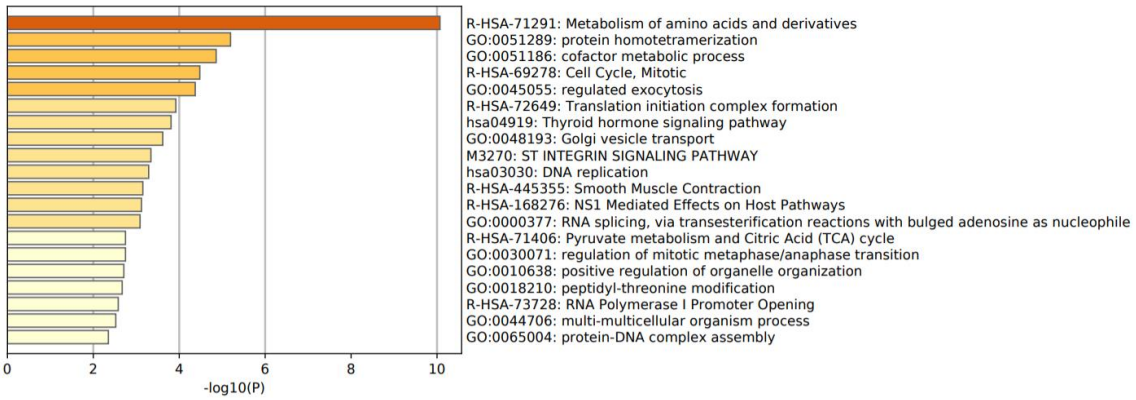

Figure S5. Bar graph of enriched biochemical pathways in MO3.13 cells treated with cannabidiol, colored by p-value, created in Metascape. Colored lines represent -$\log_{10}$(P), which significance are representing between 10^{-20} to 10^{-2}.

A

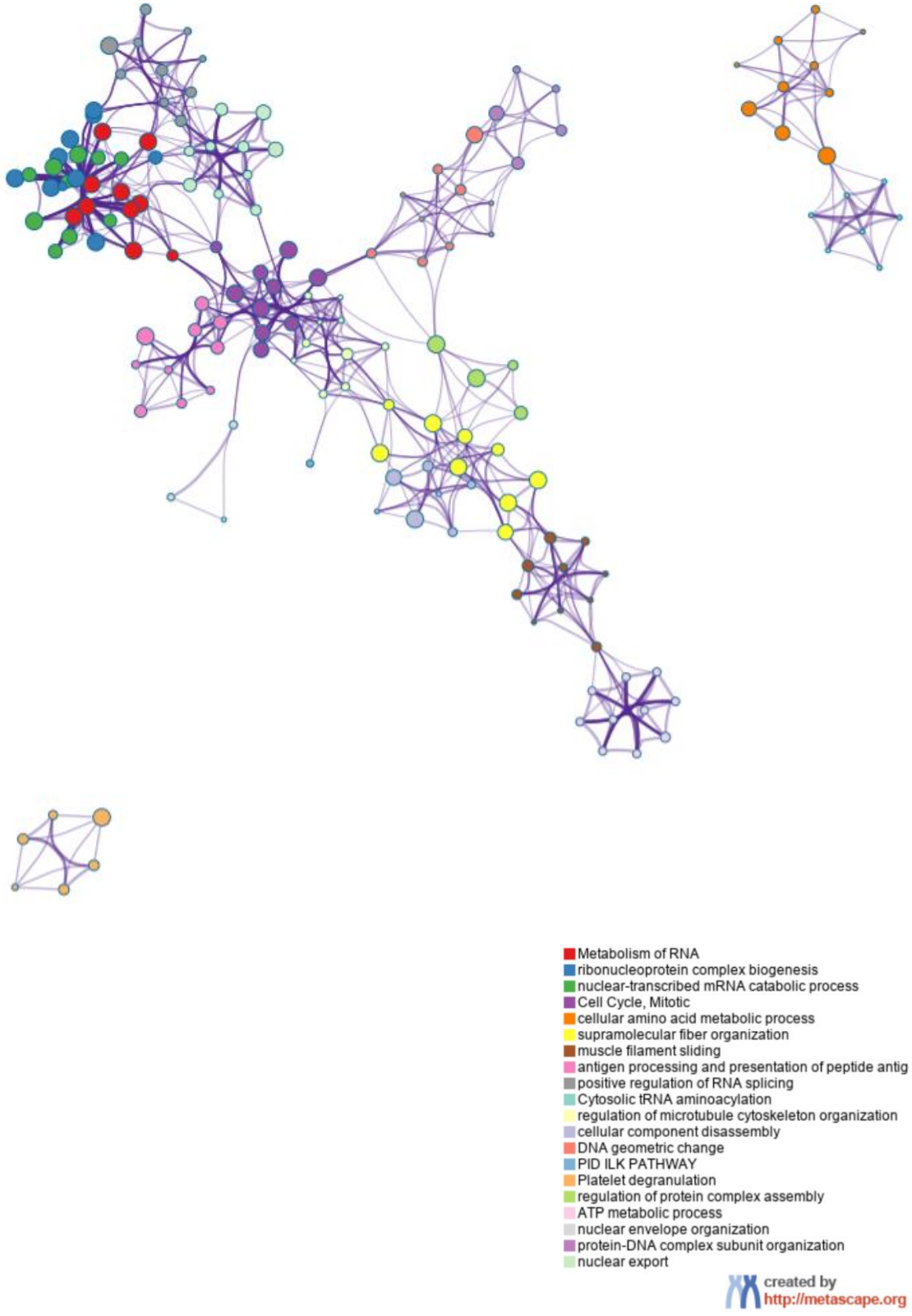
Metabolism of RNA
ribonucleoprotein complex biogenesis
nuclear-transcribed mRNA catabolic process
Cell Cycle, Mitotic
cellular amino acid metabolic process
supramolecular fiber organization
muscle filament sliding
antigen processing and presentation of peptide antig
positive regulation of RNA splicing
Cytosolic tRNA aminoacylation
regulation of microtubule cytoskeleton organization
cellular component disassembly
DNA geometric change
PID ILK PATHWAY
Platelet degranulation
regulation of protein complex assembly
ATP metabolic process
nuclear envelope organization
protein-DNA complex subunit organization
nuclear export
created by
http://metascape.org

B

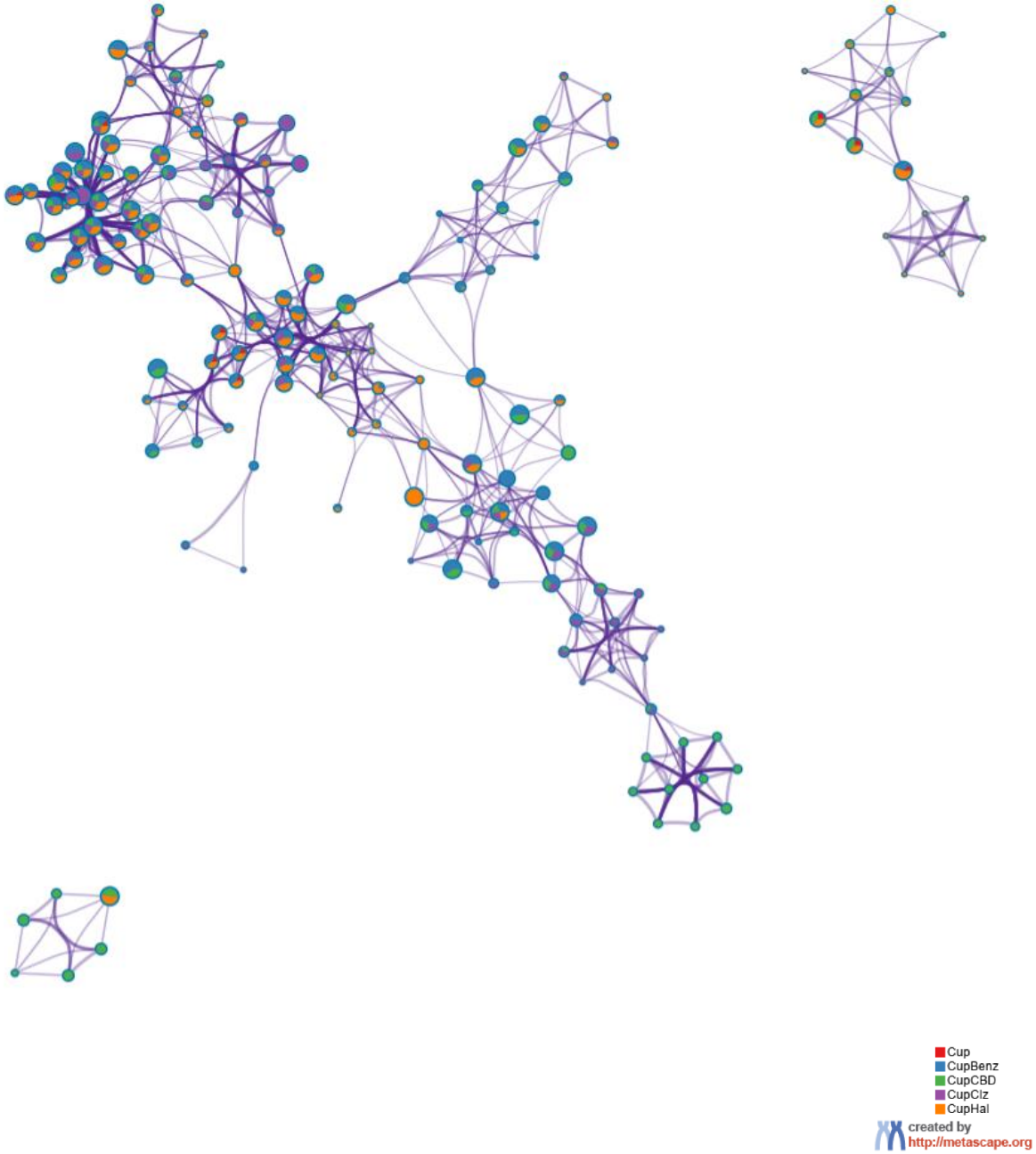

Figure S6. The network of enriched terms colored by cluster ID (A) and by network-enriched terms, represented as a pie chart (B) in treatment with cuprizone and co-treatments with cuprizone and haloperidol, clozapine, cannabidiol or benztropine, created with Metascape.

Table S1. List of proteins identified, quantified, differentially regulated, upregulated, and downregulated in treatments and co-treatments with cuprizone (Cup) and haloperidol (Hal), clozapine (Clz), cannabidiol (CBD), or benztropine (Benz).

Condition	Identified	Quantified	Differentially regulated
Cuprizone	2.019	1.744	30 (↑11 ↓19)
Haloperidol	2.802	1.886	91(↑41 ↓50)
Clozapine	2.801	1.882	292 (↑163 ↓129)
Cannabidiol	2.804	1.884	106 (↑53 ↓53)
Benztropine	2.804	1.884	196 (↑77 ↓119)
CupHal	1.946	1.608	95 (↑43 ↓52)
CupClz	2.801	1.885	91 (↑27 ↓64)
CupCBD	1.947	1.608	74 (↑40 ↓34)
Cup Benz	1.944	1.604	113 (↑55 ↓58)

Table S2. List of the differentially expressed proteins (by ANOVA, $p \leq 0.05$) seen in response to cuprizone treatment, compared with the changes seen in response to cuprizone and either haloperidol (Hal), clozapine (Clz), cannabidiol (CBD), or benztropine (Benz). Hyphens represent that the protein was not identified or not quantifiable in that sample. Highlighted p-values represent a change (ANOVA, $p \leq 0.05$) in the opposite direction of that induced by cuprizone, indicating a reversal of its putative toxic effects.

Differentially protein in CPZ	Cuprizone		CupHal		CupClz		CupCBD		CupBenz	
Protein	Log2(FC)	pValue	Log2(FC)	pValue	Log2(FC)	pValue	Log2(FC)	pValue	Log2(FC)	pValue
Citrate synthase_ mitochondrial	-0,2481354297	0,00263445082	0,4436901611	0,2935663556	-0,1322198962	0,9938722917	0,3872092341	0,7548493844	0,276937732	0,5734293488
Thioredoxin-dependent peroxide reductase_ mitochondrial	-0,7518799471	0,002885139846	-0,2295676807	0,5009169811	0,5394442793	0,1059267297	-1,632723289	0,0635277355	-0,1037505239	0,6851654379
Elongation factor 1-delta	-0,8694862715	0,00298965423	0,04251453232	0,8034585305	0,1030623117	0,6851912671	0,02321149501	0,8878958293	0,07860694537	0,7084161752
Non-POU domain-containing octamer-binding protein	-0,5273504505	0,003705681604	-0,8102484279	0,2173084731	-1,394428502	0,1906729859	-0,9256348335	0,1443311983	-0,013823854	0,9321548767
Serine/arginine-rich splicing factor 9	-0,5827770736	0,01032586779	0,6986571816	0,09529068427	-	-	-0,954735057	0,1150999992	-0,1179341066	0,6390170826
Tumor protein D54	0,4448098142	0,01050023734	0,3129735442	0,2928387642	0,1855755453	0,2618419321	0,3894142076	0,8864632279	-0,6392853084	0,1413444811
AMP deaminase 2	-0,4801237295	0,01096135793	0,3993403214	0,257752306	-0,895677751	0,01916258811	0,2710112841	0,4527034667	0,149100497	0,8256267682
Immunoglobulin lambda constant 2	3,111107227	0,01419383087	-3,00659747	0,05710726605	-	-	-3,169520297	0,0475475142	-3,192092943	0,04909105497
Metastasis-associated protein MTA2	0,2230859902	0,01441078669	0,3340446156	0,1095851903	-0,2759391389	0,3724319942	0,1416163033	0,8739551717	0,08991588288	0,7369690331
SWI/SNF complex subunit SMARCC1	-0,2983380305	0,01629854043	0,2471782048	0,05919358502	0,5275027754	0,06553570267	0,5397678607	0,007214706882	0,2553573798	0,02006282645
Annexin A5	-0,8860585173	0,02094882465	-0,2484483174	0,5713316725	-0,2893062621	0,4708681098	-0,6963256941	0,06156921966	0,27911715	0,5039692186
39S ribosomal protein L24_ mitochondrial	-0,5912590814	0,02306166696	-	-	1,060145155	0,5899003808	-	-	-	-
Procollagen-lysine_2-oxoglutarate 5-dioxygenase 2	0,2921586318	0,02987353859	1,027618255	0,2690691055	-0,6199588975	0,4952220677	0,7063652952	0,09071009502	0,5469626125	0,008606838071
Prolyl 4-hydroxylase subunit alpha-2	0,7582686936	0,0316630355	0,1618768736	0,4851293114	-0,1402108855	0,6047337477	0,03088913557	0,7954109633	0,2787638172	0,3284454822
60S ribosomal protein L3	0,3061291104	0,03266035397	1,400730995	0,1092098523	0,6903280411	0,3610962948	-0,05285023338	0,6852917798	-0,7861897203	0,8565330576
Ras-related protein Ral-A	-0,515078024	0,03390670875	0,5306664871	0,05144120106	0,6103183491	0,3144310896	-0,3318190792	0,4288564944	0,3224659555	0,2090515504
Galectin-3-binding protein	0,3930784279	0,0364676452	0,0257425054	0,8722112686	-0,1370417647	0,3060758945	0,1245210155	0,4434144939	-0,08068037785	0,7151178438
Transcription elongation regulator 1	-0,1890279228	0,03674826194	0,03183087289	0,7841625272	-0,06567032521	0,6145514284	-0,1049333596	0,5341121255	-0,1327262712	0,3997699889
Coiled-coil domain-containing protein 96	0,1814653665	0,03830210595	0,1151140526	0,4115979956	-	-	-0,02951235954	0,8017979871	-0,0967656721	0,6384139397
UTP--glucose-1-phosphate uridylyltransferase	0,3481368917	0,0473927632	-0,1661965763	0,4497235759	-0,008974857076	0,995580879	-0,05846953192	0,7298943095	-0,6144083451	0,06346339689
26S proteasome non-ATPase regulatory subunit 4	0,5141831777	0,04908990779	-0,355417386	0,1161878342	-0,3811047412	0,046168634	0,3204137689	0,4328332935	0,01165050615	0,9450426163

Table S3. Biochemical pathways highlighted in co-treatment with 10μM of cuprizone for 24 hours and 1μM of haloperidol for an additional 24 hours (CupHal), compared to cuprizone treatment alone, generated by Reactome.

Biochemical pathways - CupHal	p-value
Translation	2.05e-06
Cytosolic tRNA aminoacylation	2.69e-06
Metabolism of RNA	2.37e-05
Cellular responses to stress	3.44e-05
tRNA Aminoacylation	3.90e-05
Cellular responses to external stimuli	4.61e-05
G2/M Transition	6.82e-05
SRP-dependent cotranslational protein targeting to membrane	6.92e-05
Mitotic G2-G2/M phases	7.36e-05
Mitotic Anaphase	7.93e-05
Mitotic Prometaphase	8.23e-05
Mitotic Metaphase and Anaphase	8.23e-05
Influenza Life Cycle	9.18e-05
M Phase	1.11e-04
Metabolism of amino acids and derivatives	1.16e-04
Influenza Infection	1.44e-04
Cell Cycle, Mitotic	1.77e-04
Separation of Sister Chromatids	2.93e-04
Formation of a pool of free 40S subunits	3.05e-04
Cell Cycle	3.69e-04
rRNA processing	4.53e-04
Infectious disease	4.86e-04
L13a-mediated translational silencing of Ceruloplasmin expression	4.99e-04
GTP hydrolysis and joining of the 60S ribosomal subunit	5.22e-04
Nonsense-Mediated Decay (NMD)	6.26e-04

Table S4. Biochemical pathways highlighted in co-treatment with 10μM of cuprizone for 24 hours and 1μM of clozapine for an additional 24 hours (CupClz), compared to cuprizone treatment alone, generated by Reactome.

Biochemical pathways - CupClz	p-value
Striated Muscle Contraction	1.30e-05
Smooth Muscle Contraction	3.14e-04
Mitotic Anaphase	0.003
Mitotic Metaphase and Anaphase	0.003
M Phase	0.005
Regulation of mRNA stability by proteins that bind AU-rich elements	0.006
Muscle contraction	0.007
Depolymerisation of the Nuclear Lamina	0.008
Metabolism of RNA	0.009
Initiation of Nuclear Envelope (NE) Reformation	0.012
Abortive elongation of HIV-1 transcript in the absence of Tat	0.015
Signaling by FGFR2 IIIa TM	0.015
Mitotic Prophase	0.017
FGFR2 alternative splicing	0.019
Signaling by FGFR in disease	0.022
mRNA Capping	0.024
Nuclear Envelope (NE) Reassembly	0.026
The role of GTSE1 in G2/M progression after G2 checkpoint	0.027
Formation of the HIV-1 Early Elongation Complex	0.03
Formation of the Early Elongation Complex	0.03
Cell Cycle, Mitotic	0.031
Drug resistance in ERBB2 KD mutants	0.032
Hypusine synthesis from eIF5Alysine	0.032
Drug-mediated inhibition of ERBB2 signaling	0.032
Resistance of ERBB2 KD mutants to afatinib	0.032

Table S5. Biochemical pathways highlighted in co-treatment with 10μM of cuprizone for 24 hours and 1μM of cannabidiol for an additional 24 hours (CupCBD), compared to cuprizone treatment alone, generated by Reactome.

Biochemical pathways - CupCBD	p-value
Nephrin family interactions	4.76e-04
Platelet degranulation	0.002
Response to elevated platelet cytosolic Ca2+	0.002
Unwinding of DNA	0.003
Glutamate and glutamine metabolism	0.004
Collagen biosynthesis and modifying enzymes	0.01
rRNA processing	0.01
Orc1 removal from chromatin	0.011
Golgi-to-ER retrograde transport	0.012
Defective SLC7A7 causes lysinuric protein intolerance (LPI)	0.013
DNA strand elongation	0.019
Activation of the pre-replicative complex	0.02
Collagen formation	0.021
Switching of origins to a postreplicative state	0.022
Striated Muscle Contraction	0.023
Lysosome Vesicle Biogenesis	0.024
Activation of ATR in response to replication stress	0.024
Suppression of autophagy	0.026
The citric acid (TCA) cycle and respiratory electron transport	0.028
Formation of a pool of free 40S subunits	0.029
Platelet activation, signaling and aggregation	0.029
Major pathway of rRNA processing in the nucleolus and cytosol	0.031
NOSTRIN mediated eNOS trafficking	0.032
tRNA processing in the mitochondrion	0.032
L13a-mediated translational silencing of Ceruloplasmin expression	0.037

Table S6. Biochemical pathways highlighted in co-treatment with 10μM of cuprizone for 24 hours and 1μM of benztropine for an additional 24 hours (CupBenz), compared to cuprizone treatment alone, generated by Reactome.

Biochemical pathways - CupBenz	p-value
DNA Damage Recognition in GG-NER	7.12e-04
GTP hydrolysis and joining of the 60S ribosomal subunit	0.001
Influenza Life Cycle	0.001
Centrosome maturation	0.002
Recruitment of mitotic centrosome proteins and complexes	0.002
Cap-dependent Translation Initiation	0.002
Eukaryotic Translation Initiation	0.002
Influenza Infection	0.002
COPI-independent Golgi-to-ER retrograde traffic	0.002
Nonsense Mediated Decay (NMD) independent of the Exon Junction Complex (EJC)	0.003
Ribosomal scanning and start codon recognition	0.004
G2/M Transition	0.005
Mitotic G2-G2/M phases	0.005
Influenza Viral RNA Transcription and Replication	0.005
Intra-Golgi and retrograde Golgi-to- ER traffic	0.006
Loss of proteins required for interphase microtubule organization from the centrosome	0.006
Loss of Nlp from mitotic centrosomes	0.006
L13a-mediated translational silencing of Ceruloplasmin expression	0.007
AURKA Activation by TPX2	0.007
Nonsense-Mediated Decay (NMD)	0.008
Nonsense Mediated Decay (NMD) enhanced by the Exon Junction Complex (EJC)	0.008
Signaling by ROBO receptors	0.008

Table S7. Biochemical pathways highlighted in treatment with 1μM of haloperidol for 24 hours (Hal) compared to vehicle samples, generated by Reactome.

Biochemical pathways - Hal	p-value
Selenocysteine synthesis	1.27e-06

Eukaryotic Translation Elongation	1.37e-06
Translation	5.84e-06
Selenoamino acid metabolism	6.68e-06
Eukaryotic Translation Initiation	7.54e-06
Cap-dependent Translation Initiation	7.54e-06
Peptide chain elongation	1.08e-05
Influenza Infection	1.30e-05
Eukaryotic Translation Termination	1.42e-05
Nonsense Mediated Decay (NMD) independent of the Exon Junction Complex (EJC)	1.63e-05
Viral mRNA Translation	2.24e-05
Formation of a pool of free 40S subunits	2.39e-05
Response of EIF2AK4 (GCN2) to amino acid deficiency	2.39e-05
Metabolism of proteins	3.97e-05
L13a-mediated translational silencing of Ceruloplasmin expression	4.30e-05
SRP-dependent cotranslational protein targeting to membrane	4.55e-05
GTP hydrolysis and joining of the 60S ribosomal subunit	4.55e-05
Nonsense-Mediated Decay (NMD)	5.65e-05
Nonsense Mediated Decay (NMD) enhanced by the Exon Junction Complex (EJC)	5.65e-05
Cellular responses to stress	5.91E-05
Cellular responses to external stimuli	7.77e-05
Signaling by ROBO receptors	8.45e-05
Regulation of expression of SLITs and ROBOs	9.48e-05
Major pathway of rRNA processing in the nucleolus and cytosol	1.45e-04
rRNA processing in the nucleus and cytosol	2.07e-04

Table S8. Biochemical pathways highlighted in treatment with 1μM of clozapine for 24 hours (Clz) compared to vehicle samples, generated by Reactome.

Biochemical pathways - Clz	**p-value**

Cytosolic tRNA aminoacylation	2.88e-07
Translation	9.91e-07
tRNA Aminoacylation	1.70e-05
Metabolism of RNA	3.52e-05
Glutamate and glutamine metabolism	5.13e-05
Influenza Infection	5.35e-05
Translation initiation complex formation	1.77e-04
Ribosomal scanning and start codon recognition	1.77e-04
Activation of the mRNA upon binding of the cap-binding complex and eIFs, and subsequent binding to 43S	1.98e-04
GTP hydrolysis and joining of the 60S ribosomal subunit	2.10e-04
Processing of Capped Intron-Containing Pre-mRNA	2.65e-04
Golgi-to-ER retrograde transport	2.84e-04
Citric acid cycle (TCA cycle)	3.01e-04
mRNA Splicing - Major Pathway	3.01e-04
Cap-dependent Translation Initiation	3.47e-04
Eukaryotic Translation Initiation	3.47e-04
Metabolism of amino acids and derivatives	3.71e-04
mRNA Splicing	4.62e-04
Formation of the ternary complex, and subsequently, the 43S complex	4.67e-04
Pyruvate metabolism and Citric Acid (TCA) cycle	6.48e-04
EPH-Ephrin signaling	7.53e-04
L13a-mediated translational silencing of Ceruloplasmin expression	7.80e-04
Metabolism of proteins	8.28e-04
RMTs methylate histone arginines	0.002
Gluconeogenesis	0.002

Table S9. Biochemical pathways highlighted in treatment with 1μM of cannabidiol for 24 hours (CBD) compared to vehicle samples, generated by Reactome.

Biochemical pathways - CBD	**p-value**

L13a-mediated translational silencing of Ceruloplasmin expression	1.17e-06
GTP hydrolysis and joining of the 60S ribosomal subunit	1.26e-06
Eukaryotic Translation Initiation	2.05e-06
Cap-dependent Translation Initiation	2.05e-06
Metabolism of amino acids and derivatives	2.20e-06
Regulation of expression of SLITs and ROBOs	4.94e-04
Influenza Infection	4.94e-04
Formation of a pool of free 40S subunits	4.94e-04
Signaling by ROBO receptors	5.02e-04
Major pathway of rRNA processing in the nucleolus and cytosol	6.14e-04
SRP-dependent cotranslational protein targeting to membrane	7.50e-04
rRNA processing in the nucleus and cytosol	8.02e-04
Translation	0.001
rRNA processing	0.001
Peptide chain elongation	0.001
Nervous system development	2.76e-05
Eukaryotic Translation Termination	3.06e-05
Selenocysteine synthesis	3.06e-05
Eukaryotic Translation Elongation	3.27e-05
Nonsense Mediated Decay (NMD) independent of the Exon Junction Complex (EJC)	3.50e-05
Viral mRNA Translation	4.80e-05
Metabolism of RNA	4.91e-05
Response of EIF2AK4 (GCN2) to amino acid deficiency	5.11e-05
Axon guidance	5.84e-05
Influenza Viral RNA Transcription and Replication	9.34e-05

Table S10. Biochemical pathways highlighted in treatment with 1μM of benztropine for 24 hours (Benz) compared to vehicle samples, generated by Reactome.

Biochemical pathways - Benz	**p-value**

Influenza Infection	2.19e-09
Metabolism of RNA	2.45e-09
Cellular responses to stress	6.94e-08
Influenza Viral RNA Transcription and Replication	1.06e-07
Cellular responses to external stimuli	1.17e-07
M Phase	1.37e-07
CLEC7A (Dectin-1) signaling	2.20e-07
ISG15 antiviral mechanism	2.30e-07
RHO GTPase Effectors	3.27e-07
Host Interactions of HIV factors	3.39e-07
Regulation of mRNA stability by proteins that bind AU-rich elements	5.82e-07
Antiviral mechanism by IFN stimulated genes	6.49e-07
Cell Cycle	8.03e-07
Disorders of transmembrane transporters	8.72e-07
Metabolism of amino acids and derivatives	9.53e-07
Export of Viral Ribonucleoproteins from Nucleus	1.17e-06
Glycolysis	1.53e-06
Glucose metabolism	1.63e-06
Signaling by ROBO receptors	1.91e-06
Cell Cycle Checkpoints	2.13e-06
Response of EIF2AK4 (GCN2) to amino acid deficiency	2.39e-06
Cell Cycle, Mitotic	3.06e-06
GTP hydrolysis and joining of the 60S ribosomal subunit	6.24e-06
Selenocysteine synthesis	7.76e-06
Regulation of RUNX2 expression and activity	7.80e-06

Table S11. List of proteins differentially expressed (by ANOVA, $p \leq 0.05$) in MO3.13 oligodendrocytes exposed to cuprizone (CUP; 10µM, 48h) compared to vehicle (VEI).

Accession	Description	p-value	CUP/VEI ratio
O75390	Citrate synthase_ mitochondrial	0.002634	0.841983911
P30048	Thioredoxin-dependent peroxide reductase_	0.002885	0.593829246

	mitochondrial		
P29692	Elongation factor 1-delta	0.00299	0.547341719
Q15233	Non-POU domain-containing octamer-binding protein	0.003706	0.693827799
P22455	Fibroblast growth factor receptor 4	0.009838	0.805111207
Q13242	Serine/arginine-rich splicing factor 9	0.010326	0.667677314
O43399	Tumor protein D54	0.0105	1.361134671
Q01433	AMP deaminase 2 (EC 3.5.4.6) (AMP deaminase isoform)	0.010961	0.716916137
P0DOY2	Immunoglobulin lambda constant 2	0.014194	8.640454652
O94776	Metastasis-associated protein MTA2	0.014411	1.167227671
Q92922	SWI/SNF complex subunit SMARCC1	0.016299	0.813188642
Q9JHU4	Dynein heavy chain_ cytosolic (DYHC) (Cytoplasmic)	0.019014	0.797234958
P08758	Annexin A5	0.020949	0.541090375
Q96A35	39S ribosomal protein L24_ mitochondrial	0.023062	0.663763369
Q14258	Zinc finger protein 147 (Estrogen responsive finge)	0.023272	1.407020774
P17426	Adapter-related protein complex 2 alpha 1 subunit	0.028035	0.580740323
O00469	Procollagen-lysine_2-oxoglutarate 5-dioxygenase 2	0.029874	1.224471022
O05959	Lipoic acid synthetase (LIP-SYN) (Lipoate synthase)	0.030853	0.760985705
O15460	Prolyl 4-hydroxylase subunit alpha-2	0.031663	1.69145957
P17094	60S ribosomal protein L3	0.03266	1.236385903
Q9JLT0	Myosin heavy chain_ nonmuscle type B	0.033817	0.693456972
P11233	Ras-related protein Ral-A	0.033907	0.699755088
Q08380	Galectin-3-binding protein	0.036468	1.313192511
O14776	Transcription elongation regulator 1	0.036748	0.877196571
Q2M329	Coiled-coil domain-containing protein 96	0.038302	1.134035157
P29616	Myosin heavy chain_ cardiac muscle isoform	0.039817	0.682238114
Q15293	Reticulocalbin 1 precursor	0.040956	0.847363666
Q01240	60 kDa neurofilament protein (NF60)	0.041821	0.690599213
Q16851	UTP--glucose-1-phosphate uridylyltransferase	0.047393	1.272915712
P55036	26S proteasome non-ATPase regulatory subunit 4	0.04909	1.428185304

Table S12. List of proteins differentially expressed (by ANOVA, $p \leq 0.05$) in MO3.13 oligodendrocytes treated with haloperidol (Hal; 1µM, 24h) compared to vehicle (VEI).

Accession	Description	p-value	Hal/VEI ratio

Q9HDC9	Adipocyte plasma membrane-associated protein	9.23316E-05	1.312856574
Q6ZQQ6	WD repeat-containing protein 87	0.000167904	3.407716282
P06454	Prothymosin alpha	0.001314855	6.331514413
P52292	Importin subunit alpha-1	0.002974937	1.612108864
Q92785	Zinc finger protein ubi-d4	0.003018037	1.748412934
Q8IWJ2	GRIP and coiled-coil domain-containing protein 2	0.003208703	0.562232238
P02787	Serotransferrin	0.003622041	0.675898601
Q96B26	Exosome complex component RRP43	0.003795559	0.043622394
Q12873	Chromodomain-helicase-DNA-binding protein 3	0.003911948	0.422717298
P25398	40S ribosomal protein S12	0.004243169	3.13034976
P39748	Flap endonuclease 1	0.005692894	0.330141779
P31948	Stress-induced-phosphoprotein 1	0.006600763	0.720343076
Q13085	Acetyl-CoA carboxylase 1	0.006873453	0.785070046
Q5TCY1	Tau-tubulin kinase 1	0.006899875	1.713182141
O75477	Erlin-1	0.007342294	0.74682617
Q96KR1	Zinc finger RNA-binding protein	0.007427858	0.49390676
P62888	60S ribosomal protein L30	0.007780376	5.624567987
Q9H7B2	Ribosome production factor 2 homolog	0.008152766	0.16249862
Q13884	Beta-1-syntrophin	0.008185994	0.646060686
Q13976	cGMP-dependent protein kinase 1	0.008221527	0.576293539
P22061	Protein-L-isoaspartate(D-aspartate) O-methyltransferase	0.010935116	0.09282825
Q00577	Transcriptional activator protein Pur-alpha	0.010960811	1.330479915
P46063	ATP-dependent DNA helicase Q1	0.011924141	3.017977982
P35241	Radixin	0.012280216	0.47501204
P0DP23	Calmodulin-1	0.012614602	3.666655843
Q12840	Kinesin heavy chain isoform 5A	0.013185071	0.219779997
Q96EP5	DAZ-associated protein 1	0.013454334	0.463420342
P61088	Ubiquitin-conjugating enzyme E2 N	0.015334772	3.946390182
Q7Z2W4	Zinc finger CCCH-type antiviral protein 1	0.016765961	0.540500544
O94903	Pyridoxal phosphate homeostasis protein	0.016930731	1.210160764
P46459	Vesicle-fusing ATPase	0.01820751	0.449316354
Q15293	Reticulocalbin-1	0.018273288	0.740039576
P37802	Transgelin-2	0.018433945	0.339702161
P38571	Lysosomal acid lipase/cholesteryl ester hydrolase	0.018820373	4.825880892

P04406	Glyceraldehyde-3-phosphate dehydrogenase	0.019176775	2.674307439
P50502	Hsc70-interacting protein	0.019771818	1.294106093
O60240	Perilipin-1	0.021574922	0.108586311
P17858	ATP-dependent 6-phosphofructokinase_ liver type	0.021605046	6.491798309
Q9ULV0	Unconventional myosin-Vb	0.022599618	0.577521028
Q6FI13	Histone H2A type 2-A	0.022863195	2.440893886
P35968	Vascular endothelial growth factor receptor 2	0.02307132	1.397544802
Q08945	FACT complex subunit SSRP1	0.023591304	0.75893904
P49591	Serine--tRNA ligase_ cytoplasmic	0.02395338	0.606675819
Q13144	Translation initiation factor eIF-2B subunit epsilon	0.024017992	2.592607418
P32119	Peroxiredoxin-2	0.024058278	1.091784853
Q13200	26S proteasome non-ATPase regulatory subunit 2	0.024583026	0.452713754
P78371	T-complex protein 1 subunit beta	0.024608371	1.763917218
Q9BRV8	Suppressor of IKBKE 1	0.024748536	0.335365486
P62249	40S ribosomal protein S16	0.02490566	0.353228252
Q12926	ELAV-like protein 2	0.024954153	1.545775484
P07737	Profilin-1	0.02530649	2.560022758
P30041	Peroxiredoxin-6	0.025468981	0.571861266
P32969	60S ribosomal protein L9	0.026298469	4.995717771
Q04837	Single-stranded DNA-binding protein_ mitochondrial	0.026382881	2.139641597
O95785	Protein Wiz	0.026466899	0.19857265
Q96RP9	Elongation factor G_ mitochondrial	0.02650285	0.847397173
Q96D15	Reticulocalbin-3	0.029690632	0.259517112
O00629	Importin subunit alpha-3	0.029739773	2.781218999
P33176	Kinesin-1 heavy chain	0.030763599	0.795459736
O75923	Dysferlin	0.030856908	0.725589466
P45974	Ubiquitin carboxyl-terminal hydrolase 5	0.030939338	1.565557056
P17844	Probable ATP-dependent RNA helicase DDX5	0.031022015	0.78020866
P78356	Phosphatidylinositol 5-phosphate 4-kinase type-2 beta	0.031348212	1.681001408
Q15276	Rab GTPase-binding effector protein 1	0.031471278	0.692067452
Q05639	Elongation factor 1-alpha 2	0.031539429	1.488640265
Q13263	Transcription intermediary factor 1-beta	0.032729859	0.458604616
Q96T76	MMS19 nucleotide excision repair protein homolog	0.032979528	0.533717998
Q8WXA9	Splicing regulatory glutamine/lysine-rich protein 1	0.034320243	0.465970647
P62244	40S ribosomal protein S15a	0.034648708	16.49642671

Q13907	Isopentenyl-diphosphate Delta-isomerase 1	0.034834635	0.603184756
P61254	60S ribosomal protein L26	0.035189362	0.638225153
Q9UHD1	Cysteine and histidine-rich domain-containing protein 1	0.036560235	0.285008891
O43776	Asparagine--tRNA ligase_ cytoplasmic	0.037201917	0.669301277
Q09028	Histone-binding protein RBBP4	0.037972297	1.507236994
P54760	Ephrin type-B receptor 4	0.038707198	0.443998432
P61019	Ras-related protein Rab-2A	0.039541526	0.83831168
Q9UBS4	DnaJ homolog subfamily B member 11	0.040024668	1.241410336
Q96CW1	AP-2 complex subunit mu	0.040229227	1.81376851
Q9NRR5	Ubiquilin-4	0.040625738	0.020466719
Q96B97	SH3 domain-containing kinase-binding protein 1	0.043598601	0.489046777
Q92841	Probable ATP-dependent RNA helicase DDX17	0.043891783	0.796299382
P42677	40S ribosomal protein S27	0.044281169	40.53411752
P62805	Histone H4	0.046287787	4.265073879
Q8TBZ0	Coiled-coil domain-containing protein 110	0.046341613	0.719121165
P01011	Alpha-1-antichymotrypsin	0.046902314	31.74493361
Q9Y2J2	Band 4.1-like protein 3	0.046931239	1.281547491
Q9Y2M0	Fanconi-associated nuclease 1	0.046978427	0.321922015
P49755	Transmembrane emp24 domain-containing protein 10	0.048626748	0.72866654
P55291	Cadherin-15	0.049468688	1.304309012
Q9NP74	Palmdelphin	0.049779253	2.591706473
Q9HB71	Calcyclin-binding protein	0.04978729	1.368093104

Table S13. List of proteins differentially expressed (by ANOVA, $p \leq 0.05$) in MO3.13 oligodendrocytes treated with clozapine (Clz; 1µM, 24h) compared to vehicle (VEI).

Accession	Description	p-value	Clz/VEI ratio
Q9NPH2	Inositol-3-phosphate synthase 1	7.32124E-06	0.67719491
Q9BRV8	Suppressor of IKBKE 1	3.89809E-05	38.04180645
P33240	Cleavage stimulation factor subunit 2	0.000144748	0.441430579
P14324	Farnesyl pyrophosphate synthase	0.000159392	1.78369509
Q86VP6	Cullin-associated NEDD8-dissociated protein 1	0.000183511	2.703406479
P04181	Ornithine aminotransferase_ mitochondrial	0.000220538	1.633543869

Q9HDC9	Adipocyte plasma membrane-associated protein	0.000222658	1.396485235
P49589	Cysteine--tRNA ligase_ cytoplasmic	0.000235881	2.12118194
Q8TD55	Pleckstrin homology domain-containing family O member 2	0.000385179	3.824674125
P51149	Ras-related protein Rab-7a	0.000529204	0.787755214
Q6ZQQ6	WD repeat-containing protein 87	0.000719083	4.515936979
P52306	Rap1 GTPase-GDP dissociation stimulator 1	0.000884922	3.259871856
P00441	Superoxide dismutase [Cu-Zn]	0.000925775	0.447293981
P84090	Enhancer of rudimentary homolog	0.000979202	12.11731072
P05062	Fructose-bisphosphate aldolase B	0.001295902	2.47845427
P51665	26S proteasome non-ATPase regulatory subunit 7	0.001375626	1.641225278
Q13561	Dynactin subunit 2	0.001759184	1.897735116
P07942	Laminin subunit beta-1	0.001804532	0.464756317
Q13618	Cullin-3	0.001812523	1.710552008
Q9H993	Damage-control phosphatase ARMT1	0.001908495	24.01073188
Q9Y696	Chloride intracellular channel protein 4	0.001980398	3.682553423
Q96I25	Splicing factor 45	0.002101481	2.076191044
P48444	Coatomer subunit delta	0.002129042	3.34561157
O14531	Dihydropyrimidinase-related protein 4	0.002308075	0.522415707
P22102	Trifunctional purine biosynthetic protein adenosine-3	0.00253092	4.239459468
P12081	Histidine--tRNA ligase_ cytoplasmic	0.002575759	2.177597373
Q13363	C-terminal-binding protein 1	0.002756161	3.802567154
O75822	Eukaryotic translation initiation factor 3 subunit J	0.002782948	5.162582172
Q92922	SWI/SNF complex subunit SMARCC1	0.00289492	1.38231432
Q13884	Beta-1-syntrophin	0.003154017	0.741139116
Q9H0M0	NEDD4-like E3 ubiquitin-protein ligase WWP1	0.003167007	21.75370651
P32322	Pyrroline-5-carboxylate reductase 1_ mitochondrial	0.003216651	3.726002341
Q8N427	Thioredoxin domain-containing protein 3	0.003281211	4.659283948
P06744	Glucose-6-phosphate isomerase	0.003290233	2.084540522
Q14168	MAGUK p55 subfamily member 2	0.003402507	0.573618165
P60842	Eukaryotic initiation factor 4A-I	0.003501868	3.897145658
P62995	Transformer-2 protein homolog beta	0.003643209	0.62984495
P38919	Eukaryotic initiation factor 4A-III	0.003665622	4.020906181
O95831	Apoptosis-inducing factor 1_ mitochondrial	0.003725354	1.61253143
O96008	Mitochondrial import receptor subunit TOM40 homolog	0.00378627	1.371406495

Q9NQH7	Xaa-Pro aminopeptidase 3	0.003806587	0.277557822
P60228	Eukaryotic translation initiation factor 3 subunit E	0.003816305	3.176005093
P16403	Histone H1.2	0.003871685	2.360146488
Q9NPD3	Exosome complex component RRP41	0.004183807	2.128998307
Q02224	Centromere-associated protein E	0.004341954	0.470941598
Q08043	Alpha-actinin-3	0.004512969	0.664184856
Q7Z7K6	Centromere protein V	0.004539221	10.99352847
P17066	Heat shock 70 kDa protein 6	0.004557241	2.074321845
P54136	Arginine--tRNA ligase_ cytoplasmic	0.00478014	1.10726937
P30041	Peroxiredoxin-6	0.004822605	0.494282853
A5A3E0	POTE ankyrin domain family member F	0.004882119	6.745503999
O00629	Importin subunit alpha-3	0.005275541	4.07666093
Q96HS1	Serine/threonine-protein phosphatase PGAM5_ mitochondrial	0.00528642	0.420689121
Q9UBB4	Ataxin-10	0.005422849	6.400213204
Q2TB90	Hexokinase HKDC1	0.005497812	3.597220778
P30101	Protein disulfide-isomerase A3	0.00560315	2.276904148
Q8WUD1	Ras-related protein Rab-2B	0.005673607	0.714350663
Q8TAT6	Nuclear protein localization protein 4 homolog	0.005683708	0.757097573
Q7Z3B4	Nucleoporin p54	0.005763885	2.47149561
Q13423	NAD(P) transhydrogenase_ mitochondrial	0.005857513	0.494603774
O14735	CDP-diacylglycerol--inositol 3-phosphatidyltransferase	0.005860667	131.193224
P52292	Importin subunit alpha-1	0.005920903	1.916957444
Q99798	Aconitate hydratase_ mitochondrial	0.006179108	1.5951753
Q96BM9	ADP-ribosylation factor-like protein 8A	0.006216346	0.343230305
P04406	Glyceraldehyde-3-phosphate dehydrogenase	0.006258448	7.009479197
Q14103	Heterogeneous nuclear ribonucleoprotein D0	0.006482258	0.471292921
Q9UNL2	Translocon-associated protein subunit gamma	0.006684538	0.453234435
Q99873	Protein arginine N-methyltransferase 1	0.006694931	2.446666354
Q8IZL8	Proline-_ glutamic acid- and leucine-rich protein 1	0.006753057	4.523955138
Q9UGP8	Translocation protein SEC63 homolog	0.006827449	0.634127706
Q13616	Cullin-1	0.007010648	0.559124178
P49411	Elongation factor Tu_ mitochondrial	0.007152725	1.868347569
Q8TE73	Dynein heavy chain 5_ axonemal	0.007231534	5.965550061
P10155	60 kDa SS-A/Ro ribonucleoprotein	0.007530764	1.23676588

Q9UBS4	DnaJ homolog subfamily B member 11	0.007574009	1.704470308
Q13907	Isopentenyl-diphosphate Delta-isomerase 1	0.007694814	0.467492848
Q12904	Aminoacyl tRNA synthase complex-interacting	0.007705489	6.082500643
Q9NQT8	Kinesin-like protein KIF13B	0.007841379	2.365395459
P04075	Fructose-bisphosphate aldolase A	0.007871773	1.383948099
Q00839	Heterogeneous nuclear ribonucleoprotein U	0.007908917	2.131887422
P38571	Lysosomal acid lipase/cholesteryl ester hydrolase	0.007932562	14.02473294
Q8NFP7	Diphosphoinositol polyphosphate phosphohydrolase 3-alpha	0.00802547	4.663076369
O60701	UDP-glucose 6-dehydrogenase	0.008099634	0.489237083
P46459	Vesicle-fusing ATPase	0.00814875	0.38618117
Q9H223	EH domain-containing protein 4	0.008267659	1.856642981
P50570	Dynamin-2	0.008344696	1.789911563
Q9NTJ3	Structural maintenance of chromosomes protein 4	0.008451305	0.596792727
Q9HCD5	Nuclear receptor coactivator 5	0.008684864	2.19868488
P54578	Ubiquitin carboxyl-terminal hydrolase 14	0.008712548	2.079636603
P55884	Eukaryotic translation initiation factor 3 subunit B	0.008812753	1.783073323
P69849	Nodal modulator 3	0.009094892	2.969080631
P49591	Serine--tRNA ligase_ cytoplasmic	0.009111449	0.521766935
O75923	Dysferlin	0.009222682	0.564801398
Q9ULV0	Unconventional myosin-Vb	0.009343653	0.665402808
P41091	Eukaryotic translation initiation factor 2 subunit 3	0.009670194	0.776620649
P47895	Aldehyde dehydrogenase family 1 member A3	0.00967191	0.559145559
P62280	40S ribosomal protein S11	0.009795194	0.443256054
O60841	Eukaryotic translation initiation factor 5B	0.010165849	5.24299753
Q96EY7	Pentatricopeptide repeat domain-containing protein 3	0.010502401	11.94649783
O75533	Splicing factor 3B subunit 1	0.010506496	0.677157022
P78356	Phosphatidylinositol 5-phosphate 4-kinase type-2 beta	0.010708107	2.007863828
Q9BR76	Coronin-1B	0.011069029	0.628282477
Q8IWJ2	GRIP and coiled-coil domain-containing protein 2	0.011149115	0.617387692
P23229	Integrin alpha-6	0.011219716	1.643444337
Q14254	Flotillin-2	0.011286801	1.979215112
P28482	Mitogen-activated protein kinase 1	0.011333247	0.560134386
Q9H3K2	Growth hormone-inducible transmembrane protein	0.011757768	4.199953135
P62805	Histone H4	0.011783892	7.259184393

P31948	Stress-induced-phosphoprotein 1	0.011834665	0.641014726
Q96C90	Protein phosphatase 1 regulatory subunit 14B	0.012290388	0.061384993
Q92542	Nicastrin	0.01241813	2.364186375
P61081	NEDD8-conjugating enzyme Ubc12	0.012509728	0.654487424
P26639	Threonine--tRNA ligase 1_ cytoplasmic	0.012532415	3.883070981
Q99733	Nucleosome assembly protein 1-like 4	0.012938619	1.493326537
P36957	Dihydrolipoyllysine-residue succinyltransferase	0.013049409	0.737547671
O00410	Importin-5	0.013070535	2.199560007
P37802	Transgelin-2	0.013658401	0.166061063
O14776	Transcription elongation regulator 1	0.01374032	0.852874944
O43396	Thioredoxin-like protein 1	0.013806751	0.681729672
Q12926	ELAV-like protein 2	0.0138999	1.427950301
Q5TCY1	Tau-tubulin kinase 1	0.014082272	1.52927217
Q9UNH7	Sorting nexin-6	0.014326449	2.825781379
P23284	Peptidyl-prolyl cis-trans isomerase B	0.014411285	1.73481163
P11413	Glucose-6-phosphate 1-dehydrogenase	0.01454972	5.160330038
P62826	GTP-binding nuclear protein Ran	0.014609629	0.658331457
Q92769	Histone deacetylase 2	0.01497951	2.015434972
P61158	Actin-related protein 3	0.015476321	0.877515271
Q02413	Desmoglein-1	0.015619628	0.470497023
Q6FI13	Histone H2A type 2-A	0.015917531	3.07990662
P0C0S8	Histone H2A type 1	0.015917531	3.07990662
P10515	Dihydrolipoyllysine-residue acetyltransferase	0.016073355	6.289635556
P37268	Squalene synthase	0.016169549	1.733902218
Q9BQG0	Myb-binding protein 1A	0.016454589	2.305030856
Q8TD57	Dynein heavy chain 3_ axonemal	0.016528302	0.678414161
O15143	Actin-related protein 2/3 complex subunit 1B	0.016665961	0.731067269
P30086	Phosphatidylethanolamine-binding protein 1	0.01676297	0.627362278
P78363	Retinal-specific phospholipid-transporting ATPase ABCA4	0.016937169	1.644361289
Q9H7B2	Ribosome production factor 2 homolog	0.017221773	0.105934519
P49755	Transmembrane emp24 domain-containing protein 10	0.017251735	0.632416927
P24539	ATP synthase F(0) complex subunit B1_ mitochondrial	0.017765937	5.528422033
Q96Q15	Serine/threonine-protein kinase SMG1	0.018307679	0.654753268
P61160	Actin-related protein 2	0.018694673	0.51337617

P52788	Spermine synthase	0.018946679	0.569791645
Q8ND90	Paraneoplastic antigen Ma1	0.019303741	3.773582749
P61019	Ras-related protein Rab-2A	0.019674876	0.744916084
Q86SE5	RNA-binding Raly-like protein	0.019937708	22.31456317
Q96D15	Reticulocalbin-3	0.020897008	0.460109987
Q9NP72	Ras-related protein Rab-18	0.020968604	0.387615349
P29692	Elongation factor 1-delta	0.021115455	0.41021006
Q99961	Endophilin-A2	0.021173708	1.554961251
P06454	Prothymosin alpha	0.021451334	4.191250652
P35659	Protein DEK	0.021580522	3.675109593
Q9Y2U9	Kelch domain-containing protein 2	0.021751842	0.377469522
O75477	Erlin-1	0.021987221	0.689241542
Q99832	T-complex protein 1 subunit eta	0.02203447	0.426858672
P51795	H(+)/Cl(-) exchange transporter 5	0.022309562	0.669432184
Q96K76	Ubiquitin carboxyl-terminal hydrolase 47	0.022334513	2.108318197
O75489	NADH dehydrogenase [ubiquinone] iron-sulfur protein 3	0.02280455	0.756260597
P26583	High mobility group protein B2	0.022969262	1.401987974
P40227	T-complex protein 1 subunit zeta	0.023777959	2.06082346
Q13085	Acetyl-CoA carboxylase 1	0.024042431	0.723372845
O43852	Calumenin	0.024142243	0.804672012
P49753	Acyl-coenzyme A thioesterase 2_ mitochondrial	0.024250781	4.09688464
P02787	Serotransferrin	0.024358266	0.706210802
Q13155	Aminoacyl tRNA synthase complex-interacting	0.024418056	11.32655064
P21796	Voltage-dependent anion-selective channel protein 1	0.024483592	0.710568334
Q9NPQ8	Synembryn-A	0.024990768	0.587917776
Q15437	Protein transport protein Sec23B	0.025020279	6.867687895
Q9H488	GDP-fucose protein O-fucosyltransferase 1	0.025038028	4.029187393
P16402	Histone H1.3	0.025111516	2.590799604
Q08945	FACT complex subunit SSRP1	0.025219826	0.715716382
P19623	Spermidine synthase	0.025400348	114.8893011
Q15166	Serum paraoxonase/lactonase 3	0.025817182	1.530557767
Q86V81	THO complex subunit 4	0.026136122	0.640573475
Q4G0J3	La-related protein 7	0.026855538	0.769504466
Q96GQ7	Probable ATP-dependent RNA helicase DDX27	0.026863643	5.265879716
Q9UBW5	Bridging integrator 2	0.026902377	0.518934279

P78406	mRNA export factor	0.026967982	0.478201823
P42167	Lamina-associated polypeptide 2_ isoforms beta/gamma	0.027986635	0.778837016
P17948	Vascular endothelial growth factor receptor 1	0.028355242	44.2363056
P60468	Protein transport protein Sec61 subunit beta	0.028356049	3.123077841
Q16629	Serine/arginine-rich splicing factor 7	0.028376381	0.458398906
Q9Y2J2	Band 4.1-like protein 3	0.02841234	1.333699201
P27797	Calreticulin	0.028595541	1.507601039
Q9BV38	WD repeat-containing protein 18	0.02864427	0.710820599
P63092	Guanine nucleotide-binding protein G(s)	0.029590213	3.07335442
Q8WXF1	Paraspeckle component 1	0.029726793	0.727485778
Q9BS26	Endoplasmic reticulum resident protein 44	0.029813395	0.613418489
Q14108	Lysosome membrane protein 2	0.029911616	0.594459629
Q92692	Nectin-2	0.030629629	0.634761225
P36871	Phosphoglucomutase-1	0.030760598	1.350178182
P09874	Poly [ADP-ribose] polymerase 1	0.030810682	0.376295854
Q96CX2	BTB/POZ domain-containing protein KCTD12	0.030935669	0.5392744
Q15365	Poly(rC)-binding protein 1	0.031456283	1.838383833
Q15274	Nicotinate-nucleotide pyrophosphorylase [carboxylating]	0.031640377	1.851730603
Q6ZU15	Septin-14	0.031658127	0.023965246
Q08378	Golgin subfamily A member 3	0.031870282	1.525603454
Q8IWX7	Protein unc-45 homolog B	0.031896224	4.665392273
P21281	V-type proton ATPase subunit B_ brain isoform	0.032252599	0.669241498
O43237	Cytoplasmic dynein 1 light intermediate chain 2	0.032472273	0.799992727
P22314	Ubiquitin-like modifier-activating enzyme 1	0.03286812	1.744821054
P54577	Tyrosine--tRNA ligase_ cytoplasmic	0.033009869	0.401723017
O00560	Syntenin-1	0.033299892	1.850332003
O14980	Exportin-1	0.033527128	0.306685443
P52907	F-actin-capping protein subunit alpha-1	0.033722496	3.606182271
Q9Y230	RuvB-like 2	0.033902343	0.394988933
P45974	Ubiquitin carboxyl-terminal hydrolase 5	0.03404213	1.953166944
P33176	Kinesin-1 heavy chain	0.034258008	0.774849624
Q96B26	Exosome complex component RRP43	0.034334069	0.153153816
Q6UB35	Monofunctional C1-tetrahydrofolate synthase_ mitochondrial	0.03447681	0.727480923

Q7L014	Probable ATP-dependent RNA helicase DDX46	0.034559927	2.094151219
Q7L2E3	ATP-dependent RNA helicase DHX30	0.03523123	1.817909521
Q9BXB4	Oxysterol-binding protein-related protein 11	0.035705372	0.171557772
Q13586	Stromal interaction molecule 1	0.035810884	0.699471546
Q00325	Phosphate carrier protein_ mitochondrial	0.035855921	1.317205147
Q15392	Delta(24)-sterol reductase	0.036074315	1.681439241
P34896	Serine hydroxymethyltransferase_ cytosolic	0.036193652	2.419187375
Q9BV44	THUMP domain-containing protein 3	0.036231172	0.413795037
P31040	Succinate dehydrogenase [ubiquinone]	0.036762072	0.582820898
P18206	Vinculin	0.036922055	1.407524161
Q01433	AMP deaminase 2	0.037119928	0.5872579
P54886	Delta-1-pyrroline-5-carboxylate synthase	0.037213824	1.595634383
P40939	Trifunctional enzyme subunit alpha_ mitochondrial	0.037541846	0.774184363
Q96DU9	Polyadenylate-binding protein 5	0.037595282	0.37713659
Q14690	Protein RRP5 homolog	0.037955298	1.519936404
Q53H82	Endoribonuclease LACTB2	0.037977196	1.915945651
P54753	Ephrin type-B receptor 3	0.038223966	1.122886104
Q05707	Collagen alpha-1(XIV) chain	0.038656989	0.565460933
Q9BUF5	Tubulin beta-6 chain	0.038924736	0.365671433
Q10570	Cleavage and polyadenylation specificity factor subunit 1	0.03893459	1.365770155
O14936	Peripheral plasma membrane protein CASK	0.038956251	1.852246175
P08758	Annexin A5	0.039534717	0.442639978
P01040	Cystatin-A	0.039767956	0.030413645
Q5ZPR3	CD276 antigen	0.039851944	0.590846399
Q13283	Ras GTPase-activating protein-binding protein 1	0.040235076	3.189724024
Q9H3G5	Probable serine carboxypeptidase CPVL	0.040341851	11.27140966
P51148	Ras-related protein Rab-5C	0.04036212	2.09214512
P25398	40S ribosomal protein S12	0.040682495	3.251240364
P50502	Hsc70-interacting protein	0.040721027	1.421211622
Q07666	KH domain-containing_ RNA-binding	0.041416454	0.582748068
O60551	Glycylpeptide N-tetradecanoyltransferase 2	0.041851336	0.545191528
P33993	DNA replication licensing factor MCM7	0.041877344	0.7857795
P08133	Annexin A6	0.041969088	0.674162068
P48739	Phosphatidylinositol transfer protein beta isoform	0.041989056	1.776052039

O94760	N(G)_N(G)-dimethylarginine dimethylaminohydrolase 1	0.042046881	1.260166442
Q07065	Cytoskeleton-associated protein 4	0.04206169	1.419282639
Q6NUK1	Calcium-binding mitochondrial carrier protein SCaMC-1	0.042075357	2.169782376
O00139	Kinesin-like protein KIF2A	0.042223454	1.341317162
Q9Y2T4	Serine/threonine-protein phosphatase 2A 55 kDa regulatory	0.042395321	11.76859979
Q9Y3F4	Serine-threonine kinase receptor-associated protein	0.042738803	0.717689468
Q66K74	Microtubule-associated protein 1S	0.042781176	2.761234058
Q6YN16	Hydroxysteroid dehydrogenase-like protein 2	0.043510383	0.55988302
Q05397	Focal adhesion kinase 1	0.043684324	1.414969247
O94906	Pre-mRNA-processing factor 6	0.044080196	0.634324344
Q15691	Microtubule-associated protein RP/EB family member 1	0.044575415	0.724807608
P53597	Succinate--CoA ligase [ADP/GDP-forming]	0.044619207	0.675142842
Q9Y617	Phosphoserine aminotransferase	0.044777849	2.162233272
P48681	Nestin	0.044878739	0.492769107
Q9NZN4	EH domain-containing protein 2	0.045001102	1.234193078
Q9H361	Polyadenylate-binding protein 3	0.045198821	2.343717902
Q9HCK1	DBF4-type zinc finger-containing protein 2	0.045436429	2.681168689
P62424	60S ribosomal protein L7a	0.045453557	0.664900982
Q15375	Ephrin type-A receptor 7	0.045722107	0.355224992
P11233	Ras-related protein Ral-A	0.045730967	0.477939999
P54764	Ephrin type-A receptor 4	0.045829883	10.82466935
P06702	Protein S100-A9	0.045929626	0.584051274
P15880	40S ribosomal protein S2	0.046086278	1.672784988
Q93009	Ubiquitin carboxyl-terminal hydrolase 7	0.04609825	1.162068865
Q7LFL8	CXXC-type zinc finger protein 5	0.046122551	0.015809461
O14787	Transportin-2	0.046186629	0.017724823
P81605	Dermcidin	0.046539712	0.424742776
O75694	Nuclear pore complex protein Nup155	0.046626955	0.700046537
Q8NCM8	Cytoplasmic dynein 2 heavy chain 1	0.046638302	0.563902254
Q96NB3	Zinc finger protein 830	0.047014119	1.46262252
Q96CG8	Collagen triple helix repeat-containing protein 1	0.047064362	0.322116856
P00505	Aspartate aminotransferase_ mitochondrial	0.047103942	1.302204309
P63244	Receptor of activated protein C kinase 1	0.047337078	0.600548493
O43670	BUB3-interacting and GLEBS motif-containing protein	0.047410008	1.233365454

Q9Y265	RuvB-like 1	0.047654651	2.041036062
P17980	26S proteasome regulatory subunit 6A	0.047720962	1.395875026
Q9NR31	GTP-binding protein SAR1a	0.047729283	20.65488156
P0DP23	Calmodulin-1	0.048331466	3.655441637
Q15276	Rab GTPase-binding effector protein 1	0.048601104	0.612251902
P06753	Tropomyosin alpha-3 chain	0.048609721	0.690363991
Q15424	Scaffold attachment factor B1	0.048992773	1.997466845
Q08209	Serine/threonine-protein phosphatase 2B catalytic	0.049270015	1.599257306
P50552	Vasodilator-stimulated phosphoprotein	0.049338232	0.730332881
P49368	T-complex protein 1 subunit gamma	0.049510113	1.20137756
Q92973	Transportin-1	0.049520893	1.627720061
P62888	60S ribosomal protein L30	0.049524369	4.159240321
Q9ULV4	Coronin-1C	0.049908239	0.623447876
P01857	Immunoglobulin heavy constant gamma 1	0.049971204	0.337810807

Table S14. List of proteins differentially expressed (by ANOVA, $p \leq 0.05$) in MO3.13 oligodendrocytes treated with cannabidiol (CBD; 1µM, 24h) compared to vehicle (VEI).

Accession	Description	p-value	CBD/VEI ratio
P30041	Peroxiredoxin-6	0.000347087	0.588164574
Q8N2X6	Uncharacterized protein EXOC3-AS1	0.000511411	0.275766702
P84090	Enhancer of rudimentary homolog	0.001085072	3.374005122
P61158	Actin-related protein 3	0.001851518	0.802136405
P36957	Dihydrolipoyllysine-residue succinyltransferase component of 2-oxoglutarate dehydrogenase complex	0.00257642	0.724114199
Q16850	Lanosterol 14-alpha demethylase	0.003043294	0.550078372
O43670	BUB3-interacting and GLEBS motif-containing protein ZNF207	0.003058641	1.401434527
Q9Y696	Chloride intracellular channel protein 4	0.003947657	2.850023484
P25398	40S ribosomal protein S12	0.004001059	2.798957653
P60468	Protein transport protein Sec61 subunit beta	0.004599184	2.395864159
Q13263	Transcription intermediary factor 1-beta	0.004953115	0.757969858
Q9NQH7	Xaa-Pro aminopeptidase 3	0.00495938	0.284396936
Q7Z3B4	Nucleoporin p54	0.005125637	1.637705708

Q86YZ3	Hornerin	0.005280151	1.500296788
P54577	Tyrosine--tRNA ligase_ cytoplasmic	0.005925434	0.2044307
A1X283	SH3 and PX domain-containing protein 2B	0.005925992	1.27958553
Q04837	Single-stranded DNA-binding protein_ mitochondrial	0.006639528	1.5786977
P48443	Retinoic acid receptor RXR-gamma	0.006809798	1.449172935
Q9Y5F7	Protocadherin gamma-C4	0.006871759	0.244641221
P0DP23	Calmodulin-1	0.007802779	5.165027518
Q8WVX9	Fatty acyl-CoA reductase 1	0.008052458	1.541411482
Q9NPD3	Exosome complex component RRP41	0.008052588	1.478640659
P17480	Nucleolar transcription factor 1	0.008120102	0.724555876
P40227	T-complex protein 1 subunit zeta	0.008317303	2.077411586
Q9NZ08	Endoplasmic reticulum aminopeptidase 1	0.008697067	0.499935719
P47914	60S ribosomal protein L29	0.009594974	3.000716414
Q9P0L1	Zinc finger protein with KRAB and SCAN domains 7	0.010092106	0.193154025
Q08378	Golgin subfamily A member 3	0.0101196	1.677964371
P18031	Tyrosine-protein phosphatase non-receptor type 1	0.010376482	0.790869738
P46778	60S ribosomal protein L21	0.010569367	0.130171758
Q92542	Nicastrin	0.010761584	1.789699405
P48444	Coatomer subunit delta	0.011939149	2.988789188
Q9Y3A3	MOB-like protein phocein	0.014454285	2.296102813
P62805	Histone H4	0.015243849	4.90785507
P62888	60S ribosomal protein L30	0.015805413	4.827509291
A4QMS7	Uncharacterized protein C5orf49	0.015976687	3.332334303
Q96QR8	Transcriptional activator protein Pur-beta	0.016027979	1.418870033
O00629	Importin subunit alpha-3	0.016837963	1.959682955
Q8IY81	pre-rRNA 2'-O-ribose RNA methyltransferase FTSJ3	0.017804503	1.934717607
P49189	4-trimethylaminobutyraldehyde dehydrogenase	0.018172716	0.79854816
Q13428	Treacle protein	0.01887477	1.426949168
Q4G0J3	La-related protein 7	0.01947724	0.72291239
Q14690	Protein RRP5 homolog	0.019563771	1.345262785
Q9UBC7	Galanin-like peptide	0.019725146	0.518167891
P04075	Fructose-bisphosphate aldolase A	0.019754215	1.433694748
Q14108	Lysosome membrane protein 2	0.019912085	0.65655028
Q8IY67	Ribonucleoprotein PTB-binding 1	0.021374584	0.351454376
P46459	Vesicle-fusing ATPase	0.021597734	0.395780148

Q14764	Major vault protein	0.022018787	0.292484023
P40429	60S ribosomal protein L13a	0.02205235	1.356417472
Q8TD55	Pleckstrin homology domain-containing family O member 2	0.02212054	3.432573297
P36405	ADP-ribosylation factor-like protein 3	0.022474852	11.30487544
O95347	Structural maintenance of chromosomes protein 2	0.022853896	0.580511212
P0DN79	Cystathionine beta-synthase-like protein	0.024229116	1.10470717
P47895	Aldehyde dehydrogenase family 1 member A3	0.024461287	0.724018789
P01040	Cystatin-A	0.024607357	4.828964604
O94925	Glutaminase kidney isoform_ mitochondrial	0.025001092	0.546793653
P62244	40S ribosomal protein S15a	0.025123728	33.121333
P09972	Fructose-bisphosphate aldolase C	0.026949803	0.755672654
Q07020	60S ribosomal protein L18	0.028123546	1.820855659
Q13200	26S proteasome non-ATPase regulatory subunit 2	0.029098512	0.429181302
P0C0S8	Histone H2A type 1	0.02969026	2.488136193
Q6FI13	Histone H2A type 2-A	0.02969026	2.488136193
Q13884	Beta-1-syntrophin	0.030368639	0.749124554
Q96EP5	DAZ-associated protein 1	0.030600764	0.733270303
O00232	26S proteasome non-ATPase regulatory subunit 12	0.032753852	0.61582843
P49589	Cysteine--tRNA ligase_ cytoplasmic	0.033331148	1.402286306
Q8IYT4	Katanin p60 ATPase-containing subunit A-like 2	0.033579011	1.926749442
Q13618	Cullin-3	0.033647656	1.154456022
Q04760	Lactoylglutathione lyase	0.033923971	2.634952257
P08133	Annexin A6	0.033951765	0.667526075
Q9Y4G6	Talin-2	0.033971359	0.68510287
Q9BRP8	Partner of Y14 and mago	0.034003677	1.699917314
Q15365	Poly(rC)-binding protein 1	0.034173491	3.115505909
O75923	Dysferlin	0.034383865	0.594330223
P37802	Transgelin-2	0.035205377	0.443953098
P31040	Succinate dehydrogenase [ubiquinone] flavoprotein subunit_ mitochondrial	0.035955262	0.65490392
P49841	Glycogen synthase kinase-3 beta	0.036367735	0.73547558
P50552	Vasodilator-stimulated phosphoprotein	0.036758895	0.620096454
Q5TCY1	Tau-tubulin kinase 1	0.037247233	1.207599337
Q10471	Polypeptide N-acetylgalactosaminyltransferase 2	0.038574714	0.488102537

P19174	1-phosphatidylinositol 4_5-bisphosphate phosphodiesterase gamma-1	0.038747185	0.342886794
O15144	Actin-related protein 2/3 complex subunit 2	0.039325045	1.811557166
P40938	Replication factor C subunit 3	0.039718467	1.719912377
Q8TD57	Dynein heavy chain 3_ axonemal	0.040129269	0.79263835
P33993	DNA replication licensing factor MCM7	0.040265192	0.81173239
P43686	26S proteasome regulatory subunit 6B	0.040647979	0.724423023
O60749	Sorting nexin-2	0.041813856	0.187681245
P16615	Sarcoplasmic/endoplasmic reticulum calcium ATPase 2	0.042098401	0.680490489
P11166	Solute carrier family 2_ facilitated glucose transporter member 1	0.042289022	0.225282542
Q15056	Eukaryotic translation initiation factor 4H	0.042379279	5.958602608
Q96T76	MMS19 nucleotide excision repair protein homolog	0.043216366	0.655723727
Q8NCM8	Cytoplasmic dynein 2 heavy chain 1	0.043285633	0.669074301
Q96I25	Splicing factor 45	0.043673531	0.759575931
Q15459	Splicing factor 3A subunit 1	0.043680798	1.184662391
Q01581	Hydroxymethylglutaryl-CoA synthase_ cytoplasmic	0.043944305	0.806683618
Q02224	Centromere-associated protein E	0.044149646	0.677180721
O15372	Eukaryotic translation initiation factor 3 subunit H	0.044668427	12.55575859
Q86U42	Polyadenylate-binding protein 2	0.046613872	0.763415446
Q99523	Sortilin	0.047688963	1.89576576
P19623	Spermidine synthase	0.048086507	42.73406549
Q96KR1	Zinc finger RNA-binding protein	0.048530486	0.650284503
P53007	Tricarboxylate transport protein_ mitochondrial	0.048616236	1.63027404
Q9NPQ8	Synembryn-A	0.048779387	0.715100362
P13693	Translationally-controlled tumor protein	0.04884892	1.730764387
Q16891	MICOS complex subunit MIC60	0.04941986	0.825852009

Table S15. List of proteins differentially expressed (by ANOVA, $p \leq 0.05$) in MO3.13 oligodendrocytes treated with benztropine (Benz; 1µM, 24h) compared to vehicle (VEI).

Accession	Description	p-value	Benz/VEI ratio
P51665	26S proteasome non-ATPase regulatory subunit 7	0.000805	1.432123684

P30041	Peroxiredoxin-6	0.000894	0.50988633
P49591	Serine--tRNA ligase_ cytoplasmic	0.000991	0.52065083
P46459	Vesicle-fusing ATPase	0.001309	0.35608649
Q8N427	Thioredoxin domain-containing protein 3	0.001886	3.390757193
P62805	Histone H4	0.001959	5.93315696
Q99873	Protein arginine N-methyltransferase 1	0.002012	2.509768434
O00629	Importin subunit alpha-3	0.00212	3.504566379
Q9UBS4	DnaJ homolog subfamily B member 11	0.002171	1.9737912
P25398	40S ribosomal protein S12	0.002257	3.596583105
Q9H5X1	Cytosolic iron-sulfur assembly component 2A	0.002696	0.208120615
Q9BRV8	Suppressor of IKBKE 1	0.002832	3.413511821
O00139	Kinesin-like protein KIF2A	0.002902	1.556313228
Q9Y696	Chloride intracellular channel protein 4	0.002928	2.548714997
O96008	Mitochondrial import receptor subunit TOM40 homolog	0.003516	0.712490946
P62424	60S ribosomal protein L7a	0.003584	0.672009688
Q04837	Single-stranded DNA-binding protein_ mitochondrial	0.003853	1.773490114
P38571	Lysosomal acid lipase/cholesteryl ester hydrolase	0.004161	11.25259768
P61088	Ubiquitin-conjugating enzyme E2 N	0.004895	3.182936536
P11233	Ras-related protein Ral-A	0.005122	0.547260872
P0DMV8	Heat shock 70 kDa protein 1A	0.00525	0.553114516
O43396	Thioredoxin-like protein 1	0.005627	0.870315788
P48444	Coatomer subunit delta	0.006049	1.866799644
Q13200	26S proteasome non-ATPase regulatory subunit 2	0.006081	0.350276417
Q7L014	Probable ATP-dependent RNA helicase DDX46	0.006101	1.900155952
Q96Q15	Serine/threonine-protein kinase SMG1	0.006524	0.683588216
P62191	26S proteasome regulatory subunit 4	0.007307	0.751186389
P30086	Phosphatidylethanolamine-binding protein 1	0.007762	0.637802966
Q9UHD9	Ubiquilin-2	0.008161	0.623056921
P62888	60S ribosomal protein L30	0.008187	4.751575204
Q8ND90	Paraneoplastic antigen Ma1	0.008239	3.816386925
Q6FI13	Histone H2A type 2-A	0.008318	3.256854379
P67775	Serine/threonine-protein phosphatase 2A catalytic subunit alpha isoform	0.008385	0.671668077
Q14254	Flotillin-2	0.00843	1.739897203
Q9NTJ3	Structural maintenance of chromosomes protein 4	0.00873	0.700031755

P07942	Laminin subunit beta-1	0.008794	0.663313433
Q7LFL8	CXXC-type zinc finger protein 5	0.008796	0.00703808
Q9UGP8	Translocation protein SEC63 homolog	0.008911	0.741664978
P84090	Enhancer of rudimentary homolog	0.009053	11.44002489
O75477	Erlin-1	0.009055	0.743543723
P61160	Actin-related protein 2	0.009227	0.502694563
Q7Z7K6	Centromere protein V	0.00931	7.473875415
Q13561	Dynactin subunit 2	0.00999	1.674269544
Q96T37	RNA-binding protein 15	0.010131	0.654565584
O75923	Dysferlin	0.010204	0.706324216
Q8TEM1	Nuclear pore membrane glycoprotein 210	0.01023	0.9327971
Q96CX2	BTB/POZ domain-containing protein KCTD12	0.010425	0.55836769
P60468	Protein transport protein Sec61 subunit beta	0.011053	3.013208797
Q15392	Delta(24)-sterol reductase	0.011207	1.69266284
P07237	Protein disulfide-isomerase	0.011399	0.761210187
Q71U36	Tubulin alpha-1A chain	0.011626	0.752801355
Q99832	T-complex protein 1 subunit eta	0.011698	0.411563297
Q9H993	Damage-control phosphatase ARMT1	0.011843	13.42368257
Q5TCY1	Tau-tubulin kinase 1	0.011916	1.300742274
P07737	Profilin-1	0.012007	2.474273435
P35613	Basigin	0.012177	0.679520787
Q05682	Caldesmon	0.012312	0.895247989
Q13085	Acetyl-CoA carboxylase 1	0.012566	0.789080076
O60701	UDP-glucose 6-dehydrogenase	0.013284	0.424710678
O15143	Actin-related protein 2/3 complex subunit 1B	0.013419	0.780392827
P55854	Small ubiquitin-related modifier 3	0.013448	0.713412963
P49753	Acyl-coenzyme A thioesterase 2_ mitochondrial	0.014556	3.814242716
Q99961	Endophilin-A2	0.014698	1.38484262
Q13464	Rho-associated protein kinase 1	0.014943	0.72170605
Q9H0S4	Probable ATP-dependent RNA helicase DDX47	0.014968	0.01616522
Q8TC12	Retinol dehydrogenase 11	0.015086	1.577222075
Q01433	AMP deaminase 2	0.015315	0.50628974
Q13884	Beta-1-syntrophin	0.015776	0.59187672
P35268	60S ribosomal protein L22	0.016425	1.974477004
P12081	Histidine--tRNA ligase_ cytoplasmic	0.017199	1.712468482

P0DP23	Calmodulin-1	0.018174	3.582692816
Q96KR1	Zinc finger RNA-binding protein	0.018322	0.617078338
P22061	Protein-L-isoaspartate(D-aspartate) O-methyltransferase	0.018404	0.091534385
Q14676	Mediator of DNA damage checkpoint protein 1	0.018648	0.579425004
Q5ZPR3	CD276 antigen	0.01865	0.583125391
Q06210	Glutamine--fructose-6-phosphate aminotransferase [isomerizing] 1	0.018893	0.767159992
P16615	Sarcoplasmic/endoplasmic reticulum calcium ATPase 2	0.019512	0.666068048
Q13586	Stromal interaction molecule 1	0.01968	0.714497329
Q9P0L1	Zinc finger protein with KRAB and SCAN domains 7	0.019795	0.398081436
Q08209	Serine/threonine-protein phosphatase 2B catalytic subunit alpha isoform	0.019899	1.572177138
P04181	Ornithine aminotransferase_ mitochondrial	0.020001	1.464242515
O43491	Band 4.1-like protein 2	0.020184	0.840766032
Q9NQT8	Kinesin-like protein KIF13B	0.02044	2.024130879
P78356	Phosphatidylinositol 5-phosphate 4-kinase type-2 beta	0.020836	1.807123796
P42677	40S ribosomal protein S27	0.021337	52.13030126
Q8N8S7	Protein enabled homolog	0.021397	1.432335564
P14174	Macrophage migration inhibitory factor	0.021765	7.8509968
P62244	40S ribosomal protein S15a	0.021824	32.26417612
Q9HB71	Calcyclin-binding protein	0.021928	1.709622876
P11166	Solute carrier family 2_ facilitated glucose transporter member 1	0.022156	0.226378193
Q9Y230	RuvB-like 2	0.022811	0.466705989
Q9H0M0	NEDD4-like E3 ubiquitin-protein ligase WWP1	0.023086	17.97010417
Q92692	Nectin-2	0.023651	0.659078823
P62280	40S ribosomal protein S11	0.023768	0.602840812
O00148	ATP-dependent RNA helicase DDX39A	0.023923	0.815180956
P20073	Annexin A7	0.024482	1.880626997
Q6UB35	Monofunctional C1-tetrahydrofolate synthase_ mitochondrial	0.024526	0.705546892
P20618	Proteasome subunit beta type-1	0.024572	0.743125553
Q9UHX1	Poly(U)-binding-splicing factor PUF60	0.025093	0.363090094
Q92934	Bcl2-associated agonist of cell death	0.025695	0.773390144
Q9BS26	Endoplasmic reticulum resident protein 44	0.026337	0.674520981

Q9H223	EH domain-containing protein 4	0.026397	1.655875581
P49790	Nuclear pore complex protein Nup153	0.026871	1.659486361
P43243	Matrin-3	0.02706	0.278578866
P31040	Succinate dehydrogenase [ubiquinone] flavoprotein subunit_ mitochondrial	0.027502	0.684116012
P54578	Ubiquitin carboxyl-terminal hydrolase 14	0.027761	1.989049581
P33992	DNA replication licensing factor MCM5	0.027939	0.877944577
Q02224	Centromere-associated protein E	0.028467	0.599338685
P12270	Nucleoprotein TPR	0.028613	0.838799882
Q4G0J3	La-related protein 7	0.028994	0.845675775
Q7Z2W4	Zinc finger CCCH-type antiviral protein 1	0.029249	0.73323227
P78559	Microtubule-associated protein 1A	0.029576	0.720115964
P62316	Small nuclear ribonucleoprotein Sm D2	0.029584	30.84775332
Q9Y5F7	Protocadherin gamma-C4	0.029663	0.478654578
Q92945	Far upstream element-binding protein 2	0.029707	0.753683236
Q6ZQQ6	WD repeat-containing protein 87	0.029774	3.707343231
Q10471	Polypeptide N-acetylgalactosaminyltransferase 2	0.030021	0.569811635
P23284	Peptidyl-prolyl cis-trans isomerase B	0.03005	1.90690077
Q15758	Neutral amino acid transporter B(0)	0.03008	0.592393046
Q8TE73	Dynein heavy chain 5_ axonemal	0.030138	2.085224693
Q15366	Poly(rC)-binding protein 2	0.030595	0.797142959
P06753	Tropomyosin alpha-3 chain	0.031147	0.692408597
P32322	Pyrroline-5-carboxylate reductase 1_ mitochondrial	0.031227	3.421923013
O14980	Exportin-1	0.031273	0.335001933
P42167	Lamina-associated polypeptide 2_ isoforms beta/gamma	0.03149	0.737138319
Q07666	KH domain-containing_ RNA-binding_ signal transduction-associated protein 1	0.031583	0.499921046
Q13243	Serine/arginine-rich splicing factor 5	0.031921	1.562402921
P08243	Asparagine synthetase [glutamine-hydrolyzing]	0.032052	0.556033782
Q66K74	Microtubule-associated protein 1S	0.032269	2.020511863
P37802	Transgelin-2	0.032605	0.364088524
Q16555	Dihydropyrimidinase-related protein 2	0.0328	0.718900234
P08758	Annexin A5	0.033182	0.436846219
P40222	Alpha-taxilin	0.033253	0.701167058
Q53H82	Endoribonuclease LACTB2	0.034188	1.924556673

P27816	Microtubule-associated protein 4	0.034237	0.789528697
Q13616	Cullin-1	0.034355	0.77896068
O14530	Thioredoxin domain-containing protein 9	0.034773	0.619365059
O43776	Asparagine--tRNA ligase_ cytoplasmic	0.035176	0.688992181
Q96GQ7	Probable ATP-dependent RNA helicase DDX27	0.035213	2.72215096
Q9BR76	Coronin-1B	0.035252	0.569253614
P41091	Eukaryotic translation initiation factor 2 subunit 3	0.035733	0.860750266
O43175	D-3-phosphoglycerate dehydrogenase	0.03577	0.871675126
P61158	Actin-related protein 3	0.035789	0.916285948
P52788	Spermine synthase	0.036147	0.661661491
P61081	NEDD8-conjugating enzyme Ubc12	0.036583	0.7271843
O75718	Cartilage-associated protein	0.03699	2.051438819
P17987	T-complex protein 1 subunit alpha	0.03795	0.735329804
Q96B26	Exosome complex component RRP43	0.038467	0.111492078
Q9NUQ6	SPATS2-like protein	0.038767	0.553009157
Q8WXA9	Splicing regulatory glutamine/lysine-rich protein 1	0.038873	0.499603307
P48681	Nestin	0.039164	0.676352335
Q8TAT6	Nuclear protein localization protein 4 homolog	0.039254	0.718332034
P19087	Guanine nucleotide-binding protein G(t) subunit alpha-2	0.039835	46.62005382
P06702	Protein S100-A9	0.040203	0.701021668
P31948	Stress-induced-phosphoprotein 1	0.040222	0.712029953
O75367	Core histone macro-H2A.1	0.040579	0.65047951
P32119	Peroxiredoxin-2	0.040627	1.197539726
Q13907	Isopentenyl-diphosphate Delta-isomerase 1	0.040786	0.55820045
P09012	U1 small nuclear ribonucleoprotein A	0.040925	8.337882784
O00560	Syntenin-1	0.041187	1.765106713
P07951	Tropomyosin beta chain	0.041246	0.714592533
Q15691	Microtubule-associated protein RP/EB family member 1	0.041949	0.694614514
P53597	Succinate--CoA ligase [ADP/GDP-forming] subunit alpha_ mitochondrial	0.041981	0.733142078
P50552	Vasodilator-stimulated phosphoprotein	0.042061	0.709109292
Q9NTK5	Obg-like ATPase 1	0.042227	3.209241438
P51148	Ras-related protein Rab-5C	0.042505	1.830866843
P05062	Fructose-bisphosphate aldolase B	0.042565	2.527263589
Q9H488	GDP-fucose protein O-fucosyltransferase 1	0.042594	2.709836762

Q06203	Amidophosphoribosyltransferase	0.042638	0.276586071
Q99714	3-hydroxyacyl-CoA dehydrogenase type-2	0.04265	0.259700449
Q8NBX0	Saccharopine dehydrogenase-like oxidoreductase	0.0431	0.502219392
P01040	Cystatin-A	0.043355	0.181424694
P00558	Phosphoglycerate kinase 1	0.043748	0.471723659
Q86UP2	Kinectin	0.043918	0.747006329
P62979	Ubiquitin-40S ribosomal protein S27a	0.04415	1.329242774
P62987	Ubiquitin-60S ribosomal protein L40	0.04415	1.329242774
Q07912	Activated CDC42 kinase 1	0.044246	1.587945645
Q13423	NAD(P) transhydrogenase_ mitochondrial	0.04425	0.601383987
O43747	AP-1 complex subunit gamma-1	0.044598	1.357609503
P00505	Aspartate aminotransferase_ mitochondrial	0.044961	1.250371032
P52948	Nuclear pore complex protein Nup98-Nup96	0.045274	0.827279459
P36542	ATP synthase subunit gamma_ mitochondrial	0.045277	1.273196014
O43852	Calumenin	0.045662	0.877770451
P27348	14-3-3 protein theta	0.045727	2.705453926
Q00341	Vigilin	0.046163	0.585495245
P02751	Fibronectin	0.046293	0.806008027
O60841	Eukaryotic translation initiation factor 5B	0.047178	3.394501112
Q05655	Protein kinase C delta type	0.047236	0.534778749
O94901	SUN domain-containing protein 1	0.047443	2.808677661
P42166	Lamina-associated polypeptide 2_ isoform alpha	0.047683	0.728872208
O94925	Glutaminase kidney isoform_ mitochondrial	0.047691	0.565926924
Q969P6	DNA topoisomerase I_ mitochondrial	0.047917	2.147476816
P42224	Signal transducer and activator of transcription 1-alpha/beta	0.047982	2.400896276
Q9Y6I3	Epsin-1	0.048667	0.211248842
P06744	Glucose-6-phosphate isomerase	0.048928	1.496336125
P33240	Cleavage stimulation factor subunit 2	0.049598	0.491574107

Table S16. List of proteins differentially expressed (by ANOVA, $p \leq 0.05$) in co-treatment 10μM of cuprizone for 24 hours and 1μM of haloperidol for an additional 24 hours (CupHal), compared to cuprizone treatment alone (Cup).

Accession	Description	p-value	CupHal/Cup ratio
Q8N8S7	Protein enabled homolog	0.000875609	0.705423634
P30519	Heme oxygenase 2	0.001499796	3.942498511
P17655	Calpain-2 catalytic subunit	0.001752471	1.280544537
P61353	60S ribosomal protein L27	0.00237341	2.103871557
P13533	Myosin-6	0.002447793	0.577801094
P18085	ADP-ribosylation factor 4	0.002466583	2.275042426
O75369	Filamin-B	0.002519286	1.29657448
P62195	26S proteasome regulatory subunit 8	0.002922675	0.601208673
P00505	Aspartate aminotransferase_ mitochondrial	0.003766998	1.3936878
Q9NWV8	BRISC and BRCA1-A complex member 1	0.003859103	0.265256406
Q96QH2	PML-RARA-regulated adapter molecule 1	0.004148183	0.607411443
P23381	Tryptophan--tRNA ligase_ cytoplasmic	0.004163378	0.369420756
P0DMV8	Heat shock 70 kDa protein 1A	0.004629961	0.542425141
Q9BVC6	Transmembrane protein 109	0.004723389	2.5236424
P16949	Stathmin	0.005203852	0.831342385
Q13243	Serine/arginine-rich splicing factor 5	0.006525529	1.877441877
Q09028	Histone-binding protein RBBP4	0.006826027	0.758962147
Q15293	Reticulocalbin-1	0.006959454	1.46944861
P12081	Histidine--tRNA ligase_ cytoplasmic	0.009820601	1.380899217
O95782	AP-2 complex subunit alpha-1	0.010514844	0.956037423
O75533	Splicing factor 3B subunit 1	0.011926807	1.132179089
P26640	Valine--tRNA ligase	0.013450169	1.784528806
Q8TAQ2	SWI/SNF complex subunit SMARCC2	0.013696182	1.404579162
Q99715	Collagen alpha-1(XII) chain	0.014136872	0.816964646
Q9UBE0	SUMO-activating enzyme subunit 1	0.014183883	0.528917545
Q32MZ4	Leucine-rich repeat flightless-interacting protein 1	0.0144536	0.603987394
Q9HC35	Echinoderm microtubule-associated protein-like 4	0.014842477	1.558125379
Q15691	Microtubule-associated protein RP/EB family member 1	0.016001729	0.747198007
Q9NUQ6	SPATS2-like protein	0.018665095	0.447501228
Q12841	Follistatin-related protein 1	0.019245771	0.697990702
Q9UNF1	Melanoma-associated antigen D2	0.01951819	0.784715918

Q14204	Cytoplasmic dynein 1 heavy chain 1	0.019710386	0.734058675
O94973	AP-2 complex subunit alpha-2	0.019779111	0.423445538
P13995	Bifunctional methylenetetrahydrofolate dehydrogenase/cyclohydrolase_ mitochondrial	0.020196373	1.156921127
Q15393	Splicing factor 3B subunit 3	0.020442358	0.449066833
O14980	Exportin-1	0.020681193	2.729331561
Q14008	Cytoskeleton-associated protein 5	0.02104263	1.131954023
Q8N3K9	Cardiomyopathy-associated protein 5	0.021315258	0.392962397
P49792	E3 SUMO-protein ligase RanBP2	0.02135549	2.231275097
Q9Y5M8	Signal recognition particle receptor subunit beta	0.022253682	2.230119056
P14868	Aspartate--tRNA ligase_ cytoplasmic	0.022330578	0.867687064
P30044	Peroxiredoxin-5_ mitochondrial	0.022842919	2.435644951
Q06830	Peroxiredoxin-1	0.024153188	1.262433803
P41250	Glycine--tRNA ligase	0.024309824	0.8378035
P40429	60S ribosomal protein L13a	0.026354721	2.053316362
P55291	Cadherin-15	0.026491618	0.662109301
Q9C0B2	Cilia- and flagella-associated protein 74	0.027066759	1.434678959
Q99714	3-hydroxyacyl-CoA dehydrogenase type-2	0.027380675	1.493983238
Q14683	Structural maintenance of chromosomes protein 1A	0.027405408	0.891206109
Q03701	CCAAT/enhancer-binding protein zeta	0.027536938	9.22557294
Q9ULV5	Heat shock factor protein 4	0.027572319	0.703655994
P61619	Protein transport protein Sec61 subunit alpha isoform 1	0.029890441	1.454775033
A8MUA0	Putative UPF0607 protein ENSP00000381514	0.030327653	6.927149279
Q96T37	RNA-binding protein 15	0.030332707	0.835913692
Q96B26	Exosome complex component RRP43	0.030935979	0.285160832
P63151	Serine/threonine-protein phosphatase 2A 55 kDa regulatory subunit B alpha isoform	0.032621404	1.338205413
P20618	Proteasome subunit beta type-1	0.032828485	0.723586911
O75795	UDP-glucuronosyltransferase 2B17	0.032908243	0.604580443
O14929	Histone acetyltransferase type B catalytic subunit	0.03395749	0.672536385
P14317	Hematopoietic lineage cell-specific protein	0.034116521	0.522701267
P60660	Myosin light polypeptide 6	0.034343514	2.081579589
P17812	CTP synthase 1	0.034553064	1.87733436

Q9P0K7	Ankycorbin	0.034613936	0.410663596
P05386	60S acidic ribosomal protein P1	0.035032836	2.978010991
Q9NTJ3	Structural maintenance of chromosomes protein 4	0.035086176	0.764142383
Q9H3P7	Golgi resident protein GCP60	0.035464083	0.615361821
Q9UNZ2	NSFL1 cofactor p47	0.036684124	0.828527894
Q13573	SNW domain-containing protein 1	0.037889738	0.81883126
Q8NCI6	Beta-galactosidase-1-like protein 3	0.038024569	0.526842392
Q9H0S4	Probable ATP-dependent RNA helicase DDX47	0.038113415	0.326411228
Q9Y2Z0	Protein SGT1 homolog	0.038195094	0.816432827
Q8IYB5	Stromal membrane-associated protein 1	0.039129711	0.820439716
Q7Z5Y7	BTB/POZ domain-containing protein KCTD20	0.03934531	5.91158215
Q12873	Chromodomain-helicase-DNA-binding protein 3	0.039639557	0.320744463
P10588	Nuclear receptor subfamily 2 group F member 6	0.039813452	0.70045241
P34897	Serine hydroxymethyltransferase_ mitochondrial	0.039835093	0.890465591
P04181	Ornithine aminotransferase_ mitochondrial	0.040341882	1.439448596
P00966	Argininosuccinate synthase	0.04119813	5.444984499
P81605	Dermcidin	0.041737387	0.202515203
Q9BZK7	F-box-like/WD repeat-containing protein TBL1XR1	0.041870422	0.607379224
P30084	Enoyl-CoA hydratase_ mitochondrial	0.043788315	1.64046744
P07437	Tubulin beta chain	0.043971927	0.365885899
O14647	Chromodomain-helicase-DNA-binding protein 2	0.044056394	1.556624038
P46781	40S ribosomal protein S9	0.044076667	1.694001676
Q6P9B6	MTOR-associated protein MEAK7	0.044144651	0.541312602
Q14966	Zinc finger protein 638	0.04523991	1.155074877
P49841	Glycogen synthase kinase-3 beta	0.045629514	0.846763448
O75396	Vesicle-trafficking protein SEC22b	0.046416445	4.932656227
P30419	Glycylpeptide N-tetradecanoyltransferase 1	0.046879595	0.524561421
Q99733	Nucleosome assembly protein 1-like 4	0.047725614	0.707344681
P45973	Chromobox protein homolog 5	0.048180003	4.305289033
P14314	Glucosidase 2 subunit beta	0.048258303	1.241931952
Q14152	Eukaryotic translation initiation factor 3 subunit A	0.048300035	1.19704809
P46777	60S ribosomal protein L5	0.049947126	1.823730435
O95757	Heat shock 70 kDa protein 4L	0.049993663	0.742456968

Table S17. List of proteins differentially expressed (by ANOVA, $p \leq 0.05$) in co-treatment 10μM of cuprizone for 24 hours and 1μM of clozapine for an additional 24 hours (CupClz), compared to cuprizone treatment alone (Cup).

Accession	Description	p-value	CupClz/Cup ratio
Q13630	GDP-L-fucose synthase	0.002019516	0.502006372
Q9NUQ9	Protein FAM49B	0.002667296	1.354805129
Q8N3K9	Cardiomyopathy-associated protein 5	0.003124483	0.006270904
Q13868	Exosome complex component RRP4	0.003665968	0.673619717
Q01105	Protein SET	0.004389613	1.141883216
P0DME0	Protein SETSIP	0.004389613	1.141883216
P50440	Glycine amidinotransferase_ mitochondrial	0.004667655	0.422344136
Q96Q06	Perilipin-4	0.005979015	0.224028132
Q9H6N6	Putative uncharacterized protein MYH16	0.006468282	0.184656739
Q08J23	RNA cytosine C(5)-methyltransferase NSUN2	0.007176483	0.825039162
P18754	Regulator of chromosome condensation	0.007215832	0.65547648
P23528	Cofilin-1	0.007822902	1.410799877
Q06830	Peroxiredoxin-1	0.007935732	1.413915627
O15372	Eukaryotic translation initiation factor 3 subunit H	0.008114623	0.00089575
Q8NC56	LEM domain-containing protein 2	0.008221848	1.759215681
Q5SW79	Centrosomal protein of 170 kDa	0.008524597	0.646394352
Q96MG2	Junctional sarcoplasmic reticulum protein 1	0.008796384	0.523356021
Q96IJ6	Mannose-1-phosphate guanyltransferase alpha	0.009656243	0.506325921
Q9H081	Protein MIS12 homolog	0.014201649	1.49035866
O14929	Histone acetyltransferase type B catalytic subunit	0.014999372	0.630413012
P49755	Transmembrane emp24 domain-containing protein 10	0.015006914	1.475609169
Q9UIG0	Tyrosine-protein kinase BAZ1B	0.015421447	0.394948143
Q9UKX2	Myosin-2	0.01627744	1.381499281
P06753	Tropomyosin alpha-3 chain	0.01730038	0.683609247
Q8N2X6	Uncharacterized protein EXOC3-AS1	0.017529694	9.57914664
P13637	Sodium/potassium-transporting ATPase subunit alpha-3	0.017926646	0.612897803
P67936	Tropomyosin alpha-4 chain	0.017945719	0.705317532
Q99613	Eukaryotic translation initiation factor 3 subunit C	0.018324115	0.747806564
P48735	Isocitrate dehydrogenase [NADP]_ mitochondrial	0.018529734	0.717526421

Q01433	AMP deaminase 2	0.019162588	0.537494631
Q96HS1	Serine/threonine-protein phosphatase PGAM5_ mitochondrial	0.019297389	0.82939295
Q8WW12	PEST proteolytic signal-containing nuclear protein	0.019855294	4.307964329
O43493	Trans-Golgi network integral membrane protein 2	0.019909727	0.595645644
P55291	Cadherin-15	0.020217652	0.595236403
O94880	PHD finger protein 14	0.021251711	0.693272674
Q9BRL6	Serine/arginine-rich splicing factor 8	0.021902272	1.549925686
Q9BX67	Junctional adhesion molecule C	0.022915227	0.537694775
Q96EY1	DnaJ homolog subfamily A member 3_ mitochondrial	0.022937847	1.300350609
Q9BQS8	FYVE and coiled-coil domain-containing protein 1	0.023034767	5.071246714
Q09161	Nuclear cap-binding protein subunit 1	0.024591976	0.682011322
Q9BVC6	Transmembrane protein 109	0.026848504	1.794487452
Q92934	Bcl2-associated agonist of cell death	0.027424849	0.616944375
Q9H0A0	RNA cytidine acetyltransferase	0.027891671	0.73033018
P23381	Tryptophan--tRNA ligase_ cytoplasmic	0.030362622	0.558485314
Q8NG48	Protein Lines homolog 1	0.031100757	0.524841656
P58397	A disintegrin and metalloproteinase with thrombospondin motifs 12	0.031326824	0.386757901
Q16543	Hsp90 co-chaperone Cdc37	0.032129635	0.663367556
Q8TD57	Dynein heavy chain 3_ axonemal	0.032278646	0.843747373
Q9H3P7	Golgi resident protein GCP60	0.03259747	0.549310636
A6ND36	Protein FAM83G	0.032763152	0.677539756
Q9NX63	MICOS complex subunit MIC19	0.033304456	0.483138168
Q96DU9	Polyadenylate-binding protein 5	0.0334073	1.713869322
P81605	Dermcidin	0.033612477	0.085288405
P07951	Tropomyosin beta chain	0.034062287	0.70008989
Q5JTV8	Torsin-1A-interacting protein 1	0.035023225	0.632848756
Q9NRN5	Olfactomedin-like protein 3	0.035643173	0.294082841
Q96F86	Enhancer of mRNA-decapping protein 3	0.037141125	0.27585083
P11766	Alcohol dehydrogenase class-3	0.037364797	1.464566139
P09493	Tropomyosin alpha-1 chain	0.037739197	0.679015904
Q9NTJ3	Structural maintenance of chromosomes protein 4	0.037968855	0.752336172
Q5ZPR3	CD276 antigen	0.037991377	0.809162132
Q32MZ4	Leucine-rich repeat flightless-interacting protein 1	0.037999408	0.477013668

Q15691	Microtubule-associated protein RP/EB family member 1	0.038401311	0.730101286
Q13243	Serine/arginine-rich splicing factor 5	0.038440047	1.375456674
P07197	Neurofilament medium polypeptide	0.038580189	66.66413322
Q15785	Mitochondrial import receptor subunit TOM34	0.039101552	0.770085625
Q9NUQ6	SPATS2-like protein	0.039134319	0.254139796
Q13191	E3 ubiquitin-protein ligase CBL-B	0.03944406	0.781521929
Q96Q15	Serine/threonine-protein kinase SMG1	0.041051608	0.644990832
Q13595	Transformer-2 protein homolog alpha	0.041537977	0.544519451
Q5T1J5	Putative coiled-coil-helix-coiled-coil-helix domain-containing protein CHCHD2P9_ mitochondrial	0.042025307	11.02425566
Q8NCI6	Beta-galactosidase-1-like protein 3	0.042196106	0.557347305
O94810	Regulator of G-protein signaling 11	0.042221153	0.76042923
P28074	Proteasome subunit beta type-5	0.042397669	1.351880244
Q9NY33	Dipeptidyl peptidase 3	0.042982989	0.891487084
P10588	Nuclear receptor subfamily 2 group F member 6	0.043495579	0.766557555
P50402	Emerin	0.043791015	0.585645705
Q15149	Plectin	0.043962928	0.666218432
Q9BQ39	ATP-dependent RNA helicase DDX50	0.044855033	1.15075698
P20839	Inosine-5'-monophosphate dehydrogenase 1	0.044899905	2.708742574
Q96F05	Uncharacterized protein C11orf24	0.045088496	0.015192474
Q13418	Integrin-linked protein kinase	0.045126367	0.522007691
P55036	26S proteasome non-ATPase regulatory subunit 4	0.046168634	0.767849386
P13533	Myosin-6	0.047057021	0.27764963
Q5VYK3	Proteasome adapter and scaffold protein ECM29	0.047131022	0.496688434
P23284	Peptidyl-prolyl cis-trans isomerase B	0.047241301	1.37656196
A4QMS7	Uncharacterized protein C5orf49	0.047985457	0.072625887
Q10713	Mitochondrial-processing peptidase subunit alpha	0.048138899	0.777821777
P63241	Eukaryotic translation initiation factor 5A-1	0.049100415	4.895069291
Q0VFZ6	Coiled-coil domain-containing protein 173	0.049967279	1.806549493
O60841	Eukaryotic translation initiation factor 5B	0.049970904	1.599013642

Table S18. List of proteins differentially expressed (by ANOVA, $p \leq 0.05$) in co-treatment 10μM of cuprizone for 24 hours and 1μM of cannabidiol for an additional 24 hours (CupCBD), compared to cuprizone treatment alone (Cup).

Accession	Description	p-value	CupCBD/Cup ratio
P50570	Dynamin-2	0.000379	1.297937707
Q14011	Cold-inducible RNA-binding protein	0.000803	0.365518203
Q14152	Eukaryotic translation initiation factor 3 subunit A	0.000955	1.779787222
P31930	Cytochrome b-c1 complex subunit 1_ mitochondrial	0.00152	0.82048885
P22695	Cytochrome b-c1 complex subunit 2_ mitochondrial	0.001744	1.483167926
Q08211	ATP-dependent RNA helicase A	0.003124	1.340674243
Q14690	Protein RRP5 homolog	0.004066	0.8397594
Q8NBS9	Thioredoxin domain-containing protein 5	0.004477	1.766470614
Q15274	Nicotinate-nucleotide pyrophosphorylase [carboxylating]	0.005596	0.534865895
Q9Y2W1	Thyroid hormone receptor-associated protein 3	0.005794	1.348085446
Q92922	SWI/SNF complex subunit SMARCC1	0.007215	1.453738582
P35609	Alpha-actinin-2	0.007948	1.111244159
Q13045	Protein flightless-1 homolog	0.008938	1.220441252
Q9Y230	RuvB-like 2	0.009958	1.456801677
Q8NCI6	Beta-galactosidase-1-like protein 3	0.010734	0.346229983
P43034	Platelet-activating factor acetylhydrolase IB subunit alpha	0.012021	0.820713885
P48047	ATP synthase subunit O_ mitochondrial	0.012303	1.740773635
P00505	Aspartate aminotransferase_ mitochondrial	0.014417	1.294363998
P35658	Nuclear pore complex protein Nup214	0.014634	1.697257088
Q1KMD3	Heterogeneous nuclear ribonucleoprotein U-like protein 2	0.014639	1.279173465
P00367	Glutamate dehydrogenase 1_ mitochondrial	0.014851	1.28172984
P50993	Sodium/potassium-transporting ATPase subunit alpha-2	0.015037	1.931567626
Q08209	Serine/threonine-protein phosphatase 2B catalytic subunit alpha isoform	0.015095	1.462311679
Q9NR45	Sialic acid synthase	0.015524	0.272502571
Q9NQT8	Kinesin-like protein KIF13B	0.015587	1.875030828
P45974	Ubiquitin carboxyl-terminal hydrolase 5	0.017332	1.214383591
P17480	Nucleolar transcription factor 1	0.017479	1.869014998
Q8NBX0	Saccharopine dehydrogenase-like oxidoreductase	0.018327	0.572887598
Q01780	Exosome component 10	0.018385	0.440791646
Q9BQ52	Zinc phosphodiesterase ELAC protein 2	0.018962	1.805260474
P16949	Stathmin	0.021344	0.829442851
Q9BT09	Protein canopy homolog 3	0.021693	0.012794937

P13533	Myosin-6	0.022399	0.63885396
O60568	Multifunctional procollagen lysine hydroxylase and glycosyltransferase LH3	0.022415	1.285503339
P51149	Ras-related protein Rab-7a	0.022644	0.863183928
Q96BH1	E3 ubiquitin-protein ligase RNF25	0.023921	0.024773689
O14929	Histone acetyltransferase type B catalytic subunit	0.026103	0.680224078
Q96MG2	Junctional sarcoplasmic reticulum protein 1	0.026581	0.595705479
P62280	40S ribosomal protein S11	0.026749	0.406219837
Q01581	Hydroxymethylglutaryl-CoA synthase_ cytoplasmic	0.027462	1.360762056
Q9P2D7	Dynein heavy chain 1_ axonemal	0.027791	0.705408291
Q13620	Cullin-4B	0.028886	0.46529645
Q9NTK5	Obg-like ATPase 1	0.029068	0.512077335
A8MYA2	Uncharacterized protein CXorf49	0.029255	0.482022677
P63208	S-phase kinase-associated protein 1	0.033333	0.268580971
Q9NZ08	Endoplasmic reticulum aminopeptidase 1	0.033833	2.899816843
A4QMS7	Uncharacterized protein C5orf49	0.034369	0.27464118
P12814	Alpha-actinin-1	0.034443	1.254961078
Q9C0B2	Cilia- and flagella-associated protein 74	0.035278	1.482380988
O14602	Eukaryotic translation initiation factor 1A_ Y-chromosomal	0.035406	0.559673397
P00338	L-lactate dehydrogenase A chain	0.036969	0.716120919
Q32P28	Prolyl 3-hydroxylase 1	0.037102	1.500847414
P17035	Zinc finger protein 28	0.037622	0.669990908
P83916	Chromobox protein homolog 1	0.038127	0.4232465
P08195	4F2 cell-surface antigen heavy chain	0.038602	1.624435417
P61254	60S ribosomal protein L26	0.03882	0.501536281
P18065	Insulin-like growth factor-binding protein 2	0.038942	1.402234191
P30086	Phosphatidylethanolamine-binding protein 1	0.039414	0.376019496
Q9Y678	Coatomer subunit gamma-1	0.039872	1.221738497
P33991	DNA replication licensing factor MCM4	0.040074	1.513425784
Q9UBS4	DnaJ homolog subfamily B member 11	0.04022	1.436909053
Q14993	Collagen alpha-1(XIX) chain	0.040373	0.421042764
Q9NTJ3	Structural maintenance of chromosomes protein 4	0.040842	1.359975201
O43707	Alpha-actinin-4	0.040874	1.381079646
P14314	Glucosidase 2 subunit beta	0.04095	1.529187914

P06737	Glycogen phosphorylase_ liver form	0.041552	1.674921846
Q92974	Rho guanine nucleotide exchange factor 2	0.042325	1.440881976
Q10471	Polypeptide N-acetylgalactosaminyltransferase 2	0.043733	1.378628575
P33992	DNA replication licensing factor MCM5	0.04415	1.514875609
Q99497	Protein/nucleic acid deglycase DJ-1	0.046216	0.658077727
Q99961	Endophilin-A2	0.047219	0.746305487
P0DOY2	Immunoglobulin lambda constant 2	0.047548	0.111142284
Q96T37	RNA-binding protein 15	0.048672	1.514661286
Q7Z5Y7	BTB/POZ domain-containing protein KCTD20	0.049882	0.067631279

Table S19. List of proteins differentially expressed (by ANOVA, $p \leq 0.05$) in co-treatment 10μM of cuprizone for 24 hours and 1μM of benztropine for an additional 24 hours (CupBenz), compared to cuprizone treatment alone (Cup).

Accession	Description	p-value	CupBenz/Cup ratio
Q14203	Dynactin subunit 1	0.0003	0.655097919
Q9H3P7	Golgi resident protein GCP60	0.000439	0.393856961
P48681	Nestin	0.001076	2.040627067
Q14966	Zinc finger protein 638	0.001162	1.517765349
Q92917	G-patch domain and KOW motifs-containing protein	0.001669	0.470859088
O43395	U4/U6 small nuclear ribonucleoprotein Prp3	0.001707	1.382578559
P17480	Nucleolar transcription factor 1	0.001938	1.502790928
Q14008	Cytoskeleton-associated protein 5	0.001943	0.751628019
Q13619	Cullin-4A	0.002817	0.465065268
P43362	Melanoma-associated antigen 9	0.003209	0.051535544
P18085	ADP-ribosylation factor 4	0.003472	0.489118246
Q8N8S7	Protein enabled homolog	0.003625	0.736575453
Q13620	Cullin-4B	0.003676	0.509883852
P16949	Stathmin	0.004115	0.786165517
P29966	Myristoylated alanine-rich C-kinase substrate	0.004225	0.511319631
Q96MG2	Junctional sarcoplasmic reticulum protein 1	0.004813	0.424610118
Q8IWJ2	GRIP and coiled-coil domain-containing protein 2	0.005605	0.595835325
Q12788	Transducin beta-like protein 3	0.005686	1.304060013
P41219	Peripherin	0.006384	0.79446861

P49006	MARCKS-related protein	0.006853	0.469882149
Q9UBE0	SUMO-activating enzyme subunit 1	0.007028	0.582877932
Q6WCQ1	Myosin phosphatase Rho-interacting protein	0.007427	1.600573262
Q9C0B2	Cilia- and flagella-associated protein 74	0.007656	1.67587424
Q9NUQ6	SPATS2-like protein	0.007697	0.605189963
P09874	Poly [ADP-ribose] polymerase 1	0.007878	1.323050445
O00469	Procollagen-lysine_2-oxoglutarate 5-dioxygenase 2	0.008607	1.461006516
Q9Y2Z0	Protein SGT1 homolog	0.008812	0.728695675
P22695	Cytochrome b-c1 complex subunit 2_ mitochondrial	0.009589	1.400359291
Q96HS1	Serine/threonine-protein phosphatase PGAM5_ mitochondrial	0.010242	1.313800422
O75369	Filamin-B	0.010343	1.27949789
O14929	Histone acetyltransferase type B catalytic subunit	0.010657	0.580308513
Q9UHB6	LIM domain and actin-binding protein 1	0.010917	1.769127396
A4QMS7	Uncharacterized protein C5orf49	0.011438	0.25880031
Q9NRX5	Serine incorporator 1	0.013053	2.03511306
Q9UBB4	Ataxin-10	0.013477	0.15649551
Q9BZL4	Protein phosphatase 1 regulatory subunit 12C	0.013617	0.478376277
P51149	Ras-related protein Rab-7a	0.014715	1.309404996
Q14141	Septin-6	0.015168	0.101554777
Q13733	Sodium/potassium-transporting ATPase subunit alpha-4	0.016053	2.342922956
P23381	Tryptophan--tRNA ligase_ cytoplasmic	0.016303	0.454175229
P02751	Fibronectin	0.016707	1.233741308
P47985	Cytochrome b-c1 complex subunit Rieske_ mitochondrial	0.017232	1.815025186
P50993	Sodium/potassium-transporting ATPase subunit alpha-2	0.018235	1.380897546
Q9Y2U9	Kelch domain-containing protein 2	0.018339	3.142610514
P50440	Glycine amidinotransferase_ mitochondrial	0.018626	0.574698702
Q9BSJ8	Extended synaptotagmin-1	0.019604	1.487698713
P04083	Annexin A1	0.019623	1.396177729
P21127	Cyclin-dependent kinase 11B	0.019831	1.384864713
Q92922	SWI/SNF complex subunit SMARCC1	0.020063	1.193631389
P50502	Hsc70-interacting protein	0.0203	0.785697657
Q04637	Eukaryotic translation initiation factor 4 gamma 1	0.020757	0.764732436
P28370	Probable global transcription activator SNF2L1	0.020913	0.872782593

Q13098	COP9 signalosome complex subunit 1	0.020999	0.663377653
Q9NZV7	Zinc finger imprinted 2	0.021386	1.580844203
Q9UJU6	Drebrin-like protein	0.024017	0.623759599
Q15436	Protein transport protein Sec23A	0.024631	1.809237328
Q96QD8	Sodium-coupled neutral amino acid transporter 2	0.025293	2.528509959
Q9BS26	Endoplasmic reticulum resident protein 44	0.026166	0.720030492
Q96I99	Succinate--CoA ligase [GDP-forming] subunit beta_ mitochondrial	0.026366	1.844685972
O75915	PRA1 family protein 3	0.028781	0.712020086
Q0VFZ6	Coiled-coil domain-containing protein 173	0.029421	0.636762987
O00571	ATP-dependent RNA helicase DDX3X	0.029935	0.322886255
Q9NWH9	SAFB-like transcription modulator	0.030078	0.78895318
Q9NSE4	Isoleucine--tRNA ligase_ mitochondrial	0.030713	1.500863116
Q13439	Golgin subfamily A member 4	0.030919	1.677310453
O00273	DNA fragmentation factor subunit alpha	0.031023	0.704784609
Q9H3K2	Growth hormone-inducible transmembrane protein	0.03181	0.121191632
O95602	DNA-directed RNA polymerase I subunit RPA1	0.032888	2.027861333
P47756	F-actin-capping protein subunit beta	0.033257	0.832469108
O95202	Mitochondrial proton/calcium exchanger protein	0.033571	0.471870876
P61019	Ras-related protein Rab-2A	0.033614	1.306461562
Q86YP4	Transcriptional repressor p66-alpha	0.033742	1.289290827
P45974	Ubiquitin carboxyl-terminal hydrolase 5	0.033768	0.825146489
Q96QH2	PML-RARA-regulated adapter molecule 1	0.034903	0.758335213
Q9Y3T9	Nucleolar complex protein 2 homolog	0.035033	0.64693275
P22033	Methylmalonyl-CoA mutase_ mitochondrial	0.035302	1.366502335
P58335	Anthrax toxin receptor 2	0.035669	0.54532683
Q15758	Neutral amino acid transporter B(0)	0.036019	1.806345019
Q9NYU2	UDP-glucose:glycoprotein glucosyltransferase 1	0.036142	1.457112618
O75844	CAAX prenyl protease 1 homolog	0.036189	1.446554586
P17661	Desmin	0.036577	1.226667374
P35269	General transcription factor IIF subunit 1	0.03786	0.527949829
Q6ZR08	Dynein heavy chain 12_ axonemal	0.038712	1.566424695
P62269	40S ribosomal protein S18	0.03903	0.630421473
Q9Y2L1	Exosome complex exonuclease RRP44	0.039161	43.26231421
Q8NBJ5	Procollagen galactosyltransferase 1	0.039561	2.342348578

P00505	Aspartate aminotransferase_ mitochondrial	0.039688	1.196183392
Q9UBC7	Galanin-like peptide	0.040013	2.02908284
Q14254	Flotillin-2	0.040397	1.394606527
O75533	Splicing factor 3B subunit 1	0.041082	1.232531001
Q86UE4	Protein LYRIC	0.041119	0.708189847
Q92879	CUGBP Elav-like family member 1	0.041381	1.632678209
P43304	Glycerol-3-phosphate dehydrogenase_ mitochondrial	0.041719	0.876350801
Q96QK1	Vacuolar protein sorting-associated protein 35	0.041777	0.70177575
Q15293	Reticulocalbin-1	0.041877	1.371268423
Q99805	Transmembrane 9 superfamily member 2	0.043775	2.152893691
P05386	60S acidic ribosomal protein P1	0.044335	0.119598667
Q8NFH5	Nucleoporin NUP35	0.044814	1.672323892
P15880	40S ribosomal protein S2	0.045258	0.655654926
P62333	26S proteasome regulatory subunit 10B	0.045398	1.602036678
P51858	Hepatoma-derived growth factor	0.04543	0.69073998
O75431	Metaxin-2	0.045536	2.493188789
P78344	Eukaryotic translation initiation factor 4 gamma 2	0.046219	1.34538389
Q32MZ4	Leucine-rich repeat flightless-interacting protein 1	0.046583	0.670922305
P09936	Ubiquitin carboxyl-terminal hydrolase isozyme L1	0.046762	0.542324922
P55010	Eukaryotic translation initiation factor 5	0.047018	0.672634958
Q13557	Calcium/calmodulin-dependent protein kinase type II subunit delta	0.047622	1.493238771
P43034	Platelet-activating factor acetylhydrolase IB subunit alpha	0.047854	0.829158025
A1X283	SH3 and PX domain-containing protein 2B	0.048311	0.397760179
P0DOY2	Immunoglobulin lambda constant 2	0.049091	0.109416867
P61163	Alpha-centractin	0.049323	1.492145003
O43852	Calumenin	0.049853	1.32760096
P61254	60S ribosomal protein L26	0.049899	0.501664864

10. ANEXOS

10.1 Declaração de bioética e biossegurança

COORDENADORIA DE PÓS-GRADUAÇÃO
INSTITUTO DE BIOLOGIA
Universidade Estadual de Campinas
Caixa Postal 6109. 13083-970, Campinas, SP, Brasil
Fone (19) 3521-6378. email: cpgib@unicamp.br

DECLARAÇÃO

Em observância ao **§5º do Artigo 1º da Informação CCPG-UNICAMP/001/15**, referente a Bioética e Biossegurança, declaro que o conteúdo de minha Dissertação de Mestrado, intitulada "***Efeito de antipsicóticos e canabidiol em cultura de oligodendrócitos tratados com cuprizona: implicações para mielinização***", desenvolvida no Programa de Pós-Graduação em Biologia Funcional e Molecular do Instituto de Biologia da Unicamp, não versa sobre pesquisa envolvendo seres humanos, animais ou temas afetos a Biossegurança.

Assinatura: Ana Caroline B. Falvella
Nome do(a) aluno(a): Ana Caroline Brambilla Falvella

Assinatura: _____
Nome do(a) orientador(a): Daniel Martins de Souza

Data: 24 de novembro de 2020

10.2 Declaração de direitos autorais

Declaração

As cópias de artigos de minha autoria ou de minha co-autoria, já publicados ou submetidos para publicação em revistas científicas ou anais de congressos sujeitos a arbitragem, que constam da minha Dissertação/Tese de Mestrado/Doutorado, intitulada **"Efeito de antipsicóticos e canabidiol em cultura de oligodendrócitos tratados com cuprizona: implicações para mielinização"**, não infringem os dispositivos da Lei n.° 9.610/98, nem o direito autoral de qualquer editora.

Campinas, 24 de novembro de 2020

Assinatura : Ana Caroline B. Falvella
Nome do(a) autor(a): **Ana Caroline Brambilla Falvella**
RG n.° 38.270.664-x - SSP/SP

Assinatura : _____
Nome do(a) orientador(a): **Daniel Martins de Souza**
RG n.° 32.431.379-2 - SSP/SP